Insights into Grand Unified Theories from Current Experimental Data

Inauguraldissertation
zur
Erlangung der Würde eines Doktors der Philosophie
vorgelegt der
Philosophisch-Naturwissenschaftlichen Fakultät
der Universität Basel
von

Vinzenz Karl Maria Maurer
aus Deutschland

Basel, 2015

Genehmigt von der Philosophisch-Naturwissenschaftlichen Fakultät

auf Antrag von

Prof. Dr. Stefan Antusch, Dr. Sabine Kraml

Basel, den 21.04.2015

Prof. Dr. Jörg Schibler
Dekan

Namensnennung-Keine kommerzielle Nutzung-Keine Bearbeitung 3.0 Schweiz
(CC BY-NC-ND 3.0 CH)

Sie dürfen: **Teilen** — den Inhalt kopieren, verbreiten und zugänglich machen

Unter den folgenden Bedingungen:

Namensnennung — Sie müssen den Namen des Autors/Rechteinhabers in der von ihm festgelegten Weise nennen.

Keine kommerzielle Nutzung — Sie dürfen diesen Inhalt nicht für kommerzielle Zwecke nutzen.

Keine Bearbeitung erlaubt — Sie dürfen diesen Inhalt nicht bearbeiten, abwandeln oder in anderer Weise verändern.

Wobei gilt:

- **Verzichtserklärung —** Jede der vorgenannten Bedingungen kann **aufgehoben** werden, sofern Sie die ausdrückliche Einwilligung des Rechteinhabers dazu erhalten.
- **Public Domain (gemeinfreie oder nicht-schützbare Inhalte) —** Soweit das Werk, der Inhalt oder irgendein Teil davon zur Public Domain der jeweiligen Rechtsordnung gehört, wird dieser Status von der Lizenz in keiner Weise berührt.
- **Sonstige Rechte —** Die Lizenz hat keinerlei Einfluss auf die folgenden Rechte:
    - Die Rechte, die jedermann wegen der Schranken des Urheberrechts oder aufgrund gesetzlicher Erlaubnisse zustehen (in einigen Ländern als grundsätzliche Doktrin des **fair use** bekannt);
    - Die **Persönlichkeitsrechte** des Urhebers;
    - Rechte anderer Personen, entweder am Lizenzgegenstand selber oder bezüglich seiner Verwendung, zum Beispiel für **Werbung** oder Privatsphärenschutz.
- **Hinweis —** Bei jeder Nutzung oder Verbreitung müssen Sie anderen alle Lizenzbedingungen mitteilen, die für diesen Inhalt gelten. Am einfachsten ist es, an entsprechender Stelle einen Link auf diese Seite einzubinden.

Quelle: http://creativecommons.org/licenses/by-nc-nd/3.0/ch/ Datum: 12.11.2013

Abstract

In this thesis, we investigate several ways how the structure of a high energy particle physics model constituting a grand unification theory (GUT) in supersymmetry (SUSY) can be inferred from multiple types of information obtained at low energy.

First, we calculate the values and 1σ ranges of the running quark and lepton Yukawa couplings as well as of the quark mixing parameters at various energy scales to provide useful input for flavour model building in GUTs and other scenarios while including $\tan\beta$ enhanced SUSY threshold corrections in a simple way.

Next, we analyse the naturalness of the Minimal Supersymmetric Standard Model (MSSM) in the light of the discovery of the Higgs boson at the Large Hadron Collider (LHC). In particular, we find that among possible departures from the constrained MSSM (cMSSM) non-universal gaugino masses represent the most promising way to find parameter regions with a fine-tuning of only $\mathcal{O}(10)$ even for a Higgs mass of about 126 GeV, compared to $\mathcal{O}(100)$ for the cMSSM. In this context, we also discuss the preference for certain GUT-scale Yukawa coupling ratios over others based on fine-tuning.

Following that, we study how also the recent determination of the leptonic mixing angle $\theta_{13}^{\text{PMNS}}$ can be accommodated in a simple scenario for GUT models of flavour via charged lepton corrections. This leads us to four conditions that can easily be implemented. In addition, the interplay of the value of $\theta_{13}^{\text{PMNS}}$ with future determinations of the Dirac CP phase δ^{PMNS} is discussed using lepton mixing sum rules.

Finally, we study how the double missing partner mechanism as a solution to the doublet-triplet splitting problem can be incorporated into $SU(5)$ GUT models of flavour to comply with the bounds on proton decay. In this context, we argue that the introduction of two adjoints of $SU(5)$ is a compelling idea and calculate its constraints on the GUT scale and dimension five proton decay suppression scale at two loops. We close with general comments on the calculation of the proton lifetime in the considered scenario for flavour models.

Multiple appendices are included detailing non-obvious aspects of the calculation and other kinds of valuable information for GUT model building.

Table of Contents

Introduction

The Standard Model of elementary particle physics (SM) [1, 2] is one of the most accurately tested models in physics and successfully describes the electroweak and strong interactions of all observed particles to a remarkable precision. Nevertheless, there remain unresolved issues like the hierarchy problem, the non-unification of gauge couplings, the unexplained structure of fermion masses and mixing or the inclusion of neutrino masses. All these issues point to the conclusion that the SM is not the fundamental theory of particle physics, but has to be extended in some aspects by new physics.

One popular extension of the SM is the concept of low energy supersymmetry (SUSY). It stabilises the electroweak scale [3] against quantum corrections and modifies the renormalisation group running of the gauge couplings in such a way that they almost exactly unify at a high energy scale [4]. This makes the idea of grand unified theories (GUTs) viable.

Once the gauge couplings are unified, additional relations between the previously unrelated Yukawa couplings of the SM fermions are possible. However, exactly which relations are realised and how they can be incorporated into more extensive models of flavour is far from obvious. One possible approach – the one taken in this thesis – is to try to infer as much information as possible about the high-scale structure of GUT models (of flavour) from multiple sources at lower energies.

To this end, this thesis is organised as follows: part I gives an overview of the basics needed for part II and establishes some conventions, with chapter 1 briefly discussing the SM, chapter 2 introducing fundamental concepts for neutrino masses and mixing, chapter 3 discussing SUSY, the formulation of supersymmetric theories, SUSY breaking and the minimal supersymmetric standard model (MSSM). Lastly, in chapter 4 we give a quick overview over grand unification. Part II shows different examples of information on high-scale structures one can obtain from low energy data. In chapter 5, we derive the quantities relevant for SM flavour physics and flavour models at multiple scales, extending it to the MSSM and going as high as the GUT scale $\sim 10^{16}$ GeV. Chapter 6 shows how the growing weakness of SUSY as a solution to the hierarchy problem can be alleviated by going beyond the trodden paths of universal high-scale boundary conditions for SUSY breaking such as the constrained MSSM, how

the Large Hadron Collider (LHC) so far influences this discussion beyond not finding any new particles predicted by SUSY and what consequences non-universalities can have on GUT-scale Yukawa coupling ratios. In chapter 7, we show how the more recent observation of the reactor neutrino mixing angle makes it possible to constrain the flavour structure of GUTs and other unified models, leading to a set of four simple conditions for reproducing the experimental values. Finally, in chapter 8, we investigate how the non-observation of proton decay can be accommodated in GUT models using the so-called double missing partner mechanism. In part III, we summarise the findings and conclude.

This thesis is based on the publications [5], [6, 7], [8, 9] and [10], and presents a partially updated view on their findings.

PART I

Basics and Notation

CHAPTER 1

The Standard Model

The Standard Model (SM) [1, 2] is the quantum field theory that describes the fundamental interactions of elementary particle physics. It does so to a remarkable precision and has so far been very successful in describing and explaining the measurements done at particle colliders and other types of experiments.

In this section, we will discuss its details as far as they concern the findings in this thesis and will also give a short overview of its shortcomings of aesthetic and technical nature.

1.1 Gauge Symmetries and Field Content

The SM is formulated as a renormalisable chiral gauge theory [11] with the continuous gauge symmetry group $G_{\mathrm{SM}} = SU(3)_C \times SU(2)_L \times U(1)_Y$. The $SU(3)$ factor is responsible for quantum chromodynamics (QCD) [2], which is the theory of strong interactions between quarks and gluons, while the $SU(2) \times U(1)$ factor describes the electroweak theory (the Glashow-Weinberg-Salam model [1]), which is responsible for weak decays and electromagnetism.

The interactions between matter fermions and gauge bosons enter the Lagrangian density by replacing ordinary space-time derivatives with their gauge-covariant equivalents,

$$\partial_\mu \to D_\mu = \partial_\mu + \mathrm{i}\, g_s\, T_a G^a_\mu + \mathrm{i}\, g\, \tau_i W^i_\mu + \mathrm{i}\, g'\, Y B_\mu \,, \tag{1.1}$$

where G^a, W^i and B are the gauge vector boson fields and g_s, g, g' are the gauge couplings, corresponding to the three respective factors of G_{SM}. The matrices T_a, τ_i and Y are the generators of the respective gauge group factor. Their particular form depends on what representation they act on, e.g. $T_a = \lambda_a/2$ for $SU(3)_C$-triplets or $\tau_i = \sigma_i/2$ for $SU(2)_L$-doublets with the Gell-Mann matrices λ_a and the Pauli matrices σ_i.

	$SU(3)_C$	$SU(2)_L$	$U(1)_Y$	spin
$Q = \begin{pmatrix} u \\ d \end{pmatrix} = \begin{pmatrix} u_L \\ d_L \end{pmatrix}$	$\mathbf{3}$	$\mathbf{2}$	$\frac{1}{6}$	$\frac{1}{2}$
$u^c = u_R^*$	$\bar{\mathbf{3}}$	$\mathbf{1}$	$-\frac{2}{3}$	$\frac{1}{2}$
$d^c = d_R^*$	$\bar{\mathbf{3}}$	$\mathbf{1}$	$\frac{1}{3}$	$\frac{1}{2}$
$L = \begin{pmatrix} \nu \\ e \end{pmatrix} = \begin{pmatrix} \nu_L \\ e_L \end{pmatrix}$	$\mathbf{1}$	$\mathbf{2}$	$-\frac{1}{2}$	$\frac{1}{2}$
$e^c = e_R^*$	$\mathbf{1}$	$\mathbf{1}$	1	$\frac{1}{2}$
$H = \begin{pmatrix} H^0 \\ H^- \end{pmatrix}$	$\mathbf{1}$	$\mathbf{2}$	$-\frac{1}{2}$	0

Table 1.1: Irreducible representations of the SM fermion and scalar fields, including definitions of left-handed Weyl spinors in terms of chirality components of Dirac spinors. There are three copies of all shown fermion fields grouped together as 'generations' or 'families'.

As the SM is a chiral theory, the left- and right-handed components of fermion fields transform differently under the gauge symmetry, as described by the field representations given in tab. 1.1. As alluded therein, instead of Dirac spinors, one can also work purely with left-handed two-component Weyl spinors by converting the right-handed component fields to left-handed spinors via conjugation and implicit multiplication with the two-dimensional Levi-Civita tensor $\epsilon = -\mathrm{i}\,\sigma_2$ to take care of the pseudo-reality of the two dimensional $SU(2)$ irreducible representation[1]. For more details, see [12]. For convenience, we will make use of this scheme.

1.2 The Standard Model Lagrangian Density

In addition to the gauge invariant kinetic terms for the SM fermion and scalar fields, the Lagrangian density contains the following parts:

The self-interactions and kinetic terms of the vector bosons are contained in

$$\mathcal{L}_{\text{gauge}} = -\frac{1}{2}\,\mathrm{tr}\,G_{\mu\nu}G^{\mu\nu} - \frac{1}{2}\,\mathrm{tr}\,W_{\mu\nu}W^{\mu\nu} - \frac{1}{4}\,B_{\mu\nu}B^{\mu\nu}\,, \tag{1.2}$$

where the field strength tensors follow the definition, e.g.

$$G^a_{\mu\nu} = \partial_\mu G^a_\nu - \partial_\mu G^a_\nu + g_s f^{abc} G^b_\mu G^c_\nu\,, \tag{1.3}$$

[1] The same ϵ-tensor is also implied for products of two doublets of $SU(2)_L$.

with $G_{\mu\nu} = T_a G^a_{\mu\nu}$, the gluon fields G^a_μ and the $SU(3)$ structure constants f^{abc}. Analogous relations also apply to the vector boson fields W^i_μ and B_μ.

The potential for the electroweak doublet scalar H is given by

$$\mathcal{V}_H = \mu^2 H^\dagger H + \frac{\lambda}{4}(H^\dagger H)^2 \quad \text{with} \quad \mu^2 < 0,\, \lambda > 0\,. \tag{1.4}$$

Since, for $\mu^2 < 0$, the minimum of the potential lies at $H \neq 0$, the electroweak doublet develops a vacuum expectation value (VEV) of the form

$$\langle H \rangle = \frac{1}{\sqrt{2}} \begin{pmatrix} v = 2\sqrt{\frac{-\mu^2}{\lambda}} \\ 0 \end{pmatrix}\,, \tag{1.5}$$

which breaks the electroweak $SU(2)_L \times U(1)_Y$ part of G_{SM} down to the electromagnetic gauge symmetry $U(1)_{\text{em}}$. Thereby, three of the four electroweak gauge bosons, the W bosons $W^\pm$ and the Z boson Z^0, and the radial component[2] of the electroweak doublet H around the VEV, the Higgs boson h^0, develop masses of the form

$$M_W = \frac{1}{2}\, g\, v\,, \qquad M_Z = \frac{1}{2}\, g\, v\, (\cos\theta_W)^{-1}\,, \tag{1.6a}$$

$$m_h^2 = \frac{1}{2}\, \lambda\, v^2\,, \qquad M_\gamma = 0\,, \tag{1.6b}$$

whereas the photon γ stays massless. Here, the angle θ_W is the weak mixing angle given by

$$\sin\theta_W = \frac{g'^2}{\sqrt{g'^2 + g^2}}\,. \tag{1.7}$$

This mechanism for the generation of gauge boson masses, which constitutes spontaneous electroweak symmetry breaking (EWSB), is called the Englert-Brout-Higgs-Guralnik-Hagen-Kibble mechanism [13]. Experimental measurements of the Fermi constant $G_F = g^2/(8M_W^2)$ determine the VEV to $v \simeq 246$ GeV.

In addition to its gauge and self-interactions, the electroweak doublet scalar also has Yukawa interactions with the fermion fields, as encoded in the Lagrangian density part given by

$$\mathcal{L}_{\text{Yukawa}} = -(Y_d)_{ij}\, Q_i\, H\, d^c_j - (Y_e)_{ij}\, L_i\, H\, e^c_j + (Y_u)_{ij}\, Q_i\, \tilde{H}\, u^c_j + \text{h.c.}\,, \tag{1.8}$$

where $\tilde{H} = \epsilon H^*$ denotes the charge conjugate of the electroweak doublet H.

[2] The other would-be Goldstone boson components of H are 'eaten up' by the gauge bosons.

1.3 Fermion Masses and Mixing

After EWSB, the terms in eq. (1.8) become – in addition to Yukawa interactions with the physical Higgs boson field h^0 – mass terms for the fermion fields with mass matrices given by

$$M_u = \frac{v}{\sqrt{2}}\, Y_u \;, \quad M_d = \frac{v}{\sqrt{2}}\, Y_d \;, \quad M_e = \frac{v}{\sqrt{2}}\, Y_e \;. \tag{1.9}$$

Since these mass matrices are not generically diagonal in generation space, one has to rotate the fermion fields to the mass eigenbasis using unitary matrices as in

$$\psi_f \to V_f\, \psi_f \;, \quad \psi_{f^c} \to V_{f^c}\, \psi_{f^c} \;, \tag{1.10}$$

where the matrices V_f and V_{f^c} satisfy, e.g.

$$V_u^T\, Y_u\, V_{u^c} = \text{diagonal and positive.} \tag{1.11}$$

However, as V_u and V_d are not required to be the same, they will in general not cancel out in the weak isospin changing vertex of $W^\pm$ vector bosons to fermions. This means that the mentioned vertices will transform under eq. (1.10) as

$$g\, u_i^\dagger\, d_i\, W^+ + \text{h.c.} \quad \to \quad g\, u_i^\dagger\, (V_u^\dagger V_d)_{ij}\, d_j\, W^+ + \text{h.c.} \;. \tag{1.12}$$

The unitary matrix $V_{\text{CKM}} = V_u^\dagger V_d$ is called the Cabibbo-Kobayashi-Masukawa (CKM) mixing matrix [14] and parametrises the mixing between the three generations in each interaction vertex of fermions with a $W^\pm$ boson.

Since V_{CKM} is a unitary 3×3 matrix, it generally has nine degrees of freedom – three mixing angles and six phases. However, using the fact that V_{u^c} and V_{d^c} are not physical, one can remove five phases and is left with only four parameters, leading to the standard parametrisation [15] of V_{CKM} given by

$$V_{\text{CKM}} = \begin{pmatrix} c_{12}c_{13} & s_{12}c_{13} & s_{13}\mathrm{e}^{-\mathrm{i}\delta} \\ -s_{12}c_{23} - c_{12}s_{23}s_{13}\mathrm{e}^{\mathrm{i}\delta} & c_{12}c_{23} - s_{12}s_{23}s_{13}\mathrm{e}^{\mathrm{i}\delta} & s_{23}c_{13} \\ s_{12}s_{23} - c_{12}c_{23}s_{13}\mathrm{e}^{\mathrm{i}\delta} & -c_{12}s_{23} - s_{12}c_{23}s_{13}\mathrm{e}^{\mathrm{i}\delta} & c_{23}c_{13} \end{pmatrix} \;, \tag{1.13}$$

with $\delta = \delta^{\text{CKM}}$, $c_{ij} = \cos\theta_{ij}^{\text{CKM}}$ and $s_{ij} = \sin\theta_{ij}^{\text{CKM}}$. The angle θ_{12}^{CKM} is also called the Cabibbo angle θ_C.

Note that, as far as the SM goes, there is no mixing matrix analogous to V_{CKM} for leptons as there is only one Yukawa matrix involving lepton fields, namely Y_e, and thus only one left-handed lepton mixing matrix V_e is used. This changes if we introduce right-handed neutrino fields ν_i^c along with their Yukawa interaction terms $L_i \tilde{H} \nu_j^c$ into the SM, as we will see in the next chapter.

1.4 Open Questions

Despite its success, the SM has a couple of shortcomings that are frequently cited as motivation to study physics beyond it. In this thesis, the following ones will be relevant:

Neutrino Masses and Mixing In the present formulation of the SM, neutrinos are massless also after EWSB. However, experimental data tells us that clearly at least two of the neutrinos have very small but nevertheless non-zero masses [16]. Thus a viable extension of the SM must be able to incorporate a way to have non-zero neutrino masses and preferably explain why they are so small.

Hierarchy Problem As is general for quantum field theories including scalar particles, the scalar boson of the SM receives quantum corrections to its mass that make it as heavy as the largest scale of physics coupling to it (assuming $\mathcal{O}(1)$ couplings). If this scale of new physics is too high, e.g. the Planck scale $\sim 10^{19}$ GeV, the Higgs boson mass can only be lowered back to its measured value at the electroweak scale by tuning all contributions to some degree – 1 part in 10^{34} in the case of the Planck scale. This is usually regarded as unnatural and is frequently made unnecessary or severely improved in models going beyond the SM.

Flavour Puzzle The SM is incredibly simple as long as all fermion masses are taken to vanish, since it then only has the three gauge couplings, the electroweak VEV and the Higgs boson mass as free parameters[3]. However, as soon as one introduces Yukawa interactions to generate the fermion masses, we must introduce several new parameters, namely the nine fermion masses, the three plus one CKM mixing parameters and possibly even more leptonic mixing parameters and neutrino masses. It would therefore be very desirable to not only find some connection between the gauge couplings, but also to find some general structure in the SM flavour quantities.

[3]There is one additional parameter, the QCD angle θ from a term $\propto \theta G\tilde{G}$ in $\mathcal{L}$, with the gluon field strength tensor G and its dual $\tilde{G}$. Its experimentally required smallness is, however, a whole different puzzle in itself, which we will not address in this thesis.

CHAPTER 2

Neutrino Masses and Mixing

Neutrinos are special within the SM as they are the only fundamental fermions that are completely uncharged under symmetries respected by the vacuum. This restricts their interactions with other particles through gauge interactions, as they can only interact through the heavy vector bosons $W^{\pm}$ and Z^0 and the Higgs boson h^0, which makes them hard to detect but otherwise not very interesting.

Fortunately, it was realised in the 1960s by Pontecorvo [17] and by Maki, Nakagawa and Saki [18], that if lepton family numbers are not conserved – analogous to, for example, strangeness violation in the quark sector – and neutrinos have non-zero masses contrary to the SM, this can lead to observable neutrino flavour oscillations. Analogous to quark mixing, this can be parametrised with the unitary Maki-Nakagawa-Saki (MNS) matrix,

$$V_{\mathrm{MNS}} = \begin{pmatrix} c_{12}c_{13} & s_{12}c_{13} & s_{13}\mathrm{e}^{-\mathrm{i}\delta} \\ -s_{12}c_{23} - c_{12}s_{23}s_{13}\mathrm{e}^{\mathrm{i}\delta} & c_{12}c_{23} - s_{12}s_{23}s_{13}\mathrm{e}^{\mathrm{i}\delta} & s_{23}c_{13} \\ s_{12}s_{23} - c_{12}c_{23}s_{13}\mathrm{e}^{\mathrm{i}\delta} & -c_{12}s_{23} - s_{12}c_{23}s_{13}\mathrm{e}^{\mathrm{i}\delta} & c_{23}c_{13} \end{pmatrix} , \qquad (2.1)$$

with $\delta = \delta^{\mathrm{MNS}}$, $c_{ij} = \cos\theta_{ij}^{\mathrm{MNS}}$ and $s_{ij} = \sin\theta_{ij}^{\mathrm{MNS}}$. Depending on the parameters, electron neutrinos will then oscillate into muon neutrinos during their flight from the sun to the earth, for example. Indeed, it was found around the same time experimentally [19] that the measured solar (electron) neutrino fluxes fell short of the predictions by the standard solar model.

Nowadays, there are several experiments studying not only solar neutrinos [20], but also atmospheric ones [21] and even reactor neutrinos [22], and provide valuable information on the most straight-forward branch of flavour physics beyond the SM. Due to the fact that even the most recent global fits, e.g. [16], do not make definite statements on all quantities, it is possible to make easily falsifiable predictions for their values within models of flavour. Of particular importance in this respect are the only rather recently measured reactor angle $\theta_{13}^{\mathrm{MNS}}$, the still to be determined sign of the

neutrino mass square difference $\Delta m^2_{31} = m^2_3 - m^2_1$ and the only vaguely determined Dirac CP phase δ^{MNS}.

In the following, we will give a brief overview how to incorporate neutrino masses into the SM.

2.1 Dirac Masses

The way to generate neutrino masses that most resembles the pre-existing structure of the SM is to simply add the missing right-handed neutrino fields ν^c to the spectrum. After EWSB, neutrinos obtain masses from the new Yukawa interactions added to the SM terms of eq. (1.8),

$$\mathcal{L}_{\text{Yukawa}} \supset (Y_\nu)_{ij}\, L_i\, \tilde{H}\, \nu^c_j + \text{h.c.}\,, \tag{2.2}$$

which make it clear that the fields ν^c_i must be full gauge singlets, if this term respects the SM gauge symmetry group G_{SM}. Using the same convention for unitary transformations to the mass eigenbases as before, the MNS matrix is then given by $V_{\text{MNS}} = V_e^\dagger V_\nu$.

However, one aesthetical drawback of this mechanism becomes apparent when one determines the Yukawa couplings necessary to reproduce the neutrino masses consistent with current bounds, namely $m_\nu < 2\,\text{eV}$ from β decay experiments [23]. Assuming no large cancellations in the β decay mass, this implies a neutrino Yukawa coupling of at most about 10^{-12}. Compared to an electron Yukawa coupling of about 10^{-6}, this seems unusually small.

2.2 Majorana Masses

An alternative way to generate neutrino masses works via the non-renormalisable Weinberg operator [24],

$$\mathcal{L} \supset \frac{1}{4}\kappa_{ij}(L_i\tilde{H})(L_j\tilde{H}) + \text{h.c.} \quad \xrightarrow{\text{EWSB}} \quad -\frac{1}{2}(m_\nu)_{ij}\,\nu_i\nu_j + \text{h.c.}\,, \tag{2.3}$$

where κ and $m_\nu = -\kappa v^2/4$ are complex symmetric 3×3 matrices and now also total lepton number is broken explicitly. Due to the structure of the m_ν term, neutrinos are then Majorana particles, i.e. they do not have separate right-handed components or anti-particles, but those are given directly by the conjugate of the left-handed ones. One consequence of this is that two phases in the leptonic mixing cannot be absorbed and the unitary mixing matrix is thus given by the Pontecorvo-Maki-Nakagawa-Saki

(PMNS) matrix $V_{\rm PMNS} = V_e^\dagger V_\nu$, parametrised as

$$V_{\rm PMNS} = \begin{pmatrix} c_{12}c_{13} & s_{12}c_{13} & s_{13}\mathrm{e}^{-\mathrm{i}\delta} \\ -s_{12}c_{23} - c_{12}s_{23}s_{13}\mathrm{e}^{\mathrm{i}\delta} & c_{12}c_{23} - s_{12}s_{23}s_{13}\mathrm{e}^{\mathrm{i}\delta} & s_{23}c_{13} \\ s_{12}s_{23} - c_{12}c_{23}s_{13}\mathrm{e}^{\mathrm{i}\delta} & -c_{12}s_{23} - s_{12}c_{23}s_{13}\mathrm{e}^{\mathrm{i}\delta} & c_{23}c_{13} \end{pmatrix} P_\phi \ , \tag{2.4}$$

with $\delta = \delta^{\rm PMNS}$ and

$$P_\phi = \begin{pmatrix} \mathrm{e}^{-\frac{\mathrm{i}}{2}\varphi_1^{\rm PMNS}} & & \\ & \mathrm{e}^{-\frac{\mathrm{i}}{2}\varphi_2^{\rm PMNS}} & \\ & & 1 \end{pmatrix} \ , \tag{2.5}$$

as well as the previous definition of s_{ij} and c_{ij}. Due to their origin, the phases φ_1 and φ_2 are called Majorana phases. Note, however, that they are not observable in neutrino oscillation experiments. The unitary matrix V_ν is determined from the condition that $V_\nu^T \kappa V_\nu$ is diagonal and positive. Assuming $\kappa \sim M^{-1}$, this structure can explain the smallness of neutrino masses with a hierarchy between the electroweak scale and the supposedly high scale M.

However, since the Weinberg operator is not renormalisable, one has to worry about physics beyond the scale M. Fortunately, there is an elegant and simple solution [25] called the seesaw mechanism (strictly speaking type I): if we introduce right-handed neutrino fields as total gauge singlet fields as before and drop conservation of total lepton number, they can have Majorana mass terms themselves,

$$\mathcal{L} \supset -\frac{1}{2}(M_{\nu^c})_{ij}\nu_i^c\nu_j^c + \text{h.c.} \ , \tag{2.6}$$

even before EWSB. Thus these masses are not directly constrained in their magnitude and we can assume that they are so large that the new fields can be integrated out for calculations around the electroweak scale. This generates a contribution to the Weinberg operator of the form

$$\kappa = 2\, Y_\nu\, M_{\nu^c}^{-1}\, Y_\nu^T \ , \tag{2.7}$$

where Y_ν is the neutrino Yukawa couping matrix as in eq. (2.2). Alternatively, the type II seesaw mechanism uses a scalar $SU(2)_L$ triplet field to generate the Weinberg operator [26], while type III uses a $SU(2)_L$ triplet fermion field [27]. A general feature is that this directly connects the mass scale M associated with the Weinberg operator to the mass of the new heavy fields. So, for example, a Yukawa coupling of $\mathcal{O}(1)$ together with a light neutrino mass of $m_\nu \sim 1$ eV leads to a right-handed neutrino mass of about 10^{13} GeV, which – as we will see later – is not too far from other supposed high scales in so called grand unified theories, see chap. 4.

CHAPTER 3

Supersymmetry

3.1 The Hierarchy Problem

As mentioned in chap. 1, in the SM the Higgs boson mass parameter has to be tuned in order to obtain a hierarchy between the electroweak scale $\mathcal{O}(100\text{ GeV})$ and much higher new-physics scales. To be explicit, with a Yukawa interaction term of the form $\mathcal{L} \supset -\lambda_f H \bar{f} f$ for the scalar boson to a Dirac fermion f, the following correction arises

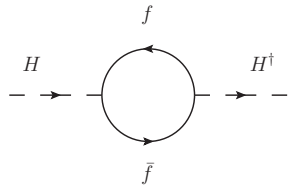

$$= -\frac{|\lambda_f|^2}{8\pi^2}\,\Lambda_{\text{UV}}^2 + \mathcal{O}\left(m_f^2 \log\left(\frac{\Lambda_{\text{UV}}}{m_f}\right)\right)\,, \tag{3.1}$$

where a simple regularisation[1] with a momentum cut-off Λ_{UV} was performed. If this cut-off is of the order of the Planck scale $M_{\text{Pl}} \sim 10^{19}$ GeV, this makes tuning of the order of 1 part in 10^{34} necessary to cancel the quantum correction and arrive back at an electroweak scale of $\mathcal{O}(100\text{ GeV})$. One possible solution to make this tuning unnecessary is motivated by the observation that introducing a complex scalar S with the interaction $\mathcal{L} \supset +\lambda_S |H|^2 |S|^2$ leads to an additional correction of the form

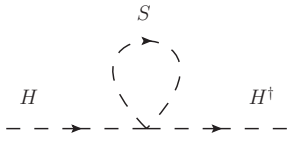

$$= +\frac{\lambda_S}{16\pi^2}\,\Lambda_{\text{UV}}^2 + \mathcal{O}\left(m_S^2 \log\left(\frac{\Lambda_{\text{UV}}}{m_S}\right)\right)\,, \tag{3.2}$$

[1] In other regularisation schemes, such as $\overline{\text{MS}}$, the cut-off dependence is replaced with a dependence on the mass of a heavy particle in the loop, e.g. when it is integrated out. The problematic instability of the hierarchy remains.

As we can see, if we introduce two scalars per Dirac fermion – or one per two-component Weyl spinor – together with the relation $\lambda_S = |\lambda_f|^2$, both quadratic cut-off dependencies cancel each other, leaving only a manageable logarithmic dependence. Thus the hierarchy between scales is stable.

Fortunately, this relation between couplings does not have to be tuned or assumed ad-hoc, but can result from the so-called supersymmetry (SUSY) that (roughly speaking) turns bosons into fermions and vice versa,

$$Q\,|\text{fermion}\rangle = |\text{boson}\rangle\ , \quad Q\,|\text{boson}\rangle = |\text{fermion}\rangle\ . \tag{3.3}$$

In the following, we will present a very quick overview over the ramifications of supersymmetry and how to quickly write down a manifestly supersymmetric theory. For more details, see e.g. [28]. To be explicit, this thesis uses $N = 1$ global supersymmetry, meaning there is only one such operator Q and SUSY transformations are taken to be independent of space-time.

3.2 Supersymmetric Theories

As sketched in eq. (3.3), supersymmetry connects fermions and bosons. More explicitly, every Weyl fermion ψ, every complex scalar ϕ and every vector boson V_μ is partnered with a field of complementary statistics each. We will call partners of fermions 'sfermions', e.g. 'stop' or 'squark'. Partners of bosons are suffixed with an '-ino', e.g. 'Higgsino' or 'gaugino'. In both cases, the new fields are labelled with a tilde on top, while the full supermultiplet containing both will be denoted with a hat on top. In cases, where the distinction between original field and supermultiplet is not necessary or obvious, the hat will be dropped.

Finally, this means that fields in the original theory become components in so-called supermultiplets that contain all fields that are connected by SUSY

$$\psi \to \hat{\psi} = (\tilde{\psi}, \psi, F)\ , \tag{3.4a}$$

$$\phi \to \hat{\phi} = (\phi, \tilde{\phi}, F)\ , \tag{3.4b}$$

$$V_\mu \to \hat{V} = (\lambda, V_\mu, D, \dots)\ , \tag{3.4c}$$

where λ, $\tilde{\phi}$ and ψ are two-component Weyl spinors, ϕ, $\tilde{\psi}$ and F are complex scalars and D is a real scalar. The introduction of the auxiliary fields F and D is necessary to balance the number of fermionic and bosonic components and make supersymmetry also survive against quantum corrections. The dots stand for additional degrees of freedom that are related to the supersymmetric generalisation of gauge symmetries. They can all be set to zero in the Wess-Zumino gauge [29], which we will assume to be the case in the rest of this thesis. Both eqs. (3.4a) and (3.4b) give a 'chiral' supermultiplet, while eq. (3.4c) gives a 'real' supermultiplet.

Note that this embedding of component fields into a supermultiplet can also be done more rigorously using superspace and superfields, see e.g. [28]. However, for the sake of simplicity, we will only review the resulting rules for the building of a supersymmetric theory. We remind the reader again that all considered fermion fields are assumed to be left-chiral two-component Weyl spinors. Additionally, we will use the term 'superfield' synonymously with 'supermultiplet'.

Using chiral and real supermultiplets, a supersymmetric theory is most easily built using the three pre-potentials:

Superpotential $W = W(\phi)$**:** A holomorphic function of all chiral supermultiplets.

Kähler potential $K = K(\phi, \phi^*)$**:** A real function of all chiral supermultiplets.

Gauge kinetic function $f_{ab} = f_{ab}(\phi)$**:** Another holomorphic function of the chiral supermultiplets.

All three can be formulated as functions of superfields or alternatively of the scalar components of each supermultiplet. Both cases follow the same rules for commutation of fields. The superpotential and Kähler potential must be singlets under all imposed symmetries, while the gauge kinetic function must transform as the symmetric product of two adjoints of the imposed gauge symmetry, symbolised by the two indices a and b. The superpotential has mass dimension 3, the Kähler potential has mass dimension 2 and the gauge kinetic function is dimensionless.

Based on these pre-potentials, the part of the Lagrangian density resulting from K is given by

$$\mathcal{L}_K = \frac{\partial^2 K}{\partial\phi_i^*\partial\phi_j}\left[(\partial_\mu\phi_i)^*(\partial^\mu\phi_j) + \mathrm{i}\psi_i^*\bar{\sigma}^\mu\partial_\mu\psi_j + F_i^*F_j\right] \tag{3.5a}$$

$$- \frac{\partial^3 K}{\partial\phi_i\partial\phi_j\partial\phi_l^*}\left[\psi_i\psi_j F_l^* - \psi_l^*\bar{\sigma}^\mu\psi_j\partial_\mu\phi_i\right] \tag{3.5b}$$

$$+ \frac{1}{4}\frac{\partial^4 K}{\partial\phi_i\partial\phi_j\partial\phi_l^*\partial\phi_m^*}(\psi_i\psi_j)(\psi_l^*\psi_m^*) \tag{3.5c}$$

$$+ \text{h.c.}\,, \tag{3.5d}$$

where ϕ_i, ψ_i, F_i are the scalar, fermionic and auxiliary component of the i'th supermultiplet respectively and K is treated as a function of only the scalar component fields. As can be seen, fully holomorphic plus anti-holomorphic parts of $K \supset f(\phi) + \text{h.c.}$ do not enter the Lagrangian density. In superfield formalism, it can easily be shown that they only result into total derivative terms that do not change the action.

Similar to K, the superpotential W generates terms in the Lagrangian density of the form

$$\mathcal{L}_W = -\frac{1}{2}\frac{\partial^2 W}{\partial\phi_i\partial\phi_j}\psi_i\psi_j + \frac{\partial W}{\partial\phi_i}F_i + \text{h.c.}\,, \tag{3.6}$$

while the gauge kinetic function generates the terms

$$\begin{aligned}\mathcal{L}_f = &-\frac{\mathrm{Re}f_{ab}}{16\pi}\left[F^a_{\mu\nu}F^{b}_{\mu\nu} - i4\lambda^{a\dagger}\bar{\sigma}^{\mu}D_{\mu}\lambda^b + 2D^aD^b\right] - \frac{\mathrm{Im}f_{ab}}{16\pi}\,F^a_{\mu\nu}\tilde{F}^{b}_{\mu\nu} \\ &-\frac{1}{16\pi}\frac{\partial f_{ab}}{\partial\phi_i}\,F_i\lambda^a\lambda^b + \mathrm{h.c.} + \dots\ ,\end{aligned} \tag{3.7}$$

where $F^a_{\mu\nu}$ is the field strength tensor of the a'th gauge vector boson field, $\tilde{F}^a_{\mu\nu}$ is its dual and λ^a is the corresponding gaugino. In both cases, the pre-potentials are again interpreted as function of the scalar supermultiplet component fields. Neglecting non-renormalisable operators for the moment, we can summarise this to the following: the Kähler potential is responsible for kinetic terms of chiral supermultiplets (and gauge interactions, though not shown here), the superpotential generates fermion masses and Yukawa couplings, and the gauge kinetic function yields the kinetic terms for gauge fields and influences the gauge couplings[2].

In the following, it is convenient to define the Kähler metric,

$$K_{i^*j} = \frac{\partial^2 K}{\partial\phi_i^*\partial\phi_j}\ , \tag{3.8}$$

and its inverse K^{ji^*}, i.e. $K^{ij^*}K_{j^*l} = \delta_{il}$.

As the Lagrangian density does not depend on derivatives of the auxiliary fields F_i, we can integrate them out by substituting them using their equations of motion,

$$F_i = K^{ij^*}\left(-\frac{\partial W^*}{\partial\phi_j^*} + \frac{\partial^3 K}{\partial\phi_l\partial\phi_m\partial\phi_j^*}\,\psi_l\psi_m + \frac{1}{16\pi}\frac{\partial f^*_{ab}}{\partial\phi_j^*}\lambda^{a\dagger}\,\lambda^{b\dagger}\right)\ . \tag{3.9}$$

With this substitution, we obtain the F-term scalar potential,

$$V_F = \frac{\partial W}{\partial\phi_i}\,K^{ij^*}\,\frac{\partial W^*}{\partial\phi_j^*}\ , \tag{3.10}$$

and field-dependent fermion 'masses',

$$M_{ij} = \frac{\partial^2 W}{\partial\phi_i\partial\phi_j} + 2\,\frac{\partial^3 K}{\partial\phi_l\partial\phi_m\partial\phi_j^\dagger}\,K^{j^*m}\,\frac{\partial W}{\partial\phi_m}\ . \tag{3.11}$$

Since the kinetic terms contained in eq. (3.5a) are not canonical, we have to normalise them with a transformation matrix P,

$$\phi_i \to P_{ij}\,\phi_j\ , \tag{3.12a}$$

$$\psi_i \to P_{ij}\,\psi_j\ , \tag{3.12b}$$

[2]At the renormalisable level, one sets $f_{ab} = \left(\frac{4\pi}{g_a^2} + \mathrm{i}\,\frac{\theta_a}{2\pi}\right)\delta_{ab}$ in the gauge boson field normalisation where g_a is set to one in the covariant derivative.

with

$$P^{\dagger}_{i^*j^*} K_{j^*l} P_{lk} = \delta_{i^*k} \ . \tag{3.13}$$

This procedure is called canonical normalisation and is general to every situation where kinetic terms are not in their canonical form.

If we only consider renormalisable interactions the situation simplifies in the following way:

- As the Kähler potential has mass dimension two, the Kähler metric is just a field-independent numerical matrix that can be transformed away using eq. (3.12). This leads to the trivial Kähler potential,

$$K = \sum_i \phi_i^* \phi_i \ , \tag{3.14}$$

  and automatically canonical kinetic terms. Often, this Kähler potential is implicitly assumed and not stated.

- The superpotential takes the form

$$W = L_i \phi_i + \frac{1}{2} m_{ij} \phi_i \phi_j + \frac{1}{6} y_{ijk} \phi_i \phi_j \phi_k \ , \tag{3.15}$$

  where $L_i \neq 0$ is only allowed for total singlet fields ϕ_i.

In this case eq. (3.10) and (3.11) simplify to

$$V_F = \sum_i \left| \frac{\partial W}{\partial \phi_i} \right|^2 \ , \tag{3.16}$$

and

$$M_{ij} = m_{ij} + y_{ijk} \phi_k \ . \tag{3.17}$$

Thus, the parameters of the superpotential directly correspond to fermion masses and Yukawa couplings.

For completeness, note that also the gauge interactions are extended in a supersymmetric theory, with additional Yukawa-type couplings to the gauginos λ^a,

$$\mathcal{L} \supset -\sqrt{2} g_a \Big(\phi_i^* (T^a)_{ij} \psi_j \Big) \lambda^a + \text{h.c.} \ , \tag{3.18}$$

and the additional D-term scalar potential,

$$V_D = \frac{1}{2} \sum_a \Big(g_a \sum_i \phi_i^{\dagger} (T^a)_{ij} \phi_j \Big)^2 \ , \tag{3.19}$$

where T^a is the generator corresponding to the a'th gauge boson and g_a is its gauge coupling. However, we will make only little use of these interactions in this thesis. For more details, see e.g. [28].

3.2.1 The Minimal Supersymmetric Standard Model

It is now straight forward to write down the minimal supersymmetric version of the SM, the MSSM [30]. The only direct complication is that one cannot use the charge conjugate $\tilde{H}$ of the SM Higgs doublet to generate the up-type quark masses, since Yukawa couplings are generated by the holomorphic superpotential. Instead, we replace the original electroweak doublet field H with a pair of charge conjugate doublet fields H_u and H_d, leading to the field content stated in tab. 3.1. Note that this also means that the spectrum of scalar particles coming from H_d, H_u contains two neutral CP-even ones (the lighter one is usually SM-like), one neutral CP-odd pseudoscalar boson A^0 and a pair of charged scalar bosons $H^\pm$.

Let us repeat that, in the following, superpartners of SM fermions are denoted by a tilde above their symbol and an 's-' prefixed to their name. The fermionic partners of H_d and H_u are suffixed with '-ino' and also receive a tilde on their symbol. Supermultiplets generally use the same symbol as the corresponding SM field, except when stated explicitly. The superpotential is to be understood as function of the supermultiplets.

Both H_u and H_d acquire non-zero VEVs and we define

$$\tan\beta = \frac{v_u}{v_d} \quad \text{with} \quad v^2 \simeq v_u^2 + v_d^2 = (246\ \text{GeV})^2\ , \tag{3.20}$$

and $\langle H_f^0 \rangle = v_f/\sqrt{2}$. Thus, the superpotential of the MSSM is given by

$$W_{\text{MSSM}} = (Y_d)_{ij} Q_i H_d d_j^c + (Y_e)_{ij} L_i H_d e_j^c - (Y_u)_{ij} Q_i H_u u_j^c + \mu H_u H_d\ , \tag{3.21}$$

with the tree-level relation to the SM Yukawa matrices of eq. (1.8) given by

$$Y_u^{\text{SM}} = Y_u^{\text{MSSM}} \sin\beta\ , \quad Y_d^{\text{SM}} = Y_d^{\text{MSSM}} \cos\beta\ , \quad Y_e^{\text{SM}} = Y_e^{\text{MSSM}} \cos\beta\ . \tag{3.22}$$

Requiring both the bottom and the top Yukawa coupling to be perturbative sufficiently above the electroweak scale, one roughly finds the constraint [28]

$$1 \lesssim \tan\beta \lesssim 60\ . \tag{3.23}$$

However, as will be important later, the matching conditions particularly for Y_d and Y_e can receive one-loop corrections that are enhanced by a factor $\tan\beta$ [31, 32, 33, 34] – interpretable as a coupling to the other larger Higgs VEV – and can thus be of significant size.

One further point is that W_{MSSM} is not the most general superpotential consistent with the SM symmetries. The following terms are also allowed

$$\Delta W = \mu_i H_u L_i + \frac{1}{2}\lambda_{ijk} L_i L_j e_k^c + \lambda'_{ijk} Q_i d_i^c L_k + \frac{1}{2}\lambda''_{ijk} u_i^c u_j^c d_k^c\ . \tag{3.24}$$

However, as these terms mediate (so far unobserved) proton decay very efficiently [35], leading to bounds such as $|\lambda_{i22}\lambda''_{112}| \lesssim \mathcal{O}(10^{-21})$, these terms are commonly assumed

	$SU(3)_C$	$SU(2)_L$	$U(1)_Y$	$\mathcal{P}_M$
Q	$\mathbf{3}$	$\mathbf{2}$	$\frac{1}{6}$	-1
u^c	$\bar{\mathbf{3}}$	$\mathbf{1}$	$-\frac{2}{3}$	-1
d^c	$\bar{\mathbf{3}}$	$\mathbf{1}$	$\frac{1}{3}$	-1
L	$\mathbf{1}$	$\mathbf{2}$	$-\frac{1}{2}$	-1
e^c	$\mathbf{1}$	$\mathbf{1}$	1	-1
H_d	$\mathbf{1}$	$\mathbf{2}$	$-\frac{1}{2}$	1
H_u	$\mathbf{1}$	$\mathbf{2}$	$\frac{1}{2}$	1

Table 3.1: Irreducible representations of the chiral supermultiplets of the MSSM. Generation indices are implicit.

to be absent. This is achieved by enforcing another global $\mathbb{Z}_2$ symmetry called R-parity [36] under which the SM fields are even while all the superpartners are odd or equivalently

$$\mathcal{P}_R = (-1)^{3(B-L)+2s} \,, \tag{3.25}$$

with the baryon number B, the lepton number L and the particle spin s. As long as angular moment is conserved, $\mathcal{P}_R$ conservation is equivalent to the conservation of matter parity [37],

$$\mathcal{P}_M = (-1)^{3(B-L)} \,, \tag{3.26}$$

which is also included in tab. 3.1.

Seesaw type I in the MSSM When incorporating the seesaw type I mechanism into the MSSM, one proceeds analogously to the SM. Additional particles called right-handed neutrinos ν^c, total singlets under gauge symmetries and odd under $\mathcal{P}_M$, are added together with their superpotential terms,

$$W_\nu = -(Y_\nu)_{ij}\, L_i H_u \nu_j^c + \frac{1}{2}(M_{\nu^c})_{ij}\, \nu_i^c \nu_j^c \,. \tag{3.27}$$

Below the scale of the right-handed neutrino masses, they are integrated out to obtain the supersymmetric equivalent of the Weinberg operator of eq. (2.3)

$$W \supset \frac{1}{4}\, \kappa_{ij}\, (L_i H_u)(L_j H_u) \,, \tag{3.28}$$

exactly mirroring the form of the usual Weinberg operator.

3.3 Breaking of Supersymmetry and $SU(2)_L \times U(1)_Y$

Supersymmetry respected by the vacuum would imply that the scalar mass matrices are given by $M^\dagger M$ with M from eq. (3.11) or (3.17), leading to the same mass eigenvalues as for the fermions. However, we have not yet observed any scalar elementary particles beyond the Higgs boson [15], not even to speak of a scalar electron at 511 keV. Thus supersymmetry has to be broken in the vacuum ground state.

In this context, the term 'soft SUSY breaking' appears. This means that SUSY is broken only by mass differences between scalars and fermions, while the relation between interaction couplings, necessary to ensure the cancellation in sec. 3.1, is still left unperturbed [38].

Attempts to directly break supersymmetry leads to the condition that at least one of the auxiliary fields F or D must acquire a non-zero VEV. Achieving this with the spectrum of the MSSM and W_{MSSM} given by eq. (3.21) does unfortunately not work satisfactorily, for details see e.g. [28]. Thus, one usually assumes that SUSY is broken in an unknown 'hidden sector' and is simply transmitted to the visible sector by some mechanism of choice. We then parametrise the general soft SUSY breaking of a general supersymmetric gauge theory as

$$-\mathcal{L}_{soft} = \frac{1}{2} M_a \lambda^a \lambda^a + \frac{1}{6} a_{ijk} \phi_i \phi_j \phi_k + \frac{1}{2} b_{ij} \phi_i \phi_j + t_i \phi_i + (\tilde{m}^2)_{ij} \phi_i^\dagger \phi_j + \text{h.c.} \,, \tag{3.29}$$

where λ^a are gaugino fields, ϕ_i are scalar components of superfields and the linear couplings t_i are only non-zero for singlets ϕ_i under all imposed symmetries. In the MSSM, the soft breaking terms thus take the form

$$\begin{aligned}
-\mathcal{L}_{soft} = {} & \frac{1}{2}(M_1 \tilde{B}\tilde{B} + M_2 \tilde{W}\tilde{W} + M_3 \tilde{g}\tilde{g} + \text{h.c.}) && \text{(3.30a)} \\
& + (m^2_{\tilde{Q}})_{ij} \tilde{Q}_i \tilde{Q}^*_j + (m^2_{\tilde{L}})_{ij} \tilde{L}_i \tilde{L}^*_j && \text{(3.30b)} \\
& + (m^2_{\tilde{u}^c})_{ij} \tilde{u}^{c*}_i \tilde{u}^c_j + (m^2_{\tilde{d}^c})_{ij} \tilde{d}^{c*}_i \tilde{d}^c_j + (m^2_{\tilde{e}^c})_{ij} \tilde{e}^{c*}_i \tilde{e}^c_j && \text{(3.30c)} \\
& + (A_d)_{ij} \tilde{Q}_i H_d \tilde{d}^c_j + (A_e)_{ij} \tilde{L}_i H_d \tilde{e}^c_j - (A_u)_{ij} \tilde{Q}_i H_u \tilde{u}^c_j + \text{h.c.} && \text{(3.30d)} \\
& + m^2_{H_u} |H_u|^2 + m^2_{H_d} |H_d|^2 + (B\mu H_u H_d + \text{h.c.}) \,, && \text{(3.30e)}
\end{aligned}$$

The average scale of superpartner masses resulting from this is commonly denoted as the SUSY scale M_{SUSY}. All of these terms potentially lead to additional flavour (FV) and CP (CPV) violation effects. To parametrise this properly, the relevant matrices are first rotated to the so-called Super CKM (SCKM) basis, see e.g. [39], where the Yukawa matrices for the fermions are diagonal and positive. Additional FV or CPV effects – like contributions to $\text{BR}(b \to s\gamma)$, $\text{BR}(B_s \to \mu^+\mu^-)$ or $\text{BR}(B_u \to \tau\nu_\tau)$ – are then generated by surviving phases and non-diagonal matrix elements. In total, the soft breaking sector gives rise to 105 new and independent parameters [40] this way.

Another important aspect of the MSSM is the fact that without the terms in eq. (3.30), the Higgs mechanism for electroweak symmetry breaking does not work as the Higgs self-interaction λ comes exclusively from gauge couplings and the SM mass square parameter μ^2 cannot be negative. Fortunately, including soft breaking terms even makes EWSB more natural in that it happens 'radiatively'. This means that the renormalisation group running of the soft term $m_{H_u}^2$ makes it turn negative at the electroweak scale if done from a sufficiently high scale. Thus $m_{H_u}^2$ plays a role similar to the parameter μ^2 in the SM and has usually a mass scale similar to the soft breaking terms. In summary, this leads to electroweak symmetry breaking of the (tree-level) form [28, 39]

$$\sin 2\beta = \frac{2B\mu}{m_{H_u}^2 + m_{H_d}^2 + 2|\mu|^2} \,, \tag{3.31a}$$

$$\frac{M_Z^2}{2} = -|\mu|^2 + \frac{m_{H_d}^2 - m_{H_u}^2 \tan^2\beta}{\tan^2\beta - 1} \,, \tag{3.31b}$$

meaning that one can trade the parameters $B\mu$, $|\mu|$ for $\tan\beta$, M_Z. Note that eq. (3.31b) only determines the modulus of the superpotential parameter μ, leaving its phase as a free parameter. However, usually μ is assumed to be real and this reduces to only an ambiguity in its sign.

3.3.1 Supersymmetry Breaking Schemes

In the following, we will give a brief overview over several SUSY breaking mediation schemes and structures that are used to bring the staggering amount of 105 new parameters under control.

Gravity-mediated SUSY breaking In this scenario, the breaking of SUSY is mediated by Planck-scale suppressed operators and supersymmetric gravity effects [41] to the visible sector. Assuming gauge coupling unification, as detailed in the next chapter, and SUSY breaking by the appearance of a non-zero F-term in Planck-scale suppressed operators with the visible sector, this leads to the minimal supergravity (mSUGRA) scenario or to the constrained MSSM (cMSSM) [42]. Then the soft breaking terms at a renormalisation scale $\mu \approx M_{\text{Pl}}$ are given by

$$M_1 = M_2 = M_3 = M_{1/2} \,, \tag{3.32a}$$

$$A_u = A_0 Y_u \,, \quad A_d = A_0 Y_d \,, \quad A_e = A_0 Y_e \,, \tag{3.32b}$$

$$m_{\tilde{Q}}^2 = m_{\tilde{L}}^2 = m_{\tilde{u}^c}^2 = m_{\tilde{d}^c}^2 = m_{\tilde{e}^c}^2 = m_0^2 \, \mathbb{1} \,, \tag{3.32c}$$

$$B\mu = B_0 \, \mu \,, \tag{3.32d}$$

where μ is the mass parameter in W_{MSSM}.

In the context of supergravity, $m_0 = m_{3/2}$ is also the gravitino mass and we have the additional relation

$$B_0 = A_0 - m_0 \ . \tag{3.33}$$

Thus, in mSUGRA, $\tan\beta$ is actually fixed in terms of the soft breaking parameters due to eq. (3.31), while it is considered a free parameter in the cMSSM. Note that it is a common approximation to implement these boundary conditions at the renormalisation scale $\mu = M_{\mathrm{GUT}}$ and not at the Planck scale M_{Pl}.

Gauge-mediated SUSY breaking Here, the breaking of SUSY is transmitted to the visible sector via the ordinary gauge interactions coupling to a new set of particles [43]. These generate the soft breaking terms of the MSSM via one- and two-loop level Feynman diagrams. We only state this mediation mechanism for completeness and will not make use of it in this thesis.

Anomaly-mediated SUSY breaking In this scheme, SUSY is broken on a separate brane (in a theory with extra dimensions) and then mediated to the visible sector via the superconformal anomaly [44]. The soft breaking terms are then parametrised at the renormalisation scale $\mu \approx M_{\mathrm{Pl}}$ (or $\mu = M_{\mathrm{GUT}}$)

$$M_a = \frac{\beta_{g_a}}{g_a}\, m_{3/2} \ , \tag{3.34a}$$

$$A_f = -\beta_{y_f}\, m_{3/2} \ , \tag{3.34b}$$

$$m_{\tilde{f}}^2 = -\frac{1}{4}\left(\beta_{g_a}\frac{\partial\gamma}{\partial g_a} + \beta_y \frac{\partial\gamma}{\partial y}\right) m_{3/2}^2 + m_0^2 \ , \tag{3.34c}$$

where y collectively denotes all Yukawa couplings, β_x is the renormalisation group equation for the quantity x and γ is the anomalous dimension matrix for the chiral superfields as a function of the gauge couplings and superpotential parameters. The introduction of m_0 analogous to mSUGRA is necessary, because slepton masses are tachyonic otherwise. In the MSSM, this leads to gaugino mass ratios of the form $M_1 : M_2 : M_3 = 33/5 : 1 : -3$ at the scale of gauge couplings unification.

Phenomenological MSSM Another complementary approach for soft SUSY breaking is the so-called phenomenological MSSM (pMSSM) [45]. It is defined directly at the low energy scale and parametrises the superpartner spectrum almost directly via their masses. This means that there is no renormalisation group (RG) evolution involved. In addition to $\tan\beta$, it has the following parameters:

- $m_{H_u}^2$, $m_{H_d}^2$: the Higgs soft mass parameters.
- M_1, M_2, M_3: the bino, wino and gluino mass parameters.

- $m_{\tilde{Q}_1}$, $m_{\tilde{u}_1^c}$, $m_{\tilde{d}_1^c}$, $m_{\tilde{L}_1}$, $m_{\tilde{e}_1^c}$: the first and second generation sfermion soft mass parameters.
- $m_{\tilde{Q}_3}$, $m_{\tilde{u}_3^c}$, $m_{\tilde{d}_3^c}$, $m_{\tilde{L}_3}$, $m_{\tilde{e}_3^c}$: the third generation sfermion soft mass parameters.
- A_u, A_d, A_e: the first and second generation trilinear couplings.
- A_t, A_b, A_τ: the third generation trilinear couplings.

Here the trilinear couplings follow the alternative convention where the trilinear matrices are given by $(A_u)_{ij} = \text{diag}(A_u y_u, A_u y_c, A_t y_t)$ in the basis where Y_u is diagonal, i.e. for the pMSSM trilinear parameters the Yukawa coupling is assumed to be factored out. Often the parameters $m_{H_u}^2$, $m_{H_d}^2$ are also traded for the parameters μ and the mass of the pseudoscalar Higgs boson M_{A^0}, which have a more clear interpretation.

CHAPTER 4

Grand Unification

4.1 Motivation

Similar to the idea of electroweak unification, one can also try to find structure in all of the three gauge interactions of the SM. Surely, the most appealing possibility in this regard would be that at a high scale the three gauge groups unify into a single one or at least into fewer group factors. In the case of one simple group, one speaks of a grand unified theory (GUT). A theory with more than one group factor is called a unified theory. A GUT would lead to equality of the three gauge couplings at a high scale denoted as M_{GUT}. Below this scale, similar to EWSB, the larger gauge symmetry group is then broken down to the SM gauge group giving rise to the low scale observed gauge couplings through quantum effects, i.e. renormalisation group running.

However, before one can analyse the equality of gauge couplings, the right normalisation for the $U(1)$ charges must be found. Looking at the generators for the SM symmetry groups T_a for $SU(3)$, τ_i for $SU(2)_L$ and Y for $U(1)_Y$, one finds

$$\mathrm{tr}(T_a T_a) = 2 \,, \tag{4.1a}$$

$$\mathrm{tr}(\tau_i \tau_i) = 2 \,, \tag{4.1b}$$

$$\mathrm{tr}(Y^2) = \frac{10}{3} \,, \tag{4.1c}$$

where there is no summation over a or i and the trace runs over one full generation of SM fermions. Due to the relation $\mathrm{tr}_R(T_A T_B) = I(R)\delta_{AB}$ for the irreducible representation R of a simple Lie group with the Dynkin index $I(R)$, the three right-hand sides must all be equal if the group factors are to be unified to one simple Lie group and each generation can be evenly divided into a number of irreducible GUT representations without remainder. This leads to the so-called GUT normalisation of hypercharge,

$$\tilde{Y} = \sqrt{\tfrac{3}{5}}\, Y \,, \quad g_1 = \sqrt{\tfrac{5}{3}}\, g' \,. \tag{4.2}$$

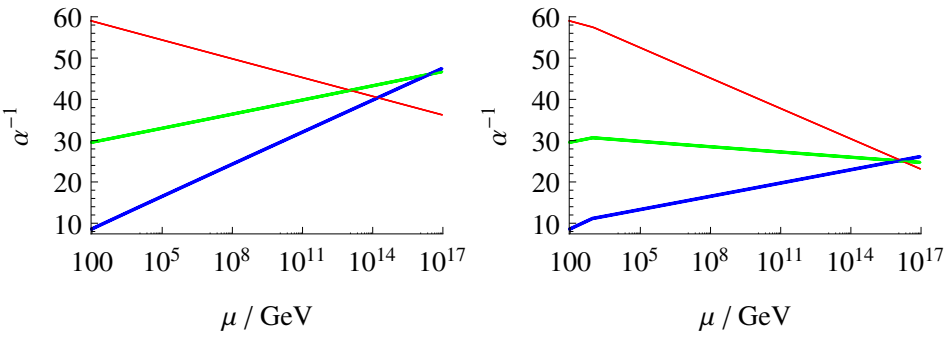

Figure 4.1: Running of all three gauge couplings of the SM (left) and MSSM (right) at the two loop level. Line thickness corresponds to the 1σ range. The structure constants $\alpha_1 = g_1^2/4\pi$, α_2 and α_3 are red, green and blue respectively. The threshold between MSSM and SM was set to 1 TeV for the right plot.

Analogously, we define $g_2 = g$ and $g_3 = g_s$. Grand unification would thus imply

$$g_1 = g_2 = g_3 \ , \tag{4.3}$$

at a high renormalisation scale M_{GUT}.

Within this normalisation and identification, we can now analyse whether eq. (4.3) is satisfied at some scale when taking into account renormalisation group running. As shown in fig. 4.1, in the SM the three gauge couplings come close to each other at a scale of about $\mu = 10^{14}$ GeV, but do not meet within their uncertainty. On the other hand, in the MSSM with a SUSY scale of about 1 TeV, the gauge couplings meet to a good accuracy at about $\mu \approx 10^{16}$ GeV, however not exactly within their uncertainty requiring some small finite threshold corrections. We will come back to the subject of gauge coupling unification later in chap. 8, where a more in-depth analysis is performed.

Thus, GUTs are usually considered most natural and motivated as a high-scale extension of the MSSM. In the following, we will give a quick overview over how such extensions work. All considerations are to be taken in the context of the MSSM.

4.2 Embedding of the Standard Model

While the relation in eq. (4.3) is already a very good start, it does not determine how the various SM gauge group representations are embedded into the larger unified gauge group. For analysing representations, we will use the notation $(r_1, r_2)_q$ for r_1 under $SU(3)_C$, r_2 under $SU(2)_L$ and q under $U(1)$ with an additional global normalisation change compared to $U(1)_Y$ to obtain integer charges for all representations. Then, the

chiral fields of the MSSM transform as

$$\begin{aligned} Q &\sim (\mathbf{3},\mathbf{2})_{-1} \,, \quad L \sim (\mathbf{1},\mathbf{2})_{3} \,, \\ u^c &\sim (\bar{\mathbf{3}},\mathbf{1})_{4} \,, \quad d^c \sim (\bar{\mathbf{3}},\mathbf{1})_{-2} \,, \quad e^c \sim (\mathbf{1},\mathbf{1})_{-6} \,, \\ H_d &\sim (\mathbf{1},\mathbf{2})_{3} \,, \quad H_u \sim (\mathbf{1},\mathbf{2})_{-3} \,, \end{aligned} \tag{4.4}$$

which means that the $U(1)$ differs from $U(1)_Y$ by a factor of -6. Likewise, the SM gauge bosons transform as

$$G \sim (\mathbf{8},\mathbf{1})_0 \,, \quad W \sim (\mathbf{1},\mathbf{3})_0 \,, \quad B \sim (\mathbf{1},\mathbf{1})_0 \,. \tag{4.5}$$

4.2.1 Embedding into $SU(5)$

The smallest possible group for grand unification of the SM gauge group is the simple Lie group $SU(5)$ [46]. It embeds the three gauge boson representations into the adjoint representation,

$$\mathbf{24} = (\mathbf{8},\mathbf{1})_0 + (\mathbf{1},\mathbf{3})_0 + (\mathbf{1},\mathbf{1})_0 + (\mathbf{3},\mathbf{2})_{-5} + (\bar{\mathbf{3}},\mathbf{2})_5 \,, \tag{4.6}$$

where the last two representations form an additional pair of vector-like leptoquark vector boson fields that acquire a mass $M_V \sim M_{\mathrm{GUT}}$ from spontaneous symmetry breaking to the SM gauge group. In total, a **24**-plet can be most easily represented by a hermitian traceless 5×5 matrix. The breaking of $SU(5)$ to the SM gauge group can be achieved by a VEV of an additional Higgs field in this **24** representation in the direction of hypercharge.

Each generation of matter superfields of the MSSM is embedded into the two representations $\bar{\mathbf{5}}$ and **10** as in

$$\begin{aligned} \bar{\mathbf{5}} &= (\mathbf{1},\mathbf{2})_3 + (\bar{\mathbf{3}},\mathbf{1})_{-2} = L + d^c \,, \\ \mathbf{10} &= (\mathbf{1},\mathbf{1})_{-6} + (\bar{\mathbf{3}},\mathbf{1})_4 + (\mathbf{3},\mathbf{2})_{-1} = e^c + u^c + Q \,, \end{aligned} \tag{4.7}$$

which can be modelled as a 5-dimensional vector $\mathcal{F}^\alpha$ and an antisymmetric 5×5 tensor $\mathcal{T}_{\alpha\beta}$ respectively.

The doublet fields H_u, H_d can either be embedded into a pair of $\mathbf{5}$, $\bar{\mathbf{5}}$ or alternatively also into **45** or $\overline{\mathbf{45}}$ respectively. For details on the branching of **45** into SM representations, see e.g. [47].

As shown above, beyond eq. (4.3), one major feature of GUTs is the embedding of multiple SM matter field representations into one GUT representation. This naturally leads to GUT-scale relations between previously unrelated Yukawa couplings. At the renormalisable level, the two choices for the $SU(5)$ representation of H_d lead to two distinct and predictive ratios between charged lepton and down-type quark Yukawa couplings,

$$W \supset \lambda\, \mathcal{F}_i \mathcal{T}_j H_{\bar{5}} \quad \to \quad \mathcal{N}\lambda\, (L_i e^c_j + Q_j d^c_i)\, H_d \,, \tag{4.8a}$$

$$W \supset \lambda\, \mathcal{F}_i \mathcal{T}_j H_{\overline{45}} \quad \to \quad \mathcal{N}\lambda\, (-3 L_i e^c_j + Q_j d^c_i)\, H_d \,, \tag{4.8b}$$

where $\mathcal{N}$ is some normalisation factor and i, j are generation indices. As can be seen, the matrix Y_e will be connected to the transposed matrix Y_d^T by a factor that is not a free parameter, in this case 1 or -3, and purely originates from the ratio of two group theoretical Clebsch-Gordan coefficients. Hence, we will call such factors Clebsch-Gordan (CG) factors. The first CG factor of above is often used for the third family where it leads b-τ unification $y_b = y_\tau$. The latter can be used for the muon to strange Yukawa coupling ratio, where it can lead to the so-called Georgi-Jarlskog mass relations [48], $m_\mu \approx 3\, m_s$, $m_e \approx m_d/3$ (at the GUT scale).

Beyond the renormalisable level, one can also introduce powers of GUT breaking VEVs of Higgs superfield in the **24** representation. This leads to index structures (before contracting to an $SU(5)$ singlet) of, e.g.

$$\mathcal{F}^\alpha \mathcal{T}_{\beta\gamma} (H_{24})^\epsilon_\delta (H_{\bar{5}})^\rho \,, \tag{4.9}$$

where now all upper indices have to be contracted with lower ones to obtain an $SU(5)$ invariant term for the superpotential. One way to fix this otherwise undetermined structure of index contractions is to generate such a non-renormalisable operator using heavy vector-like messenger fields, as shown in [49], see also [50]. As the structure of the VEV of H_{24} is fixed by the breaking of $SU(5)$ to the SM gauge group, once an index contraction is fixed, the resulting ratio between Yukawa couplings is also fixed to a value that can again be interpreted as ratio of two Clebsch-Gordan coefficients and is thus also included in our denotation of CG factors. One interesting example is given by [49]

$$W \supset \frac{1}{\Lambda} \left(\mathcal{F}_i H_{24}\right)_{\bar{\mathbf{5}}} \left(\mathcal{T}_j H_{\bar{5}}\right)_{\mathbf{5}} \to \mathcal{N} \frac{\langle H_{24} \rangle}{\Lambda} \left(-\frac{3}{2} L_i e^c_j + Q_j d^c_i \right) H_d \,, \tag{4.10}$$

where the index below the brackets specifies the representation of the index contraction of the fields inside, which coincides with the representation of the messenger field. Using this approach, ratios between $(Y_e)_{ij}$ and $(Y_d)_{ji}$ can be fixed to the values[1]: $-\frac{1}{2}$, 1, $\pm\frac{3}{2}$, -3, $\frac{9}{2}$, 6, 9.

At the renormalisable level and without involving **24**-plets, the up-type quark Yukawa matrix originates from operators of the form

$$W \supset \mathcal{T}_i \mathcal{T}_j H_5 \,, \tag{4.11}$$

which simply leads to the relation $Y_u = Y_u^T$, or alternatively $Y_u = -Y_u^T$ in the case of H_u transforming as a **45** representation.

For a more exhaustive list of possible ratios and more details, see app. D, ref. [49] or also [51].

[1] This list also includes the alternate representation for the GUT breaking Higgs field, **75**, and the electroweak doublet Higgs field, $\overline{\mathbf{45}}$.

4.2.2 Embedding into $SO(10)$ and Pati-Salam

About as old as the idea of $SU(5)$ grand unification is the one of grand unification to $SO(10)$ [52]. Here the three matter field generations are each unified into a single spinorial representation **16** of $SO(10)$,

$$\begin{aligned}\mathbf{16} &= (\mathbf{1},\mathbf{2})_3 + (\bar{\mathbf{3}},\mathbf{1})_{-2} + (\mathbf{1},\mathbf{1})_{-6} + (\bar{\mathbf{3}},\mathbf{1})_4 + (\mathbf{3},\mathbf{2})_{-1} + (\mathbf{1},\mathbf{1})_0 \\ &= L + d^c + e^c + u^c + Q + \nu^c \,,\end{aligned} \tag{4.12}$$

where merely symmetry requirements already force us to introduce three generations of right-handed neutrinos ν^c. Likewise, the two electroweak doublets H_d and H_u are most easily embedded into a **10** of $SO(10)$,

$$\begin{aligned}\mathbf{10} &= (\mathbf{1},\mathbf{2})_3 + (\mathbf{1},\mathbf{2})_{-3} + (\bar{\mathbf{3}},\mathbf{1})_{-2} + (\mathbf{3},\mathbf{1})_2 \\ &= H_d + H_u + \dots \,,\end{aligned} \tag{4.13}$$

where the dots stand for additional colour triplet fields, analogous to the embedding of H_d, H_u into fiveplets in $SU(5)$. Note that we will not state the branching rules for adjoints or other GUT breaking Higgs choices for $SO(10)$ as the breaking to the SM can be quite complicated and goes beyond the scope of this thesis.

At the renormalisable level, the MSSM Yukawa couplings stem from operators of the form

$$\begin{aligned}W \supset\ & \lambda_{ij}(\Phi_{16})_i(\Phi_{16})_j\Phi_{10} \\ \to\quad & \mathcal{N}\,\lambda_{ij}\,(Q_i u_j^c H_u \,+\, Q_i d_j^c H_d \,+\, L_i e_j^c H_d \,+\, (i \leftrightarrow j) + \dots)\,,\end{aligned} \tag{4.14}$$

with generation indices i, j and the dots stand for additional couplings involving right-handed neutrinos. As can be seen, this leads to the relation $Y_u = Y_d = Y_e$ as well as symmetry for all three Yukawa matrices.

Of particular interest is also a subgroup of $SO(10)$ that only leads to partial unification of $SU(3)_C$ and $U(1)_Y$, but incorporates some left-right symmetry missing from the SM: the Pati-Salam (PS) symmetry group $SU(4) \times SU(2)_L \times SU(2)_R$ [53]. The PS representations are embedded into $SO(10)$ as in

$$\mathbf{16} = (\mathbf{4},\mathbf{2},\mathbf{1}) + (\bar{\mathbf{4}},\mathbf{1},\mathbf{2})\,, \quad \mathbf{10} = (\mathbf{1},\mathbf{2},\mathbf{2}) + (\mathbf{6},\mathbf{1},\mathbf{1})\,, \tag{4.15}$$

where (r_1, r_2, r_3) denotes the three representations corresponding to the PS group factors. The PS field representations, in turn, branch into the SM representations following

$$(\mathbf{4},\mathbf{2},\mathbf{1}) = (\mathbf{3},\mathbf{2})_{-1} + (\mathbf{1},\mathbf{2})_3 \qquad = Q + L\,, \tag{4.16a}$$

$$(\bar{\mathbf{4}},\mathbf{1},\mathbf{2}) = (\bar{\mathbf{3}},\mathbf{1})_{-2} + (\bar{\mathbf{3}},\mathbf{1})_4 + (\mathbf{1},\mathbf{1})_{-6} + (\mathbf{1},\mathbf{1})_0 \qquad = d^c + u^c + e^c + \nu^c\,, \tag{4.16b}$$

$$(\mathbf{1},\mathbf{2},\mathbf{2}) = (\mathbf{1},\mathbf{2})_3 + (\mathbf{1},\mathbf{2})_{-3} \qquad = H_d + H_u\,, \tag{4.16c}$$

where we again see the existence of three right-handed neutrino fields ν^c implied by the PS symmetry. Yukawa matrices are then generated by terms of the form

$$\begin{aligned} W \supset\ & \lambda_{ij}\ (\Phi_{421})_i(\Phi_{\bar{4}12})_j\Phi_{122} \\ \to\ & \mathcal{N}\lambda_{ij}\ (Q_i u_j^c H_u + Q_i d_j^c H_d + L_i e_j^c H_d + \dots)\ , \end{aligned} \tag{4.17}$$

with generation indices i, j and the indices of Φ signifying PS group representations. As in the case of $SO(10)$, this yields the relation $Y_u = Y_d = Y_e$. However, the matrices are not required to be symmetric anymore, although such symmetry can come as a consequence of embedding PS into $SO(10)$. Analogously to the case of $SU(5)$, the above relation, valid at the renormalisable level, can be modified using a VEV breaking PS to the SM gauge group and fixing index contractions with the use of messenger fields. In particular for this thesis, the most interesting CG factors between $(Y_e)_{ij}$ and $(Y_d)_{ij}$ are given by: $\frac{3}{4}$, 1, 2, -3, 9. For more details, see [49, 54].

4.3 Soft Supersymmetry Breaking in GUTs

Since, in unified theories, multiple MSSM superfield representations are put together in a smaller set of irreducible representation of the unified gauge group, this naturally also has some consequences for the soft breaking terms, given in their most general form in eq. (3.30). In particular, if we do not assume a very restrictive SUSY breaking scheme such as the cMSSM, the restrictions from certain symmetries can still provide breaking schemes that are not as arbitrary as the parametrisation of the pMSSM. In the following, we will give a very brief review over the structures obtained this way, as will become important later in chap. 6.

4.3.1 Soft Scalar Masses

We divide the effects that unified symmetries have on the scalar soft masses $m_{\tilde{f}}^2$ into two categories: the ones caused by the unified symmetry itself and those caused by symmetry breaking patterns.

The first category is rather trivial. Namely, if two or more MSSM fields ϕ_i are part of one single unified irreducible representations Φ, the unified symmetry imposes the condition that their soft SUSY breaking scalar masses are equal,

$$m_{\tilde{\phi}_1}^2 = m_{\tilde{\phi}_2}^2 = \dots = m_{\tilde{\Phi}}^2\ , \tag{4.18}$$

at the scale of unified symmetry break-down.

Another possibility, as discussed in [55], is that the larger unified symmetry group contains a $U(1)$ factor as subgroup, which is broken both by a regular scalar component VEV and by a VEV in the D component of some field. The latter constitutes direct

SUSY breaking which is mediated to the visible sector via the D-term potential, leading to contributions to their soft scalar masses proportional to their $U(1)$ charge,

$$\Delta m^2_{\tilde{\phi}_i} = q(\phi_i) D \ , \tag{4.19}$$

where $q(\phi_i)$ is the charge of the field ϕ_i under the broken $U(1)$ symmetry and D is the SUSY breaking D component VEV. Assuming unification at most to the exceptional Lie group E_6, which contains two $U(1)$ factors in addition to hypercharge $U(1)_Y$, this yields a basis of three linearly independent D-term contributions D_S, D_X and D_Y, with charges defined in [55], that have the form

$$\begin{aligned}
\Delta m^2_{\tilde{Q}} &= \frac{1}{6} D_Y - \frac{1}{3} D_X - \frac{1}{3} D_S \ , & \Delta m^2_{\tilde{e}^c} &= D_Y - \frac{1}{3} D_X - \frac{1}{3} D_S \ , \\
\Delta m^2_{\tilde{L}} &= -\frac{1}{2} D_Y + D_X - \frac{2}{3} D_S \ , & \Delta m^2_{H_u} &= \frac{1}{2} D_Y + \frac{2}{3} D_X + \frac{2}{3} D_S \ , \\
\Delta m^2_{\tilde{u}^c} &= -\frac{2}{3} D_Y - \frac{1}{3} D_X - \frac{1}{3} D_S \ , & \Delta m^2_{H_d} &= -\frac{1}{2} D_Y - \frac{2}{3} D_X + D_S \ , \\
\Delta m^2_{\tilde{d}^c} &= \frac{1}{3} D_Y + D_X - \frac{2}{3} D_S \ ,
\end{aligned} \tag{4.20}$$

with D_i being of the order M^2_{SUSY}, i.e. of the size of usual soft SUSY breaking terms. In the absence of effects that leave the unified symmetry in tact and give universal contributions, this results in ratios between the soft term fixed by the symmetry group structure. For more information, we refer the reader to [55].

4.3.2 Gaugino Masses

The case of gaugino masses proceeds quite similar to the one of soft scalar masses. In the case of purely symmetry based situations, the MSSM gaugino masses are required to be equal,

$$M_1 = M_2 = M_3 \ , \tag{4.21}$$

at the scale of GUT symmetry break-down, or some subset of these equations in the case of non-grand unification.

Symmetry breaking effects for gaugino masses, on the other hand, can enter via GUT non-singlet fields that develop SUSY breaking VEVs in their F component and appear in the gauge kinetic function. This way, as can be seen from eq. (3.7), they can generate possibly non-universal gaugino mass terms [56]. Since the VEVs of such F-terms are determined by the structure of symmetry break-down, these gaugino masses exhibit fixed ratios between the different MSSM gaugino mass parameters. For example, following the F-term VEV of a GUT Higgs field H in the **200** representation of $SU(5)$, we obtain gaugino mass ratios of

$$M_1 : M_2 : M_3 = 10 : 2 : 1 \ , \tag{4.22}$$

assuming the field H appears to linear order in $f_{ab} \supset H$. For more information and a review over possible ratios generated this way, we refer the reader to [56].

Another possibility is provided in string theories via contributions to f_{ab} related to anomalies and string threshold corrections [57]. In this thesis, we will only consider a simplified model based on orbifold compactification, called the O-II model. It generates gaugino mass ratios of the form

$$M_1 : M_2 : M_3 = \left(-\delta_{\mathrm{GS}} + \frac{33}{5}\right) : (-\delta_{\mathrm{GS}} + 1) : (-\delta_{\mathrm{GS}} - 3) \ , \tag{4.23}$$

with a negative integer constant δ_{GS} as required by an anomaly cancellation condition. This is effectively a combination of universal gaugino masses and the ratios found in anomaly mediation, see sec. 3.3.1. For more details, see [57].

4.4 Proton-Decay and Doublet-Triplet Splitting

Unfortunately, GUTs also have a problem where they possibly clash with experimental results: they break baryon and lepton number explicitly since they incorporate baryons and leptons into joined representations under the gauge symmetry. This in turn leads to the instability of the proton which has not been observed yet [15] (even if matter parity is conserved as assumed here). In the following, we give a very brief review over what contributions to the proton decay width can be expected. We will restrict our discussion to the unification to $SU(5)$ – unification to $SO(10)$ encompasses the same contributions and more as it contains $SU(5)$ as a subgroup.

Mediation via Vector Bosons From eq. (4.6), we know that the adjoint representation of $SU(5)$ contains a vector-like pair of leptoquark superfields with mass $M_V \sim M_{\mathrm{GUT}}$. As gauge bosons, they have interactions where they couple at the same time to quarks and leptons contained in the same GUT multiplet. Thus, when they are integrated out, they give rise to dimension six operators in the Kähler potential of the form

$$K \supset \frac{g_5^2}{M_V^2} \left(Q^\dagger Q^\dagger u^c e^c + Q^\dagger L^\dagger d^c u^c\right) + \text{h.c.} \ , \tag{4.24}$$

where we suppressed generation indices and g_5 is the $SU(5)$ gauge coupling. They give rise to proton decay via diagrams of the form shown in fig. 4.2. The naively expected structure of vector boson couplings involving σ_μ can be reconciled with eq. (3.5) via the identity $(\sigma^\mu)_{a\dot{b}}(\sigma_\mu)_{c\dot{d}} = 2\epsilon_{ac}\epsilon_{\dot{b}\dot{d}}$ as is relevant for two component spinors. Using a naive estimate for proton decay width,

$$\Gamma_p \approx \alpha_5^2 \, \frac{m_p^5}{M_V^4} \ , \tag{4.25}$$

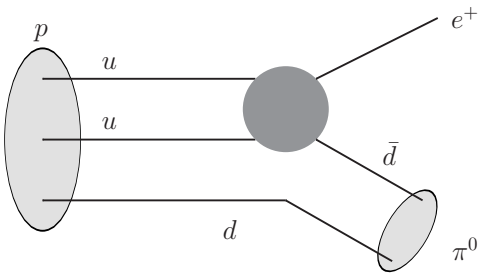

Figure 4.2: Schematic diagram of proton decay via a four fermion dimension six operator (dark grey dot) originating from the terms in eq. (4.24) (but not exclusive to supersymmetry).

with the unified structure constant $\alpha_5 \approx g_5^2/4\pi$ and the proton mass m_p, together with the experimental constraint $\tau(p \to \pi^0 e^+) > 1.6 \cdot 10^{33}$ years, we find a lower bound on the mass of the leptoquark vector boson M_V of

$$M_V \gtrsim 3 \cdot 10^{15} \text{ GeV} , \tag{4.26}$$

where we used $\alpha_5 = 1/25$ as motivated by fig. 4.1 and also chap. 5, see also [58]. Since the GUT scale is about 10^{16} GeV, GUT models usually have no problem with this bound.

Mediation via Higgs Triplets Another additional superfield that couples to quarks and leptons is given by colour triplet partners T and $\bar{T}$ of the Higgs doublet $H_{u,d}$ as implied by their SM decomposition in eq. (4.7).[2] These colour triplets couple to the MSSM multiplets via Yukawa interactions of the form

$$W \supset -\frac{1}{2} Y_{qq}\, QQT + Y_{ql}\, QL\bar{T} + Y_{ue}\, u^c e^c T - Y_{ud}\, u^c d^c \bar{T} + m_T\, T\bar{T} , \tag{4.27}$$

where we again suppressed generation indices for simplicity. These Yukawa coupling matrices Y_{qq}, Y_{ql}, Y_{ue} and Y_{ud} are automatically implied by the $SU(5)$ Yukawa couplings of eqs. (4.8) and (4.11) when taking into account T and $\bar{T}$. As gauge coupling unification assumes only the MSSM spectrum up to the GUT scale, these colour triplets must be quite heavy and split from the doublets, leading to the "doublet-triplet splitting problem". When they are subsequently integrated out, they generate dimension five

[2]Note that this assumes the embedding $H_u, H_d \to \mathbf{5}, \bar{\mathbf{5}}$. In the case of 45 dimensional representations, the following also applies and is even exacerbated by the additional SM multiplets contained in the representation **45**.

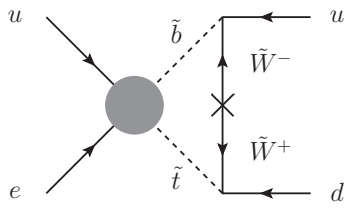

Figure 4.3: Example diagram of superpartner dressing for dimension five operators (dark grey dot) originating to arrive at dimension six operators for use in fig. 4.2. For more details, see [58].

and six operators that lead to proton decay and are schematically given by

$$W \supset \frac{1}{m_T}\left[\frac{1}{2}Y_{qq}Y_{ql}\,QQQL + Y_{ue}Y_{ud}\,u^c e^c u^c d^c\right] , \tag{4.28a}$$

$$K \supset \frac{Y_{qq}^* Y_{ue}}{m_T^2}\,Q^\dagger Q^\dagger u^c e^c + \frac{Y_{ql}^* Y_{ud}}{m_T^2}\,Q^\dagger L^\dagger d^c u^c + \text{h.c.} , \tag{4.28b}$$

again with generation indices suppressed. Similar to the case of leptoquark vector bosons, we can again make a naive estimate of the lower bound on the triplet mass due to the dimension six operator: since Y_{ql} and Y_{ud} are related to Y_d by GUT relations, we substitute α_5 in eq. (4.25) with the square of the GUT-scale Yukawa coupling $y_d \approx 0.5 \cdot 10^{-5}/\cos\beta$ as taken from chap. 5. For $\tan\beta = 30$, this yields a equally naive bound of

$$m_T \gtrsim 2 \cdot 10^{12}\ \text{GeV} . \tag{4.29}$$

For the dimension five operators, the situation is not as straight forward as they do not directly lead to proton decay. Only when the superpartners of the SM fields are integrated out at their mass scale M_{SUSY}, 'dressing' of the dimension five operators with loops of superpartners (see fig. 4.3 for an example) leads to dimension six proton decay operators similar to the four fermion interactions resulting from the other dimension six operators. However, this dressing only results in a suppression mass scale of $m_T \cdot M_{\text{SUSY}}$ instead of m_T^2. Subsequently, the lower bound for the colour triplet mass (appearing in the dimension five operators) was found to be [59]

$$m_T \gtrsim 10^{17}\ \text{GeV} , \tag{4.30}$$

for which $M_{\text{SUSY}} \lesssim 1$ TeV was considered. Thus, the doublet-triplet problem (DTS) is one important shortcoming of GUTs, as (naively) the colour triplets must not only be split from the Higgs doublets but also partially from the GUT scale itself.

PART II

Insights on Unified Theories

CHAPTER 5

Running Flavour Parameters

5.1 Motivation

For finding the structure of a theory that implements grand unification and tries to explain the structure of the fermion masses and mixing parameters, one important ingredient is the determination of the Yukawa couplings and other quantities at the relevant renormalisation scales. This is done using renormalisation group (RG) running with intermediate thresholds between different effective theories where appropriate. GUT models of flavour can then be compared with experimental data at the scale where the model is defined or alternatively at a single energy scale without the need to explicitly replicate experimentally determined quantities from more accessible ones. Both of these approaches have been recognised as useful [60].

Concerning experimental data, over the last years, while precision has increased in the lepton mixing sector with the measurement of the mixing angle $\theta_{13}^{\text{PMNS}}$ [22] and subsequent improvement in global fits [16], also in the quark sector, the precision for light quark masses has improved significantly, as reported by the Flavour Averaging Group (FLAG) [61] and as stated in the more recent update of the Particle Data Group (PDG) review [15]. Combined, both sectors have now become powerful constraints on models for fermion masses and mixing.

Therefore, it is worth to revisit what consequences these advancements in precision have on the values and allowed ranges of the running quark and charged lepton flavour parameters at various energy scales. After a calculation of this strictly in the SM up to a few TeV, we match the SM to the MSSM and take into account $\tan\beta$ enhanced threshold corrections [31, 32, 33, 34] and run all flavour parameters up to the GUT scale $M_{\text{GUT}} = 2 \cdot 10^{16}$ GeV. For this, the threshold corrections are parametrised in a simple way, so that they can easily be included in GUT model building considerations.

This chapter is therefore organised as follows. After describing the numerical input and procedure in sec. 5.2, our parametrisation for the inclusion of SUSY threshold

corrections is shown in sec. 5.3. In sec. 5.4 and 5.5, we present our results for the flavour parameters at the renormalisation scales $\mu = M_Z$, 1 TeV, 3 TeV and 10 TeV and at M_{GUT}, respectively.

5.2 Numerical Analysis

Using the same notation as in [62], with M_f denoting pole masses and $m_f(\mu)$ the running $\overline{\text{MS}}$ masses, the low energy input values used in our analysis are as follows:

For the light quark masses (at $\mu = 2$ GeV, with $n_f = 2+1$ active flavours), we use the values from the PDG review of 2014 [15],

$$\frac{m_s}{m_{ud}} = 27.5 \pm 1 \,, \quad m_d = 4.8^{+0.5}_{-0.3} \text{ MeV} \,, \quad m_s = 95 \pm 5 \text{ MeV} \,, \tag{5.1}$$

where $m_{ud} = (m_u + m_d)/2$. Furthermore, also from [15], we use

$$m_c(m_c) = 1.275 \pm 0.025 \text{ GeV} \qquad (n_f = 4) \,, \tag{5.2a}$$
$$m_b(m_b) = 4.18 \pm 0.03 \text{ GeV} \qquad (n_f = 5) \,, \tag{5.2b}$$
$$M_t = 173.21 \pm 1.22 \text{ GeV} \qquad (\text{pole mass}) \,, \tag{5.2c}$$
$$\alpha_s(M_Z) = 0.1185 \pm 0.0006 \qquad (\text{with } n_f = 5) \,, \tag{5.2d}$$
$$M_e = 0.510998928 \pm 0.000000011 \text{ MeV} \,, \tag{5.2e}$$
$$M_\mu = 105.6583715 \pm 0.0000035 \text{ MeV} \,, \tag{5.2f}$$
$$M_\tau = 1776.82 \pm 0.16 \text{ MeV} \,, \tag{5.2g}$$
$$1/\alpha(M_Z) = 127.940 \pm 0.014 \,, \tag{5.2h}$$
$$\hat{s}^2_{\theta_W} = 0.231258 \pm 0.000089 \,. \tag{5.2i}$$

For the quark mixing parameters, we use the values as determined by the UTFit collaboration [63] as of summer 2014:

$$\sin\theta_{12} = 0.2255 \pm 0.0005 \,, \qquad \sin\theta_{23} = 0.0417 \pm 0.0006 \,, \tag{5.3a}$$
$$\sin\theta_{13} = 0.00363 \pm 0.00012 \,, \qquad \delta = 1.211 \pm 0.059 \,. \tag{5.3b}$$

The Higgs self-coupling is extracted from its mass $m_h = 125.7 \pm 0.4$ GeV [15].

The input values for the QCD parameters (quark masses and α_s) are evolved to $M_Z = 91.1876$ GeV [15] using the Mathematica package `RunDec` [62], as described in app. A. The running lepton masses at M_Z in the low energy theory of QED are computed from their pole masses as in [64]. All fermion masses are then matched from QCD $\times$ QED to the standard model, taking into account electroweak and Higgs boson contributions to the running masses as described in app. B. Subsequently, the running fermion masses are converted to Yukawa couplings according to $m_f = y_f v/\sqrt{2}$ with

the Higgs VEV $v = 246.220$ GeV as obtained from G_F, while α_s, α and $\sin\theta_W$ are used to calculate the gauge couplings g_i (in GUT normalisation, see sec. 4.1).

The parameters at M_Z are passed to a modified version of the Mathematica package `REAP` [65], which performs the running to the desired higher scales. The modifications compared to the standard version of `REAP` include two loop SM and MSSM RG equations [66, 67] for all quantities, automatic conversion of $\overline{\text{MS}}$ to $\overline{\text{DR}}$ quantities [68] at the SM-MSSM threshold as well as the handling of $\tan\beta$ enhanced threshold corrections as described in the next section.

Note that all quantities are calculated in the context of the SM or MSSM, i.e. with vanishing neutrino masses. Due to the fact that the Weinberg operator does not enter the running of Yukawa couplings in the MSSM with Majorana neutrino masses, it is straight-forward to generalise our results also to models with seesaw mechanism at high energies. Only above the seesaw scale, where neutrino Yukawa couplings appear in the effective theory, this approach is merely an approximation. We will come back to this sec. 5.5.

5.3 Inclusion of the SUSY Threshold Corrections

Most commonly, to obtain parameters at high energies in a supersymmetric theory, the SM has to be matched to the MSSM at some scale. A common approximation, which we will also use in this study, is to do this at one single threshold scale M_{SUSY}, where all superpartners and fields beyond the SM are integrated out simultaneously. In particular for moderate or large $\tan\beta$, radiative threshold corrections to Yukawa couplings [31, 32, 33, 34] can be large since some of the contributing diagrams are enhanced by a factor $\tan\beta$. Due to this enhancement, they can even exceed the one-loop running contribution and all relevant uncertainties. It is therefore mandatory to include them for the analysis of the running quark and charged lepton Yukawa couplings in SUSY models.

These $\tan\beta$ enhanced corrections are most conveniently described in the basis where the up-type quark Yukawa matrix Y_u is diagonal. Then one can write the matching conditions for the quark Yukawa couplings as

$$Y_u^{\text{SM}} \simeq Y_u^{\text{MSSM}} \sin\beta \,, \tag{5.4a}$$

$$Y_d^{\text{SM}} \simeq (\mathbb{1} + \Delta_d + \Delta_u)\, Y_d^{\text{MSSM}} \cos\beta \,, \tag{5.4b}$$

with the matrices $(16\pi^2)\Delta_d^* = V_{\text{CKM}}\Gamma_d V_{\text{CKM}}^\dagger \tan\beta$ and $(16\pi^2)\Delta_u^* = \Gamma_u \tan\beta$ defined in terms of the matrices Γ_d and Γ_u as defined in [32]. Contributions without $\tan\beta$ enhancement have been dropped from eq. (5.4) as they amount to corrections at less than percent-level. In the following, we neglect them since we will not claim better accuracy for the relevant GUT-scale Yukawa couplings. The correction matrix Γ_d

corresponds to the contribution from gluinos, while Γ_u gives the contribution coming from charginos and up-type squarks – in particular it contains the correction involving the trilinear soft breaking matrix A_u. Note that the formulae given in [32] do not include correction due to neutralinos, i.e. the bino and one wino, which we do include in the following discussion.

Neglecting effects from inter-generation mixing in Δ_d and Δ_u and extending the concept to charged leptons, the matching conditions can be simplified to

$$Y_u^{\mathrm{SM}} \simeq Y_u^{\mathrm{MSSM}} \sin\beta \,, \tag{5.5a}$$

$$Y_d^{\mathrm{SM}} \simeq (\mathbb{1} + \mathrm{diag}(\eta_q, \eta_q, \eta'_q + \eta_A))\, Y_d^{\mathrm{MSSM}} \cos\beta \,, \tag{5.5b}$$

$$Y_e^{\mathrm{SM}} \simeq (\mathbb{1} + \mathrm{diag}(\eta_\ell, \eta_\ell, \eta'_\ell))\, Y_e^{\mathrm{MSSM}} \cos\beta \,. \tag{5.5c}$$

Additionally, we approximate that the first two generations of down-type quarks and charged leptons each receive the same threshold corrections, which is a good approximation as long as there is no significant mass difference between first and second generation squarks and sleptons respectively, which is a common feature of many SUSY scenarios.

Six parameters appear in eqs. (5.5): η_q and η'_q are dominated by the gluino contribution but also include the corrections from loops with winos and binos. The parameters η_ℓ and η'_ℓ only parametrise corrections from electroweak gauginos and are thus often smaller than η_q and η'_q. The parameter η_A originates from chargino-stop loops and depends mainly on the trilinear soft SUSY breaking term A_u. Assuming the trilinear soft breaking matrix A_u to be hierarchical (like the quark and charged lepton Yukawa matrices), the correction only enters for the third generation. An analogous correction does not appear for the charged leptons due to the absence of right-handed neutrinos. As the η's all contain a factor of $\tan\beta$, they are often also written as $\eta_i = \varepsilon_i \tan\beta$. They can be calculated explicitly once a SUSY scenario is specified. For formulae for the one-loop results in the electroweak-unbroken phase, we refer the reader to e.g. [31, 32, 33].

From eqs. (5.5) one can see that the Yukawa matrices only depend on four combinations of the six parameters, which means two can be absorbed. First, the parameter η'_ℓ can be absorbed in a re-definition of $\beta \to \bar{\beta}$, such that

$$\cos\bar{\beta} := (1 + \eta'_\ell)\cos\beta \,, \tag{5.6}$$

or equivalently (to a good approximation) $\tan\bar{\beta} := (1 + \eta'_\ell)^{-1} \tan\beta$. Introducing furthermore the parameters $\bar{\eta}_b$, $\bar{\eta}_q$ and $\bar{\eta}_\ell$ as

$$\bar{\eta}_b := \eta'_q + \eta_A - \eta'_\ell \,, \tag{5.7a}$$

$$\bar{\eta}_q := \eta_q - \eta'_\ell \,, \tag{5.7b}$$

$$\bar{\eta}_\ell := \eta_\ell - \eta'_\ell \,, \tag{5.7c}$$

we can rewrite the matching conditions of eqs. (5.5) as

$$Y_u^{\mathrm{SM}} \simeq Y_u^{\mathrm{MSSM}} \sin\bar{\beta} \,, \tag{5.8a}$$
$$Y_d^{\mathrm{SM}} \simeq (\mathbb{1} + \mathrm{diag}(\bar{\eta}_q, \bar{\eta}_q, \bar{\eta}_b))\, Y_d^{\mathrm{MSSM}} \cos\bar{\beta} \,, \tag{5.8b}$$
$$Y_e^{\mathrm{SM}} \simeq (\mathbb{1} + \mathrm{diag}(\bar{\eta}_\ell, \bar{\eta}_\ell, 1))\, Y_e^{\mathrm{MSSM}} \cos\bar{\beta} \,. \tag{5.8c}$$

In the following, we consider moderate or large $\tan\beta$, i.e. $\tan\beta \geq 5$, where we can approximate $\sin\beta \simeq \sin\bar{\beta}$. As mentioned above, the lepton correction parameters η_ℓ, η'_ℓ are typically smaller than η_q, η'_q and are therefore often neglected. In our parametrisation neglecting η_ℓ, η'_ℓ would simplify eqs. (5.8) with $\bar{\beta} = \beta$. However, since the effects of η_ℓ and η'_ℓ can be relevant (cf. e.g. [33]), we prefer to include them in the analysis.

In tab. 5.2, we give the values of the running SM parameters, converted to the $\overline{\mathrm{DR}}$ scheme as used in the analysis above M_{SUSY}. They can be used to calculate the MSSM Yukawa matrices Y_u, Y_d and Y_e at M_{SUSY}, with threshold corrections included, from eqs. (5.8). Explicitly, in the basis where Y_u and Y_e are diagonal, we obtain the Yukawa matrices from tab. 5.2 as

$$Y_u^{\mathrm{SM}} = \mathrm{diag}(y_u^{\mathrm{SM}}, y_c^{\mathrm{SM}}, y_t^{\mathrm{SM}}) \,, \tag{5.9a}$$
$$Y_d^{\mathrm{SM}} = V_{\mathrm{CKM}}^T(\theta_{12}^{q,\mathrm{SM}}, \theta_{23}^{q,\mathrm{SM}}, \theta_{13}^{q,\mathrm{SM}}, \delta^{q,\mathrm{SM}})\ \mathrm{diag}(y_d^{\mathrm{SM}}, y_s^{\mathrm{SM}}, y_b^{\mathrm{SM}}) \,, \tag{5.9b}$$
$$Y_e^{\mathrm{SM}} = \mathrm{diag}(y_e^{\mathrm{SM}}, y_\mu^{\mathrm{SM}}, y_\tau^{\mathrm{SM}}) \,, \tag{5.9c}$$

in the parametrisation of chap. 1, i.e. conjugated compared to PDG parametrisation for Yukawa matrices [15]. Using these expressions for the SM Yukawa matrices, the MSSM Yukawa matrices at M_{SUSY} are then given as

$$Y_u^{\mathrm{MSSM}} \simeq Y_u^{\mathrm{SM}} \frac{1}{\sin\bar{\beta}} \,, \tag{5.10a}$$
$$Y_d^{\mathrm{MSSM}} \simeq \mathrm{diag}\left(\frac{1}{1+\bar{\eta}_q}, \frac{1}{1+\bar{\eta}_q}, \frac{1}{1+\bar{\eta}_b}\right) Y_d^{\mathrm{SM}} \frac{1}{\cos\bar{\beta}} \,, \tag{5.10b}$$
$$Y_e^{\mathrm{MSSM}} \simeq \mathrm{diag}\left(\frac{1}{1+\bar{\eta}_\ell}, \frac{1}{1+\bar{\eta}_\ell}, 1\right) Y_e^{\mathrm{SM}} \frac{1}{\cos\bar{\beta}} \,. \tag{5.10c}$$

Finally, we emphasise that the parameters $\bar{\eta}_q$ and $\bar{\eta}_\ell$ only correct the Yukawa couplings of the first two generations of down-type quarks and charged leptons, whereas $\bar{\eta}_b$ affects the third generation. This has the following advantage: since $\bar{\eta}_q$ and $\bar{\eta}_\ell$ only induce corrections to Yukawa couplings which are comparatively small, their effect can be neglected in the β-functions when calculating the RG evolution of the parameters. To a good approximation, the RG evolution thus only depends on $\bar{\eta}_b$ and $\tan\bar{\beta}$. This will be useful to simplify the discussion of the effects of the SUSY threshold corrections on the running parameters at M_{GUT} in sec. 5.5.

5.4 Results at Low Scales

The results at renormalisation scales $\mu = M_Z$, 1 TeV, 3 TeV and 10 TeV, as calculated within the SM in the $\overline{\text{MS}}$ scheme, are given in tab. 5.1. All quantities converted to the $\overline{\text{DR}}$ scheme can be found in tab. 5.2. The stated uncertainties were obtained from a Monte Carlo analysis based on the uncertainties of the input parameters as stated in sec. 5.2. They are given as (marginalised) highest posterior density (HPD) intervals (corresponding to the 1σ uncertainties). For more information on the used statistical relations, see app. C.

5.5 Results at the GUT Scale

To determine the running parameters at the GUT scale $M_{\text{GUT}} = 2 \cdot 10^{16}$ GeV, we perform the matching between the SM and the MSSM at the scale M_{SUSY}, as described in sec. 5.3. From eqs. (5.8), in leading order in small mixing approximation, one can explicitly obtain the relations between the eigenvalues (or rather singular values) of the SM and MSSM Yukawa matrices as

$$y_{u,c,t}^{\text{SM}} \simeq y_{u,c,t}^{\text{MSSM}} \sin\bar{\beta} \,, \tag{5.11a}$$

$$y_{d,s}^{\text{SM}} \simeq (1+\bar{\eta}_q)\; y_{d,s}^{\text{MSSM}} \cos\bar{\beta} \,, \tag{5.11b}$$

$$y_{b}^{\text{SM}} \simeq (1+\bar{\eta}_b)\; y_{b}^{\text{MSSM}} \cos\bar{\beta} \,, \tag{5.11c}$$

$$y_{e,\mu}^{\text{SM}} \simeq (1+\bar{\eta}_\ell)\; y_{e,\mu}^{\text{MSSM}} \cos\bar{\beta} \,, \tag{5.11d}$$

$$y_{\tau}^{\text{SM}} \simeq y_{\tau}^{\text{MSSM}} \cos\bar{\beta} \,. \tag{5.11e}$$

The relation between the SM and MSSM mixing parameters of the CKM matrix is given by (again in leading order in a small mixing approximation)

$$\theta_{i3}^{q,\text{SM}} \simeq \frac{1+\bar{\eta}_q}{1+\bar{\eta}_b}\; \theta_{i3}^{q,\text{MSSM}} \,, \tag{5.12a}$$

$$\theta_{12}^{q,\text{SM}} \simeq \theta_{12}^{q,\text{MSSM}} \,, \tag{5.12b}$$

$$\delta^{q,\text{SM}} \simeq \delta^{q,\text{MSSM}} \,. \tag{5.12c}$$

In addition to not being affected by threshold corrections (for the given parametrisation) to a very good approximation, $\theta_{12}^{q,\text{SM}}$ and $\delta^{q,\text{SM}}$ are also stable under the RG evolution. Having calculated the other MSSM quantities, their running between M_{SUSY} and M_{GUT} indeed depends to a good approximation only on $\bar{\eta}_b$ and $\tan\bar{\beta}$, as already mentioned in sec. 5.3. This allows to present their GUT-scale values as only two-dimensional plots of functions of $\bar{\eta}_b$ and $\tan\bar{\beta}$ only (for a fixed M_{SUSY}). Since the left hand sides of eqs. (5.11) and (5.12) do not depend on any threshold correction parameters, the $\bar{\eta}_b$ and $\tan\bar{\beta}$ dependence of the quantities on the right side at the GUT scale

is given purely by the non-commuting of RG evolution and application of the matching conditions and is therefore not as strong.

The resulting GUT-scale quantities for $M_{\text{SUSY}} = 1$ TeV are shown in figs. 5.1–5.6, and the relative 1σ uncertainties for the GUT-scale parameters are given in tab. 5.3. For the third generation Yukawa couplings, the uncertainties depend on $\bar{\eta}_b$ and $\tan\bar{\beta}$, and are given in fig. 5.4. The relative uncertainties for the other parameters are practically independent of $\bar{\eta}_b$ and $\tan\bar{\beta}$ for most of the parameter space. Only in the parameter regions in the GUT-scale figures very close to the grey area, where one of the third generation Yukawa couplings becomes non-perturbatively large, i.e. larger than $\sqrt{4\pi}$, also these uncertainties can increase accordingly.

In addition, we also show the values of the GUT-scale ratios y_t/y_b and y_τ/y_b as functions of $\tan\bar{\beta}$ and $\bar{\eta}_b$ in fig. 5.7. As one can see both the ratios $y_\tau/y_b = 1$ and the alternative ratio $y_\tau/y_b = 3/2$ [49] are accessible for reasonable SUSY threshold correction and $\tan\bar{\beta}$ values. The $SO(10)$ relation $y_t = y_b = y_\tau$ would imply $\bar{\eta}_b = -0.159$, $\tan\bar{\beta} = 49.8$. It is interesting to note that the GUT-scale Yukawa coupling ratios y_μ/y_s and y_e/y_d do not depend on $\tan\bar{\beta}$ and $\bar{\eta}_b$ to a good approximation. This happens because the factor $\cos\bar{\beta}$ from the matching conditions cancels out and $\bar{\eta}_b$ affects the RG evolution of both the numerator and denominator quantities in the same way, i.e. via the trace terms in the RG equations. The ratios at M_{GUT} (assuming $M_{\text{SUSY}} = 1$ TeV) are then given by

$$\frac{(1+\bar{\eta}_\ell)y_\mu}{(1+\bar{\eta}_q)y_s} \approx 4.38^{+0.22}_{-0.25}\,, \qquad \frac{(1+\bar{\eta}_\ell)y_e}{(1+\bar{\eta}_q)y_d} \approx 0.41^{+0.02}_{-0.04}\,. \tag{5.13}$$

One can also derive the following relation at M_{GUT},

$$\frac{y_\mu}{y_s}\frac{y_d}{y_e} \approx 10.7^{+1.3}_{-0.8}\,, \tag{5.14}$$

where the dependence on all threshold correction parameters and even on M_{SUSY} drops out to an excellent approximation[1].

Effect of Neutrino Yukawa Couplings As mentioned earlier, due to the use of the SM and MSSM only, the shown results are only valid for vanishing neutrino masses. However, in the case of Majorana neutrino masses generated by the Weinberg operator of eq. (2.3) or its SUSY equivalent, the RG equations for all dimensionless quantities remain unchanged. When the Weinberg operator is generated by a seesaw mechanism[2], at the high scale of right-handed neutrino Majorana masses M_N the theory has to be matched with one that also contains neutrino Yukawa coupling matrices Y_ν in its RG

[1] Note that, of course, this is not the case if first and second generation threshold corrections are not approximately equal.

[2] To be specific, we assume a seesaw type I mechanism hereafter.

equations. If we estimate their relative effect on the RG running from the scale M_N to M_{GUT} as

$$\delta_\nu \approx \frac{1}{16\pi^2}||Y_\nu||^2 \ln\left(\frac{M_N}{M_{\text{GUT}}}\right) , \tag{5.15}$$

with the Euclidean norm of the neutrino Yukawa matrix $||Y_\nu||$, and the heaviest light neutrino mass by

$$m_\nu = \frac{v_u^2}{2}\,\frac{||Y_\nu||^2}{M_N} , \tag{5.16}$$

we arrive at the relation

$$\delta_\nu \approx 0.0041\,\frac{m_\nu}{2\text{ eV}}\,\frac{M_N}{10^{12}\text{ GeV}}\left(1+\frac{1}{\tan^2\beta}\right)\left(1+0.1\ln\frac{M_N}{10^{12}\text{ GeV}}\right) . \tag{5.17}$$

Thus, assuming $\tan\beta \gtrsim 5$ and light neutrino masses saturating the limit of 2 eV given by [15], demanding $\delta_\nu < 0.5\%$, i.e. an effect on the charged lepton Yukawa couplings below the allotted relative uncertainty, requires right-handed neutrino masses of the order $M_N \lesssim 10^{12}$ GeV, or in other words $Y_\nu \lesssim \mathcal{O}(0.1)$, following eq. (5.16). Since the other flavour quantities have larger uncertainties or are affected less directly than the charged lepton Yukawa couplings, they provide no further constraints on the applicability of our results.

Dependence on the SUSY Scale Of course, the GUT-scale quantities also depend on the SUSY scale M_{SUSY}. To quantify this, we performed the same analysis also for $M_{\text{SUSY}} = 3$ TeV and 10 TeV. Generally speaking, we find deviations from the values in the figures at the few percent-level, which additionally also depend on the parameters $\tan\bar{\beta}$ and $\bar{\eta}_b$, while the relative uncertainties as given in tab. 5.3 do not change significantly. It is unfortunately not possible to simplify the data and eliminate one of those two parameters by a change of parametrisation due to the fact that different quantities depend differently on y_b^{MSSM} and y_τ^{MSSM}, thereby picking up independent combinations of $\tan\bar{\beta}$ and $\bar{\eta}_b$.

Thus, the only possibility to show an accurate picture of the deviation is to replicate all figures for the other SUSY scales, which we will do not do in this thesis for the sake of briefness. Nevertheless, one can find some trends in the change of the GUT-scale quantities from M_{SUSY} from 1 TeV to 10 TeV:

- CKM mixing angles θ_{13} and θ_{23} generally increase by about 3 to 5% in most parts of the shown parameter space, but also up to 10% in parts where one Yukawa coupling is large, i.e. near the non-perturbativity (NP) region.
- The top Yukawa coupling decreases by about 2 to 5%, with up to $\sim 10\%$ near the NP region.

- All other Yukawa couplings tend to increase by varying amounts, but can nevertheless also decrease near the NP region, although the parameter space where this happens is quite small (in the parametrisation shown in the figures). The effect for the first two generations of down type quarks, up type quarks and charged leptons is equal to a good approximation, respectively.

For further details, we refer the reader to the full data set available online at

`http://particlesandcosmology.unibas.ch/files/maurerv/RunningParameters-thesis.tar.gz` ,

which should be used when actual numbers rather than trends are necessary.

SM Quantity	$\mu = M_Z$		= 1 TeV		= 3 TeV		= 10 TeV	
$y_u^{\rm SM} \,/\, 10^{-6}$	6.9	$^{+1.5}_{-2.4}$	6.0	$^{+1.3}_{-2.1}$	5.6	$^{+1.2}_{-2.0}$	5.3	$^{+1.2}_{-1.9}$
$y_d^{\rm SM} \,/\, 10^{-5}$	1.577	$^{+0.168}_{-0.096}$	1.362	$^{+0.144}_{-0.084}$	1.289	$^{+0.136}_{-0.080}$	1.220	$^{+0.129}_{-0.075}$
$y_s^{\rm SM} \,/\, 10^{-4}$	3.12	$^{+0.16}_{-0.17}$	2.70	$^{+0.14}_{-0.15}$	2.55	$^{+0.13}_{-0.14}$	2.42	± 0.13
$y_c^{\rm SM} \,/\, 10^{-3}$	3.59	$^{+0.10}_{-0.11}$	3.098	$^{+0.091}_{-0.095}$	2.928	$^{+0.085}_{-0.092}$	2.770	$^{+0.080}_{-0.087}$
$y_b^{\rm SM} \,/\, 10^{-2}$	1.643	± 0.015	1.390	± 0.013	1.305	$^{+0.012}_{-0.013}$	1.226	± 0.012
$y_t^{\rm SM}$	0.9833	$^{+0.0073}_{-0.0076}$	0.8656	$^{+0.0076}_{-0.0074}$	0.8248	± 0.0075	0.7864	± 0.0075
$\theta_{12}^{q,\rm SM}$	0.22746	± 0.00051	0.22746	± 0.00051	0.22746	± 0.00051	0.22747	± 0.00051
$\theta_{23}^{q,\rm SM} \,/\, 10^{-2}$	4.171	± 0.060	4.258	$^{+0.062}_{-0.060}$	4.291	$^{+0.060}_{-0.063}$	4.325	± 0.062
$\theta_{13}^{q,\rm SM} \,/\, 10^{-3}$	3.63	± 0.12	3.71	± 0.12	3.73	± 0.12	3.76	± 0.12
$\delta^{q,\rm SM}$	1.211	± 0.059	1.211	± 0.059	1.211	± 0.059	1.211	± 0.059
$y_e^{\rm SM} \,/\, 10^{-6}$	2.795169	± 0.000016	2.8479	$^{+0.0018}_{-0.0019}$	2.8640	$^{+0.0027}_{-0.0026}$	2.8773	$^{+0.0035}_{-0.0034}$
$y_\mu^{\rm SM} \,/\, 10^{-4}$	5.900762	$^{+0.000020}_{-0.000019}$	6.0121	$^{+0.0038}_{-0.0040}$	6.0461	$^{+0.0056}_{-0.0055}$	6.0742	± 0.0073
$y_\tau^{\rm SM} \,/\, 10^{-2}$	1.003101	$^{+0.000092}_{-0.000089}$	1.02204	$^{+0.00065}_{-0.00069}$	1.02781	$^{+0.00098}_{-0.00092}$	1.0326	± 0.0012
g_3	1.2148	$^{+0.0031}_{-0.0030}$	1.0563	± 0.0020	1.0020	± 0.0017	0.9513	± 0.0014
g_2	0.65171	± 0.00013	0.63923	± 0.00012	0.63371	± 0.00012	0.62781	± 0.00012
g_1	0.461462	$^{+0.000038}_{-0.000036}$	0.467812	$^{+0.000039}_{-0.000037}$	0.470806	$^{+0.000040}_{-0.000038}$	0.474150	± 0.000040

Table 5.1: Values of the running SM quantities in the $\overline{\rm MS}$ scheme at multiple renormalisation scales μ together their marginalised highest posterior density (HPD) intervals (corresponding to the 1σ uncertainties). The gauge coupling g_1 is given in GUT normalisation, i.e. $g_1^2 = 5/3\, g'^2$. The uncertainties are calculated with a Monte Carlo analysis from the uncertainties for the input parameters as given in sec. 5.2.

SM Quantity	$\mu = 1$ TeV		$= 3$ TeV		$= 10$ TeV	
$y_u^{\rm SM} \,/\, 10^{-6}$	5.9	$^{+1.3}_{-2.1}$	5.6	$^{+1.2}_{-2.0}$	5.3	$^{+1.2}_{-1.9}$
$y_d^{\rm SM} \,/\, 10^{-5}$	1.351	$^{+0.143}_{-0.083}$	1.279	$^{+0.135}_{-0.079}$	1.212	$^{+0.129}_{-0.075}$
$y_s^{\rm SM} \,/\, 10^{-4}$	2.67	$^{+0.14}_{-0.15}$	2.53	$^{+0.13}_{-0.14}$	2.40	$^{+0.12}_{-0.13}$
$y_c^{\rm SM} \,/\, 10^{-3}$	3.072	$^{+0.090}_{-0.094}$	2.907	$^{+0.084}_{-0.091}$	2.752	$^{+0.080}_{-0.087}$
$y_b^{\rm SM} \,/\, 10^{-2}$	1.379	± 0.013	1.296	$^{+0.012}_{-0.013}$	1.218	± 0.012
$y_t^{\rm SM}$	0.8584	$^{+0.0075}_{-0.0073}$	0.8187	$^{+0.0075}_{-0.0074}$	0.7812	$^{+0.0074}_{-0.0075}$
$\theta_{12}^{q,\rm SM}$	0.22746	± 0.00051	0.22746	± 0.00051	0.22747	± 0.00051
$\theta_{23}^{q,\rm SM} \,/\, 10^{-2}$	4.258	$^{+0.062}_{-0.060}$	4.291	$^{+0.060}_{-0.063}$	4.325	± 0.062
$\theta_{13}^{q,\rm SM} \,/\, 10^{-3}$	3.71	± 0.12	3.73	± 0.12	3.76	± 0.12
$\delta^{q,\rm SM}$	1.211	± 0.059	1.211	± 0.059	1.211	± 0.059
$y_e^{\rm SM} \,/\, 10^{-6}$	2.8498	$^{+0.0018}_{-0.0019}$	2.8658	$^{+0.0027}_{-0.0026}$	2.8791	$^{+0.0035}_{-0.0034}$
$y_\mu^{\rm SM} \,/\, 10^{-4}$	6.0161	$^{+0.0038}_{-0.0040}$	6.0500	$^{+0.0056}_{-0.0055}$	6.0779	± 0.0073
$y_\tau^{\rm SM} \,/\, 10^{-2}$	1.02271	$^{+0.00065}_{-0.00069}$	1.02847	$^{+0.00098}_{-0.00092}$	1.0332	± 0.0012
g_3	1.0601	± 0.0020	1.0052	± 0.0017	0.9540	± 0.0015
g_2	0.63978	± 0.00012	0.63425	± 0.00012	0.62833	± 0.00012
g_1	0.467812	$^{+0.000039}_{-0.000037}$	0.470806	$^{+0.000040}_{-0.000038}$	0.474150	± 0.000040

Table 5.2: Values of the running SM quantities at renormalisation scales $\mu = 1$ TeV, 3 TeV and 10 TeV, converted to the $\overline{\rm DR}$ scheme for use in an analysis above $M_{\rm SUSY}$, together their marginalised highest posterior density (HPD) intervals (corresponding to the 1σ uncertainties). The gauge coupling g_1 is given in GUT normalisation $g_1^2 = 5/3\, g'^2$. The values can be used when applying the matching rules of eqs. (5.10) which include the $\tan\beta$-enhanced SUSY threshold corrections. When calculating the uncertainties for the Yukawa couplings of the charged leptons, we recommend to use a relative uncertainty of 0.5% instead of the smaller statistical error given above, in order to account for theoretical uncertainties, e.g. from the non-$\tan\beta$-enhanced SUSY threshold corrections.

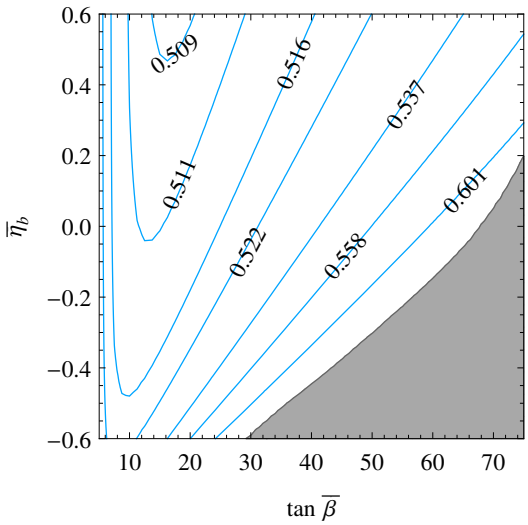

(a) $y_t^{\mathrm{MSSM}}\ \sin\bar{\beta}$

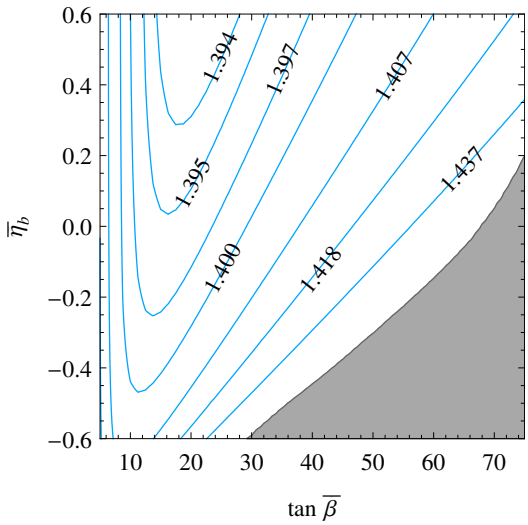

(b) $y_c^{\mathrm{MSSM}}\ \sin\bar{\beta}\ /\ 10^{-3}$

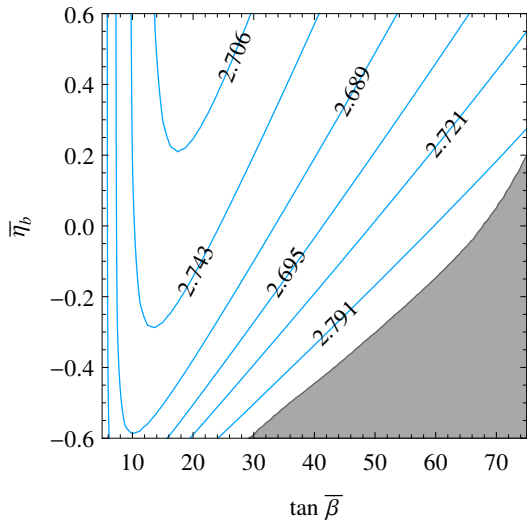

(c) $y_u^{\mathrm{MSSM}}\ \sin\bar{\beta}\ /\ 10^{-6}$

Figure 5.1: Results for the running Yukawa couplings y_t^{MSSM}, y_c^{MSSM} and y_u^{MSSM} at M_{GUT} in the $\overline{\mathrm{DR}}$ scheme, multiplied by $\sin\bar{\beta}$ (assuming $M_{\mathrm{SUSY}} = 1$ TeV). As discussed in sec. 5.3, the GUT-scale quantities can be given to a good approximation as functions of the two parameters $\tan\bar{\beta}$ and $\bar{\eta}_b$ only. They are defined in eqs. (5.6) and (5.7), respectively. If the threshold effects for the charged leptons are neglected, $\tan\bar{\beta}$ simply reduces to the usual $\tan\beta$. In the dark grey regions of the plots, at least one of the Yukawa couplings becomes non-perturbative before or at M_{GUT}. The relative uncertainties for the parameters are summarised in tab. 5.3. The dependence of the relative uncertainties for the third generation Yukawa couplings on $\tan\bar{\beta}$ and $\bar{\eta}_b$ is shown in fig. 5.4. For the other parameters the relative uncertainties are independent of $\tan\bar{\beta}$ and $\bar{\eta}_b$ to a very good approximation.

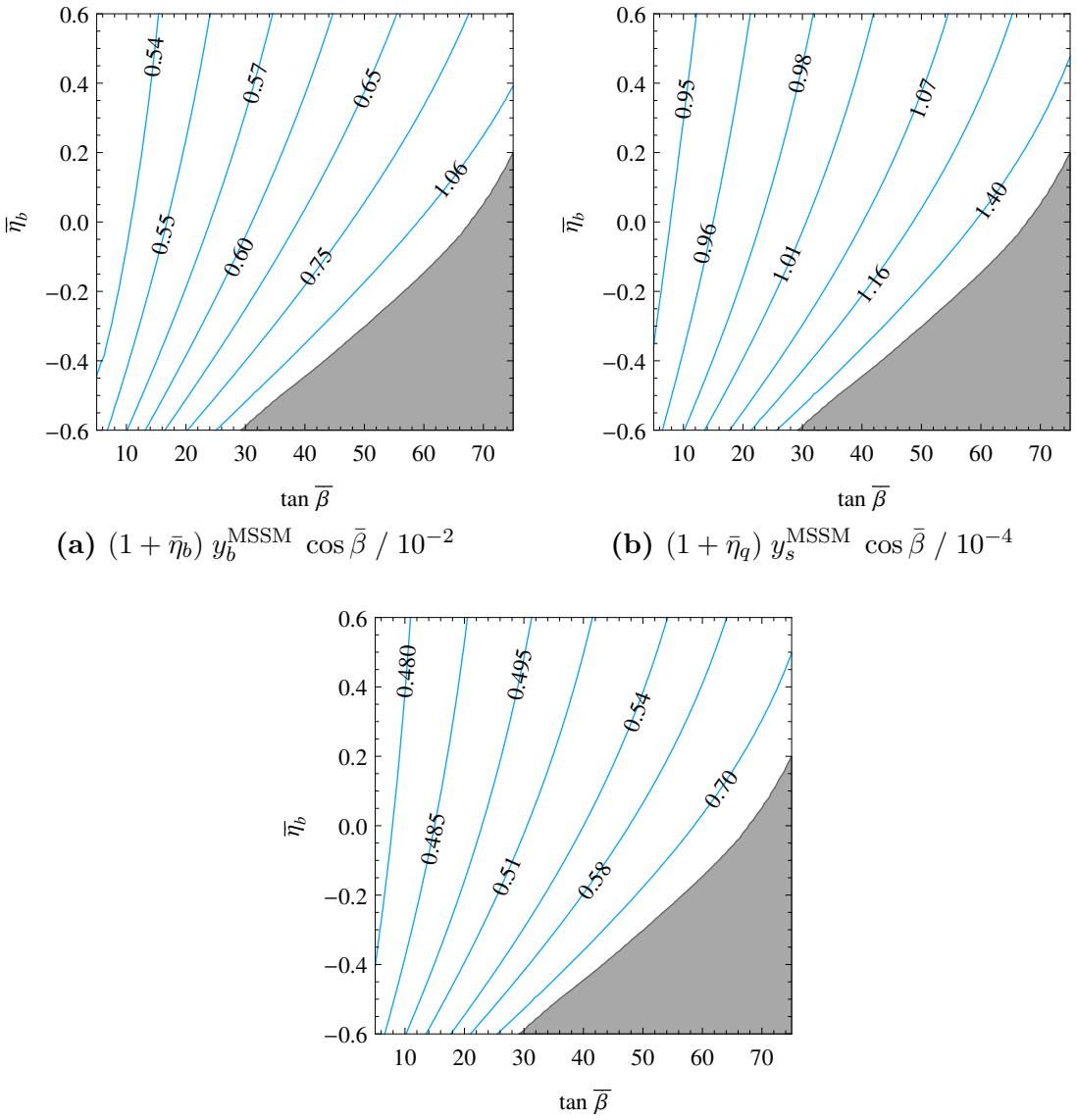

(a) $(1+\bar{\eta}_b)\, y_b^{\text{MSSM}}\, \cos\bar{\beta}\, /\, 10^{-2}$

(b) $(1+\bar{\eta}_q)\, y_s^{\text{MSSM}}\, \cos\bar{\beta}\, /\, 10^{-4}$

(c) $(1+\bar{\eta}_q)\, y_d^{\text{MSSM}}\, \cos\bar{\beta}\, /\, 10^{-5}$

Figure 5.2: Results for the running Yukawa couplings y_b^{MSSM}, y_s^{MSSM} and y_d^{MSSM} at M_{GUT} in the $\overline{\text{DR}}$ scheme (assuming $M_{\text{SUSY}} = 1$ TeV), multiplied by the respective threshold correction factor and $\cos\bar{\beta}$, cf. eqs. (5.11b) and (5.11c). As discussed in sec. 5.3, the GUT-scale quantities can be given to a good approximation as functions of the two parameters $\tan\bar{\beta}$ and $\bar{\eta}_b$ only. They are defined in eqs. (5.6) and (5.7), respectively. If the threshold effects for the charged leptons are neglected, $\tan\bar{\beta}$ simply reduces to the usual $\tan\beta$. In the dark grey regions of the plots, at least one of the Yukawa couplings becomes non-perturbative before or at M_{GUT}. For further details, see the caption of fig. 5.1.

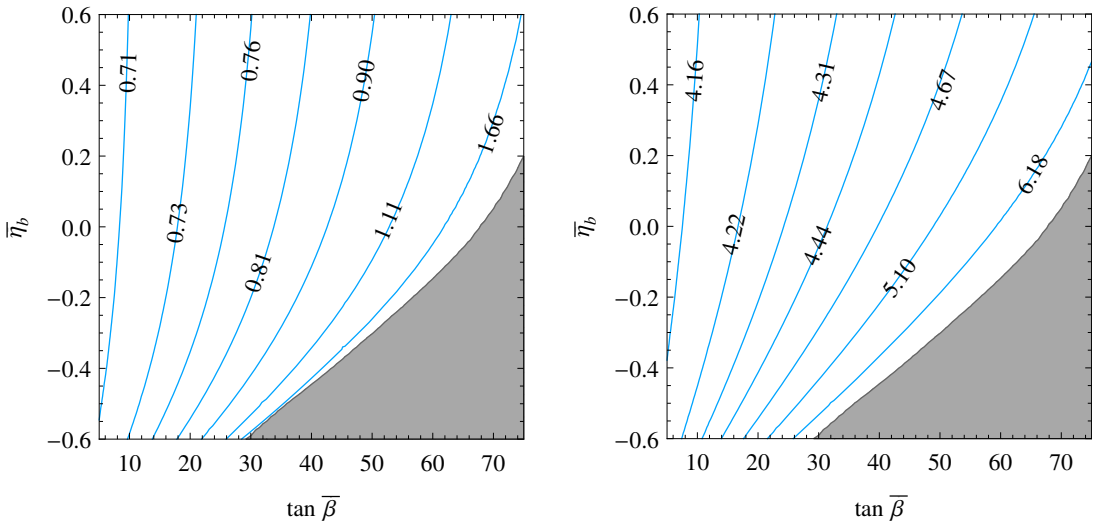

(a) $y_\tau^{\text{MSSM}} \cos\bar{\beta} \,/\, 10^{-2}$ **(b)** $(1+\bar{\eta}_\ell)\, y_\mu^{\text{MSSM}} \cos\bar{\beta} \,/\, 10^{-4}$

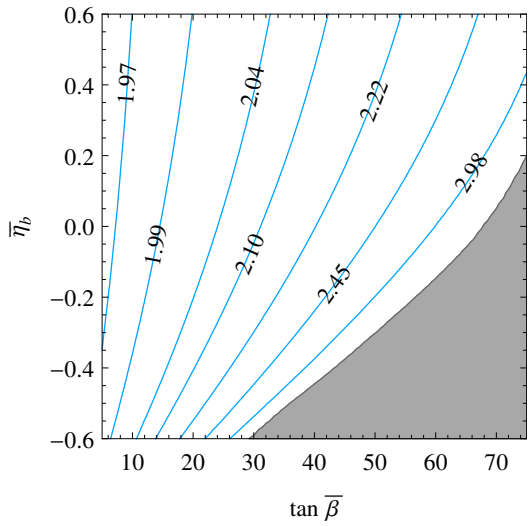

(c) $(1+\bar{\eta}_\ell)\, y_e^{\text{MSSM}} \cos\bar{\beta} \,/\, 10^{-6}$

Figure 5.3: Results for the running Yukawa couplings y_τ^{MSSM}, y_μ^{MSSM} and y_e^{MSSM} at M_{GUT} in the $\overline{\text{DR}}$ scheme (assuming $M_{\text{SUSY}} = 1$ TeV), multiplied by the respective threshold correction factor and $\cos\bar{\beta}$, cf. eqs. (5.11d) and (5.11e). As discussed in sec. 5.3, the GUT-scale quantities can be given to a good approximation as functions of the two parameters $\tan\bar{\beta}$ and $\bar{\eta}_b$ only. They are defined in eqs. (5.6) and (5.7), respectively. If the threshold effects for the charged leptons are neglected, $\tan\bar{\beta}$ simply reduces to the usual $\tan\beta$. In the dark grey regions of the plots, at least one of the Yukawa couplings becomes non-perturbative before or at M_{GUT}. For further details, see the caption of fig. 5.1.

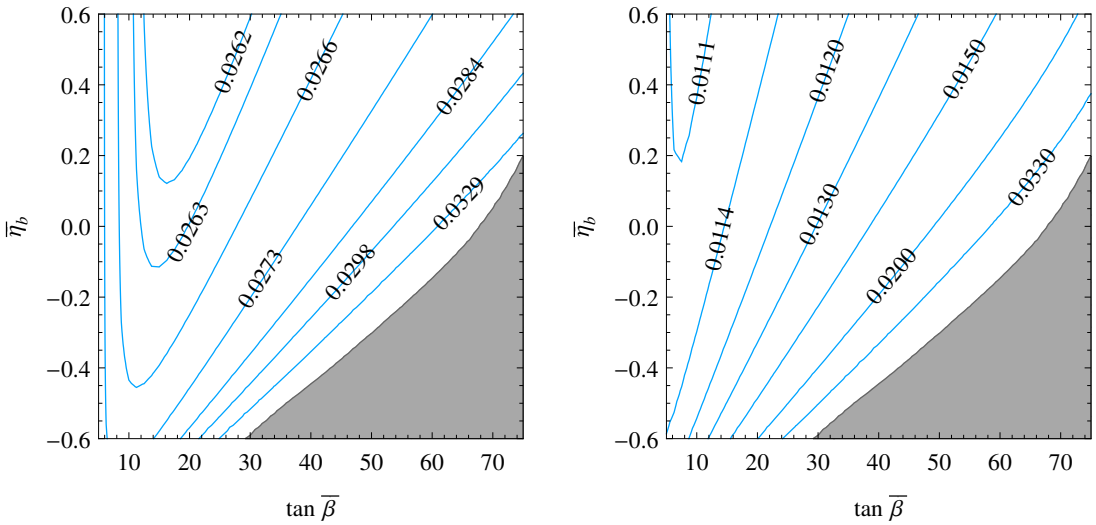

(a) $\sigma(y_t^{\mathrm{MSSM}})/y_t^{\mathrm{MSSM}}$ **(b)** $\sigma(y_b^{\mathrm{MSSM}})/y_b^{\mathrm{MSSM}}$

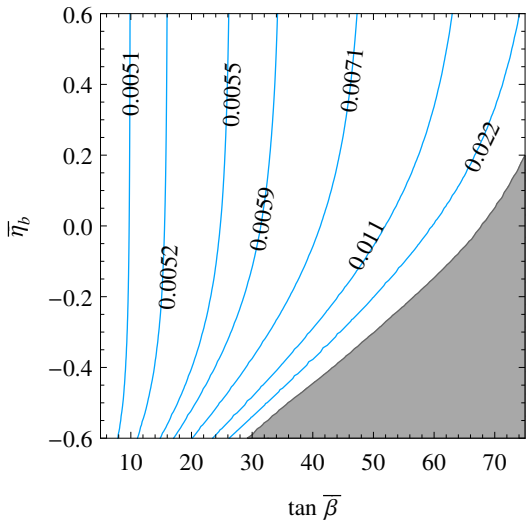

(c) $\sigma(y_\tau^{\mathrm{MSSM}})/y_\tau^{\mathrm{MSSM}}$

Figure 5.4: Relative uncertainties for the GUT-scale values of the running third generation Yukawa couplings y_t^{MSSM}, y_b^{MSSM} and y_τ^{MSSM} (assuming $M_{\mathrm{SUSY}} = 1$ TeV). Analogous to the GUT-scale Yukawa couplings themselves, their uncertainties can also be given as functions of only $\tan\bar{\beta}$ and $\bar{\eta}_b$ to a good approximation. The parameters $\bar{\beta}$ and $\bar{\eta}_b$ are defined in eqs. (5.6) and (5.7), respectively. If the threshold effects for the charged leptons are neglected, $\tan\bar{\beta}$ simply reduces to the usual $\tan\beta$. In the dark grey regions of the plots, at least one of the Yukawa couplings becomes non-perturbative before or at M_{GUT}. For further details, see the caption of fig. 5.1. The relative errors for the other parameters are summarised in tab. 5.3.

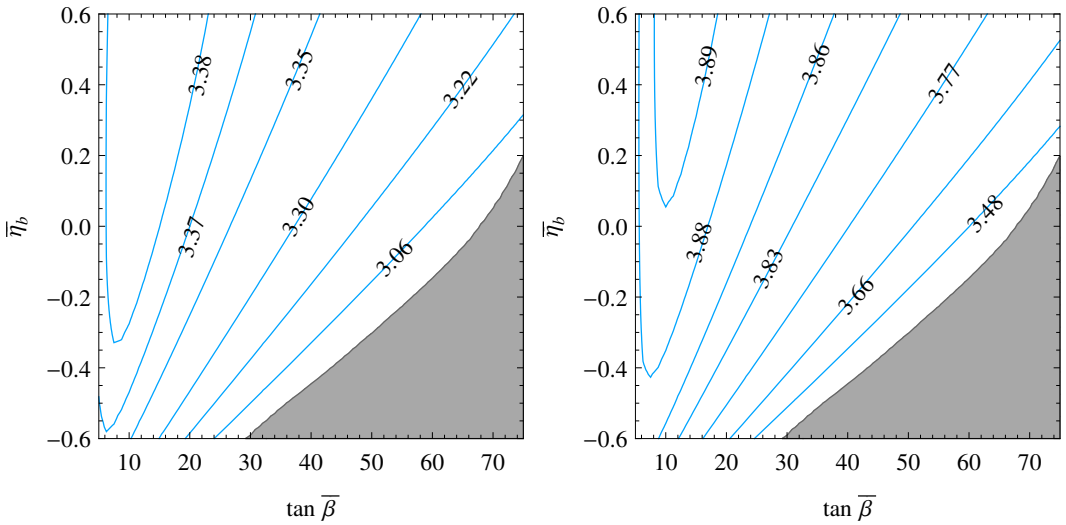

(a) $(1+\bar{\eta}_q)/(1+\bar{\eta}_b)\ \theta_{13}^{q,\mathrm{MSSM}}\ /\ 10^{-3}$ **(b)** $(1+\bar{\eta}_q)/(1+\bar{\eta}_b)\ \theta_{23}^{q,\mathrm{MSSM}}\ /\ 10^{-2}$

Figure 5.5: Results for the CKM mixing angles $\theta_{13}^{q,\mathrm{MSSM}}$ and $\theta_{13}^{q,\mathrm{MSSM}}$ at M_{GUT} in the $\overline{\mathrm{DR}}$ scheme (assuming $M_{\mathrm{SUSY}} = 1$ TeV), multiplied by the respective threshold correction factor, cf. eq. (5.12a). The results of the mixing angles at the GUT scale can be obtained by multiplying the values in the plots by $[(1+\bar{\eta}_q)/(1+\bar{\eta}_b)]^{-1}$. As discussed in sec. 5.3, the GUT-scale quantities can be given as functions of only $\tan\bar{\beta}$ and $\bar{\eta}_b$ to a good approximation. The parameters $\bar{\beta}$ and $\bar{\eta}_b$ are defined in eqs. (5.6) and (5.7), respectively. If the threshold effects for the charged leptons are neglected, $\tan\bar{\beta}$ simply reduces to the usual $\tan\beta$. In the dark grey regions of the plots, at least one of the Yukawa couplings becomes non-perturbative before or at M_{GUT}.

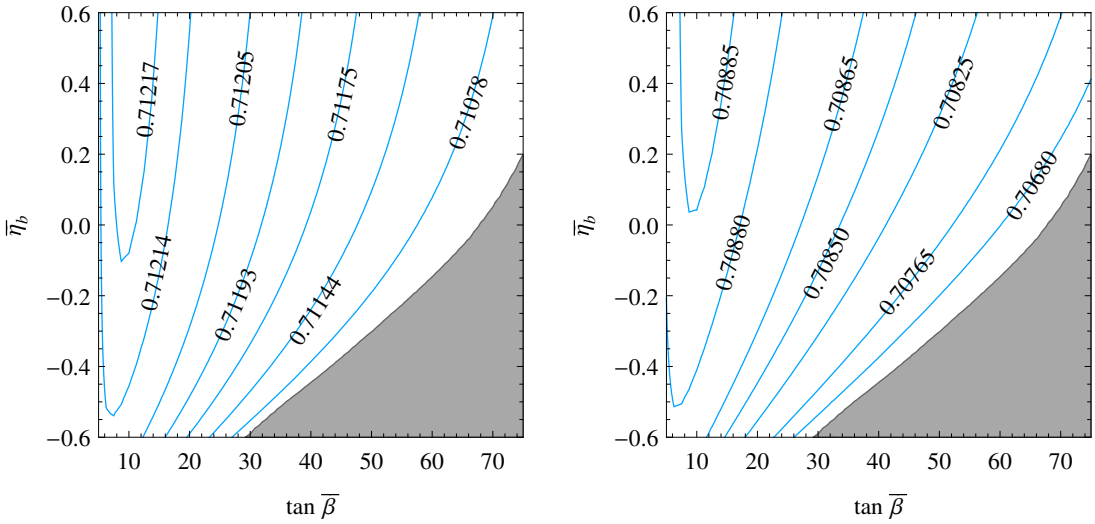

(a) g_1 **(b)** g_2

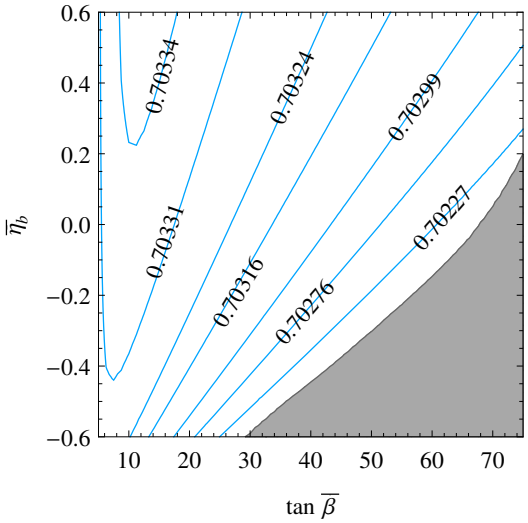

(c) g_3

Figure 5.6: Results for the gauge couplings g_1, g_2 and g_3 at $M_{\mathrm{GUT}} = 2 \cdot 10^{16}$ GeV in the $\overline{\mathrm{DR}}$ scheme (assuming $M_{\mathrm{SUSY}} = 1$ TeV), in GUT normalisation, i.e. $g_1^2 = 5/3\, g'^2$. As discussed in sec. 5.3, the GUT-scale quantities can be given as functions of only $\tan\bar{\beta}$ and $\bar{\eta}_b$ to a good approximation. The parameters $\bar{\beta}$ and $\bar{\eta}_b$ are defined in eqs. (5.6) and (5.7), respectively. If the threshold effects for the charged leptons are neglected, $\tan\bar{\beta}$ simply reduces to the usual $\tan\beta$. In the dark grey regions of the plots, at least one of the Yukawa couplings becomes non-perturbative before or at M_{GUT}.

MSSM Quantity z_i	Relative Uncertainty $\sigma(z_i)/z_i$ at $M_{\rm GUT}$
$y_u^{\rm MSSM}$	29%
$y_d^{\rm MSSM}$	8.5%
$y_s^{\rm MSSM}$	5.3%
$y_c^{\rm MSSM}$	3.3%
$y_b^{\rm MSSM}$	see fig. 5.4
$y_t^{\rm MSSM}$	see fig. 5.4
$\theta_{12}^{q,\rm MSSM}$	0.22%
$\theta_{23}^{q,\rm MSSM}$	1.5%
$\theta_{13}^{q,\rm MSSM}$	3.3%
$\delta^{q,\rm MSSM}$	4.9%
$y_e^{\rm MSSM}$	0.6%
$y_\mu^{\rm MSSM}$	0.6%
$y_\tau^{\rm MSSM}$	see fig. 5.4
g_3	0.09%
g_2	0.025%
g_1	0.020%

Table 5.3: Relative uncertainties $\sigma(z_i)/z_i$ for the running GUT-scale parameters z_i, assuming $M_{\rm SUSY} = 1$ TeV. For the third generation Yukawa couplings the relative uncertainties depend on $\tan\bar{\beta}$ and $\bar{\eta}_b$ as shown in fig. 5.4. As explained in the caption of tab. 5.2, we have used 0.5% relative uncertainty for the charged lepton Yukawa couplings at $M_{\rm SUSY}$. This is enlarged to 0.6% uncertainty at $M_{\rm GUT}$, as shown here, due to RG effects and the uncertainties for the other parameters.

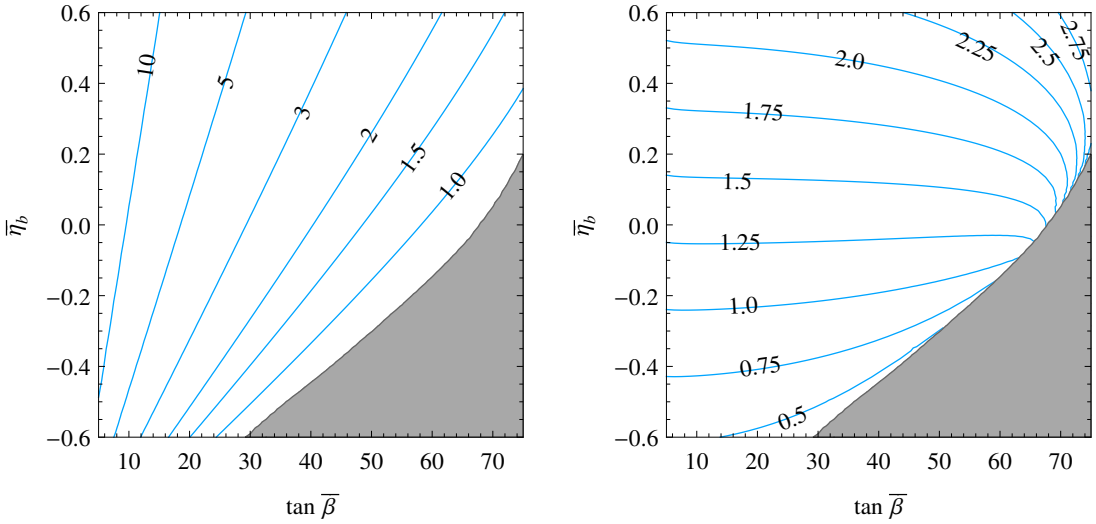

(a) $y_t^{\mathrm{MSSM}}/y_b^{\mathrm{MSSM}}$ **(b)** $y_\tau^{\mathrm{MSSM}}/y_b^{\mathrm{MSSM}}$

Figure 5.7: Values of the GUT-scale Yukawa coupling ratios $y_t^{\mathrm{MSSM}}/y_b^{\mathrm{MSSM}}$ and $y_\tau^{\mathrm{MSSM}}/y_b^{\mathrm{MSSM}}$ as functions of $\tan\bar{\beta}$ and $\bar{\eta}_b$ for $M_{\mathrm{SUSY}} = 1$ TeV. The parameters $\bar{\beta}$ and $\bar{\eta}_b$ are defined in eqs. (5.6) and (5.7), respectively. If the threshold effects for the charged leptons are neglected, $\tan\bar{\beta}$ simply reduces to the usual $\tan\beta$. In the dark grey regions of the plots, at least one of the Yukawa couplings becomes non-perturbative before or at M_{GUT}.

CHAPTER 6

Hints from Electroweak Fine-tuning

6.1 Motivation

For quite some time, the LHC experiments ATLAS and CMS only found negative results in their search for new particles, e.g. in direct searches for superpartners [69], based on ~ 5 fb^{-1} of data. Fortunately, they did find a new resonance, mainly based on excesses of events in the $\gamma\gamma$ and ZZ^* channels. Soon after the report of this discovery, found to be consistent with a SM Higgs boson with a mass of $m_h = 125.7 \pm 0.4$ GeV [15], it was realised that such a mass was compatible with low-energy SUSY, specifically the MSSM, provided quite heavy top squarks (with masses $\gtrsim \mathcal{O}(1)$ TeV) and/or large left-right stop mixing (see for instance [70]) are present.

At first glance, the negative results of direct SUSY searches and the comparatively heavy Higgs boson mass are thus consistent with each other. However, since a major motivation for the postulation of SUSY is the solution of the hierarchy problem – naively requiring superpartner masses of the electroweak symmetry breaking scale – it suggests itself to ask whether the MSSM can accomplish this task in a still satisfyingly natural way.

Regarding high-scale (i.e. GUT-scale) SUSY breaking scenarios, it turns out that in the cMSSM a significant amount of fine-tuning (at least $\gtrsim \mathcal{O}(100)$) is unavoidable to explain a Higgs mass of $m_h \approx 126$ GeV for stabilising the electroweak scale. We thus want to investigate this issue of naturalness in the context of models where one or more of the soft breaking parameter universality assumptions of the cMSSM are relaxed.

To find promising and simple GUT-scale SUSY breaking schemes that deviate from the cMSSM, we adopt the following strategy: we start by considering a generic setup with 17 independent parameters, resembling the phenomenological MSSM (pMSSM) (see sec. 3.3.1), but defined at the GUT scale, in order to identify the parameters that are most significant for the fine-tuning of the electroweak scale. This allows

to find rigid relations among the parameters where fine-tuning is decreased. After discussing multiple possibilities, we mainly focus on non-universal relations among gaugino masses, whose possible impact on fine-tuning has also been studied before the LHC results by [71, 72, 73].[1]

In this context, we will then study the interplay between fine-tuning, model predictions for the Higgs boson mass and the GUT-scale ratios of gaugino masses as well as third family Yukawa couplings. In our numerical analysis, we include various experimental constraints, e.g. from BR($b \to s\gamma$), BR($B_s \to \mu^+\mu^-$) and BR($B_u \to \tau\nu_\tau$). We do not impose strict constraints from requiring that the $(g-2)_\mu$ deviation from the SM is reconciled using SUSY particles.

The rest of this chapter is organised as follows: in the next section we present a semi-analytical way to study the dependence of the electroweak scale on the parameters of the GUT-scale boundary conditions as inspired by the pMSSM. Thanks to this, we can examine regions with low fine-tuning and identify non-universal gaugino masses as most promising candidate. In sec. 6.3, we briefly revisit the dependence of GUT-scale Yukawa coupling ratios on low energy SUSY threshold corrections and the dependence of the latter on the SUSY spectrum. Subsequently in sec. 6.4, we present the results of an extensive numerical analysis of fine-tuning in the MSSM scenario with non-universal gaugino masses (at the GUT scale) and compare the results to various experimental constraints, most importantly the discovery of the Higgs boson at around 126 GeV.

6.2 Fine-Tuning in the MSSM

Fine-tuning in the MSSM has been extensively studied in the literature, starting with [77].[2] In the following, we present a brief review of the problem in order to introduce the concepts of our analysis and comment on the corrections beyond tree-level that we have included [73, 79].

As shown in eq. (3.31b), in the MSSM, the Z-boson mass can be expressed in terms of $\tan\beta$, the supersymmetric mass parameter μ and the soft SUSY breaking mass terms of H_u and H_d. For moderate and large $\tan\beta$, the relation can be simplified (to a good approximation) to

$$\frac{M_Z^2}{2} \approx -|\mu|^2 - m_{H_u}^2 + \mathcal{O}(m_{H_{u,d}}^2/(\tan\beta)^2) \; . \tag{6.1}$$

The right-hand side can be expressed in terms of fundamental parameters of the SUSY breaking scheme by considering the renormalisation group evolution of μ and $m_{H_u}^2$ from the GUT scale to the low energy scale. Since experimental constraints force the

[1] A discussion of the fine-tuning price of a 126 GeV Higgs after the first hints in December 2011 within several SUSY models has been also given in [74] (see also [75, 76]).

[2] For an extensive list of references, see e.g. [78, 74].

soft SUSY breaking parameters to be somewhat larger than M_Z, a certain amount of tuning between μ and $m_{H_u}^2$ is needed. In order to quantify this fine-tuning, the following measure has been introduced [77]

$$\Delta_a = \left| \frac{\partial \log M_Z}{\partial \log a} \right| = \left| \frac{a}{2M_Z^2} \frac{\partial M_Z^2}{\partial a} \right| . \tag{6.2}$$

The value of Δ_a gives the dependence of M_Z on variations of a given fundamental – i.e. presumably GUT-scale – Lagrangian parameter a. The value of such a quantity has an intuitive interpretation: for instance $\Delta_a = 100$ implies a necessary cancellation to 1 part in 100. This definition not only covers the obvious fine-tuning needed for μ needed to fulfil eq. (6.1), but also the tuning needed for cases where cancellations between large fundamental parameters result in a small $m_{H_u}^2$ via competing RG evolution effects. The global measure of fine-tuning for a given point in parameter space is then defined as the maximum of all single parameter Δ_a's as in

$$\Delta = \max_a \Delta_a . \tag{6.3}$$

Going through the single parameter contributions Δ_a one by one, one first sees that the fine-tuning in μ is special as its low energy value is determined by demanding the experimentally measured value of M_Z. Hence, neglecting RG effects for the moment, Δ_μ can be approximately expressed in terms of $m_{H_u}^2$ as

$$\Delta_\mu \approx \left| 2\frac{m_{H_u}^2}{M_Z^2} + 1 \right| . \tag{6.4}$$

Of course, in our numerical analysis later, the running of μ is included.

The discussion of the fine-tuning measures Δ_a of other parameters is more involved as they enter eq. (6.1) only via the RG evolution of $m_{H_u}^2$. It is, however, possible to approximately express $m_{H_u}^2$ as a polynomial in the high-energy parameters of the theory, such that

$$\Delta_a \approx \left| \frac{a}{M_Z^2} \frac{\partial m_{H_u}^2}{\partial a} \right| , \tag{6.5}$$

for all parameters $a \not\equiv \mu$.

The coefficients of this polynomial depend strongly on the top Yukawa coupling y_t and the strong gauge coupling constant α_s. Therefore it was argued in the literature that these two parameters should be included in the fine-tuning measure as well, see, e.g. [80, 81]. However, since they are measured – in contrast to the parameters introduced in the SM to MSSM transition – there are different approaches for including them in the global fine-tuning measure Δ. In this study, we will follow previous works [80, 81] and use the approach to weight them with their experimental uncertainty σ, e.g. for y_t,

$$\Delta_{y_t} = \left| \frac{\sigma_{y_t}}{2M_Z^2} \frac{\partial M_Z^2}{\partial y_t} \right| = \left| \frac{\sigma_{y_t}}{y_t} \frac{y_t}{2M_Z^2} \frac{\partial M_Z^2}{\partial y_t} \right| , \tag{6.6}$$

and similarly for the strong coupling constant. Note that we have to use the RG evolved experimental error at the GUT scale, which is bigger than the lower energy one for the top Yukawa coupling and smaller for the strong coupling constant. In our numerical analysis later on, we used the mean values at low energies $M_t = 172.9 \pm 0.6 \pm 0.9$ GeV (the top quark pole mass) [82] and $\alpha_s(M_Z) = 0.1184 \pm 0.0007$ [82] with the relative uncertainties $\sigma_{y_t}^{\text{rel}} = 4\%$ and $\sigma_{\alpha_s}^{\text{rel}} = 0.2\%$ at the GUT scale.

In the following, we present semi-analytical formulae for the dependence of the low-scale $m_{H_u}^2$ on the assumed fundamental soft SUSY breaking GUT-scale parameters, which can be used to tell where one can expect a reduction in fine-tuning. Note that, for the sake of simplicity and manageable equation size, we do not include the parameters y_t and α_s in our semi-analytical discussion. Nevertheless, their effect will be included in the numerical analysis as described above.

Going beyond tree level, one has to take into account loop effects [73, 79], which modify the original eq. (6.1). The effect of this is two-fold. On the one hand, the Higgs potential is obviously modified; on the other hand loop corrections also affect the Higgs vacuum expectation value v. We will not go into a detailed discussion here, but we notice that taking into account all the relevant corrections roughly reduces the fine-tuning by a factor M_Z^2/m_h^2, where m_h is the light Higgs boson mass. Such an effect is clearly sizeable in the parameter region of interest, where $m_h \sim 126$ GeV.

Before we come to the semi-analytical discussion, we would like to remark that a fine-tuning measure should be taken with some caution. It is a matter of personal taste how much fine-tuning one accepts as "natural" and also the used definition might differ according to preference. Thus, we want to stress that the aim of this study is mainly a comparison of different parameter regions. A relative difference in fine-tuning would then render one region more attractive to us than another one.

6.2.1 Fine-Tuning with pMSSM Parameters

As mentioned above, we express $m_{H_u}^2$ in terms of the GUT-scale parameters inspired by the pMSSM low energy parametrisation, shown in sec. 3.3.1. In particular, we consider the same parametrisation with one scalar soft mass for the first and second generation and one for the third generation per sfermion type and take the gaugino masses to be non-universal also at the GUT scale. Regarding the trilinear couplings, we ignore the parameters for the first two generations and set them equal to the third generation one. Instead of low-scale μ and the CP-odd Higgs mass m_{A_0}, we use the GUT-scale value of $m_{H_u}^2$ and $m_{H_d}^2$ as free parameters and denote them by $m_{h_u}^2$ and $m_{h_d}^2$ respectively the minimise the potential for confusion.

Due to the form of the RG equations of the soft breaking parameters (see e.g. [67]), the dependence of the low energy scale $m_{H_u}^2$ on the GUT-scale parameters can be

written as

$$m_{H_u}^2 = \sum_i a_i m_i^2 + \frac{1}{2}\sum_{i,j} N_i b_{ij} N_j \ , \tag{6.7}$$

where the parameters m_i^2 are soft scalar masses and the parameters $N_i \equiv (M_1, M_2, M_3, A_t, A_b, A_\tau)$ are the gaugino masses and trilinear couplings[3], which we assume to be real. The parameters a_i are real and the matrix b_{ij} is a general symmetric (and real) 6×6 matrix.

To make the deviation from the universality assumptions of the cMSSM more obvious, we introduce the following dimensionless quantities:

$$\eta_\alpha = M_\alpha / M_3 \quad \text{with } \alpha = 1,2,3 \ , \quad \eta_i = A_i / M_3 \quad \text{with } i = t, b, \tau \ , \tag{6.8}$$

which, of course, implies $\eta_3 = 1$. Thus we can write

$$N_i = M_3 \cdot (\eta_1, \eta_2, \eta_3, \eta_t, \eta_b, \eta_\tau) \ . \tag{6.9}$$

The fine-tuning measure as introduced in eq. (6.3) can now be easily written down as

$$\Delta_{m_i} = \left| 2 a_i \frac{m_i^2}{M_Z^2} \right| \ , \quad \Delta_m = \max_i \Delta_{m_i} \ , \tag{6.10}$$

for the scalar masses, and for the other soft terms

$$\Delta_{N_i} = \left| \frac{\sum_j N_i b_{ij} N_j}{M_Z^2} \right| \quad (\text{no sum over } i) \ , \quad \Delta_N = \max_i \Delta_{N_i} \ , \tag{6.11}$$

and for μ

$$\Delta_\mu \approx \left| 2 \frac{\sum_i a_i m_i^2 + \frac{1}{2}\sum_{i,j} N_i b_{ij} N_j}{M_Z^2} + 1 \right| \ . \tag{6.12}$$

Having this in mind, we turn to expressing $m_{H_u}^2$ at the SUSY scale in the mentioned parameters. For this, we use the best fit point found by the global cMSSM parameter fit Fittino [83], corresponding to $M_3 = 1.016$ TeV, $m_i = 0.504$ TeV for every i, $\eta_i = N_i/M_3 = (1, 1, 1, -2.825, -2.825, -2.825)$, $\tan\beta = 18$ and μ positive. Using `softSUSY 3.2.3` [84], we find the semi-analytical expansion

$$\begin{aligned} m_{H_u}^2\big|_{M_{\text{SUSY}}} = {} & 0.655\, m_{h_u}^2 + 0.026\, m_{h_d}^2 \\ & - 0.048\, m_{\tilde{Q}_1}^2 + 0.108\, m_{\tilde{u}_1^c}^2 - 0.049\, m_{\tilde{d}_1^c}^2 + 0.051\, m_{\tilde{L}_1}^2 - 0.051\, m_{\tilde{e}_1^c}^2 \\ & - 0.342\, m_{\tilde{Q}_3}^2 - 0.267\, m_{\tilde{u}_3^c}^2 - 0.022\, m_{\tilde{d}_3^c}^2 + 0.025\, m_{\tilde{L}_3}^2 - 0.025\, m_{\tilde{e}_3^c}^2 \end{aligned}$$

[3] To be explicit, the trilinear parameters A_x are defined such that, e.g., the trilinear matrix A_u is given by $A_u = A_t Y_u$ at the GUT scale. They are thus a generalisation of the cMSSM parameter A_0.

$$
\begin{aligned}
&+ M_3^2\,(0.0030\,\eta_b^2 - 0.1191\eta_t^2 + 0.0018\,\eta_\tau^2) \\
&+ M_3^2\,(0.0008\,\eta_b\eta_t + 0.0006\,\eta_b\,\eta_\tau + 0.0003\,\eta_t\,\eta_\tau) \\
&+ M_3^2\,(0.2790\,\eta_t + 0.0066\,\eta_b + 0.0118\,\eta_\tau) \\
&+ M_3^2\,\eta_1\,(0.0131\,\eta_t + 0.0001\,\eta_b + 0.0001\,\eta_\tau) \\
&+ M_3^2\,\eta_2\,(0.0713\,\eta_t - 0.0006\,\eta_b - 0.0012\,\eta_\tau) \\
&- M_3^2\,(1.3460 + 0.0346\,\eta_1 - 0.0165\,\eta_1^2 \\
&\qquad\qquad + 0.1392\,\eta_2 - 0.2256\,\eta_2^2 + 0.0052\,\eta_1\,\eta_2)\,,
\end{aligned}
\tag{6.13}
$$

where η_3 has already been replaced with 1. Already at first glance, it is easy to see that the most significant contributions come from the stop and Higgs soft mass parameters and from the gluino mass.

The coefficients a_i of eq. (6.7) can be directly read off from eq. (6.13). In order to show the terms involving the parameters $\eta_i = N_i/M_3$ in a transparent way, we also display the coefficients b_{ij} as a (symmetric) matrix:

$$
b_{ij} = \begin{pmatrix}
0.033 & -0.0052 & -0.0346 & 0.0131 & 0.0001 & 0.0001 \\
 & 0.4512 & -0.1392 & 0.0713 & -0.0006 & 0.0012 \\
 & & -2.6920 & 0.2790 & 0.0066 & 0.0118 \\
 & & & -0.2382 & 0.0008 & 0.0003 \\
 & & & & 0.0060 & 0.0006 \\
 & & & & & 0.0036
\end{pmatrix} . \tag{6.14}
$$

Even though the coefficients a_i and b_{ij} were numerically obtained in the vicinity of a specific point in parameter space, we checked that they provide a reasonably accurate estimate of $m_{H_u}^2$ in wide regions of parameter space. The corresponding uncertainty of the coefficients can be estimated as roughly of the order of $10 - 20\%$. This is good enough for the qualitative discussion we present on possible strategies to reduce the fine-tuning in the following subsections. Nevertheless, the results we present in sec. 6.4 are based on a full numerical analysis, with the RG evolution and fine-tuning of all parameters computed in each point of the parameter space separately.

6.2.2 Our Strategy

In order to find SUSY breaking schemes with reduced fine-tuning, we assume that the underlying model of SUSY breaking predicts certain fixed relations between the SUSY breaking parameters at a high energy scale (e.g. at the GUT scale). As a consequence, cancellations among different terms in eq. (6.13) can occur naturally, which can lead to a reduced fine-tuning. Such a behaviour is a well-known property of models with universal scalar masses (like the cMSSM), for which the coefficients a_i in eq. (6.13) cancel almost completely.[4]

[4]This property is known as "focus point" [85, 86].

As mentioned above, the coefficients a_i and b_{ij} depend strongly on the top Yukawa coupling and the strong coupling constant and thereby both enter the fine-tuning measure. Following our discussion before, we weight the individual fine-tuning in these quantities by their experimental uncertainty. It turns out that the fine-tuning in the strong coupling constant is then very small and only the fine-tuning in y_t plays a role. Due to the rather involved dependence of the coefficients on these two parameters we will only include their effects in the numerical results. For the semi-analytical discussion here, we have fixed y_t and α_s, and checked that varying them within their experimentally allowed ranges does not change the results qualitatively.

In the light of the Higgs discovery, the cMSSM unavoidably has a certain amount of fine-tuning either from quite heavy squarks or from a large A-term (in maximal mixing scenarios). In this study, we therefore consider the possibility that the underlying theory predicts different, non-universal (but fixed) boundary conditions at the GUT scale, namely non-universal scalar masses (NUSM) and non-universal gaugino masses (NUGM). Although such relations may not hold exactly in realistic models, they may guide towards more natural SUSY scenarios.

6.2.3 Fine-Tuning from the Scalar Sector Parameters

We will now discuss possible NUSM scenarios motivated by different unified theory symmetry groups. First, let us point out that the assumption of sfermion soft mass universality as in the cMSSM features a significant reduction of fine-tuning due to an almost-complete cancellation between the largest contributions in eq. (6.13), i.e. between the term with $m^2_{h_u}$ and the terms with $m^2_{\tilde{Q}_3}$ and $m^2_{\tilde{u}^c_3}$. From the point of view of naturalness, a similar relation between $m^2_{h_u}$ and $m^2_{\tilde{Q}_3}, m^2_{\tilde{u}^c_3}$ is therefore desirable.

Let us now consider non-universal fixed ratios for the soft scalar masses motivated by unified theories: if we assume that the gauge couplings and the SM fields are (partially) unified into a smaller set of couplings or irreducible representations as shown in sec. 4.2, this automatically also means that certain soft breaking terms are related by symmetry, i.e. they have a fixed ratio. The three candidates for the defining symmetry groups we consider are $SU(5)$ [46] and Pati–Salam [53], which can in turn both be embedded in $SO(10)$ [52]. For simplicity, we assume that possible higher order GUT symmetry breaking corrections that induce further splittings within one irreducible representation can be neglected in each case and that there is no splitting between the soft terms of the first two generations as before.

- In the case of $SU(5)$, eq. (6.13) reduces to

$$\begin{aligned} m^2_{H_u}\big|_{M_{\text{SUSY}}} = &-0.009\, m^2_{\tilde{\mathcal{T}}_1} + 0.002\, m^2_{\tilde{\mathcal{F}}_1} - 0.634\, m^2_{\tilde{\mathcal{T}}_3} + 0.003\, m^2_{\tilde{\mathcal{F}}_3} \\ &+ 0.655\, m^2_{h_u} + 0.026\, m^2_{h_d} \\ &+ \text{gaugino masses and trilinear terms}\,, \end{aligned} \tag{6.15}$$

where $m^2_{\tilde{\mathcal{T}}_i}$ stands for the masses of the tenplets of $SU(5)$, which contain the coloured doublet, the up-type coloured singlet and charged lepton singlet fields ($m^2_{\tilde{Q}_i} = m^2_{\tilde{u}^c_i} = m^2_{\tilde{e}^c_i} = m^2_{\tilde{\mathcal{T}}_i}$), and $m^2_{\tilde{\mathcal{F}}_i}$ of the fiveplets of $SU(5)$, which contain the down-type coloured singlet and the lepton doublet fields ($m^2_{\tilde{d}^c_i} = m^2_{\tilde{L}_i} = m^2_{\tilde{\mathcal{F}}_i}$). We allow an arbitrary splitting of the Higgs fields from the other scalar mass parameters and also between up and down Higgs themselves. One can clearly see that the simplest option in order not to strongly increase the fine-tuning is to impose a fixed relation where $m^2_{\tilde{\mathcal{T}}_3} \approx m^2_{h_u}$, because otherwise one has to consider the fine-tuning from each parameter separately and has to deal with the two large coefficients, cf. eq. (6.3).

- Turning to the case of Pati–Salam, we find

$$\begin{aligned} m^2_{H_u}\big|_{M_{\text{SUSY}}} = {} & 0.003\, m^2_{\tilde{l}_1} + 0.008\, m^2_{\tilde{r}_1} - 0.317\, m^2_{\tilde{l}_3} - 0.314\, m^2_{\tilde{r}_3} + 0.681\, m^2_h \\ & + \text{gaugino masses and trilinear terms} , \end{aligned} \tag{6.16}$$

  where, in this case, $\tilde{l}$ denotes the left-handed doublet fields ($m^2_{\tilde{Q}_i} = m^2_{\tilde{L}_i} = m^2_{\tilde{l}_i}$), $\tilde{r}$ denotes the right-handed doublet fields ($m^2_{\tilde{u}^c_i} = m^2_{\tilde{d}^c_i} = m^2_{\tilde{e}^c_i} = m^2_{\tilde{r}_i}$) and h denotes the Higgs bi-doublet ($m^2_{h_u} = m^2_{h_d} = m^2_h$). The conclusions are similar to the $SU(5)$ case. The simplest fixed relation one can impose in order not to increase fine-tuning compared to the cMSSM is $m^2_{\tilde{l}_3} \approx m^2_{\tilde{r}_3} \approx m^2_h$.

- Finally, let us discuss the situation in $SO(10)$ GUTs. Here, our assumptions allow for independent soft mass terms of the matter fields, $m^2_{16_1}$ and $m^2_{16_3}$ and for the Higgs fields $m^2_{h_u} = m^2_{h_d} = m^2_{10}$, yielding

$$\begin{aligned} m^2_{H_u}\big|_{M_{\text{SUSY}}} = {} & -0.011\, m^2_{16_1} - 0.631\, m^2_{16_3} + 0.681\, m^2_{10} \\ & + \text{gaugino masses, trilinear terms} , \end{aligned} \tag{6.17}$$

  which implies that again, a fixed relation beyond the ones from the GUT itself would have to be imposed (e.g. between m^2_{10} and $m^2_{16_3}$) in order to not to strongly increase fine-tuning.

- A further more advanced possibility is given by the possibility that the sfermion soft mass terms are given predominantly by D-term potential contributions, see sec. 4.3.1. Parametrising the three possible linearly independent D-term contributions as D_Y, D_X and D_S as defined in [55], one finds

$$\begin{aligned} m^2_{H_u}\big|_{M_{\text{SUSY}}} = {} & 0.217\, D_Y + 0.634\, D_X + 0.668\, D_S \\ & + \text{gaugino masses, trilinear terms} . \end{aligned} \tag{6.18}$$

Demanding that all D-term contributions to the sfermion soft breaking terms remain non-negative, there is a unique fixed relation between the D_i that minimises the resulting coefficient in eq. (6.18): $D_X = -D_S$, $D_Y = 0$. This can be achieved via the existence (and spontaneous breaking) of a $U(1)$ symmetry with charges $q(Q) = q(u^c) = q(e^c) = 0 = q(H_u)$ and $q(d^c) = q(L) = 1 = -q(H_d)$ up to normalisation. It might thus be compatible with $SU(5)$ and would imply vanishing sfermion soft mass terms for all component fields inside ten-plets (as well as H_u) at the GUT scale. Unfortunately, this simply means that there is no fine-tuning because the parameters with the largest coefficients are zero.

A few further comments are in order. First, one can see that the soft terms for the first two families enter with small coefficients into $m_{H_u}^2$. This illustrates the well-known fact that these soft masses can be significantly larger than the third family ones, without paying a large price in fine-tuning. Furthermore, in the above discussion, we have focused on fixed relations from GUT structures. As we have shown, with most fixed relations alone one would increase fine-tuning compared to the cMSSM case. From the above equations one can imagine additional fixed relations on top of these structures which could come from a more fundamental theory and can in principle reduce fine-tuning by leading to a cancellation in the contributions to $m_{H_u}^2$. However, we will not investigate such cases in more detail here.

Another relevant point is that we have only discussed "direct" effects on the fine-tuning, i.e. the effects on the fine-tuning measure around a given SUSY parameter point. We note that there can also be "indirect" effects: namely when introducing a non-universality allows to avoid certain constraints on the SUSY parameter space and makes regions with lower fine-tuning accessible (e.g. a "compressed" spectrum helps to evade constraints from direct SUSY searches at the LHC [87]).

Finally, let us note that small splittings in models where the soft parameters are universal (cMSSM-like) at the leading order and get only corrected by small additional contributions (e.g. by higher dimensional operators in flavour models, see, for instance, [88]) can have a certain degree of non-universality without increasing the fine-tuning too much. However, large non-universalities ($\mathcal{O}(1)$) again lead back to the same situation as in the general case, as shown above.

In summary, the possibilities to reduce the fine-tuning with fixed relations between sfermion soft mass parameters seem rather limited and mostly lead to the same relation: sfermion mass universality as in the cMSSM. Otherwise, the fine-tuning increases rather than decreases. We therefore consider this case complete and not study it in more detail numerically.

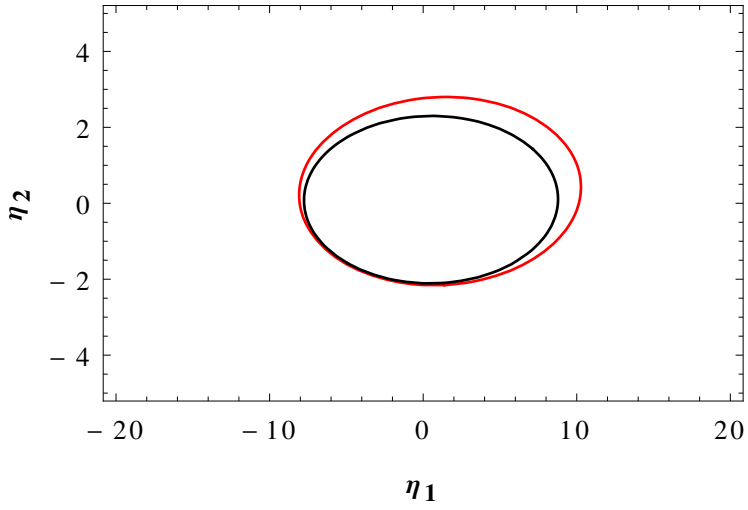

Figure 6.1: The two ellipses in the η_1-η_2 plane which minimise the fine-tuning in the case on non-universal gaugino masses. The red ellipse corresponds to eq. (6.21a) and the black one to eq. (6.21b).

6.2.4 Fine-Tuning from Gaugino Masses and Trilinears

Having discussed non-universalities in the scalar soft mass terms, we now turn to gaugino masses and trilinear SUSY breaking couplings. Since they appear together in the polynomial of eq. (6.13), they cannot be discussed separately. For simplicity, we concentrate on the case where the trilinear couplings are universal $\eta_t = \eta_b = \eta_\tau = \eta_A$. In principle, one can also try to reduce the fine-tuning by assuming fixed relations for η_t, η_b, and η_τ. This leads to a similar discussion as for gaugino masses except that the required ratios will be quite large due to the smallness of the coefficients involving η_b and η_τ in eq. (6.13).

For the case of non-universality strictly in gaugino masses, the $m_{H_u}^2$ polynomial simplifies to

$$\begin{aligned} m_{H_u}^2(M_{\text{SUSY}}) = &-M_3^2\,(1.3460 + 0.0346\,\eta_1 - 0.0165\,\eta_1^2 \\ &\qquad + 0.1392\,\eta_2 - 0.2256\,\eta_2^2 + 0.0052\,\eta_1\,\eta_2) \\ &+ M_3^2\,\eta_A(0.2974 + 0.0132\,\eta_1 + 0.0718\,\eta_2) - 0.1125\,M_3^2\,\eta_A^2 \\ &+ \text{scalar masses} \\ \equiv &\,(f_1(\eta_1,\eta_2) + f_2(\eta_1,\eta_2)\,\eta_A + f_3\,\eta_A^2)\,M_3^2 + \dots\,, \end{aligned} \tag{6.19}$$

where we have again used $\eta_3 = 1$. The question is now under which conditions the fine-tuning, as defined in eqs. (6.10) and (6.12), is minimised.

Considering only the sector at hand, the overall fine-tuning is given by

$$\Delta \approx \left|\frac{M_3^2}{M_Z^2}\right| \max\left\{\begin{array}{c} |2\,f_3\,\eta_A^2 + f_2(\eta_1,\eta_2)\,\eta_A|, \\ |2\,f_1(\eta_1,\eta_2) + f_2(\eta_1,\eta_2)\,\eta_A| \end{array}\right\} . \tag{6.20}$$

Setting these two contributions to zero yields two possible solutions:

$$\textbf{Solution 1:}\ f_1(\eta_1,\eta_2) = 0, \qquad \eta_A = 0\ , \tag{6.21a}$$

$$\textbf{Solution 2:}\ f_1(\eta_1,\eta_2) = \frac{f_2(\eta_1,\eta_2)^2}{4f_3}, \qquad \eta_A = -\frac{f_2(\eta_1,\eta_2)}{2f_3}\ . \tag{6.21b}$$

With the parameters in eq. (6.19), the two solutions define two distinct ellipses in the η_1-η_2 plane, as shown in fig. 6.1. Later, in our numerical analysis, we will see that this is indeed a feature found in the parameter space.

Since the trilinear terms have a strong impact on the prediction of the Higgs boson mass, it is important to discuss the behaviour of η_A in more detail. For the first solution, the situation is trivial. The second solution can be re-written as

$$\begin{aligned} \eta_A &= 1.3516 + 0.0593\,\eta_1 \pm 0.7033\,\sqrt{(1-0.1138\,\eta_1)(1+0.1288\,\eta_1)}\ , \\ \eta_2 &= 0.0934 + 0.0021\,\eta_1 \pm 2.2040\,\sqrt{(1-0.1138\,\eta_1)(1+0.1288\,\eta_1)}\ , \end{aligned} \tag{6.22}$$

which implies that $0.52 < \eta_A < 2.24$. Interestingly, this implies for example that in the Fittino best fit point with $\eta_A = -2.825$, which we use as benchmark, the fine-tuning cannot be made arbitrarily small by choosing appropriate η_1 and η_2. Nevertheless, the fine-tuning can be reduced by a sizable factor: adjusting the gaugino mass ratios in the benchmark point, we find a minimal fine-tuning in this sub-sector of

$$\Delta = 1.93\left|\frac{M_3^2}{M_Z^2}\right| \quad \text{for } \eta_1 = -4.60 \text{ and } \eta_2 = -2.64\ , \tag{6.23}$$

compared to $\Delta = 3.65|M_3^2/M_Z^2|$ for $\eta_1 = \eta_2 = 1$.

Having discussed the fine-tuning in M_3 and η_A, we note that there are regions of parameter space where the fine-tuning in μ is the dominant contribution to the over-all Δ. If we insert the solutions of eqs. (6.21a), (6.21b) into eq. (6.19), we see that in both cases the contribution to $m_{H_u}^2$ proportional to M_3 vanishes completely (assuming η_A fixed to the solution). Assuming there are no significant cancellations, this means that $|m_{H_u}^2|$ is decreased as well, which in turn also decreases Δ_μ via eq. (6.4).

Regarding prior literature, we note that the first solution for the case $\eta_A = 0$ was already found in [73] – albeit with a slightly different notation setting $\eta_2 = 1$ instead of $\eta_3 = 1$. Consequently, hyperbolas were found instead of ellipses. The second solution, however, was not discussed therein. Instead, in [71] a related case was studied where also a fixed relation between the masses scales of gauginos and trilinear parameters was assumed, while in our analysis η_A is a free parameter.

6.3 Comments on SUSY Threshold Corrections

As shown in the previous chapter, the Yukawa coupling ratios at the GUT scale strongly depend on the SUSY threshold correction at low scales. Notably for the third family, phenomenologically interesting possibilities are, e.g., the standard bottom-tau Yukawa unification $y_\tau/y_b = 1$ or the alternative ratio $y_\tau/y_b = 3/2$, see also [49]. Based on the spectrum dependence of the SUSY threshold corrections, the GUT-scale Yukawa ratios are thus interesting discriminators between GUT models and SUSY breaking schemes respectively. Therefore, in this chapter, we also want to address the question whether one GUT-scale Yukawa coupling relations might be preferred based on fine-tuning.

In the following, we discuss some details of the parameter dependence of the $\tan\beta$ enhanced one-loop corrections to the Yukawa couplings of the down-type quarks and the charged leptons [31, 32]. For example, for the bottom quark Yukawa coupling, we can write

$$y_b^{\mathrm{SM}} = y_b^{\mathrm{MSSM}}(1 + \varepsilon_b \tan\beta)\cos\beta \; . \tag{6.24}$$

The correction ε_b can be decomposed into [89, 33, 90]

$$\varepsilon_b \approx \varepsilon^G + \varepsilon^B + \varepsilon^W + \varepsilon^y \; , \tag{6.25}$$

where[5]

$$\varepsilon^G = -\frac{2\alpha_S}{3\pi}\frac{\mu}{M_3} H_2(u_{\tilde{Q}_3}, u_{\tilde{d}_3}) \; , \tag{6.26a}$$

$$\varepsilon^B = \frac{1}{16\pi^2}\left[\frac{g'^2}{6}\frac{\eta_1 M_3}{\mu}\left(H_2(v_{\tilde{Q}_3}, x_1) + 2H_2(v_{\tilde{d}_i}, x_1)\right) + \frac{g'^2}{9}\frac{\mu}{\eta_1 M_3} H_2(w_{\tilde{Q}_3}, w_{\tilde{d}_3})\right] \; , \tag{6.26b}$$

$$\varepsilon^W = \frac{1}{16\pi^2}\frac{3g^2}{2}\frac{\eta_2 M_3}{\mu} H_2(v_{\tilde{Q}_3}, x_2) \; , \tag{6.26c}$$

$$\varepsilon^y = -\frac{y_t^2}{16\pi^2}\frac{\eta_t M_3}{\mu} H_2(v_{\tilde{Q}_3}, v_{\tilde{u}_3^c}) \; . \tag{6.26d}$$

Here $u_{\tilde{f}} = m_{\tilde{f}}^2/M_3^2$, $v_{\tilde{f}} = m_{\tilde{f}}^2/\mu^2$, $w_{\tilde{f}} = m_{\tilde{f}}^2/(\eta_1^2 M_3^2)$, $x_i = (\eta_i^2 M_3^2)/\mu^2$ for $i = 1, 2$ and the loop function H_2 is given by

$$H_2(x, y) = \frac{x \ln x}{(1-x)(x-y)} + \frac{y \ln y}{(1-y)(y-x)} \; . \tag{6.27}$$

In the cMSSM, it is possible to neglect ε^B and ε^W in a first approximation since they are suppressed by the smaller gauge couplings. In NUGM scenarios, this is in general

[5] Here, all parameters η_i are to be understood as SUSY-scale values. These are, however, directly proportional to the corresponding GUT-scale values to a good approximation (except for η_t).

not true anymore because the suppression might be compensated by an enhancement of the bino or wino mass parameter compared to the gluino one. This becomes quite important if (and when) our expectation of $\eta_1 \sim \mathcal{O}(10)$ from fig. 6.1 also applies numerically and can result in larger corrections than otherwise available.

Without some in-depth knowledge of the parameter space or simplifying assumptions, a quantitative statement is thus quite difficult. In general, one can expect significant corrections up to 50% for the GUT-scale Yukawa coupling ratios, see e.g. [33, 90].

6.4 Numerical Analysis

To improve our understanding obtained from the semi-analytical treatment, we turn to our numerical analysis. To this end, we use a modified version of the spectrum calculator `softSUSY` [84] to calculate the SUSY spectra, GUT-scale Yukawa coupling ratios and the fine-tuning. The modifications to `softSUSY` consist of including the already mentioned one-loop corrections to fine-tuning and the SUSY threshold corrections for the Yukawa couplings of all three fermion generations [31, 32, 89, 33, 90].

In a second step, we use the program `SuperIso` [91] in order to check experimental constraints for the observables $\mathrm{BR}(b \to s\gamma)$, $\mathrm{BR}(B_s \to \mu^+\mu^-)$ and $\mathrm{BR}(B_u \to \tau\nu_\tau)$. The experimental ranges that were considered are: $\mathrm{BR}(b \to s\gamma) = (355 \pm 24 \pm 9) \cdot 10^{-6}$ [92], $\mathrm{BR}(B_s \to \mu^+\mu^-) < 4.5 \cdot 10^{-9}$ at 95% CL [93] and $\mathrm{BR}(B_u \to \tau\nu_\tau) = (1.41 \pm 0.43) \cdot 10^{-4}$ [94].

Additionally, LEP bounds [82] on sparticle masses were applied and we discarded points where the $\tilde{\tau}$ is the lightest supersymmetric particle (LSP) and points leading to colour and charge breaking (CCB) vacua[6]. To study the impact of the Higgs boson discovery, we present results both with and without the Higgs mass constraint. Note that including constraints from direct SUSY searches at the LHC is not as straightforward and we will therefore only show a comparison with simplified model searches for illustrative purposes.

Concerning the 3.2σ level $(g-2)_\mu$ discrepancy from the Standard Model expectation [96], for this study, we consider it an experimental evidence that, while certainly interesting, still requires a full experimental confirmation from next generation experiments, such as those proposed at J-PARC [97] and at Fermilab [98]. For this reason, we have not imposed strict constraints on the spectrum based on this discrepancy. In fact, in the considered scenario, we find only very few and isolated points which satisfy $(g-2)_\mu$ at 2σ and predict a Higgs boson mass in agreement with the recent results. However, all of them correspond to a fine-tuning larger than $\mathcal{O}(100)$.

We have also not imposed constraints for the neutralino relic density nor from direct and indirect dark matter searches. Such constraints can be evaded by non-standard

[6] We use the so called 'traditional' bound [95]: $|(A_u)_{33}|^2 < 3\, y_t^2\, [(m^2_{\tilde{Q}})_{33} + (m^2_{\tilde{u}^c})_{33} + m^2_{H_u} + |\mu|^2]$ and similar formulae for A_d and A_e.

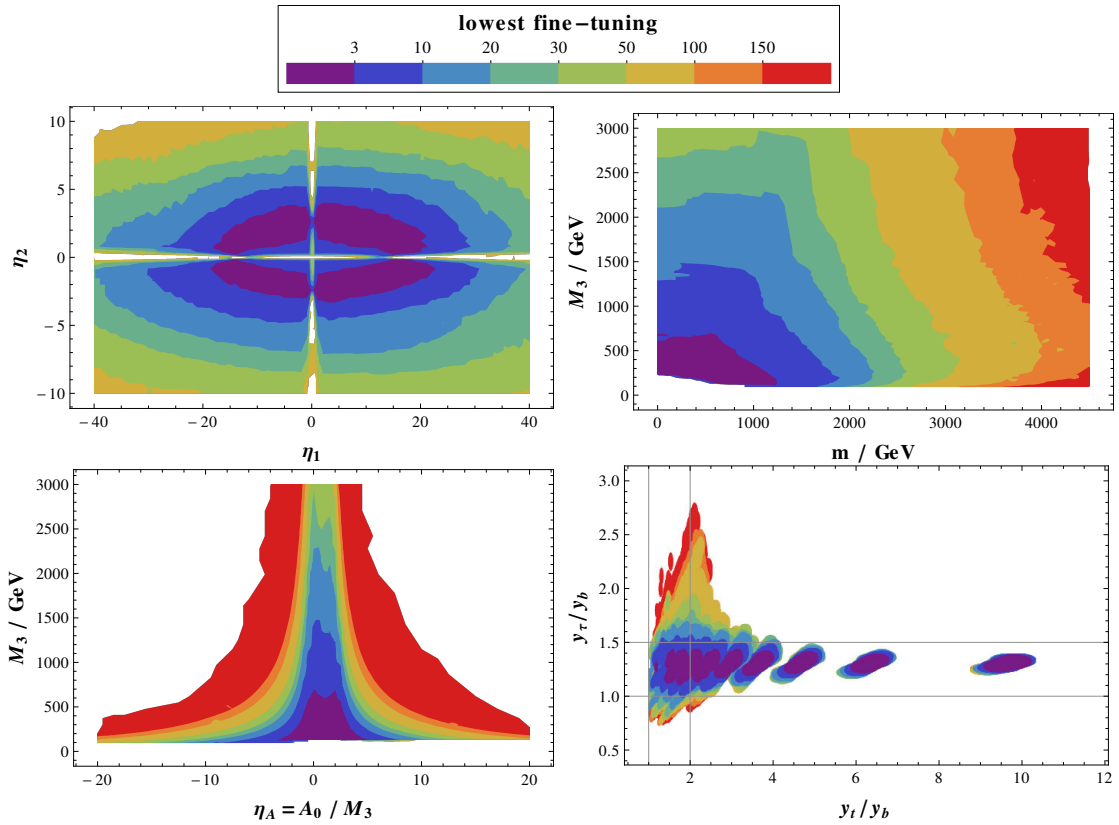

Figure 6.2: Lowest fine-tuning in the (a) η_1-η_2, (b) m-M_3, (c) η_A-M_3 and (d) y_t/y_b-y_τ/y_b planes consistent with the experimental bounds described in the text. For explanations of the parameters, see main text. The Higgs mass constraint is not included. The 1σ errors on the quark masses [82] are taken into account by scaling data points into error ellipses in the last plot correspondingly.

cosmological histories or a different LSP like the gravitino or the axino. Nevertheless, it is interesting to note that, in the region $\eta_2 \lesssim 0.5\,\eta_1$, the lightest neutralino is predominantly wino- or Higgsino-like, which implies that the canonically determined relic density is strongly suppressed. For these parameter regions, one cannot explain dark matter by thermal relic neutralinos, but at least there is no overproduction of them.

6.4.1 Before LHC Higgs and SUSY Results

As discussed previously, we expect to find an ellipse shaped region in the η_1-η_2 plane where fine-tuning is significantly lower than in the other parts of the parameter space, especially compared to the cMSSM.

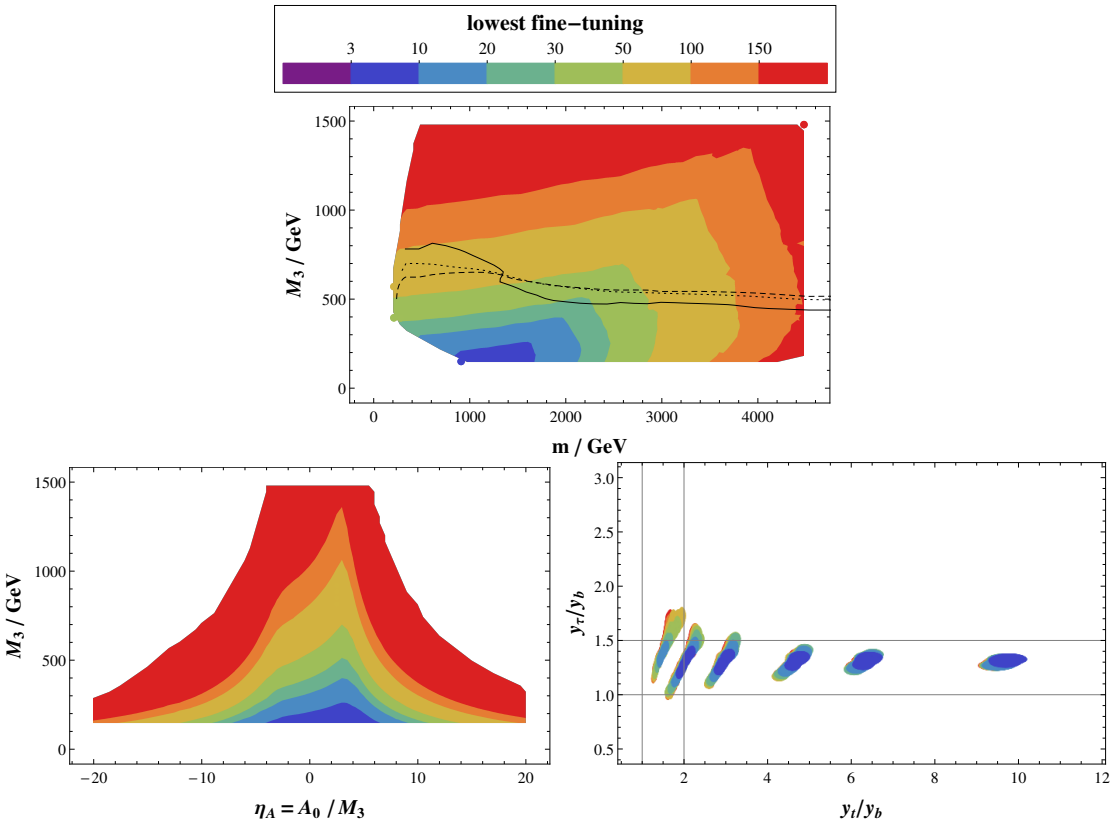

Figure 6.3: Lowest fine-tuning in the cMSSM in the (a) m_0-M_3, (b) η_A-M_3 and (c) y_t/y_b-y_τ/y_b planes consistent with the experimental bounds described in the text. For explanations of the parameters, see main text. The Higgs mass constraint is not included. The 1σ errors on the quark masses [82] are taken into account by scaling data points into error ellipses in the last plot correspondingly. In plot (a), we also included the LHC exclusion limits [99, 100, 101] as solid, dashed and dotted lines respectively for illustrative purposes – these were not applied as constraint anywhere. Note the different scale for M_3 and different point density for y_t/y_b due to different values for $\tan\beta$ compared to fig. 6.2.

To study this in detail, we performed a parameter scan over the following region in NUGM parameter space: the soft scalar mass parameters were set to be universal $m_i = m$ for every i and varied from 0 to 4.5 TeV, the GUT-scale gluino mass M_3 from 0.15 to 2 TeV, and $\eta_t = \eta_b = \eta_\tau = \eta_A$ from -20 to 20 for $\tan\beta = 2, 10, 15, 20, \ldots, 60$.[7] For the ranges of the gaugino mass ratios, we scanned over $-40 \leq \eta_1 \leq 45$ and $-10 \leq \eta_2 \leq 10$. Both signs for μ were allowed. In the scan, we have dropped all points

[7] Note that in the data for the cMSSM part of the scan, taken from [6], $\tan\beta$ only takes the values $10, 15, 20, 30, 40, 50$.

with a fine-tuning larger than 200.

Fine-tuning was calculated for the parameters m, μ, $A_0 = \eta_A M_3$, M_3, y_t and α_s. Tuning in the ratios η_1, η_2 was neglected as they were assumed to be fixed by some underlying model. In all plots where contours are shown instead of points only, outliers that are very far away from their neighbours are still shown as isolated points instead of being incorporated into the contour. In addition, unless stated otherwise, all plots show values marginalised over parameters not shown.

As shown in fig. 6.2a, we indeed find an ellipse shaped region that allows for quite low fine-tuning without being excluded by experimental bounds. While the semi-analytical results shown in fig. 6.1 do not exactly reproduce the numerical results, they still give a good qualitative understanding. Compared to the cMSSM with the same experimental bounds, we find a fine-tuning Δ lower than 3 instead of just below 10, see fig. 6.3. In the following, we will focus on this elliptical region of low fine-tuning and consider only points in the η_1-η_2 plane where the minimal fine-tuning is $\Delta_{\text{min}} < 10$.[8] The curve in fig. 6.2a, where the fine-tuning has its minimum in the η_1-η_2 plane, is approximately given by the ellipse

$$\left(\frac{\eta_1}{15.0}\right)^2 + \left(\frac{\eta_2}{2.6}\right)^2 = 1\,. \tag{6.28}$$

Next, we take a closer look at the dependence of fine-tuning on the other parameters. In fig. 6.2b, we can clearly see that introducing non-universal gaugino masses can significantly weaken the dependence of Δ_{min} on the gaugino mass scale compared to the cMSSM in fig. 6.3a. While the latter only allows for a minimal fine-tuning lower than 20 for $M_3 < 400$, the same now applies up to $M_3 \sim 2.2$ TeV. On the other hand, the fine-tuning dependence on m (resp. m_0 in the cMSSM) remains largely unchanged.

Furthermore from fig. 6.2c, we can roughly see the same behaviour for large η_A as in fig. 6.3b, while for small η_A from -2 to 4 we find two peaks at $\eta_A = 0$ and $\eta_A \sim 2$. These are the values for η_A required for solution 1 and the upper end of the range quoted for solution 2 of eqs. (6.21a), (6.21b) respectively.

Finally, for the GUT-scale Yukawa coupling ratios shown in fig. 6.2d and 6.3c, a few comments are in order. First, we note that the semi-discrete nature of the plot in the y_t/y_b direction is directly related to the discrete values over which we scanned $\tan\beta$. Next, we notice that, in contrast to our analysis in [6], the ratios in the cMSSM found here are much more restricted – however, with the same conclusion that a b-τ Yukawa coupling ratio of 3/2 is favoured by fine-tuning compared to 1. This difference is made up entirely by the exclusion of colour and charge breaking vacua. On the other hand, going to non-universal gaugino masses restores most of the freedom in Yukawa coupling ratios (as expected from possible enhancements of ε^W and ε^B) and

[8] Depending on the other parameters, this restriction can cause the minimal fine-tuning in other projections to increase but, interestingly, this does not significantly change the appearance of all affected plots, indicating that being on the ellipse is indeed a necessary condition for small fine-tuning.

as expected the fine-tuning price of all ratios is reduced greatly. Again comparing the b-τ Yukawa coupling ratio of 3/2 with the case of b-τ Yukawa unification yields a slight preference for 3/2 with a minimal fine-tuning of $\Delta \sim 5$ vs. 9.

6.4.2 Results including LHC Higgs and SUSY Searches

In the light of the discovery of the Higgs boson at the LHC, it is interesting to analyse the consequences of non-universal gaugino masses for naturalness of the (non-universal) MSSM under this additional aspect. In fig. 6.4, we show the same plots as in fig. 6.2 with the additional experimental constraint from the CMS experiment, $m_h = 125.3 \pm 0.6$ GeV [102], on top of which we include a theoretical uncertainty of ± 3 GeV [103] for the Higgs mass calculation at each point in parameter space.

As one can see in fig. 6.4a, non-universal gaugino masses can accommodate this additional constraint even with a fine-tuning lower than 20 – actually just above 10 and in a very small region of parameter space even slightly below 10. This happens, e.g., around $\eta_2 \sim 0$, $\eta_1 \sim 15$ and to a lesser degree also around $\eta_1 \sim 0$, $\eta_2 \sim 2.6$ and in the part of the ellipse in between. The reasons why these regions are favoured after including the Higgs results can readily be deduced from the beta functions [67] of the stop soft masses and the stop trilinear coupling (at the GUT scale):

$$16\pi^2 \beta_{m^2_{\tilde{Q}}} \supset -g^2_{\mathrm{GUT}} M_3^2 \left(\frac{32}{3} + 6\eta_2^2 + \frac{2}{15}\eta_1^2 \right) \equiv -g^2_{\mathrm{GUT}}\, M_3^2\, f_Q(\eta_1, \eta_2) \,, \tag{6.29a}$$

$$16\pi^2 \beta_{m^2_{\tilde{u}^c}} \supset -g^2_{\mathrm{GUT}} M_3^2 \left(\frac{32}{3} + \frac{32}{15}\eta_1^2 \right) \equiv -g^2_{\mathrm{GUT}}\, M_3^2\, f_u(\eta_1, \eta_2) \,, \tag{6.29b}$$

$$16\pi^2 \beta_{A_t} \supset -g^2_{\mathrm{GUT}} M_3 \left(\frac{32}{3} + 6\eta_2 + \frac{26}{15}\eta_1 \right) \equiv -g^2_{\mathrm{GUT}} M_3\, f_A(\eta_1, \eta_2) \,. \tag{6.29c}$$

The dependence of the functions f_Q, f_u and f_A on $\eta_1 \equiv r_\eta \cos\phi$, $\eta_2 \equiv r_\eta \sin\phi$ on the approximative ellipse given by eq. (6.28) is shown in fig. 6.5. It can easily be seen that the gaugino mass contribution to right-handed stop masses is greatly enhanced for the angles $\phi = 0, \pi$, i.e. $\eta_2 = 0$, $|\eta_1| \sim 15$, while it does not significantly differ from the cMSSM value elsewhere. The contribution to the left-handed stop mass, on the other hand, receives a smaller but still sizable enhancement over the cMSSM value, but does not vary as much along the ellipse. Furthermore for $\phi = 0$, i.e. $\eta_1 \sim 15$ and $\eta_2 = 0$, the contribution to the running of A_t receives a sizeable enhancement, which is present to a lesser degree also for $\phi = \pi/2$, i.e. $\eta_1 = 0$ and $\eta_2 \sim 2.6$. However, for angles in the other quadrants, where at least one η_i is negative, the cancellation with the large gluino mass running contribution precludes a similar enhancement in f_A. In practice, these three effects turn out to be effective only when they work in unison to obtain a high enough Higgs mass without entailing increased fine-tuning.

The changes in fig. 6.4b are not very surprising: regions with low masses get cut off. Also the changes in fig. 6.4c are not unexpected, the solution with $\eta_A > 0$ is

disfavoured more than the solution with $\eta_A \sim 0$, as the latter does not suffer from the cancellation with the gluino mass contribution to the running of the top trilinear soft term. Unsurprisingly, either large η_A or large M_3 (hence large top trilinear coupling) is needed to accommodate a consistently large Higgs mass.

Regarding the Yukawa coupling ratios shown in fig. 6.4d, we see that the minimal fine-tuning required for a unified b-τ Yukawa coupling ratio suffers more from the requirement of a consistent Higgs mass than the ratio of 3/2. Namely after applying the constraint, the fine-tuning for $y_\tau/y_b = 3/2$ can go down to $\Delta = 30$, while $y_\tau = y_b$ requires at least a Δ of 60. This is also nicely illustrated in fig. 6.6, where we have shown the interplay between the Higgs mass, the GUT-scale y_τ/y_b ratio and the minimal amount of fine-tuning Δ.

Another important aspect of LHC experiments are the searches for superpartner particles. Since changes in the gaugino mass ratios η_1 and η_2 can significantly alter the composition of the lightest neutralino[9] as well as the mass splittings controlling jet energies and missing E_T from the cascade decays, the exclusion regions for the cMSSM do not apply anymore. A full event and detector simulation would, however, go beyond the scope of this study. Instead, we make use of exclusion bounds derived in so-called simplified model searches [104, 69]. For simplicity, we simply juxtapose the spectra found by the numerical scan with some representative bounds in several simplified model types. While this is not a rigorous approach, it should serve as general guidance how endangered by exclusion each point is.

The resulting situation is shown in fig. 6.7. Without the Higgs mass constraint, in most plots, the region with $\Delta < 3$ is partially inside the excluded region, while even $\Delta < 10$ extends far beyond the bounds. Requiring a Higgs boson within 1σ of the experimental measurement [102] (including 3 GeV theoretical uncertainty as explained before) even excludes more than what direct SUSY searches exclude in some areas. It is important to note that, even in this quite restrictive approach, all of the parameter space with high m_h and $\Delta < 20$ is safe from being excluded by the shown constraints.

Furthermore, it is also interesting to look at the correlation between the Higgs and several sparticle masses, which is shown in fig. 6.8. Here, we can see that for low fine-tuning relatively light neutralinos and charginos are expected. This is due to the fact that μ is small in this region, so that Higgsinos are expected to be light. Also, the gluinos and the lightest stop can be rather heavy in our scenario with low fine-tuning ($\Delta < 20$ for $m_{\tilde{g}} \gtrsim 1.5$ TeV and $m_{\tilde{t}_1} \gtrsim 1.0$ TeV). The LHC still has not reached this region of parameter space. Hence stating that all natural regions of the MSSM parameter space are already ruled out seems to be premature.

[9] Actually, low fine-tuning generally also means quite low μ, so Higgsino-like lightest neutralinos and charginos are quite likely.

η_1, η_2	Δ_{min}	Origin	
1, 1	118	cMSSM (Gaugino Unification)	
10, 2	12	**200** of $SU(5)$	[56]
$\frac{19}{10}$, $\frac{5}{2}$	18	**770** of $SO(10) \to (1,1)$ of $SU(4) \times SU(2)_R$	[56]
$\frac{77}{5}$, 1	36	**770** of $SO(10) \to (1,0)$ of $(SU(5)' \times U(1))_{\text{flipped}}$	[56]
$-\frac{1}{5}$, 3	46	**210** of $SO(10) \to (75,0)$ of $(SU(5)' \times U(1))_{\text{flipped}}$	[56]
$\frac{21}{5}$, $\frac{7}{3}$	13	O-II with $\delta_{\text{GS}} = -6$	[57, 73]
$\frac{17}{5}$, 2	28	O-II with $\delta_{\text{GS}} = -7$	[57, 73]
$\frac{29}{5}$, 3	44	O-II with $\delta_{\text{GS}} = -5$	[57, 73]

Table 6.1: Selected theoretically motivated ratios and the minimal possible fine-tuning they allow after imposing the experimental constraint $m_h = 125.3 \pm 0.6$ GeV [102] with a theoretical uncertainty of ± 3 GeV [103] for the Higgs mass calculation. Only ratios that can reduce the fine-tuning by at least 50% compared to the unified (cMSSM) scenario are shown. For more details on the origin of these ratios, see e.g. [56, 73, 57]. The results are illustrated graphically in fig. 6.9.

6.4.3 Favoured Non-Universal Gaugino Mass Ratios

As mentioned in sec. 4.3.2, fixed non-universal gaugino mass ratios may originate from various high energy models, for instance from GUTs or orbifold scenarios (see, e.g. [56, 73, 57] for discussions). In tab. 6.1 and fig. 6.9, we show examples of proposed fixed ratios η_1, η_2 for which we find that the fine-tuning can be reduced by more than 50% compared to the cMSSM.

Interestingly, among the orbifold models O-II of [57, 73], from the full numerical results including the constraints from the LHC Higgs results, we find that the option $(\eta_1, \eta_2) = (\frac{21}{5}, \frac{7}{3})$ based on $\delta_{\text{GS}} = -6$ has the lowest possible fine-tuning with $\Delta_{\text{min}} = 13$. In contrast, based on analytical estimates in [73] and before the Higgs results were available, the preferred ratio was $(\eta_1, \eta_2) = (\frac{29}{5}, 3)$ with $\delta_{\text{GS}} = -5$.[10]

The GUT ratios with the lowest fine tuning, with $\Delta_{\text{min}} = 12$, turns out to be $(\eta_1, \eta_2) = (10, 2)$. For the ratios found to be favoured in [73], we find significantly higher fine-tuning, e.g.: $\Delta_{\text{min}} = 82$ for $(\eta_1, \eta_2) = (-5, 3)$, $\Delta_{\text{min}} = 141$ for $(\eta_1, \eta_2) = (-\frac{101}{10}, -\frac{3}{2})$, $\Delta_{\text{min}} = 143$ for $(\eta_1, \eta_2) = (1, -\frac{7}{3})$.

Finally, as discussed at the beginning of sec. 6.4, for $\eta_2 < 0.5\,\eta_1$, the neutralino is dominated by its wino (or Higgsino) component. This implies that the relic density

[10] The parameter δ_{GS} is a negative integer constant associated with Green-Schwarz anomaly cancellation, cf. [57, 73]. The gaugino mass ratios are then $\eta_i = -\delta_{\text{GS}} + b_i$, with the beta function coefficients $b_i = (33/5, 1, -3)$.

is strongly suppressed and there is therefore no danger of overproducing thermal neutralino dark matter. Among the ratios listed in tab. 6.1, this applies to $(\eta_1, \eta_2) = (10, 2)$ and $(\eta_1, \eta_2) = (\frac{77}{5}, 1)$. For the other ratios of tab. 6.1, $\eta_2 > 0.5\,\eta_1$ holds and, at least in principle, thermal neutralino dark matter could be possible, assuming a standard thermal history of the universe. As already mentioned, we have not applied dark matter constraints in our analysis to not impose model-dependent choices on the thermal history of the universe.

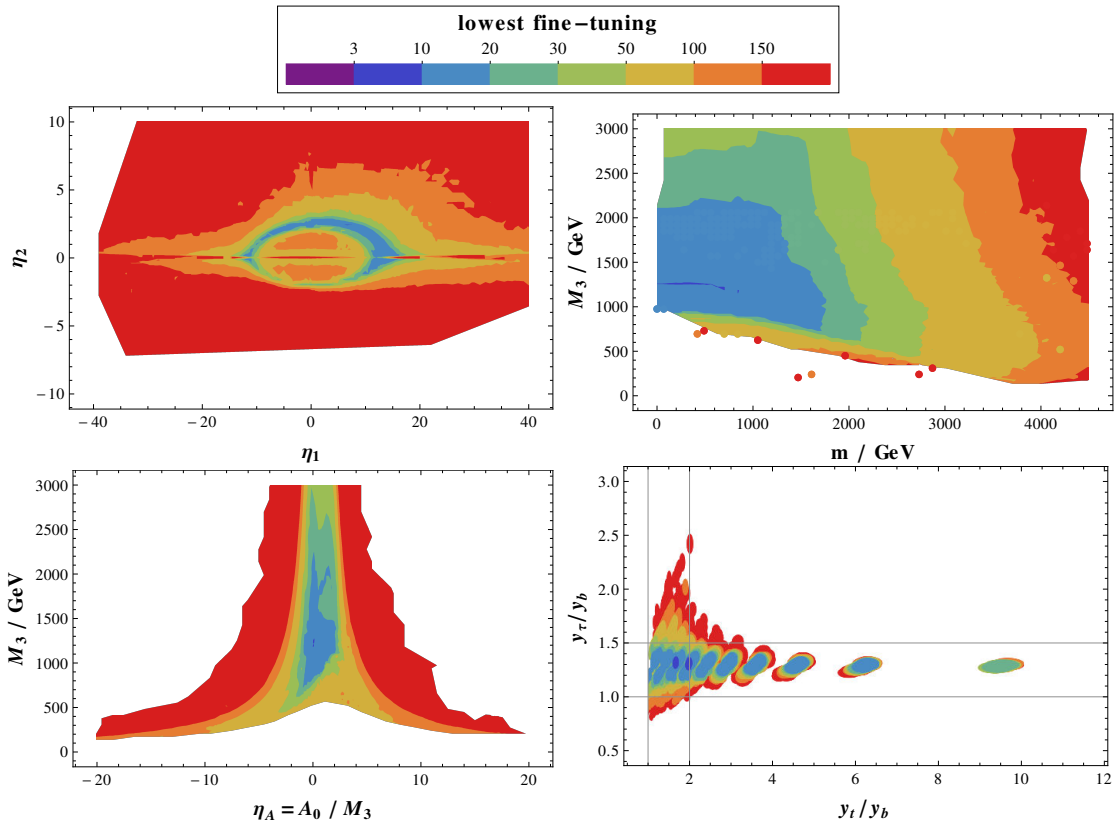

Figure 6.4: Lowest fine-tuning in the (a) η_1-η_2, (b) m-M_3, (c) η_A-M_3 and (d) y_t/y_b-y_τ/y_b planes consistent with the experimental bounds described in the text. For explanations of the parameters, see main text. In contrast to fig. 6.2, we have included the CMS experimental constraint $m_h = 125.3 \pm 0.6$ GeV [102] and a theoretical uncertainty of ± 3 GeV [103] for the Higgs mass calculation at each data point. The 1σ errors on the quark masses [82] are taken into account by scaling data points into error ellipses in the last plot correspondingly.

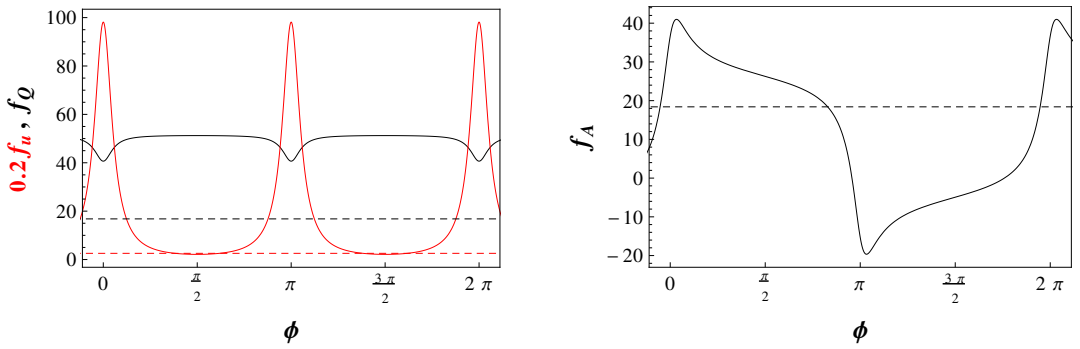

Figure 6.5: Dependence of the gaugino mass contribution functions f_Q, f_u, f_A (left plot/black, left plot/red, right plot respectively) to left-handed stop soft squared mass $m^2_{\tilde{Q}}$, right-handed stop soft squared mass $m^2_{\tilde{u}^c}$ and stop trilinear coupling A_t as defined by eq. (6.29). For the ellipse of low fine-tuning, the rough form of eq. (6.28) was used with the definition $\phi = \arg(\eta_1 + \mathrm{i}\eta_2)$. The corresponding value of f_x for the cMSSM with $\eta_1 = \eta_2 = 1$ is shown as a dashed line in the same colour. Note that f_u has been rescaled by a factor 5 for illustrative purposes.

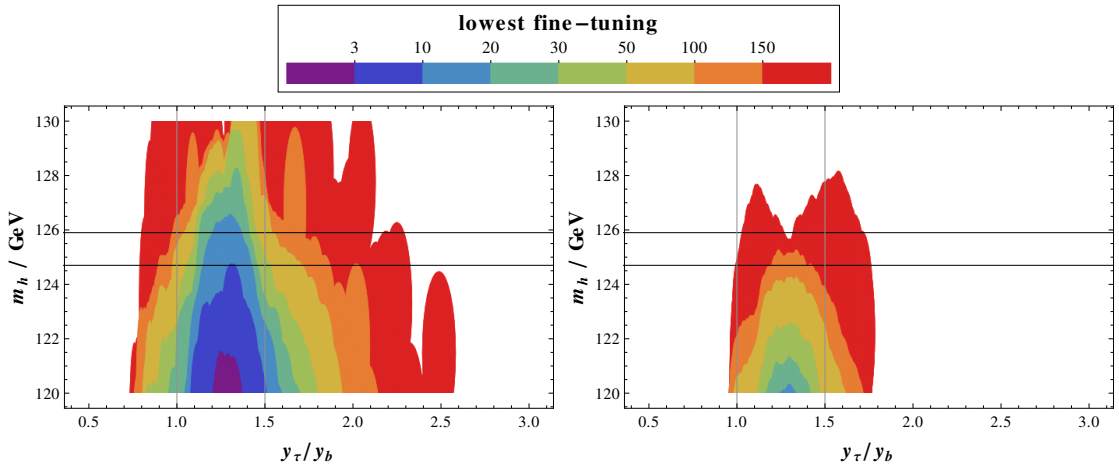

Figure 6.6: Lowest fine-tuning in the m_h-y_τ/y_b plane consistent with experimental bounds described in the text for non-universal gaugino masses (left) and universal gaugino masses (right). The horizontal lines correspond to the 1σ error of 0.6 GeV around 125.3 GeV as claimed by the CMS collaboration [102]. The 1σ errors on the quark masses [82] are taken into account by scaling the data points into error ellipses correspondingly. In addition, a theoretical uncertainty of 3 GeV [103] for the Higgs mass calculation at each point in parameter space is included.

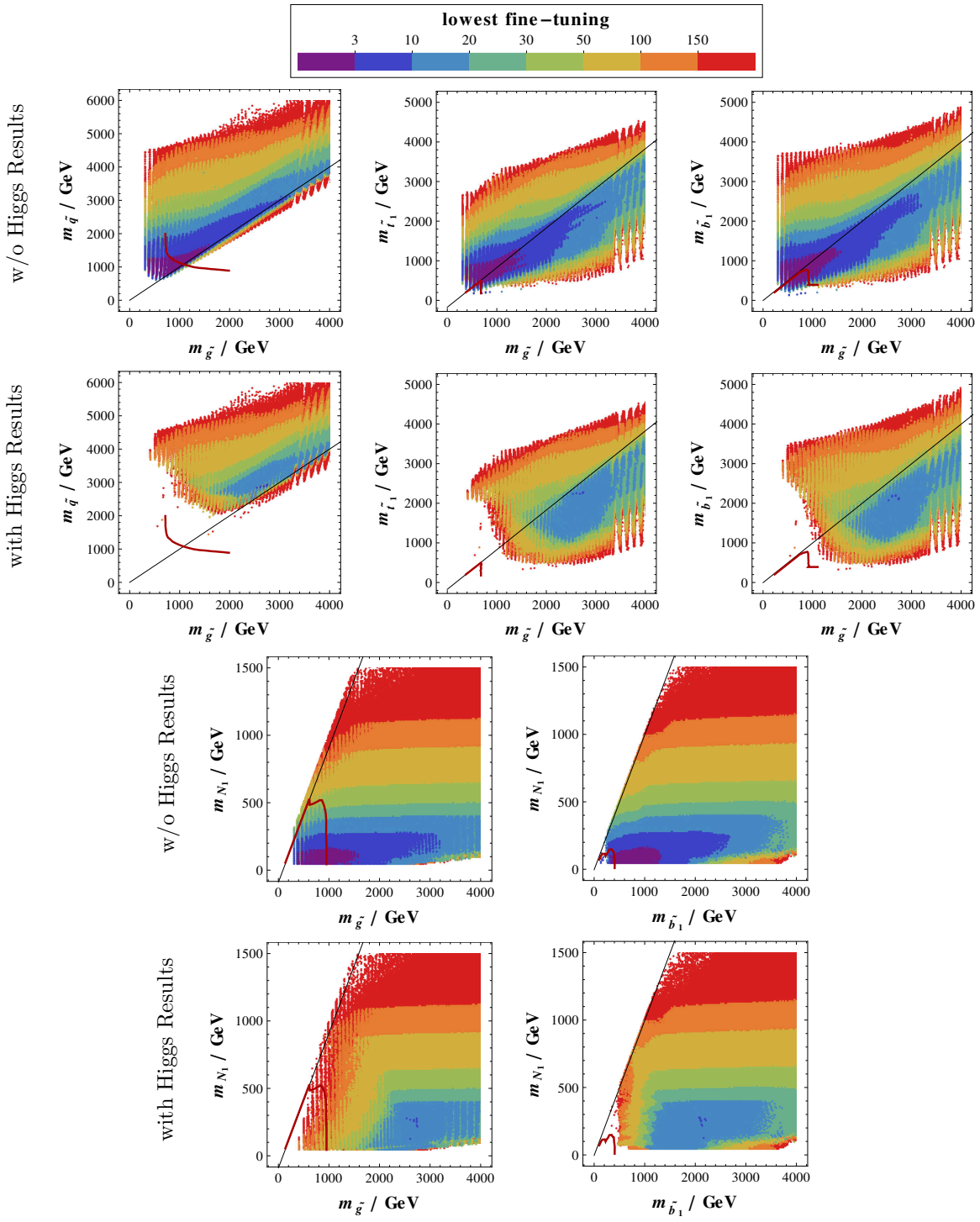

Figure 6.7: Lowest fine-tuning in various planes used for simplified models. Only points consistent with experimental bounds described in the text are shown. In addition, for the plots on the second and fourth line, the points are subjected to the experimental constraint $m_h = 125.3 \pm 0.6$ GeV [102] assuming an additional theoretical uncertainty of ± 3 GeV [103] for the Higgs mass calculation. The corresponding bounds due to LHC SUSY searches [69] are shown as thick dark red lines. Note that the bounds should only be used for general guidance on how direct SUSY searches at the LHC affect our results, as we did not perform a full detector simulation. For more details, see the main text.

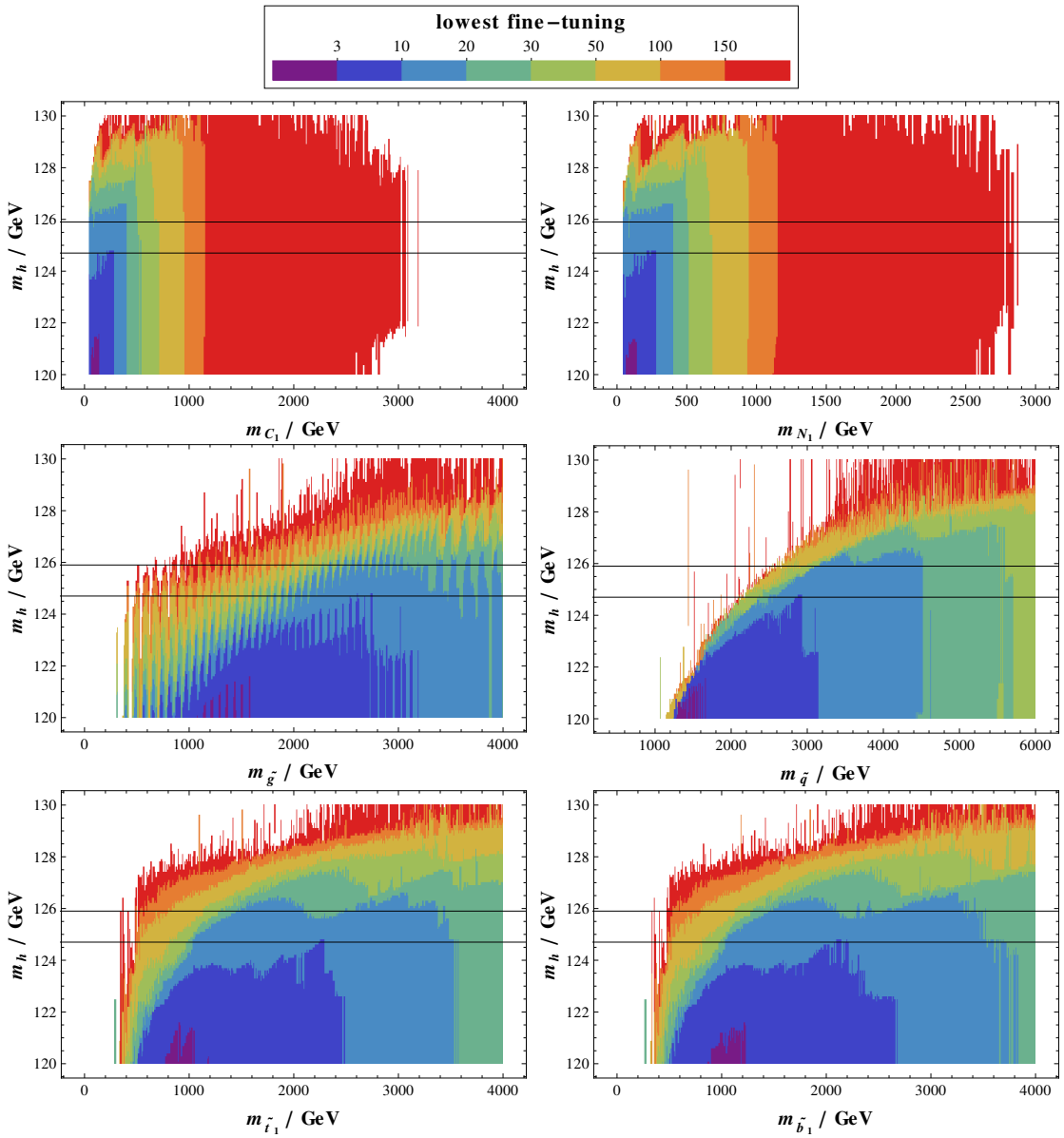

Figure 6.8: Lowest fine-tuning shown for the Higgs mass vs. important sparticle masses including the experimental constraint $m_h = 125.3 \pm 0.6$ GeV [102] and a theoretical uncertainty of ± 3 GeV [103] for the Higgs mass calculation at each point.

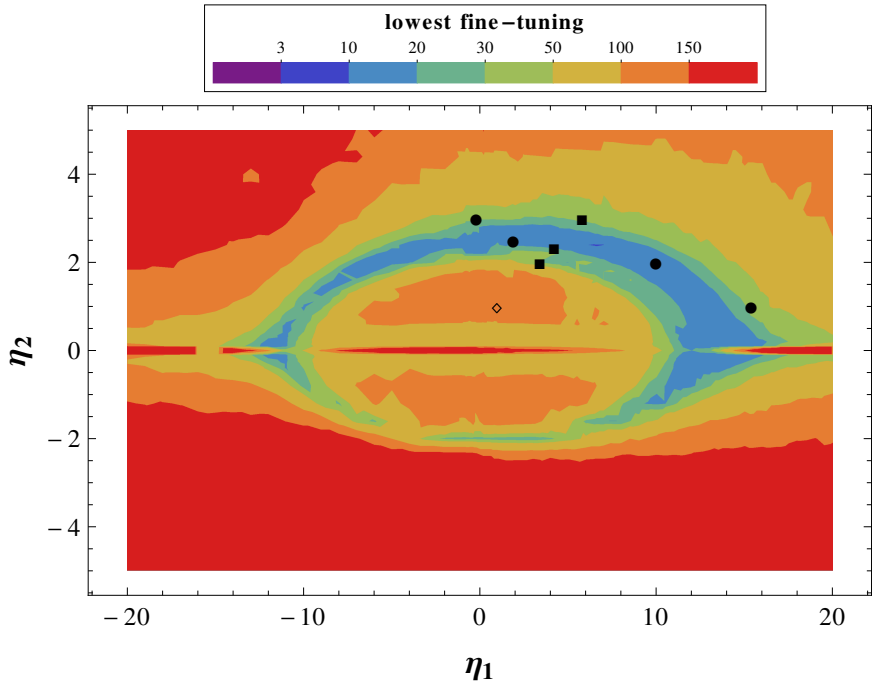

Figure 6.9: Lowest fine-tuning in the η_1-η_2 plane consistent with the experimental constraint $m_h = 125.3 \pm 0.6$ GeV [102] including a theoretical uncertainty of ± 3 GeV [103] for the Higgs mass calculation. Theoretically motivated ratios that reduce the fine-tuning compared to the unified scenario by at least 50% and the analytical expectation are marked as follows: the gaugino unification, i.e. cMSSM, is marked as empty diamond, circles correspond to ratios derived from GUT symmetry breaking [56] and squares to ratios found in the so-called O-II model in [57, 73]. For more details see tab. 6.1.

CHAPTER 7

Large $\theta_{13}^{\rm PMNS}$ in Unified Theories

7.1 Motivation

The origin of the quark and lepton masses and mixing parameters and the structure of their sizes is and has been one of the biggest mysteries in particle physics. As seen in chap. 5, the quark mixing angles and Yukawa couplings are rather small and hierarchical with

$$\theta_{13}^{\rm CKM} \approx 0.20^\circ \ , \quad \theta_{23}^{\rm CKM} \approx 2.4^\circ \ , \quad \theta_{12}^{\rm CKM} \equiv \theta_C = 13.02^\circ \ , \tag{7.1}$$

while the neutrino mixing angles [16] are rather large with

$$\theta_{23}^{\rm PMNS} \approx 45^\circ \ , \quad \theta_{12}^{\rm PMNS} \approx 35^\circ \ . \tag{7.2}$$

Soon it was realised that the smallness of mixing angles and Yukawa couplings can be realised by associating them with a vacuum expectation value that spontaneously breaks a so-called family symmetry and induces Yukawa couplings by appearing in appropriate effective higher-dimensional operators [105], leading to relations of the form $y \sim \langle H \rangle / M$ for some suppression scale M and symmetry breaking field H. On the other hand, the large lepton mixing angles were found to be realised to good precision within the framework of (discrete) family symmetries, leading exactly to so-called tri-bimaximal mixing [106]

$$\theta_{23}^{\rm PMNS} = 45^\circ \ , \quad \theta_{12}^{\rm PMNS} = 35.3^\circ \ , \quad \theta_{13}^{\rm PMNS} = 0 \ . \tag{7.3}$$

This is, of course, a very discouraging prediction for experiments that are trying to observe $\theta_{13}^{\rm PMNS}$ at a sensitivity of a few degrees.

One way to deviate from this without sacrificing predictivity is to use a structure of the following form. The quark mixing is assumed to come only from the down-type

quark sector. Thus setting the 1-1 element of the Yukawa matrix of the down and strange subsector to 0 as in

$$Y_d = \begin{pmatrix} 0 & a \\ b & c \end{pmatrix} , \tag{7.4}$$

fixes all parameters as functions of y_d, y_s and θ_C (neglecting SUSY threshold corrections and assuming no significant effects from third generation mixing). If we now impose an $SU(5)$ connection between Y_d and Y_e with a Clebsch-Gordan (CG) factor of -3 in the 2-2 matrix entry of Y_e, e.g. via H_d contained (partially) in a $\overline{\mathbf{45}}$ representation, we get

$$Y_e^T = \begin{pmatrix} 0 & a \\ b & -3\,c \end{pmatrix} . \tag{7.5}$$

This leads to the "Georgi-Jarlskog" [48] mass relations

$$m_\mu = 3\, m_s , \quad m_e = \frac{1}{3}\, m_d , \tag{7.6}$$

if we interpret theses masses to be GUT-scale Yukawa couplings times the electroweak VEV. Additionally, the non-vanishing mixing $\theta_{12}^e \approx \theta_C/3$ in the e-μ sector corrects a tri-bimaximal neutrino sector so that

$$\theta_{13}^{\mathrm{PMNS}} \approx \frac{1}{3\sqrt{2}}\, \theta_C \approx 3^\circ . \tag{7.7}$$

For a time, this was an interesting if somewhat common prediction [107], which was at least within the realm of possibility for detection at reactor neutrino experiments.

However, in 2011 and 2012 it became falsified when the third leptonic mixing angle $\theta_{13}^{\mathrm{PMNS}}$ was measured by T2K, DoubleCHOOZ, DayaBay and RENO, see [22], such that recent global fits [16] find

$$\theta_{13}^{\mathrm{PMNS}} = 8.5^\circ \pm 0.2^\circ . \tag{7.8}$$

Additionally, judging from eq. (5.14), the Georgi-Jarlskog mass relations of eq. (7.6) are now also in tension with experimental data or demand more involved SUSY threshold corrections to be valid.

Thus, it is interesting to address the following questions:

- How can one get such a large reactor angle $\theta_{13}^{\mathrm{PMNS}}$ without sacrificing the predictivity of the Georgi-Jarlskog setup?
- Can we generalise the Georgi-Jarlskog relation in a way that is consistent with current flavour data for neutrino mixing and fermion masses?
- Can we still postdict $\theta_{13}^{\mathrm{PMNS}}$ as a simple function of other flavour quantities?

- What are the possible values for $\theta_{13}^{\mathrm{PMNS}}$ in such a setup, in particular, is there a maximum and what is it?
- What constraints does this impose on the structure of the flavour model?

This chapter will thus show a simple generalisation of the Georgi-Jarlskog mass relations and what conditions it has to fulfil to reproduce all relevant data sufficiently well. It is based on the publications [8] and [9] and represents an updated view on their contents.

7.2 Non-GUT Conditions and Assumptions

First, we will formulate some general conditions and assumptions that characterise the Georgi-Jarlskog scenario and incidentally find application in many flavour models. Nonetheless, let it be noted that, while these conditions are satisfied very frequently, they may not be the only way to realise a flavour model that reproduces all current data with less parameters than fitted flavour quantities, although such models might then not resemble the Georgi-Jarlskog scenario very much.

Motivated by the hierarchical structure of quark masses and mixing angles, we will assume that the three Yukawa matrices Y_u, Y_d and Y_e are also hierarchical in structure, which in particular implies that the left-mixing angles (denoted as θ_{ij}^u, θ_{ij}^d and θ_{ij}^e) are all comparatively small, i.e. of at most size comparable to the Cabibbo angle θ_C, as is typical for GUT flavour models in the flavour basis. Let us revisit the relations among the mixing parameters in these three sectors together with the mixing in the neutrino sector (angles denoted by θ_{ij}^ν). For this, it is useful to remind ourselves of the standard parametrisation for unitary matrices using Euler angles and all complex phases

$$U = \mathrm{diag}(\mathrm{e}^{\mathrm{i}\delta_e}, \mathrm{e}^{\mathrm{i}\delta_\mu}, \mathrm{e}^{\mathrm{i}\delta_\tau}) \cdot V \cdot \mathrm{diag}(e^{-\mathrm{i}\varphi_1/2}, e^{-\mathrm{i}\varphi_2/2}, 1) \tag{7.9}$$

where

$$V = \begin{pmatrix} c_{12}c_{13} & s_{12}c_{13} & s_{13}\mathrm{e}^{-\mathrm{i}\delta} \\ -c_{23}s_{12} - s_{23}s_{13}c_{12}\mathrm{e}^{\mathrm{i}\delta} & c_{23}c_{12} - s_{23}s_{13}s_{12}\mathrm{e}^{\mathrm{i}\delta} & s_{23}c_{13} \\ s_{23}s_{12} - c_{23}s_{13}c_{12}\mathrm{e}^{\mathrm{i}\delta} & -s_{23}c_{12} - c_{23}s_{13}s_{12}\mathrm{e}^{\mathrm{i}\delta} & c_{23}c_{13} \end{pmatrix} \tag{7.10}$$

with c_{ij} and s_{ij} denoting $\cos\theta_{ij}$ and $\sin\theta_{ij}$, respectively. The mixing matrices appearing in charged currents in terms of the sub-sector mixing matrices are given by

$$V_{\mathrm{CKM}} = V_u^\dagger V_d \ , \quad V_{\mathrm{PMNS}} = V_e^\dagger V_\nu \ , \tag{7.11}$$

Beginning with the quark sector and expanding to leading order in the small mixing angles, we obtain the following relations between CKM angles and up- and down-type

quark mixing [108]:

$$\theta_{12}^{\rm CKM} e^{-{\rm i}\delta_{12}^{\rm CKM}} = \theta_{12}^{d} e^{-{\rm i}\delta_{12}^{d}} - \theta_{12}^{u} e^{-{\rm i}\delta_{12}^{u}} \,, \tag{7.12a}$$

$$\theta_{23}^{\rm CKM} e^{-{\rm i}\delta_{23}^{\rm CKM}} = \theta_{23}^{d} e^{-{\rm i}\delta_{23}^{d}} - \theta_{23}^{u} e^{-{\rm i}\delta_{23}^{u}} \,, \tag{7.12b}$$

$$\theta_{13}^{\rm CKM} e^{-{\rm i}\delta_{13}^{\rm CKM}} = \theta_{13}^{d} e^{-{\rm i}\delta_{13}^{d}} - \theta_{13}^{u} e^{-{\rm i}\delta_{13}^{u}} - \theta_{12}^{u} e^{-{\rm i}\delta_{12}^{u}} (\theta_{23}^{d} e^{-{\rm i}\delta_{23}^{d}} - \theta_{23}^{u} e^{-{\rm i}\delta_{23}^{u}}) \,, \tag{7.12c}$$

where the standard Dirac CP phase $\delta^{\rm CKM}$ in $V_{\rm CKM}$ can be identified as (cf. [109])

$$\delta_{\rm CKM} = \delta_{13}^{\rm CKM} - \delta_{23}^{\rm CKM} - \delta_{12}^{\rm CKM} \,, \tag{7.13}$$

and the phases δ_{ij}^{u} and δ_{ij}^{d} are associated with the rotation angles θ_{ij}^{u} and θ_{ij}^{d} in the up- and down-type quark sectors, using the same notation as in [108]. As can be seen, this alternative phase convention has advantages for the formulation of mixing sum rules and is straightforward in its translation back to standard parametrisation.

Similar formulae are also valid in the lepton sector, where we obtain to leading order in a small angle expansion treating $\theta_{13}^{\rm PMNS}$ as a small parameter [110] and assuming that the 2-3 and 1-2 neutrino mixing angles are large:

$$s_{12}^{\rm PMNS} {\rm e}^{-{\rm i}\delta_{12}^{\rm PMNS}} = s_{12}^{\nu} {\rm e}^{-{\rm i}\delta_{12}^{\nu}} + \theta_{13}^{e} c_{12}^{\nu} s_{23}^{\nu} {\rm e}^{{\rm i}(\delta_{23}^{\nu} - \delta_{13}^{e})} - \theta_{12}^{e} c_{23}^{\nu} c_{12}^{\nu} {\rm e}^{-i\delta_{12}^{e}} \,, \tag{7.14a}$$

$$s_{23}^{\rm PMNS} {\rm e}^{-{\rm i}\delta_{23}^{\rm PMNS}} = s_{23}^{\nu} {\rm e}^{-{\rm i}\delta_{23}^{\nu}} - \theta_{23}^{e} c_{23}^{\nu} {\rm e}^{-{\rm i}\delta_{23}^{e}} \,, \tag{7.14b}$$

$$\theta_{13}^{\rm PMNS} {\rm e}^{-i\delta_{13}^{\rm PMNS}} = \theta_{13}^{\nu} {\rm e}^{-{\rm i}\delta_{13}^{\nu}} - \theta_{13}^{e} c_{23}^{\nu} {\rm e}^{-{\rm i}\delta_{13}^{e}} - \theta_{12}^{e} {\rm e}^{-{\rm i}\delta_{12}^{e}} (s_{23}^{\nu} {\rm e}^{-{\rm i}\delta_{23}^{\nu}} - \theta_{23}^{e} {\rm e}^{-{\rm i}\delta_{23}^{e}}) \,, \tag{7.14c}$$

where the leptonic CP phases follow the relations

$$\delta_{23}^{\rm PMNS} = -\frac{\varphi_2^{\rm PMNS}}{2} \,, \; \delta_{13}^{\rm PMNS} = \delta^{\rm PMNS} - \frac{\varphi_1^{\rm PMNS}}{2} \,, \; \delta_{12}^{\rm PMNS} = \frac{1}{2} \left(\varphi_2^{\rm PMNS} - \varphi_1^{\rm PMNS} \right) \,. \tag{7.15}$$

The phases $\varphi_1^{\rm PMNS}$ and $\varphi_2^{\rm PMNS}$ are the Majorana phases and $\delta^{\rm PMNS}$ is the Dirac CP phase. The relations of eqs. (7.12) and (7.14) quickly lead us to two conditions.

Condition 1: As can be seen from eqs. (7.14), $\theta_{13}^{\rm PMNS}$ is comprised of contributions from θ_{13}^{ν}, θ_{13}^{e} and θ_{12}^{e} (at leading order). Taking into account the assumed hierarchical structure of the quark mixing angles also replicated in θ_{ij}^{e}, the contribution from θ_{13}^{e} is usually too small to generate $\theta_{13}^{\rm PMNS}$ of sufficient magnitude. On the other hand, θ_{13}^{ν} constitutes a so far unconstrained parameter, so it would a priori not be beneficial for predictivity to use it as the source of $\theta_{13}^{\rm PMNS}$. Thankfully, the Cabibbo angle, i.e. the 1-2 CKM angle, is just of the same order of magnitude as $\theta_{13}^{\rm PMNS}$. Thus we formulate the first condition to be given by

$$\theta_{13}^{\nu} \approx 0 \,, \quad \theta_{13}^{e} \approx 0 \,. \tag{7.16}$$

Then the first two summands on the right side of eq. (7.14c) drop out and we obtain, at leading order in small angles and independently of any phases,

$$\theta_{13}^{\mathrm{PMNS}} \approx \theta_{12}^{e} s_{23}^{\nu} \approx \frac{1}{\sqrt{2}}\,\theta_{12}^{e}\ . \tag{7.17}$$

In the last step, we have for now inserted a maximal neutrino mixing angle, i.e. $\theta_{23}^{\nu} = 45°$, to keep the discussion simple. We will come back to the effect of this simplification later.

A second important ingredient of the Georgi-Jarlskog mass relations is given by the connection between the Y_d and Y_e matrices. We will stick to this, even though a connection between Y_u and Y_e might also be possible. However, the stronger hierarchy in the up-type quark masses makes it more difficult to obtain mixing angles of order $\mathcal{O}(\theta_C)$ in Y_u. Keeping this in mind, we arrive at the second condition.

Condition 2: Using Y_d as source of mixing in Y_e via GUT relations, we require that

$$\theta_{12}^{d} = \theta_C \tag{7.18}$$

to a good approximation. This may be a consequence of $\theta_{12}^{u} \ll \theta_{12}^{d}$, which is a typical feature of models with hierarchical Yukawa matrices where the stronger hierarchy in the up-quark sector implies the smaller mixing angles as mentioned above.

Alternatively, one can also require $\theta_{12}^{d} = \mathcal{O}(\theta_C)$, where, however, the right hand side is to be understood as a predictive (i.e. practically fixed) value involving a model-dependent fixed number. One example is given by the scenario where θ_{13}^{u}, $\theta_{13}^{d} \approx 0$. This leads to $\theta_{12}^{d} \approx 12.0° \pm 0.3°$ via the quark mixing sum rule,

$$\theta_{12}^{d} \approx \left| \theta_{12}^{\mathrm{CKM}} - \frac{\theta_{13}^{\mathrm{CKM}}}{\theta_{23}^{\mathrm{CKM}}} \mathrm{e}^{-\mathrm{i}\delta^{\mathrm{CKM}}} \right| . \tag{7.19}$$

For more details, see. [108].

7.3 Conditions on Flavour GUT Structures

To arrive at a predictive setup for $\theta_{13}^{\mathrm{PMNS}}$, we want to use the same style of GUT relations as in the Georgi-Jarlskog scenario. It is desirable to keep the number of parameters as small as possible, which means that the connection between parameters of Y_d and Y_e must be one-to-one. We formulate this as the following condition:

Condition 3: To obtain predictive GUT relations, we require that the elements of the Yukawa matrices Y_e and Y_d are each dominantly generated by one single joint

GUT operator. In this case, the matrix elements are closely linked by group theoretical CG factors, as discussed in sec. 4.2.

Focusing explicitly on the 1-2 submatrix of the first two families, which is a good approximation since we assume a hierarchical structure of Y_e and Y_d, and on Pati-Salam (PS) or $SU(5)$ theories, we can write

$$Y_d = \begin{pmatrix} d & b \\ a & c \end{pmatrix} \Rightarrow \begin{cases} \text{In PS:} & Y_e = \begin{pmatrix} c_d\, d & c_b\, b \\ c_a\, a & c_c\, c \end{pmatrix} , \\ \text{In } SU(5): & Y_e = \begin{pmatrix} c_d\, d & c_a\, a \\ c_b\, b & c_c\, c \end{pmatrix} . \end{cases} \tag{7.20}$$

Here, c_a, c_b, c_c and c_d are the CG factors which relate the elements in the Yukawa matrices Y_d and Y_e. Note that, in $SU(5)$ GUTs, Y_d is related to Y_e^T, whereas in Pati-Salam unified theories Y_d is related directly to Y_e. As can be seen, this generalises the Georgi-Jarlskog scenario to more than the single CG factor of $c_c = -3$ and (initially) more parameters.

Available CG factors in $SU(5)$ GUTs are, e.g.,

$$c_a, c_b, c_c, c_d \in \left\{ -\frac{1}{2}, 1, \pm\frac{3}{2}, -3, \frac{9}{2}, 6, 9 \right\} , \tag{7.21}$$

and in Pati-Salam models, e.g.,

$$c_a, c_b, c_c, c_d \in \left\{ \frac{3}{4}, 1, 2, -3, 9 \right\} , \tag{7.22}$$

see [49] and [54]. For details on their viability in supersymmetric scenarios, see e.g. [49]. For simplicity, we will restrict ourselves to these CG factors.

Note that this condition can be somewhat relaxed in some cases. For instance, only the matrix elements that enter the determination of θ_{12}^e are inevitably subject to this requirement, while other elements are somewhat less constrained. However, this can still lead to undesired consequences when considering corrections beyond the small angle approximation, where all matrix elements might enter significantly, see sec. 7.5.

Additionally, the case where two operators featuring the same CG factor contribute to the same matrix element is also implicitly covered by this condition as it does not change the predictivity of the one-to-one connection between Y_d and Y_e. Note, however, that in this case other connections between Yukawa matrices, namely the ones responsible for proton decay might indeed lose predictivity, cf. app. D and sec. 8.4.

From the above, it is clear that the CG factors play an important role. For a successful model, a consistent set of CG factors, leading also to viable mass relations

for the first two families, has to be found. As has been studied in [8, 111], multiple combinations of phenomenologically viable CG factors exist which can lead to a large $\theta_{13}^{\text{PMNS}}$ compared to the Georgi-Jarlskog case. A viable prediction only follows from a subset of these combinations of CG factors, as we will now discuss in the context of $SU(5)$ GUTs and Pati-Salam unified theories.

7.3.1 Predictive Setups for $\theta_{13}^{\text{PMNS}}$ in Pati-Salam Theories

To obtain a condition for the structure of the CG factors, it is useful to note that in both $SU(5)$ GUTs as well as Pati-Salam models the mixing angle θ_{12}^d is given to leading order in small angle approximation by

$$\theta_{12}^d \approx \left|\frac{b}{c}\right| \overset{!}{\approx} \theta_C \,. \tag{7.23}$$

On the other hand, the 1-2 mixing angle θ_{12}^e is (in Pati-Salam models) given by

$$\theta_{12}^e \approx \left|\frac{c_b\, b}{c_c\, c}\right| \approx \left|\frac{c_b}{c_c}\right| \theta_C \,, \tag{7.24}$$

where the previous equation has been inserted in the last step. Finally, using eq. (7.17) we obtain

$$\theta_{13}^{\text{PMNS}} \approx \frac{\theta_{12}^e}{\sqrt{2}} \approx \left|\frac{c_b}{c_c}\right| \frac{\theta_C}{\sqrt{2}} = 9.2^\circ \left|\frac{c_b}{c_c}\right| \,. \tag{7.25}$$

In the spirit of the original Georgi-Jarlskog setup, we will first consider the case where the 1-1 entry of both Y_d and Y_e is set to $d = 0$. Then, to leading order in small angle approximation, the quark-lepton Yukawa coupling ratios are given by

$$\frac{y_\mu}{y_s} \approx |c_c| \,, \quad \frac{y_e}{y_d} \approx \left|\frac{c_a c_b}{c_c}\right| \,. \tag{7.26}$$

Note that these relations are assumed to be valid at a very high scale. Thus they already include possible SUSY threshold corrections.

In the following, we will restrict ourselves to the case $c_c = -3$, as even the two other choices closest to the (uncorrected) GUT-scale μ-s ratio of eq. (5.13), $c_c = 2$ or 9, would need SUSY threshold correction exceeding 40%. Unfortunately, this leads to the same mass relation as the Georgi-Jarlskog scenario [48] and thus no improvement in this respect.

Assuming that the combined effect of the SUSY threshold corrections to quark and lepton Yukawa couplings are such that c_c is consistent with the relation for $\frac{y_\mu}{y_s}$ given in eq. (5.13) within the 1σ uncertainty, we can derive the corresponding e-d mass ratio, assuming that the corrections are the same for the first and second generation. From

this, we calculate the allowed range for the product $|c_a c_b|$ requiring to also be in the 1σ uncertainty range for the first generation mass ratio. The resulting range is given by

$$c_c = \quad -3 \quad \Rightarrow \quad |c_a c_b| \in [0.72, 0.94] \; . \tag{7.27}$$

This reduces the list of viable values for c_a and c_b, as given in [54], to $c_a = 3/4$, $c_b = 1$ or vice versa and hence the ratio $|\frac{c_b}{c_c}|$ to the discrete values

$$\left|\frac{c_b}{c_c}\right| \in \left\{\frac{1}{4}, \frac{1}{3}\right\} \; , \tag{7.28}$$

As one can see, even the largest ratio only reproduces the same value for $\theta_{13}^{\text{PMNS}}$ as the original Georgi-Jarlskog scenario in eq. (7.7), as shown in tab. 7.1, and is thus not large enough to be consistent with the global fit value of 8.5°, even if one includes corrections as discussed later. Thus we conclude that a Pati-Salam model with a texture zero in the 1-1 element of Y_d and Y_e is not viable.

Fortunately, in the case of $d \neq 0$, eq. (7.25) still applies to leading order in small angle approximation and we can formulate a final condition for the GUT structure:

Condition 4 (PS): In Pati-Salam unified models, the CG factors for the operators generating the 2-2 element and the 1-2 element are required to be equal,

$$|c_b| = |c_c| \; . \tag{7.29}$$

The predictivity of the model can then be saved by requiring the matrices Y_d and Y_e to be symmetric, reducing the number of parameters to the same as in the $d = 0$ case. One example of such a scenario is discussed in sec. 7.5.

Note that, independently, this condition was also formalised in [112], where, however, the following case of $SU(5)$ GUTs was not treated.

7.3.2 Predictive Setups for $\theta_{13}^{\text{PMNS}}$ in $SU(5)$ GUTs

As before, we will first focus on the case with vanishing 1-1 matrix element $d = 0$. Then, contrary to Pati-Salam the charged lepton mixing angle is given by

$$\theta_{12}^e \approx \left|\frac{c_a\, a}{c_c\, c}\right| \; . \tag{7.30}$$

Putting this together with the still valid eq. (7.26) yields a new relation for the reactor angle,

$$\theta_{13}^{\text{PMNS}} \approx \frac{1}{\sqrt{2}} \frac{y_e}{y_\mu} \left|\frac{c_c}{c_b}\right| \frac{1}{\theta_{12}^d} \approx 0.85° \left|\frac{c_c}{c_b}\right| \frac{\theta_C}{\theta_{12}^d} \; , \tag{7.31}$$

where it is interesting to note that the dependence on the quark mixing angle is now inverted. Analogous to Pati-Salam case, only a subset of values for c_c is consistent with the requirement of threshold corrections below 40%, namely -3, $\frac{9}{2}$ and 6. These restrict the CG factors c_a and c_b like before to

$$c_c = -3 \quad \Rightarrow \quad |c_a c_b| \in [0.72, 0.94] \,, \tag{7.32a}$$
$$c_c = \tfrac{9}{2} \quad \Rightarrow \quad |c_a c_b| \in [1.6, 2.1] \,, \tag{7.32b}$$
$$c_c = 6 \quad \Rightarrow \quad |c_a c_b| \in [2.9, 3.7] \,. \tag{7.32c}$$

Unfortunately, the choice $c_c = \frac{9}{2}$ yields no combinations of c_a and c_b that fall into this range, as the threshold correction to the μ-s ratio is too small to shift the e-d ratio to any of the values available from CG factors, assuming universality of the threshold corrections over the first two generations.[1] The other combinations lead to ratios as appearing in eq. (7.31) of

$$c_c = -3 \quad \Rightarrow \quad \left|\tfrac{c_c}{c_b}\right| \in \{2, 6\} \,, \tag{7.33a}$$
$$c_c = \tfrac{9}{2} \quad \Rightarrow \quad \left|\tfrac{c_c}{c_b}\right| \in \{\} \,, \tag{7.33b}$$
$$c_c = 6 \quad \Rightarrow \quad \left|\tfrac{c_c}{c_b}\right| \in \{1, 2, 6, 12\} \,. \tag{7.33c}$$

As we can see from the corresponding values in tab. 7.1, only the single combination with $|c_c/c_b| = 12$ yields a sufficiently large $\theta_{13}^{\text{PMNS}}$ that can possibly be made consistent with experimental data. Interestingly, it is also the only combination that was found in [111] that was additionally consistent with the value for the ratio of down and strange quark masses of [113].

This leads us to the following (first) formulation of the final condition for the case of $SU(5)$ GUTs:

Condition 4a ($SU(5)$): In case of vanishing 1-1 matrix elements of Y_d and Y_e, $d = 0$, the group theoretical CG factors linking both matrices must have the values

$$c_c = c_a = 6 \,, \quad c_b = -\frac{1}{2} \,, \tag{7.34}$$

assuming that no CG factors other than the ones of eq. (7.21), i.e. originating from dimension five effective operators as discussed in [49], are available.

Alternatively and analogously to the Pati-Salam case, one can retain the same amount of predictivity and allow non-zero 1-1 matrix elements and instead require symmetric matrices. This leads to the following modified (and arguably simpler) condition:

[1] Also taking into account other CG factors such as the other ones shown in chap. D provides some possibilities after all. However, the largest $|c_c/c_b|$ available is still only 6 with $c_a = \pm 9/4$, $c_b = 3/4$. Other c_c choices are not affected qualitatively and new ones do not become available with this extension.

c_c	-3 in PS		-3 in $SU(5)$		6 in $SU(5)$			
$\theta_{13}^{\mathrm{PMNS}}$	2.3°	3.1°	1.7°	5.1°	0.8°	1.7°	5.1°	10.1°
c_a	1	$\frac{3}{4}$	$-\frac{1}{2}$	$\pm\frac{3}{2}$	$-\frac{1}{2}$	1	-3	6
c_b	$\frac{3}{4}$	1	$\pm\frac{3}{2}$	$-\frac{1}{2}$	6	-3	1	$-\frac{1}{2}$

Table 7.1: Predicted values for $\theta_{13}^{\mathrm{PMNS}}$ (in small angle approximation), which arise with CG factors c_c, c_a, c_b and $(Y_d)_{11} = (Y_e)_{11} = 0$, assuming $\theta_{12}^d = \theta_C$.

Condition 4b ($SU(5)$): If the Yukawa matrices Y_d and Y_e are symmetric, the CG factors of the 1-2 and 2-2 matrix elements have to be the same,

$$|c_a| \equiv |c_b| = |c_c| \,. \tag{7.35}$$

This symmetry may, for example, be a consequence of the way that the flavour structure arises out of the breaking of a (non-Abelian) family symmetry.

Note that unlike in the Pati-Salam case, here the symmetry is also desired for a consistent value of $\theta_{13}^{\mathrm{PMNS}}$ due to the additional transposition in the connection between Y_d and Y_e, whereas in the former case, symmetry is only needed for full predictivity of all flavour variables and part of the corrections. For an example on what specific CG factors can work in this case, see the discussion in sec. 7.5.

7.4 Scenario Overview

For clarity, let us again review the discussed scenario and conditions formulated above in shorter form. To this end, the general conditions that characterise this scenario are illustrated summarily in fig. 7.1. In more detail, they are given by:

Condition 1: The 1-3 mixings in m_ν and Y_e shall be small, i.e. much smaller than the Cabibbo angle θ_C,

$$\theta_{13}^\nu \approx 0 \,, \quad \theta_{13}^e \approx 0 \,. \tag{7.36}$$

Condition 2: The 1-2 mixing in Y_d shall be given by the Cabibbo angle to a good approximation,

$$\theta_{12}^d \approx \theta_C \,, \tag{7.37}$$

which is, for example, automatically satisfied in models with $\theta_{12}^u \ll \theta_{12}^d$.

Condition 3: The matrix elements of the first two generation subsector of Y_d and Y_e have to be generated dominantly by one single GUT operator per element (or by operators with the same group theoretical Clebsch-Gordan factors).

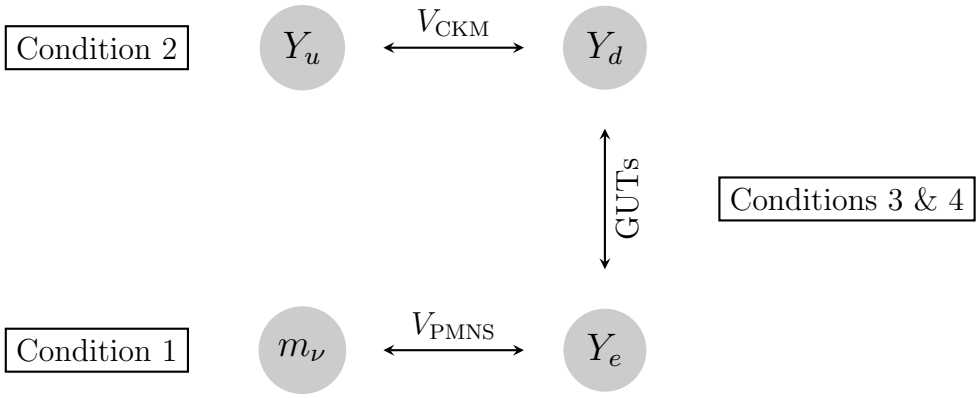

Figure 7.1: Under conditions 1 to 4, a predictive and consistent relation for $\theta_{13}^{\text{PMNS}}$ generalising the Georgi-Jarlskog scenario is obtained by linking the charged lepton and quark sectors via GUTs.

Condition 4: Two of the CG factors shall be equal, i.e. $|c_b| = |c_c|$ in Pati-Salam models and $|c_a| = |c_c|$ in $SU(5)$ GUTs. In $SU(5)$ GUTs, one additional constraint has to be imposed on the structure of the mass matrices, such as a symmetry in the 1-2 submatrix or zero 1-1 elements of Y_d and Y_e with $c_a = 6$ and $c_b = -1/2$.

As such, they provide a good starting point for GUT models of flavour that predict (or postdict) a viable value for $\theta_{13}^{\text{PMNS}}$.

7.5 Corrections

While the discussion above is quite simple and intuitive, it is only a first order approximation and there are some systematic and possibly significant corrections, as we will discuss now.

Corrections due to small mixing approximation

In the formulae above, we neglected higher order terms in a small angle and mass ratio approximation for the sake of simplicity. The error introduced by this is dependent on the structure of the mass matrices and the CG factors, but can be computed easily.

Consider, for example, the scenario of an $SU(5)$ GUT with a texture zero in the 1-1 matrix element of Y_d and Y_e, together with CG factors $c_c = c_a = 6$, $c_b = -\frac{1}{2}$,

$$Y_d = \begin{pmatrix} 0 & b \\ a & c \end{pmatrix}, \quad Y_e = \begin{pmatrix} 0 & 6\,a \\ -\frac{1}{2}\,b & 6\,c \end{pmatrix}. \tag{7.38}$$

Performing an exact diagonalisation and fitting to the experimental values of y_e/y_μ, y_s/y_d and θ_C (as given in tab. 5.2 with uncertainties as given in tab. 5.3)

yields $\theta_{12}^e = 13.9°$ instead of the previous value $\theta_{12}^e = 13.02°$. Consequently, instead of $\theta_{13}^{\text{PMNS}} \approx \theta_C/\sqrt{2} = 9.2°$, the more precise GUT-scale prediction is given by

$$\begin{gathered} SU(5) \text{ with } d = 0,\ c_c = c_a = 6,\ c_b = \tfrac{1}{2} \text{ and } \theta_{12}^d = \theta_C\text{:} \\ \theta_{13}^{\text{PMNS}} = 9.8° \ . \end{gathered} \tag{7.39}$$

Alternatively, one can use the scenario of symmetric Y_d and Y_e together with non-vanishing 1-1 element d. Performing an analogous fit yields a GUT-scale prediction of

$$\begin{gathered} SU(5) \text{ with } a \equiv b,\ d \neq 0,\ c_d = -\tfrac{3}{2} \text{ and } c_b = c_c = -3\text{:} \\ \theta_{13}^{\text{PMNS}} = 8.8° \ . \end{gathered} \tag{7.40}$$

Corrections from $\theta_{12}^d \neq \theta_C$

In an explicit GUT flavour model, the condition $\theta_{12}^d = \theta_C$ may not be fulfilled exactly. Model independently, this constitutes a source of theoretical uncertainty. Within a specific model, it will result in a different value for θ_{12}^e and consequently in a modified prediction for $\theta_{13}^{\text{PMNS}}$. Thus different models with different θ_{12}^d might be able to be distinguished with future more precise measurements of $\theta_{13}^{\text{PMNS}}$.

For example, consider the scenario where θ_{13}^u, $\theta_{13}^d \approx 0$, which in turn leads to $\theta_{12}^d \approx 12.0° \pm 0.3°$ via the quark mixing sum rule [108] instead of $\theta_{12}^d = \theta_C$. Furthermore, let us assume a model with symmetric Yukawa matrices (it does not matter whether Pati-Salam or $SU(5)$) and CG factors $c_d = 9$ and $c_b = c_c = -3$, leading to matrices of the form

$$Y_d = \begin{pmatrix} d & b \\ b & c \end{pmatrix} \ , \quad Y_e = \begin{pmatrix} c_d\, d & c_b\, b \\ c_b\, b & c_c\, c \end{pmatrix} \ . \tag{7.41}$$

Again using exact diagonalisation and fitting the experimental values, we obtain the modified GUT-scale prediction assuming $\theta_{23}^\nu = 45°$

$$\begin{gathered} \text{PS}/SU(5) \text{ with } \theta_{13}^u, \theta_{13}^d \approx 0, a \equiv b, c_d = 9 \text{ and } c_b = c_c = -3 : \\ \theta_{13}^{\text{PMNS}} = 8.9° \, . \end{gathered} \tag{7.42}$$

Note that this is only one example CG factor combination and others might lead to a slightly better fitting $\theta_{13}^{\text{PMNS}}$.

Corrections due to deviations from $\theta_{23}^\nu = 45°$

Another simplification we have made is using the relation for $\theta_{13}^{\text{PMNS}}$ in eqs. (7.14) only to leading order and assuming $\theta_{23}^\nu = 45°$. Thankfully, both corrections can be incorporated simultaneously and actually lead to a more accessible formula.

Namely, careful consideration of eqs. (7.14) reveals that the next-to-leading order contribution to $\theta_{13}^{\text{PMNS}}$ turns s_{23}^{ν} exactly into the term representing s_{23}^{PMNS}, leading to the modified relation

$$\theta_{13}^{\text{PMNS}} = \theta_{12}^{e} s_{23}^{\text{PMNS}} \,, \tag{7.43}$$

up to further corrections of $\mathcal{O}((\theta_{13}^{\text{PMNS}})^3)$. With the measured range for $\theta_{23}^{\text{PMNS}}$, this already introduces an uncertainty of about 5% as well as a dependence on the neutrino mass hierarchy [16]. For instance in a normal mass hierarchy, the predicted value for $\theta_{13}^{\text{PMNS}}$ from eq. (7.43) is reduced from the value of 9.8° of eq. (7.39) to 9.3° and to 8.3° in the case of eq. (7.40). An improved experimental accuracy for $\theta_{23}^{\text{PMNS}}$ and/or a determination of the mass hierarchy would thus be important for more precise tests of such $\theta_{13}^{\text{PMNS}}$ predictions.

Corrections due to Renormalisation Group Effects

Another important correction comes from RG evolution. For simplicity, we will restrict ourselves to the case of a strongly hierarchical neutrino mass spectrum, i.e. $m_1 = 0$ in the case of a normal hierarchy (NH) and $m_3 = 0$ in the case of an inverted hierarchy (IH). The used RG equations will be those valid in the MSSM extended with the Weinberg operator.

Taking into account the previous point, we will base our discussion on the relation

$$\theta_{13}^{\text{PMNS}} = \theta_C \, s_{23}^{\text{PMNS}} \,, \tag{7.44}$$

which assumes that $\theta_{12}^{e} = \theta_C$ and allows for application to general $\theta_{23}^{\text{PMNS}}$. Since, for a GUT flavour model, this relation is defined at the GUT scale M_{GUT}, to compare experimental data with those predicted by the model the following strategy is used:

The measured values of θ_C and $\theta_{23}^{\text{PMNS}}$ are run up to M_{GUT} to determine the value $\theta_{13}^{\text{PMNS}}|_{M_{\text{GUT}}}$. Then, the RG running of $\theta_{13}^{\text{PMNS}}|_{M_{\text{GUT}}}$ down to the electroweak scale M_{EW} is performed to obtain $\theta_{13}^{\text{PMNS}}|_{M_{\text{EW}}}$, the parameter measurable in experiments.

As discussed in chap. 5, the running of θ_C is very small and can be neglected in the following.

Using the analytical results of [114], one can estimate the change in the 2-3 mixing angle induced by running, $\Delta s_{23}^{\text{PMNS}} \equiv s_{23}^{\text{PMNS}}|_{M_{\text{EW}}} - s_{23}^{\text{PMNS}}|_{M_{\text{GUT}}}$, in leading logarithmic approximation and in leading (zeroth) order in $\theta_{13}^{\text{PMNS}}$ to:

$$\text{NH:} \quad \Delta s_{23}^{\text{PMNS}} \approx \frac{(y_\tau^{\text{SM}})^2(1+\tan^2\beta)}{16\pi^2} \ln\left(\frac{M_{\text{GUT}}}{M_{\text{EW}}}\right) (c_{23}^{\text{PMNS}})^2 s_{23}^{\text{PMNS}} \,, \tag{7.45a}$$

$$\text{IH:} \quad \Delta s_{23}^{\text{PMNS}} \approx -\frac{(y_\tau^{\text{SM}})^2(1+\tan^2\beta)}{16\pi^2} \ln\left(\frac{M_{\text{GUT}}}{M_{\text{EW}}}\right) (c_{23}^{\text{PMNS}})^2 s_{23}^{\text{PMNS}} \,. \tag{7.45b}$$

For the running of $\theta_{13}^{\mathrm{PMNS}}$, we also have to include the terms of $\mathcal{O}(\theta_{13}^{\mathrm{PMNS}})$, and obtain for $\Delta\theta_{13}^{\mathrm{PMNS}} \equiv \theta_{13}^{\mathrm{PMNS}}|_{M_{\mathrm{EW}}} - \theta_{13}^{\mathrm{PMNS}}|_{M_{\mathrm{GUT}}}$ in leading order in the small parameters $\theta_{13}^{\mathrm{PMNS}}$ and $\sqrt{|\Delta m_{21}^2/\Delta m_{31}^2|}$ (with $\Delta m_{ij}^2 = m_i^2 - m_j^2$ being the neutrino mass square differences) [114]:

$$\text{NH:}\quad \Delta\theta_{13}^{\mathrm{PMNS}} \approx \frac{(y_\tau^{\mathrm{SM}})^2(1+\tan^2\beta)}{16\pi^2}\ln\left(\frac{M_{\mathrm{GUT}}}{M_{\mathrm{EW}}}\right)\Bigg((c_{23}^{\mathrm{PMNS}})^2\theta_{13}^{\mathrm{PMNS}} + 2\,\frac{m_2}{m_3}\cos(\delta^{\mathrm{PMNS}}-\varphi_2^{\mathrm{PMNS}})c_{12}^{\mathrm{PMNS}}s_{12}^{\mathrm{PMNS}}c_{23}^{\mathrm{PMNS}}s_{23}^{\mathrm{PMNS}}\Bigg)\,, \tag{7.46a}$$

$$\text{IH:}\quad \Delta\theta_{13}^{\mathrm{PMNS}} \approx -\frac{(y_\tau^{\mathrm{SM}})^2(1+\tan^2\beta)}{16\pi^2}\ln\left(\frac{M_{\mathrm{GUT}}}{M_{\mathrm{EW}}}\right)(c_{23}^{\mathrm{PMNS}})^2\theta_{13}^{\mathrm{PMNS}}\,. \tag{7.46b}$$

Putting both corrections together and using the GUT-scale relation of eq. (7.44) yields

$$\theta_{13}^{\mathrm{PMNS}}|_{M_{\mathrm{EW}}} = \theta_C\, s_{23}^{\mathrm{PMNS}}|_{M_{\mathrm{GUT}}} + \Delta\theta_{13}^{\mathrm{PMNS}} \tag{7.47}$$

$$= \theta_C\,(s_{23}^{\mathrm{PMNS}}|_{M_{\mathrm{EW}}} - \Delta s_{23}^{\mathrm{PMNS}}) + \Delta\theta_{13}^{\mathrm{PMNS}}\,. \tag{7.48}$$

As one can see, for the IH case the terms $\Delta\theta_{13}^{\mathrm{PMNS}}$ and $\theta_C\,\Delta s_{23}^{\mathrm{PMNS}}$ cancel each other at leading order, while for NH only the term proportional to the neutrino mass ratio $\frac{m_2}{m_3}$ remains. Plugging in the experimental values of the mixing parameters and $y_\tau^{\mathrm{SM}} \approx 0.01$, we obtain the following estimate for RG corrected relation:

$$\text{NH:}\quad \theta_{13}^{\mathrm{PMNS}}|_{M_{\mathrm{EW}}} \approx \theta_C\, s_{23}^{\mathrm{PMNS}}|_{M_{\mathrm{EW}}} + 0.2^\circ\cos(\delta^{\mathrm{PMNS}}-\varphi_2^{\mathrm{PMNS}})\left(\frac{\tan\beta}{50}\right)^2\,, \tag{7.49a}$$

$$\text{IH:}\quad \theta_{13}^{\mathrm{PMNS}}|_{M_{\mathrm{EW}}} \approx \theta_C\, s_{23}^{\mathrm{PMNS}}|_{M_{\mathrm{EW}}}\,. \tag{7.49b}$$

The remaining (next to leading order) corrections in the IH case can be estimated to about $\mathcal{O}(0.05^\circ)\left(\frac{\tan\beta}{50}\right)^2$.

In conclusion, it is a rather good approximation to use parameters measured at low energies in eq. (7.44). Furthermore, for the IH case, the prediction is remarkably insensitive to RG effects.

Note that the above does not include effects from neutrino Yukawa couplings, which may enter above the mass thresholds of heavy right-handed neutrinos in seesaw type I models. These effects are more model-dependent and can be estimated using the analytical results of [65] or alternatively calculated numerically using the Mathematica package `REAP` (introduced in [65]).

For hierarchical neutrino Yukawa matrices, i.e. ones dominated by the 3-3 element y^ν_{33}, one can estimate the additional correction by replacing

$$(y_\tau^{\rm SM})^2(1+\tan^2\beta)\ln\left(\frac{M_{\rm GUT}}{M_{\rm EW}}\right)$$

in the previous equations with

$$(y^\nu_{33})^2\ln\left(\frac{M_{\rm GUT}}{M_{\rm R3}}\right)\ ,$$

where $M_{\rm R3}$ is the mass of the corresponding right-handed neutrino.

Corrections from canonical normalisation

Additional effects that can lead to deviations from $\theta_{13}^{\rm PMNS} = \theta_C\, s_{23}^{\rm PMNS}$ are due to the necessity of canonical normalisation of the kinetic terms. These effects often appear when heavy messenger fields are integrated out to generate effective operators that lead to Yukawa couplings, which inevitably also leads to effective operators in the Kähler potential. When these corrections to kinetic terms are dominated by third family effects, such that the Kähler metric for the lepton doublet fields is given by

$$K_L \approx k_0\,{\rm diag}(1,1,1+\eta^{\rm CN})\ , \tag{7.50}$$

they can be estimated, as has been discussed in [115, 116]. In this case, the corrections from canonical normalisation can be parametrised by a single (yet model-dependent) parameter $\eta^{\rm CN}$, while k_0 drops out as it is only an overall rescaling. Similar to before, an estimate of this correction can then be obtained from eqs. (7.45) and (7.46) via the replacement

$$(y_\tau^{\rm SM})^2(1+\tan^2\beta)\ln\left(\frac{M_{\rm GUT}}{M_{\rm EW}}\right) \quad \to \quad 8\pi^2\eta^{\rm CN}\ .$$

Analogous to case of RG corrections, the relation for $\theta_{13}^{\rm PMNS}$ is quite insensitive to CN corrections in the IH case. The actual value of $\eta^{\rm CN}$, on the other hand, is highly model-dependent. In the NH case, the CN effects may therefore well be of the order of the RG corrections (or even larger) in some specific models. On the other hand, there are classes of models where the CN corrections are negligible, cf. [115].

In summary, we conclude that the theoretical uncertainties for $\theta_{13}^{\rm PMNS}$ can amount to up to about $\mathcal{O}(10\%)$, which is larger than the current experimental uncertainty [16], but still not excessively so. It may even be desirable to have such corrections to reduce

tension between the theoretical and experimental values. The discussed scenario is thus interesting and well motivated, but in order to make a final verdict a careful model-by-model analysis including all corrections has to be performed. For two such models that realise all mentioned conditions and are in good agreement with experiment, see [117, 118].

7.6 The Mixing Sum Rule and Underlying Mixing Patterns

In the light of the determination of $\theta_{13}^{\rm PMNS}$, it is also interesting to discuss the following. When θ_{13}^{ν}, $\theta_{13}^{e} \ll \theta_C$ (**Condition 1**), the mixing angle θ_{12}^{ν} is related to $\theta_{13}^{\rm PMNS}$ and $\theta_{12}^{\rm PMNS}$ by the lepton mixing sum rule[2] [110, 119, 120]

$$\theta_{12}^{\rm PMNS} - \theta_{13}^{\rm PMNS} \cos(\delta^{\rm PMNS}) \approx \theta_{12}^{\nu} \, . \tag{7.51}$$

Thus, the size of $\theta_{13}^{\rm PMNS}$ has interesting consequences:

- Assuming tri-bimaximal mixing in the neutrino sector [106], i.e. $\sin(\theta_{12}^{\nu}) = 1/\sqrt{3}$, the sum rule becomes

$$\theta_{12}^{\rm PMNS} - 8.5^\circ \cos(\delta^{\rm PMNS}) \approx \arcsin\left(\frac{1}{\sqrt{3}}\right) \, . \tag{7.52}$$

  This can only be consistent if $\delta^{\rm PMNS} \approx \pm 90^\circ$.[3]

- Another possibility would be bi-maximal neutrino mixing [123], i.e. $\theta_{12}^{\nu} = 45^\circ$. Then the sum rule reads

$$\theta_{12}^{\rm PMNS} - 8.5^\circ \cos(\delta^{\rm PMNS}) \approx 45^\circ \, , \tag{7.53}$$

  which is similar to the common form of the 'quark-lepton complementarity' relation $\theta_{12}^{\rm PMNS} + \theta_C \approx 45^\circ$ [124, 125, 126]. In contrast to before, the relation above requires $\delta^{\rm PMNS} \approx 180^\circ$ to agree reasonably well with the present experimental data.

We emphasise that neither tri-bimaximal nor bi-maximal neutrino mixing are required for the specific scenario. As stated above, it only depends on the value of the PMNS angle $\theta_{23}^{\rm PMNS}$ and the discussed conditions. In this sense, a future measurement of $\delta^{\rm PMNS}$

[2] The sum rule becomes $\theta_{12}^{\rm PMNS} - \theta_{13}^{\rm PMNS} \cot(\theta_{23}^{\rm PMNS}) \cos(\delta^{\rm PMNS}) \approx \theta_{12}^{\nu}$ if $\theta_{23}^{\rm PMNS}$ deviates from maximal mixing [110, 119, 120]. RG corrections to the sum rule have been discussed in [121].

[3] Such specific phases may emerge from flavour models with $\mathbb{Z}_2$ or $\mathbb{Z}_4$ shaping symmetries that can also explain a right-angled CKM unitarity triangle (with $\alpha \approx 90^\circ$), as discussed in [122].

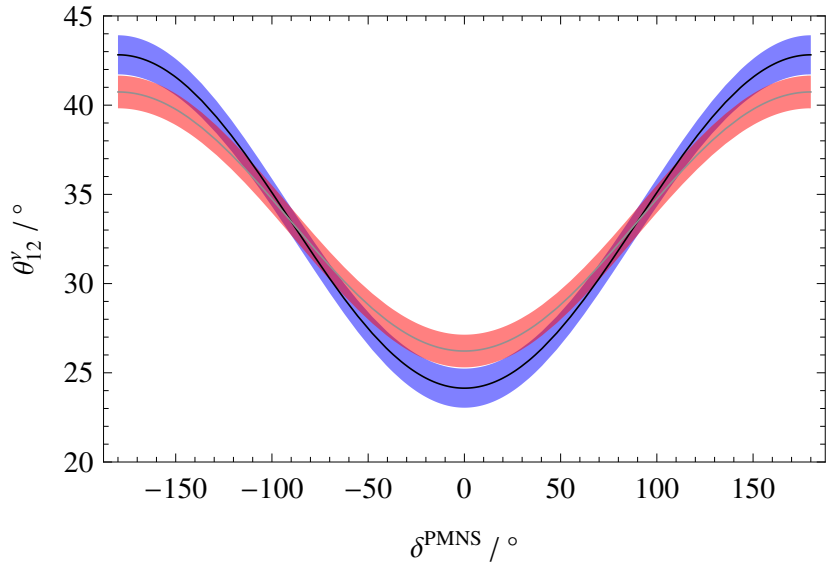

Figure 7.2: The value of θ_{12}^{ν} as reconstructed using the lepton mixing sum rule of eq. (7.51) (under the condition θ_{13}^{ν}, $\theta_{13}^{e} \ll \theta_C$). The shaded region denotes the 1σ uncertainty obtained from the uncertainties of $\theta_{12}^{\mathrm{PMNS}}$, $\theta_{13}^{\mathrm{PMNS}}$ and $\theta_{23}^{\mathrm{PMNS}}$, also including deviations of $\theta_{23}^{\mathrm{PMNS}}$ from 45°. Blue (red) corresponds to global fit values for normal (inverted) hierarchy.

can be viewed as "reconstructing" the underlying neutrino mixing value θ_{12}^{ν}, as shown in fig. 7.2. Thus, using the mixing sum rule of eq. (7.51), a precise measurement of $\theta_{12}^{\mathrm{PMNS}}$, $\theta_{13}^{\mathrm{PMNS}}$ and δ^{PMNS} may hint at a specific neutrino mixing pattern. The measurement of large $\theta_{13}^{\mathrm{PMNS}}$ provides a valuable input in this context.

Incidentally, it may be interesting to note that, while models with tri-bimaximal neutrino mixing seem to be associated with a normal neutrino mass hierarchy, see e.g. [117], models with bi-maximal mixing or similar rather tend to emerge in the context of models with inverse neutrino mass hierarchy, e.g. [118].

CHAPTER 8

Proton Decay and the Double Missing Partner Mechanism

8.1 Motivation

Regarding proton decay, most existing GUT models fall into two broad categories. On one hand, there are those that focus on the flavour sector and obtain viable mass and mixing relations while neglecting proton decay. On the other hand, there are those that manage to naturally suppress proton decay by solving the doublet-triplet splitting problem of GUTs, but have problems with the flavour sector. For example, they predict the unrealistic quark-lepton Yukawa relation $Y_e = Y_d^T$ (e.g. [127]), which may only be viable in the presence of extensive uncontrolled higher order corrections (e.g. [128]) rendering the model non-predictive, or the experimentally disfavoured Georgi-Jarlskog relations $y_\mu = 3y_s$ and $y_e = \frac{1}{3}y_d$ [48] (as e.g. in [129]). Alternatively, they rely on linear combinations of GUT Yukawa operators (e.g. [130]), which again implies the loss of predictivity. Also many flavour models assume certain Abelian 'shaping' symmetries for their fields valid at high scales, but do not include in their discussion what form the GUT Higgs potential should take and what consequences this entails. It is therefore worthwhile to study how the aspects of viable flavour structure and proton decay can be combined into a predictive and more complete setup than what was previously done.

Therefore, in the following, we intend to study one proposed solution to the doublet-triplet splitting problem (in four space-time dimensions) called the "missing partner mechanism" (MPM) [131, 132] and its improved version, the "double missing partner mechanism" (DMPM) [133] (as is used in most of the articles cited above) in the context of supersymmetric $SU(5)$ GUT models of flavour. In this context, we are again guided by the approach of [49] and later publications (e.g. [8, 111] and [9, 134, 117, 118]) involving higher-dimensional operators which contain a GUT breaking Higgs field and lead to Clebsch-Gordan (CG) factors appearing as Yukawa coupling ratios, as is also

discussed in chap. 7.

This chapter is organised into three parts: first in sec. 8.2, we discuss the features of the MPM and DMPM as solution to the doublet-triplet splitting problem (DTS) in the context of both dimension five and six proton decay operators generated by the Higgs colour triplets. Here we ultimately arrive at the conclusion that for the considered structure of Yukawa coupling relations more than one GUT Higgs field in the adjoint representation **24** of $SU(5)$ is necessary. Consequently in sec. 8.3, we study the implications of this together with gauge coupling unification in the context of the DMPM for the proton decay operator suppression scales and the GUT scale. Finally in sec. 8.4, we discuss further features of the assumed structure for predictions of the proton decay width, for which particularly app. D can be helpful material for GUT model building.

8.2 Single and Double Missing Partner Mechanism for Flavour Models

In the following, we review the missing partner mechanism and double missing partner mechanism such that it can be used with GUT Higgs fields in the adjoint representation **24** of $SU(5)$. This makes it possible to integrate it into scenarios where discrete CG ratios are used for relations between Yukawa couplings, e.g. the scenario shown in chap. 7.

Throughout this section, for illustrative purposes, we consider that the bounds on proton decay rate require the effective mass of the colour triplets to be of at least $M_T^{\text{dim=5}} \approx 10^{17}$ GeV [59], while the effective mass suppressing dimension six proton decay mediated by the colour triplets is required to be $M_T^{\text{dim=6}} \gtrsim 10^{12}$ GeV, see sec. 4.4 and [58].

8.2.1 The Missing Partner Mechanism

The basic idea of the missing partner mechanism (MPM) is the introduction of a pair of superfields Z_{50} and $\bar{Z}_{50}$ in **50** and $\overline{\mathbf{50}}$ representations of $SU(5)$ based on the fact that the decomposition of a **50** under the SM gauge group contains the same $SU(3)$ triplet as in the **5**, but not an $SU(2)$ doublet. Thus, using the **50**-plets to generate an effective mass term for the colour triplets in the **5** fields keeps the electroweak doublets massless, while the colour triplets acquire masses of the order of the GUT scale. The superpotential for the MPM is given by[1]

$$W_{\text{MPM}} = \bar{H}_5 H_{75} Z_{50} + \bar{Z}_{50} H_{75} H_5 + M_{50} Z_{50} \bar{Z}_{50} \,, \tag{8.1}$$

[1]For simplicity we omit most order one coefficients in the superpotentials, except where they are relevant to the discussion.

where H_{75} is a superfield transforming in the **75** representation of $SU(5)$, which contains a SM singlet. When H_{75} acquires a vacuum expectation value in that direction, $SU(5)$ is broken to the SM gauge group. With the triplet mass contribution from $\langle H_{75}\rangle$ denoted as V, the mass matrices of the Higgs doublet and triplet fields in H_5, $\bar{H}_5$ and Z_{50}, $\bar{Z}_{50}$ are given by

$$m_D = 0 \ , \quad m_T = \begin{pmatrix} 0 & V \\ V & M_{50} \end{pmatrix} \ , \tag{8.2}$$

where the first row and column refers to the triplet and anti-triplet contained in the 5-dimensional representations. Let us assume that the colour triplet Yukawa couplings for dimension five proton decay are obtained from terms of the form

$$W_{\text{Yuk}} = \mathcal{T}_i \mathcal{F}_j \bar{H}_5 + \mathcal{T}_i \mathcal{T}_j H_5 \ , \tag{8.3}$$

where the families of the MSSM matter superfields are embedded in the standard way in $\mathcal{T}_i$ and $\mathcal{F}_j$, transforming as **10** and $\bar{\mathbf{5}}$ of $SU(5)$, respectively. To calculate the effective dimension five proton decay operators all Higgs triplets from 5- and 50-dimensional representations have to be integrated out, but considering W_{Yuk} as above only the triplets in the 5-dimensional representations dominantly couple to matter. Denoting the triplet mass eigenvalues as $\tilde{M}_1$ and $\tilde{M}_2$, and the corresponding mass eigenstates as $\tilde{T}_1$ and $\tilde{T}_2$, the triplets that couple to matter are then given by the combinations

$$T^{(5)} = \sum_i U^*_{1i} \tilde{T}_i \ , \quad \bar{T}^{(5)} = \sum_i V_{1i} \bar{\tilde{T}}_i \ , \tag{8.4}$$

where U and V are unitary matrices such that $U^\dagger m_T V = \text{diag}(\tilde{M}_1, \tilde{M}_2) \equiv m_T^{\text{diag}}$. Integrating out all triplet mass eigenstates $\tilde{T}_i$ and $\bar{\tilde{T}}_i$ generates a contribution to the dimension five operators for proton decay proportional to the inverse of the "effective triplet mass"

$$(M_T^{\text{dim=5}})^{-1} := V_{1i} \left(m_T^{\text{diag}}\right)^{-1}_{ij} U^*_{1j} = V_{1i} \left(m_T^{\text{diag}}\right)^{-1}_{ij} U^\dagger_{j1} = (m_T^{-1})_{11} \ . \tag{8.5}$$

Also inserting the equations of motion in the Kähler potential of the colour triplets,

$$K_T = T^{(5)} T^{(5)\dagger} + \bar{T}^{(5)} \bar{T}^{(5)\dagger} + T^{(50)} T^{(50)\dagger} + \bar{T}^{(50)} \bar{T}^{(50)\dagger} \ , \tag{8.6}$$

yields contributions to the dimension six proton decay operators proportional to

$$\left(M_{\bar{T}}^{\text{dim=6}}\right)^{-2} := V_{1i} \left(m_T^{\text{diag}}\right)^{-1}_{ij} U^\dagger_{jk} U_{km} \left(m_T^{\text{diag}}\right)^{-1}_{ml} V^\dagger_{l1} = \left(m_T^{-1} m_T^{\dagger -1}\right)_{11} \ , \tag{8.7}$$

for the $Q^\dagger L^\dagger d^c u^c$ operator and proportional to $(M_T^{\text{dim=6}})^{-2} = (m_T^{\dagger -1} m_T^{-1})_{11}$ for the $Q^\dagger Q^\dagger u^c e^c$ operator as given in eq. (4.28b). With the mass matrix m_T given in eq. (8.2),

the effective triplet mass is thus[2]

$$M_T^{\text{dim=5}} = \left(m_T^{-1}\right)_{11}^{-1} = -\frac{V^2}{M_{50}} \,, \tag{8.8}$$

while the suppression scales of the dimension six operators are given by

$$\left(M_{\bar{T}}^{\text{dim=6}}\right)^2 = \left(M_T^{\text{dim=6}}\right)^2 = \left(m_T^{-1} m_T^{\dagger -1}\right)_{11}^{-1} = \frac{|V|^4}{|M_{50}|^2 + |V|^2} \,. \tag{8.9}$$

With a GUT scale of $V \approx 10^{16}$ GeV and M_{50} below the Planck scale, the dimension six proton decay is suppressed sufficiently with values of $M_T^{\text{dim=6}}$ between 10^{13} and 10^{16} GeV. Since the doublets obtain no mass terms, the splitting of doublet mass and effective triplet mass is successful. However, requiring $M_T^{\text{dim=5}} \gtrsim 10^{17}$ GeV one obtains an upper bound for $M_{50} \lesssim 10^{15}$ GeV. Having the large representations **50** and $\overline{\mathbf{50}}$ enter the renormalisation group (RG) running of the gauge couplings at this scale leads to the break down of perturbativity just above the GUT scale. Thus, the MPM solves the DTS problem, but trades it for $SU(5)$ becoming non-perturbative much below the Planck scale M_{Pl}.

8.2.2 The Double Missing Partner Mechanism

This trade-off is avoided in the double missing partner mechanism (DMPM), which owes its name to the doubling of the number of Higgs fields in **5**, $\bar{\mathbf{5}}$, **50** and $\overline{\mathbf{50}}$ representations [133]. The original fields H_5 and $\bar{H}_5$ are still the only ones that couple to the matter fields $\mathcal{F}_i$ and $\mathcal{T}_i$, whereas their new siblings H_5' and $\bar{H}_5'$ do not. The superpotential for the DMPM is given by

$$\begin{aligned} W_{\text{DMPM}} = {} & \bar{H}_5 H_{75} Z_{50} + \bar{Z}_{50} H_{75} H_5' + \bar{H}_5' H_{75} Z_{50}' + \bar{Z}_{50}' H_{75} H_5 \\ & + M_{50} Z_{50} \bar{Z}_{50} + M_{50}' Z_{50}' \bar{Z}_{50}' \\ & + \mu' H_5' \bar{H}_5' \,. \end{aligned} \tag{8.10}$$

The mass matrices of the doublet and triplet components of the Higgs fields H_5, H_5', Z_{50}, Z_{50}' and their corresponding barred fields, after H_{75} gets a VEV V, are given by

$$m_D = \begin{pmatrix} 0 & 0 \\ 0 & \mu' \end{pmatrix} \,, \quad m_T = \begin{pmatrix} 0 & 0 & 0 & V \\ 0 & \mu' & V & 0 \\ V & 0 & M_{50} & 0 \\ 0 & V & 0 & M_{50}' \end{pmatrix} \,. \tag{8.11}$$

[2]Whenever we quote numbers for $M_T^{\text{dim=5}}$, $M_{\bar{T}}^{\text{dim=6}}$ and $M_T^{\text{dim=6}}$ in the text, we will always refer to their absolute values.

While the Higgs doublets coupling to matter remain massless, the second pair of Higgs doublets contained in H_5' and $\bar{H}_5'$ has mass μ'. The improvement of the DMPM compared to the MPM can be seen in the effective triplet mass $M_T^{\text{dim=5}}$

$$M_T^{\text{dim=5}} = \left(m_T^{-1}\right)_{11}^{-1} = -\frac{V^4}{\mu' M_{50} M_{50}'} \,. \tag{8.12}$$

The same effective triplet mass of $M_T^{\text{dim=5}} \approx 10^{17}$ GeV can now be reached with masses $M_{50} \approx M_{50}' \approx 10^{18}$ GeV, provided the heavier doublet pair has a (relatively) small mass $\mu' \approx 10^{11}$ GeV. With the large representations of $SU(5)$ having high masses, the perturbativity of the model can be preserved up to (almost) the Planck scale. Finally, the dimension six proton decay operators are suppressed by

$$\begin{aligned}
\left(M_{\bar{T}}^{\text{dim=6}}\right)^2 &= \left(m_T^{-1} m_T^{\dagger -1}\right)_{11}^{-1} \\
&= \frac{|V|^8}{|V|^6 + |M_{50}|^2 \left(|V|^4 + |M_{50}' \mu'|^2 + |V\mu'|^2\right)} \approx (10^{14}\ \text{GeV})^2 \,, \qquad (8.13a) \\
\left(M_T^{\text{dim=6}}\right)^2 &= \left(m_T^{\dagger -1} m_T^{-1}\right)_{11}^{-1} \\
&= \frac{|V|^8}{|V|^6 + |M_{50}'|^2 \left(|V|^4 + |M_{50} \mu'|^2 + |V\mu'|^2\right)} \approx (10^{14}\ \text{GeV})^2 \,, \qquad (8.13b)
\end{aligned}$$

without tension with the bounds on proton decay.

8.2.3 Dealing with Planck-Scale Suppressed Operators

Considering the inherently non-renormalisable structure of supergravity (the extension of global SUSY to a local symmetry which automatically includes gravitational interactions) [41], it is reasonable to assume that all higher dimensional operators allowed by the imposed symmetries are present and suppressed by some power of the Planck-scale if they are not already generated via some other means. In that case, the naive implementations of the MPM and DMPM run into the following problem.

The superpotentials given in eq. (8.1) and eq. (8.10) include direct mass terms for the 50-dimensional fields. As a consequence, one cannot use symmetries to forbid non-renormalisable Planck-scale suppressed operators such as

$$W \supset \frac{1}{M_{\text{Pl}}} H_5 H_{75}^2 \bar{H}_5 \tag{8.14}$$

for the MPM and

$$W \supset \frac{1}{M_{\text{Pl}}} H_5 H_{75}^2 \bar{H}_5' + \frac{1}{M_{\text{Pl}}} H_5' H_{75}^2 \bar{H}_5 \tag{8.15}$$

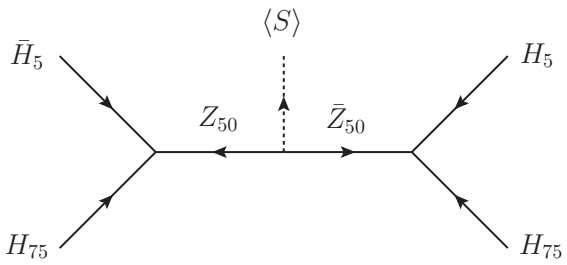

Figure 8.1: MPM diagram with an external S field generating the mass term for the 50-dimensional messengers after acquiring a VEV.

for the DMPM. These Planck-scale suppressed higher dimensional operators do not involve the 50-dimensional messengers and therefore generate dangerously large contributions to the masses of the doublets contained in the 5-dimensional representations, effectively spoiling the doublet-triplet splitting mechanism.

Given the above philosophy, we must forbid these operators through a symmetry, which we call a shaping symmetry. The MPM and the DMPM can then be restored by adding a singlet field S, responsible for giving mass to the 50-dimensional superfields through couplings of the form $SZ_{50}\bar{Z}_{50}$, $SZ'_{50}\bar{Z}'_{50}$ and a VEV $\langle S \rangle \neq 0$, as seen in the diagram in fig. 8.1 (note that S is not acting as an external field but generating the mass term). The non-trivial charge of S under a shaping symmetry forbids the dangerous Planck-suppressed operators.

It is interesting to note that this strategy of generating masses for the messenger fields through an additional singlet field also stabilises the predictions for the Yukawa coupling ratios in models using CG factors by forbidding unwanted index contractions that would appear with Planck-scale suppression, cf. the example models given in [10].

8.2.4 The Double Missing Partner Mechanism with an Adjoint of $SU(5)$

As was seen in chap. 7, Clebsch-Gordan factors originating from couplings to a GUT breaking Higgs field H_{24} in the adjoint representation **24** of $SU(5)$ can be particularly useful for GUT model building. It is thus well motivated to replace the GUT Higgs field H_{75} needed in the DMPM with the effective combination H_{24}^2/Λ, see also [127]. This can be achieved at the renormalisable level by integrating out heavy messenger fields in the **45** and $\overline{\mathbf{45}}$ representations of $SU(5)$ [130].

To replace the H_{75} in the MPM, we thus have to introduce a set of messenger fields X_{45}, $\bar{X}_{45}$, Y_{45} and $\bar{Y}_{45}$. For the DMPM, we also need to add a second set X'_{45}, $\bar{X}'_{45}$, Y'_{45} and $\bar{Y}'_{45}$. In fig. 8.2 we show the supergraphs generating the non-diagonal entries of the triplet mass matrix in the DMPM with an adjoint H_{24}.

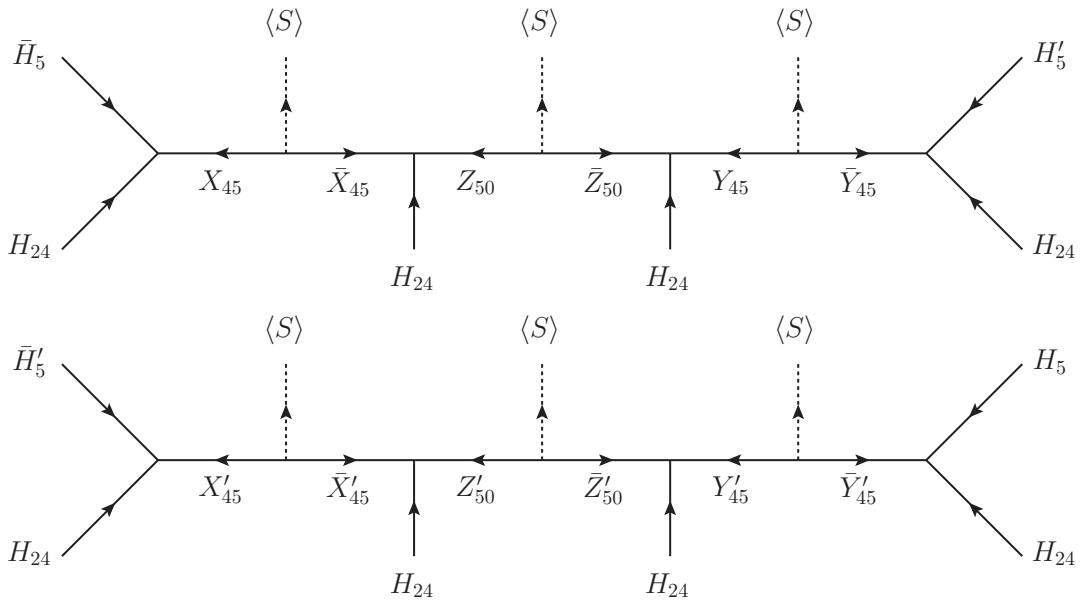

Figure 8.2: Supergraphs generating the non-diagonal entries of the triplet mass matrix as in eq. (8.18).

Related to the discussion in sec. 8.2.3, we avoid direct mass terms in order to forbid dangerous Planck-suppressed operators that would generate universal mass contributions for Higgs doublets and triplets. Instead, the messenger pairs $X_{45}\bar{X}_{45}$, $Y_{45}\bar{Y}_{45}$, $Z_{50}\bar{Z}_{50}$ and their corresponding primed versions obtain masses from the VEV of a singlet field S, charged under an additional shaping symmetry.

The renormalisable superpotential is then given by:

$$\begin{aligned} W_{\text{DMPM24}} = {} & \bar{H}_5 H_{24} X_{45} + \bar{X}_{45} H_{24} Z_{50} + \bar{Z}_{50} H_{24} Y_{45} + \bar{Y}_{45} H_{24} H_5' \\ & + \bar{H}_5' H_{24} X_{45}' + \bar{X}_{45}' H_{24} Z_{50}' + \bar{Z}_{50}' H_{24} Y_{45}' + \bar{Y}_{45}' H_{24} H_5 \\ & + S X_{45}\bar{X}_{45} + S Y_{45}\bar{Y}_{45} + S Z_{50}\bar{Z}_{50} + S X_{45}'\bar{X}_{45}' + S Y_{45}'\bar{Y}_{45}' + S Z_{50}'\bar{Z}_{50}' \\ & + \mu' H_5'\bar{H}_5' \,, \end{aligned} \tag{8.16}$$

where we carefully checked that, with this messenger field content, no dangerous Planck-suppressed operators appear that spoil the mechanism.

After H_{24} and S obtain their VEVs and after integrating out the 45-dimensional messenger fields, we find the following mass matrices for the Higgs doublets and triplets

$$m_D = \begin{pmatrix} 0 & 0 \\ 0 & \mu' \end{pmatrix} \,, \qquad m_T = \begin{pmatrix} 0 & 0 & 0 & -\frac{V^2}{\langle S\rangle} \\ 0 & \mu' & -\frac{V^2}{\langle S\rangle} & 0 \\ -\frac{V^2}{\langle S\rangle} & 0 & \langle S\rangle & 0 \\ 0 & -\frac{V^2}{\langle S\rangle} & 0 & \langle S\rangle \end{pmatrix} \,, \tag{8.17}$$

which is, of course, highly reminiscent of eq. (8.11). Here V is defined by $\langle H_{24}\rangle \equiv V\mathrm{diag}(1,1,1,-\frac{3}{2},-\frac{3}{2})$. Integrating out the heavy 50-dimensional fields in a next step, the mass matrices become

$$m_D = \begin{pmatrix} 0 & 0 \\ 0 & \mu' \end{pmatrix} , \quad m_T = \begin{pmatrix} 0 & -\frac{V^4}{\langle S\rangle^3} \\ -\frac{V^4}{\langle S\rangle^3} & \mu' \end{pmatrix} . \tag{8.18}$$

Thus, the doublets in the pair $H_5\bar{H}_5$ stay massless, while the doublet pair in $H_5'\bar{H}_5'$ is heavy. Using only H_5 and $\bar{H}_5$ for the Yukawa couplings of the SM fermions, the effective triplet component mass relevant for dimension five proton decay is given by

$$M_T^{\mathrm{dim=5}} = \left(m_T^{-1}\right)^{-1}_{11} = -\frac{V^8}{\langle S\rangle^6\mu'} , \tag{8.19}$$

while the effective masses suppressing dimension six proton decay mediated by colour triplets are given by

$$\left(M_{\bar{T}}^{\mathrm{dim=6}}\right)^2 = \left(M_T^{\mathrm{dim=6}}\right)^2 \approx \frac{|V|^8}{|\langle S\rangle|^6} , \tag{8.20}$$

where we approximated using $|\langle S\rangle| \gg |V|$ and $|\langle S\rangle^3\mu'| \ll |V|^4$. Hence, the requirement of $M_T^{\mathrm{dim=6}} \gtrsim 10^{12}$ GeV can only be obtained with $\langle S\rangle \approx 10^{18}$ GeV if the GUT-scale value is larger than $V \gtrsim 10^{16}$ GeV. In this case one needs $\mu' \approx 10^7$ GeV to obtain an effective triplet mass $M_T^{\mathrm{dim=5}} \approx 10^{17}$ GeV for dimension five proton decay operators. Therefore, if the GUT-scale is high enough, the effective triplet mass can be large enough to stabilise the proton and the large $SU(5)$ representations used in the DMPM can be heavy enough to keep the theory perturbative up to the Planck scale.

When H_{24} is uncharged under additional symmetries, having μ' several orders of magnitude smaller than V requires μ' to arise from the spontaneous breakdown of a shaping symmetry, to avoid the term $\langle H_{24}\rangle H_5'\bar{H}_5'$, which would give rise to a too large contribution to μ' and consequently a too small effective triplet mass. Note that the effective triplet masses entering the dimension five proton decay operators can be expressed in terms of the mass eigenstates of doublet and triplet components as $M_T^{\mathrm{dim=5}} = -\tilde{M}_1\tilde{M}_2/\mu'$. The effective triplet mass of dimension six proton decay is then excellently approximated by $M_T^{\mathrm{dim=6}} = M_{\bar{T}}^{\mathrm{dim=6}} \approx \sqrt{M_T^{\mathrm{dim=5}}\mu'}$.

Finally, one may wonder if some of the heavy messengers are redundant and could be merged with others, so that the number of fields in the spectrum would be reduced while preserving the structure of the mechanism. However, if either $X_{45} \equiv Y_{45}$ or $X_{45}' \equiv Y_{45}'$, it can be seen from fig. 8.2 that supergraphs without the $Z_{50}\bar{Z}_{50}$ mass insertion would be allowed, spoiling the splitting of doublets and triplets and generating large non-diagonal entries in the doublet mass matrix m_D. On the other hand, if either $X_{45} \equiv X_{45}'$, $Y_{45} \equiv Y_{45}'$ or $Z_{50} \equiv Z_{50}'$, the DMPM is reduced to the MPM, reintroducing the issue of perturbativity. Finally, an identification of $X_{45} \equiv Y_{45}'$ would allow diagrams

bypassing the 50-dimensional fields, generating unwanted mass term for both doublet and triplet components of H_5, $\bar{H}_5$, and thus a too large μ-term. In conclusion, we see no way to shrink the messenger spectrum of this variant of the DMPM.

8.2.5 Introducing a Second Adjoint Field

As we have seen above, the DMPM with an adjoint GUT breaking Higgs H_{24} instead of a **75** solves the DTS problem while providing the necessary building block for the desirable CG factors for flavour model building. In the following, we will argue why it is compelling to introduce a second adjoint Higgs field:

- In the minimal SUSY $SU(5)$ model [37], the single GUT breaking **24** contains an $SU(2)_L$ triplet component and an $SU(3)_C$ octet component with equal masses. Demanding gauge coupling unification, the mass of the Higgs colour triplets is required to be about 10^{15} GeV [135], ruling out this model due to proton decay. Non-renormalisable operators in the GUT breaking superpotential, as in

$$W \supset M \,\mathrm{tr} H_{24}^2 + \frac{1}{\Lambda} \left(\mathrm{tr} H_{24}^2\right)^2 + \frac{1}{\Lambda'} \,\mathrm{tr} H_{24}^4 \,, \tag{8.21}$$

  can split the **24** component masses, allowing for a higher effective triplet mass, see [136] and also sec. 8.3. An additional **24** can be used to realise this non-renormalisable superpotential in a renormalisable way.

- It turns out that the introduction of an additional **24** is not just a UV-completion of the non-renormalisable superpotential of [136]. When both adjoints have approximately the same mass and therefore the second **24** is not integrated out, the additional colour octet and electroweak triplet in the spectrum lead to more freedom for the GUT scale and effective triplet mass. In the following section, we thus discuss all feasible renormalisable superpotentials with two adjoints and their impact on M_{GUT} and $M_T^{\mathrm{dim}=5}$ in a gauge coupling unification analysis.

- A renormalisable superpotential for one **24** requires it to be uncharged under shaping symmetries to acquire a VEV. However, a shaping symmetry charge is vital in the type of flavour models considered here and in chap. 7 to enforce texture zeros and avoid unwanted admixtures of additional CG factors involving less insertions of H_{24}. With a second **24**, the adjoint fields can acquire non-vanishing VEVs also when charged under such shaping symmetries.

The features of renormalisable superpotentials for two adjoints are discussed in detail in the next section.

8.3 Gauge Coupling Unification and the Effective Triplet Mass

In GUT extensions of the SM, it is common to have additional fields somewhere below the GUT scale that modify the RG running of the gauge couplings up to the GUT scale. This is also the case in the class of models we want to investigate here. It ts therefore necessary to re-evaluate the unification of gauge couplings within our extended spectrum.

8.3.1 Gauge Coupling Unification with the Additional Fields

To study the gauge coupling unification, we start with the modified equality condition at one-loop level,

$$\frac{1}{\alpha_u} = \frac{1}{\alpha_i} - \frac{1}{2\pi}\left(b_i^{(\mathrm{SM})} \log\frac{M_{\mathrm{SUSY}}}{M_Z} + b_i^{(\mathrm{MSSM})} \log\frac{M_{\mathrm{GUT}}}{M_{\mathrm{SUSY}}} + \sum_f b_i^{(f)} \log\frac{M_{\mathrm{GUT}}}{M_f} \right) , \quad (8.22)$$

where $i = 1, 2, 3$ labels the SM gauge interactions and f labels the additional superfields (compared to the MSSM), with masses M_f and one-loop beta coefficients $b_i^{(f)}$. For the full SM spectrum, the one-loop beta-function coefficients are $b_i^{(\mathrm{SM})} = (41/10, -19/6, -7)$, while for the full MSSM spectrum we have $b_i^{(\mathrm{MSSM})} = (33/5, 1, -3)$. We define the SUSY scale M_{SUSY} here as the scale where we make the transition from the SM beta coefficients to the MSSM ones, so all superpartners enter the theory at the same scale. The α_i appearing in eq. (8.22) are those at low energies $\alpha_i \equiv \alpha_i(M_Z)$, while α_u is the unified gauge coupling at the GUT scale $\alpha_u \equiv \alpha_i(M_{\mathrm{GUT}})$. The GUT scale M_{GUT} is defined here as the scale where the last $SU(5)$ multiplet is completed, in other words the scale where all three one-loop beta coefficients for the SM gauge couplings become equal.

In the following, we assume that the heaviest incomplete $SU(5)$ multiplets to enter the RG equations are the leptoquark vector bosons such that the GUT scale corresponds to their mass $M_{\mathrm{GUT}} = M_V$. While other cases can certainly arise, we focus on this one as it is quite common in our setup to have heavy leptoquark vector bosons. We verified that in this case the effective colour triplet mass can be made very heavy as well.

Coming to the differences in field content between MSSM and DMPM, we see that the latter introduces one additional pair of $SU(2)$-doublets, $D^{(5)}$ and $\bar{D}^{(5)}$, and two additional pairs of $SU(3)$-triplets, $T_i^{(5)}$ and $\bar{T}_i^{(5)}$, $i = 1, 2$. They enter the beta-functions with the coefficients $b_i^{(5,D)} = (3/5, 1, 0)$ for the Dirac pair of doublets and $b_i^{(5,T)} = (2/5, 0, 1)$ per Dirac pair of triplet and anti-triplet.

Furthermore, we have two $SU(5)$ breaking GUT Higgs fields H_{24} and H'_{24} in the adjoint representation. They each contain one SM-singlet component, one $SU(2)$-triplet, $T^{(24)}$ with $b_i^{(24,T)} = (0,2,0)$, an $SU(3)$-octet, $O^{(24)}$ with $b_i^{(24,O)} = (0,0,3)$ and a leptoquark superfield pair, $L^{(24)}$ with $b_i^{(24,L)} = (5,3,2)$. Since one leptoquark superfield pair is eaten up during the spontaneous breaking of $SU(5)$, we are left with two triplets with masses $M_{T_1^{(24)}}$ and $M_{T_2^{(24)}}$, two octets with masses $M_{O_1^{(24)}}$ and $M_{O_2^{(24)}}$ and one leptoquark superfield pair with mass $M_{L^{(24)}}$. For convenience, we define the geometric means of the masses $M^2_{T^{(5)}} = M_{T_1^{(5)}} M_{T_2^{(5)}}$ for the colour triplets and analogously $M^2_{T^{(24)}} = M_{T_1^{(24)}} M_{T_2^{(24)}}$, $M^2_{O^{(24)}} = M_{O_1^{(24)}} M_{O_2^{(24)}}$ for the components of H_{24} and H'_{24}.

Having this at hand, we can solve eq. (8.22) for $M_{D^{(5)}}$, $M_{T^{(5)}}$ and M_{GUT}, to obtain the relations[3]

$$\begin{aligned}
\log M_{D^{(5)}} &= \frac{15\pi}{4\alpha_1} - \frac{17\pi}{4\alpha_2} - \frac{3\pi}{2\alpha_3} + \frac{59}{3}\log M_Z && \text{(8.23a)}\\
&\quad + \frac{2\pi}{\alpha_u} + \frac{3}{2}\log M_{L^{(24)}} - \frac{17}{2}\log M_{T^{(24)}} - \frac{9}{2}\log M_{O^{(24)}} - \frac{43}{6}\log M_{\mathrm{SUSY}}\,,\\
\log M_{T^{(5)}} &= \frac{35\pi}{24\alpha_1} - \frac{7\pi}{8\alpha_2} - \frac{19\pi}{12\alpha_3} + \frac{119}{12}\log M_Z && \text{(8.23b)}\\
&\quad + \frac{\pi}{\alpha_u} + \frac{3}{4}\log M_{L^{(24)}} - \frac{7}{4}\log M_{T^{(24)}} - \frac{19}{4}\log M_{O^{(24)}} - \frac{19}{6}\log M_{\mathrm{SUSY}}\,,\\
\log M_{\mathrm{GUT}} &= \frac{5\pi}{12\alpha_1} - \frac{\pi}{4\alpha_2} - \frac{\pi}{6\alpha_3} + \frac{11}{6}\log M_Z && \text{(8.23c)}\\
&\quad + \frac{1}{2}\log M_{L^{(24)}} - \frac{1}{2}\log M_{T^{(24)}} - \frac{1}{2}\log M_{O^{(24)}} - \frac{1}{3}\log M_{\mathrm{SUSY}}\,.
\end{aligned}$$

For the study of proton decay, it is more convenient to instead solve eq. (8.22) for the GUT-scale gauge coupling α_u and the effective triplet mass $M_T^{\mathrm{dim=5}} = M^2_{T^{(5)}}/M_{D^{(5)}}$, which gives the suppression of the dimension five proton decay operators (cf. the discussion in sec. 8.2.4). Then we get the relations

$$\begin{aligned}
\frac{\pi}{\alpha_u} &= -\frac{43\pi}{24\alpha_1} + \frac{15\pi}{8\alpha_2} + \frac{11\pi}{12\alpha_3} - \frac{197}{20}\log M_Z + \frac{3}{5}\log M_{DT} && \text{(8.24a)}\\
&\quad - \frac{3}{4}\log M_{L^{(24)}} + \frac{15}{4}\log M_{T^{(24)}} + \frac{11}{4}\log M_{O^{(24)}} + \frac{7}{2}\log M_{\mathrm{SUSY}}\,,\\
\log M_T^{\mathrm{dim=5}} &= -\frac{5\pi}{6\alpha_1} + \frac{5\pi}{2\alpha_2} - \frac{5\pi}{3\alpha_3} + \frac{1}{6}\log M_Z && \text{(8.24b)}\\
&\quad + 5\log M_{T^{(24)}} - 5\log M_{O^{(24)}} + \frac{5}{6}\log M_{\mathrm{SUSY}}\,,
\end{aligned}$$

[3] In the following, "log" of a mass is to be understood as the natural logarithm of the mass divided by one common mass scale, e.g. $\log m \equiv \log(m/\mathrm{GeV})$.

$$\begin{aligned}\log M_{\mathrm{GUT}} = {} & \frac{5\pi}{12\alpha_1} - \frac{\pi}{4\alpha_2} - \frac{\pi}{6\alpha_3} + \frac{11}{6}\log M_Z \\ & + \frac{1}{2}\log M_{L^{(24)}} - \frac{1}{2}\log M_{T^{(24)}} - \frac{1}{2}\log M_{O^{(24)}} - \frac{1}{3}\log M_{\mathrm{SUSY}}\ ,\end{aligned} \tag{8.24c}$$

where we have introduced the mass $M_{DT}^3 = M_{D^{(5)}}^2 M_{T^{(5)}}$. As one can see only α_u depends on M_{DT}, which one can explain using the fact that doublets and colour triplets together form a complete representation of $SU(5)$. Thus, following eq. (8.22), one can see that a simultaneous rescaling $M_{D^{(5)}} \to q^2 M_{D^{(5)}}$ and $M_{T^{(5)}} \to q M_{T^{(5)}}$ leaves the GUT scale invariant and only shifts α_u, while $M_T^{\mathrm{dim}=5} \propto q^0$ remains unchanged and $M_{DT} \propto q$ parametrises this rescaling. Further interdependencies between α_u, $M_T^{\mathrm{dim}=5}$ and M_{GUT} are then implicit via their shared dependence on the other masses.

Thus, gauge coupling unification implies that the effective triplet mass follows the relation

$$\begin{aligned}M_T^{\mathrm{dim}=5} &= \exp\left(\frac{5}{6}\pi\left(\frac{3}{\alpha_2} - \frac{2}{\alpha_3} - \frac{1}{\alpha_1}\right)\right) M_Z^{1/6} M_{\mathrm{SUSY}}^{\frac{5}{6}} \left(\frac{M_{T^{(24)}}}{M_{O^{(24)}}}\right)^5 \\ &= 2.5^{+0.6}_{-0.8} \cdot 10^{17}\ \mathrm{GeV} \left(\frac{M_{\mathrm{SUSY}}}{1\,\mathrm{TeV}}\right)^{\frac{5}{6}} \left(\frac{M_{T^{(24)}}}{M_{O^{(24)}}}\right)^5\ ,\end{aligned} \tag{8.25}$$

while the GUT scale is given by

$$M_{\mathrm{GUT}} = 1.37^{+0.05}_{-0.05} \cdot 10^{16}\ \mathrm{GeV} \left(\frac{M_{\mathrm{SUSY}}}{1\,\mathrm{TeV}}\right)^{-\frac{1}{3}} \left(\frac{M_{L^{(24)}}}{10^{16}\,\mathrm{GeV}}\right)^{\frac{1}{2}} \left(\frac{M_{T^{(24)}} M_{O^{(24)}}}{(10^{16}\,\mathrm{GeV})^2}\right)^{-\frac{1}{2}}\ . \tag{8.26}$$

For completeness, the unified gauge coupling is given by

$$\begin{aligned}\frac{1}{\alpha_u} = {} & 24.58 \pm 0.06 + \frac{7}{2\pi}\ln\frac{M_{\mathrm{SUSY}}}{1\,\mathrm{TeV}} + \frac{3}{5\pi}\ln\frac{M_{DT}}{10^{14}\,\mathrm{GeV}} \\ & - \frac{3}{4\pi}\ln\frac{M_{L^{(24)}}}{10^{16}\,\mathrm{GeV}} + \frac{15}{4\pi}\ln\frac{M_{T^{(24)}}}{10^{16}\,\mathrm{GeV}} + \frac{11}{4\pi}\ln\frac{M_{O^{(24)}}}{10^{16}\,\mathrm{GeV}}\ .\end{aligned} \tag{8.27}$$

For these numbers, we have used the experimental values and uncertainties for the gauge couplings as given in tab. 5.2. Note that for all three quantities the full uncertainty is dominated by the experimental error of g_3. In the following, we will not quote any uncertainties of these masses anymore since the relative uncertainty changes only negligibly for the different superpotentials and when switching over to two-loop running. The reference scale 10^{14} GeV is chosen due to the fact that $M_{DT} = 10^{14}$ GeV and $M_{T^{(5)}} = 10^{16}$ GeV implies $M_T^{\mathrm{dim}=5} = 10^{19}$ GeV.

Since the relation for the effective triplet mass $M_T^{\mathrm{dim}=5}$ receives significant two-loop contributions (cf. for instance [135]), we have also performed a numerical two-loop analysis using the following procedure with the Mathematica package `REAP` as modified for chap. 5. We start with SM values for the gauge and Yukawa couplings at M_Z as

given in tab. 5.2, run up to a scale of 1 TeV with the full two-loop SM RG equations and match the SM to the MSSM (including the $\overline{\text{MS}}$ to $\overline{\text{DR}}$ scheme conversion). From there we run and match using full two-loop MSSM RG equations while step-by-step including all additional multiplets at their mass scale via their one-loop gauge coupling threshold corrections[4] as well as contributions to the one- and two-loop gauge coupling RG equations, see app. E. The Yukawa couplings of the Higgs colour triplets are well approximated by using the Yukawa couplings of the corresponding doublets. We do not take into account any other Yukawa couplings. We verified that this approximation affects the numerical results at below percent level.

8.3.2 Superpotentials with Two Adjoints of $SU(5)$

In the following, we systematically study all renormalisable superpotentials with two adjoints that can break SU(5) to the SM gauge group. We find only four possibilities with non-vanishing VEVs and masses, classified based on their symmetry. These are:

(a) $W = M_{24}\,\mathrm{tr}H_{24}^2 + M'_{24}\mathrm{tr}H_{24}'^2 + \kappa'\,\mathrm{tr}H_{24}H_{24}'^2 + \lambda\,\mathrm{tr}H_{24}^3$,
$\mathbb{Z}_2$ symmetry where H_{24} is uncharged and H'_{24} charged.

(b) $W = \tilde{M}_{24}\,\mathrm{tr}H_{24}H'_{24} + \lambda\,\mathrm{tr}H_{24}^3 + \lambda'\,\mathrm{tr}H_{24}'^3$,
$\mathbb{Z}_3$ symmetry, where H_{24} has charge 2 and H'_{24} charge 1.

(c) $W = \tilde{M}_{24}\,\mathrm{tr}H_{24}H'_{24} + \lambda\,\mathrm{tr}H_{24}^3 + \kappa'\,\mathrm{tr}H_{24}H_{24}'^2$,
$\mathbb{Z}_4^R$ symmetry where H_{24} has a charge of 2 (with $q_\theta = 1$) and H'_{24} is uncharged.

(d) The trivial case with both fields only charged under $SU(5)$ and all (non-linear) terms allowed. We will not consider this case any further.

Since there are two adjoint Higgs fields, it is convenient to define a quantity $\tan\beta_V$ similar to $\tan\beta$ of the MSSM, so that

$$\langle H_{24}\rangle = V_1\ \mathrm{e}^{\mathrm{i}\phi_1}\ \mathrm{diag}(1,1,1,-3/2,-3/2)\ , \tag{8.28}$$

$$\langle H'_{24}\rangle = V_2\ \mathrm{e}^{\mathrm{i}\phi_2}\ \mathrm{diag}(1,1,1,-3/2,-3/2)\ , \tag{8.29}$$

with $V_1, V_2 > 0$ and $\tan\beta_V = V_1/V_2$.

Superpotential (a)

We will begin our discussion with superpotential (a) which turns out to be the most complicated case since it has the most parameters. As it contains two mass parameters, we introduce a second angle β_M and mean mass $M > 0$ such that $M_{24} = M\mathrm{e}^{\mathrm{i}\alpha_1}\sin\beta_M$

[4] When one integrates out particles at a threshold scale equal to their mass, these threshold corrections vanish, as can be seen in [137].

and $M'_{24} = M\mathrm{e}^{\mathrm{i}\alpha_2}\cos\beta_M$. The vacuum expectation values in terms of superpotential parameters are given by

$$V_1\mathrm{e}^{\mathrm{i}\phi_1} = \frac{4M'_{24}}{\kappa'} \quad \text{and} \quad V_2^2\mathrm{e}^{2\mathrm{i}\phi_2} = 4\,M'_{24}\frac{2M_{24}\kappa' - 3M'_{24}\lambda}{\kappa'^3}\,, \tag{8.30}$$

which can as well be expressed as $3\lambda/\kappa' = 2\mathrm{e}^{\mathrm{i}(\alpha_1-\alpha_2)}\tan\beta_M - \mathrm{e}^{-2\mathrm{i}(\phi_1-\phi_2)}\cot^2\beta_V$. For the geometric means of the masses of the additional fields inside the adjoints, we find

$$M^2_{T^{(24)}} = 5\,M^2\,\cos\beta_M\sqrt{(2\cos\beta_M - 3\sin\beta_M\tan^2\beta_V)^2 + \Delta}\,, \tag{8.31a}$$

$$M^2_{O^{(24)}} = 5\,M^2\,\cos\beta_M\sqrt{(3\cos\beta_M - 2\sin\beta_M\tan^2\beta_V)^2 + \Delta}\,, \tag{8.31b}$$

$$M^2_{L^{(24)}} = \frac{1}{4}\,M^2\,\frac{\cos^2\beta_M}{\sin^4\beta_V}\,, \tag{8.31c}$$

with $\Delta = 12\,\sin(2\beta_M)\,\cot^2(\beta_V)\,\sin^2\bar{\phi}$ and $\bar{\phi} = (\alpha_1-\alpha_2)/2 + \phi_1 - \phi_2$. Note that not only the geometric mean masses, but also the mass eigenvalues themselves only depend on this phase combination $\bar{\phi}$ and are invariant under $\bar{\phi}\to\bar{\phi}+\pi$.

The effective triplet mass as of eq. (8.25) is heaviest if the phase $\bar{\phi}$ is 0, π or 2π, since then the ratio $M_{T^{(24)}}/M_{O^{(24)}}$ is not bounded from above (or below), which allows for the maximal range for $M_T^{\mathrm{dim}=5}$. Thus, in the following, we choose $\bar{\phi}$ and thus Δ to vanish.

The resulting plots for $M_T^{\mathrm{dim}=5}$ and for M_{GUT} are shown in fig. 8.3 for $M_{\mathrm{SUSY}} = 1$ TeV, $M = 10^{15}$ GeV, $M_{D^{(5)}} = 1000$ TeV and $\bar{\phi} = 0$, including also a comparison between one- and two-loop results. Note that gauge coupling unification depends only weakly on $M_{D^{(5)}}$. The dimension six masses $M_{\bar{T}}^{\mathrm{dim}=6}$ and $M_T^{\mathrm{dim}=6}$ are still given by $\sqrt{M_T^{\mathrm{dim}=5}M_{D^{(5)}}}$ to a good approximation.

Superpotential (b) and (c)

These two superpotentials have only one massive parameter $\tilde{M}_{24} = M\mathrm{e}^{\mathrm{i}\alpha}$ and hence the analytic results become much less cumbersome. The vacuum solutions are given by

$$V_1\mathrm{e}^{\mathrm{i}\phi_1} = \frac{2}{3}\frac{M\mathrm{e}^{\mathrm{i}\alpha}}{\sqrt[3]{\lambda^2\lambda'}} \quad \text{and} \quad V_2\mathrm{e}^{\mathrm{i}\phi_2} = \frac{2}{3}\frac{M\mathrm{e}^{\mathrm{i}\alpha}}{\sqrt[3]{\lambda\lambda'^2}}\,, \tag{8.32}$$

up to a $\mathbb{Z}_3$ symmetry transformation for superpotential (b) and

$$V_1\mathrm{e}^{\mathrm{i}\phi_1} = \frac{1}{\sqrt{3}}\frac{M\mathrm{e}^{\mathrm{i}\alpha}}{\sqrt{\lambda\kappa'}} \quad \text{and} \quad V_2\mathrm{e}^{\mathrm{i}\phi_2} = \frac{M\mathrm{e}^{\mathrm{i}\alpha}}{\kappa'}\,, \tag{8.33}$$

up to a minus sign in V_1 for superpotential (c). In other words, the couplings fulfil the relation $\lambda'/\lambda = \mathrm{e}^{3\mathrm{i}(\phi_2-\phi_1)}\tan^3\beta_V$ for superpotential (b) and $\kappa'/\lambda = 3\mathrm{e}^{2\mathrm{i}(\phi_1-\phi_2)}\tan^2\beta_V$ for superpotential (c).

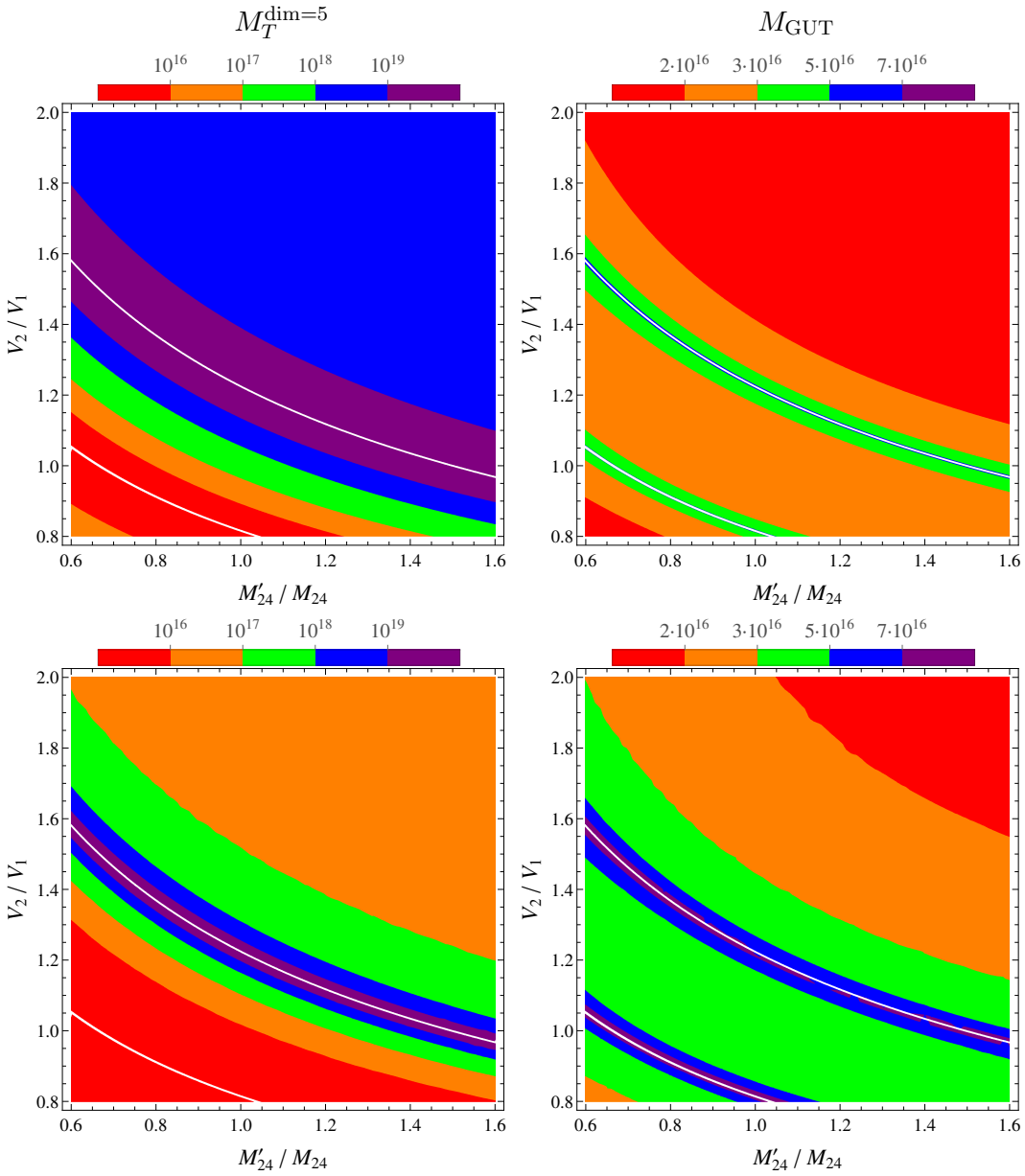

Figure 8.3: The effective colour triplet mass $M_T^{\text{dim=5}}$ (left) and GUT scale M_{GUT} (right) in GeV at one-loop (upper) and two-loop (lower) order as resulting from superpotential (a) for $M_{\text{SUSY}} = 1$ TeV, $M = 10^{15}$ GeV, $M_{D^{(5)}} = 1000$ TeV and $\bar{\phi} = 0$. Note the different colour coding of left and right. For illustration, the white strips denote areas with light $M_{T^{(24)}}$ or $M_{O^{(24)}}$ ($< 10^{13}$ GeV). Such relatively low values for these components can arise either from cancellation between terms, or from a generic suppression due to small parameters, cf. eqs. (8.31).

For the geometric means of the masses of the colour triplets, octets and the mass of the left-over leptoquark superfield in H_{24} and H'_{24}, we find

$$M^2_{T^{(24)}} = \frac{35}{4}\,M^2\ ,\quad M^2_{O^{(24)}} = \frac{15}{4}\,M^2 \text{ and } M^2_{L^{(24)}} = \frac{1}{\sin^2(2\beta_V)}\,M^2\ , \tag{8.34}$$

for superpotential (b) and

$$M^2_{T^{(24)}} = \frac{5}{4}\,M^2\ ,\quad M^2_{O^{(24)}} = \frac{5}{4}\,M^2 \text{ and } M^2_{L^{(24)}} = \frac{1}{4\sin^2(2\beta_V)}\,M^2\ , \tag{8.35}$$

for superpotential (c). Note that in both cases also all mass eigenvalues turn out to be phase-independent. Therefore, applying eq. (8.25), i.e. unification of the gauge couplings at one-loop, implies

$$M_T^{\text{dim=5, 1-loop}} = 2.5\cdot 10^{17}\text{ GeV}\left(\frac{M_{\text{SUSY}}}{1\,\text{TeV}}\right)^{\frac{5}{6}}\cdot\begin{cases}\left(\frac{7}{3}\right)^{\frac{5}{2}}\approx 8.3 & \text{(b)}\\ 1 & \text{(c)}\end{cases}\ , \tag{8.36}$$

and

$$M_{\text{GUT}}^{\text{1-loop}} = \frac{1.37\cdot 10^{16}\text{ GeV}}{\sqrt{|\sin 2\beta_V|}}\left(\frac{M_{\text{SUSY}}}{1\,\text{TeV}}\right)^{-\frac{1}{3}}\left(\frac{M}{10^{15}\,\text{GeV}}\right)^{-\frac{1}{2}}\cdot\begin{cases}\sqrt{\frac{8}{\sqrt{21}}}\approx 1.3 & \text{(b)}\\ 2 & \text{(c)}\end{cases}\ . \tag{8.37}$$

Assuming the same parameters, we find an almost ten times heavier effective triplet mass in superpotential (b) than in (c).

At two-loop, we find the following approximate behaviour for the masses

$$M_T^{\text{dim=5, 2-loop}} = \left(\frac{M_{\text{SUSY}}}{1\,\text{TeV}}\right)^{0.74}\cdot\begin{cases}5.2\cdot 10^{16}\text{ GeV}\left(\frac{M}{10^{15}\,\text{GeV}}\right)^{-0.15} & \text{(b)}\\ 6.8\cdot 10^{15}\text{ GeV}\left(\frac{M}{10^{15}\,\text{GeV}}\right)^{-0.18} & \text{(c)}\end{cases}\ , \tag{8.38}$$

and

$$M_{\text{GUT}}^{\text{2-loop}} = |\sin 2\beta_V|^{-0.48}\left(\frac{M_{\text{SUSY}}}{1\,\text{TeV}}\right)^{-0.4}\cdot\begin{cases}2.89\cdot 10^{16}\text{ GeV}\left(\frac{M}{10^{15}\,\text{GeV}}\right)^{-0.61} & \text{(b)}\\ 4.78\cdot 10^{16}\text{ GeV}\left(\frac{M}{10^{15}\,\text{GeV}}\right)^{-0.63} & \text{(c)}\end{cases}\ . \tag{8.39}$$

The dependence on other parameters is negligible. Based on this, having $M_T^{\text{dim=5}} \gtrsim 10^{17}$ GeV requires $M_{\text{SUSY}} \gtrsim 2.3$ TeV and 35 TeV for superpotential (b) and (c) respectively. Again, $M_{D^{(5)}} = 1000$ TeV has been fixed and the values of $M_T^{\text{dim=6, 1-loop}}$ and $M_T^{\text{dim=6, 2-loop}}$ can be approximated by the square root of the product of $M_{D^{(5)}}$ and $M_T^{\text{dim=5, 1-loop}}$ or $M_T^{\text{dim=5, 2-loop}}$ respectively.

Note that there is a claim [138] that the MSSM with an additional unbroken R-symmetry cannot be obtained from the spontaneous breaking of a four-dimensional

(SUSY) GUT. Note that this is not in conflict with our superpotentials, because the R-symmetry is either absent (a, b, d) or spontaneously broken at the GUT scale (c). Superpotential (c) is particularly interesting for model building purposes because R-symmetries are very popular in flavour models with non-Abelian family symmetries (and spontaneous CP violation). For more details, see also app. D in [10].

8.4 Proton Decay in Models with Fixed Ratios

Even with the knowledge of the mass scale appearing in the dimension five and six proton decay operators, we unfortunately still do not have enough information to fully determine whether a GUT model of flavour is excluded by a too short proton lifetime. Namely, considering the dimension five and six proton decay operators as mediated by colour triplets,

$$W_{p\to?} = \frac{1}{M_T^{\dim=5}} \left[\frac{1}{2}(Y_{qq})_{ij}(Y_{ql})_{mn}\, Q_i\, Q_j\, Q_m\, L_n + (Y_{ue})_{ij}(Y_{ud})_{mn}\, u_i^c\, e_j^c\, u_m^c\, d_n^c\right] , \quad (8.40a)$$

$$\begin{aligned} K_{p\to?} = &- \frac{1}{\left(M_T^{\dim=6}\right)^2}\frac{1}{2}(Y_{qq})^*_{ij}(Y_{ue})_{mn}\, Q_i^\dagger\, Q_j^\dagger\, u_m^c\, e_n^c \\ &- \frac{1}{\left(M_T^{\dim=6}\right)^2}(Y_{ql})^*_{ij}(Y_{ud})_{mn}\, Q_i^\dagger\, L_j^\dagger\, u_m^c\, d_n^c + \text{h.c.} , \end{aligned} \quad (8.40b)$$

we see that two ingredients are still missing. First the dimension five proton decay operator has to be dressed with a closed loop of superpartners introducing a dependence on the SUSY breaking scheme. Second, a priori a flavour model usually only takes into account the MSSM Yukawa matrices Y_u, Y_d, Y_e neglecting the fact that the colour triplets have their own Yukawa coupling matrices Y_{qq}, Y_{ue}, Y_{ql}, Y_{ud}, which are the ones appearing in proton decay.

Let us focus on the latter point first. Consider e.g. the example models (a) and (b) shown in [10] with superpotentials generating Y_d and Y_e of the schematical form

$$\begin{aligned} W_{(\text{a})} = &\frac{1}{\Lambda_3}(H'_{24}\mathcal{F}_3)_{\bar5}(\bar H_5\mathcal{T}_3)_5 + \frac{1}{\Lambda_2}(H'_{24}\mathcal{T}_2)_{10}(\bar H_5\mathcal{F}_2)_{\overline{10}} \\ &+ \frac{1}{\Lambda_1^2}(H'_{24}\mathcal{F}_1)_{\overline{45}}(\mathcal{T}_1 H_{24}\bar H_5)_{45} , \end{aligned} \quad (8.41a)$$

$$\begin{aligned} W_{(\text{b})} = &\frac{1}{\Lambda_3}(H'_{24}\mathcal{F}_3)_{\bar5}(\bar H_5\mathcal{T}_3)_5 + \frac{1}{\Lambda_{22}}(H'_{24}\mathcal{T}_2)_{10}(\bar H_5\mathcal{F}_2)_{\overline{10}} \\ &+ \frac{1}{\Lambda_{21}}(H_{24}\mathcal{T}_2)_{10}(\bar H_5\mathcal{F}_1)_{\overline{10}} + \frac{1}{\Lambda_{12}}(H_{24}\mathcal{F}_2)_{\overline{45}}(\mathcal{T}_1 H_{24}\bar H_5)_{45} , \end{aligned} \quad (8.41b)$$

where indices under parentheses specify index contraction to a specific $SU(5)$ representation and Λ_i are some generic suppression scales associated with messengers leading

to the respective index contractions (for more details see [10] and app. D). The fields H_{24} and H'_{24} are GUT Higgs fields in the adjoint representation **24** as appearing in the superpotentials (a) and (b) in sec. 8.3.2 in model (a) and (b) respectively. The up-type Yukawa matrix entries are assumed to originate from usual $SU(5)$ symmetric Yukawa coupling terms not involving powers of **24** similar to the ones in eq. (4.11). Resulting from these superpotentials, we find MSSM Yukawa matrices for (a) given by

$$Y_d = \mathrm{diag}\,(y_d, y_s, y_b) \ , \quad Y_e = \mathrm{diag}\left(-\frac{1}{2}y_d, 6y_s, -\frac{3}{2}y_b\right) \ , \tag{8.42}$$

and for (b)

$$Y_d = \begin{pmatrix} 0 & y_{d,12} & 0 \\ y_{d,21} & y_s & 0 \\ 0 & 0 & y_b \end{pmatrix} \ , \quad Y_e^T = \begin{pmatrix} 0 & -\frac{1}{2}y_{d,12} & 0 \\ 6y_{d,21} & 6y_s & 0 \\ 0 & 0 & -\frac{3}{2}y_b \end{pmatrix} \ , \tag{8.43}$$

where the last is also reminiscent of the scenario discussed in chap. 7. One additional virtue of the Yukawa coupling ratios introduced this way is that similar fixed ratios also apply between the usual matrices Y_d, Y_e and the couplings to the colour triplets Y_{qq}, Y_{ue}, Y_{ql}, Y_{ud}. For these example structures, we thus find for (a)

$$Y_{ql} = \mathrm{diag}\left(y_d, y_s, -\frac{3}{2}y_b\right) \ , \quad Y_{ud} = \mathrm{diag}\left(\frac{2}{3}y_d, -4y_s, y_b\right) \ , \tag{8.44}$$

and for (b)

$$Y_{ql} = \begin{pmatrix} 0 & y_{d,12} & 0 \\ y_{d,21} & y_s & 0 \\ 0 & 0 & -\frac{3}{2}y_b \end{pmatrix} \ , \quad Y_{ud} = \begin{pmatrix} 0 & \frac{2}{3}y_{d,12} & 0 \\ -4y_{d,21} & -4y_s & 0 \\ 0 & 0 & y_b \end{pmatrix} \ , \tag{8.45}$$

while the other matrices follow the minimal $SU(5)$ relation $Y_{qq} = Y_{ue} = Y_u$. For an extensive list of ratios between all involved Yukawa couplings in such schemes with powers of fields in the **24** representation and a description on how they were obtained, see app. D. The approach using discrete CG factors thus not only leads to desirable predictions for the SUSY spectrum via the SUSY threshold corrections, but also to predictions for proton decay with fewer free parameters than e.g. just assuming that unspecified higher order operators fix the relation $Y_d = Y_e^T$ of minimal $SU(5)$, see for instance [136, 139, 140]. This advantage was also mentioned in [141, 140] for GUT textures instead of more complete models like in [10].

Note, however, there is one caveat to this. In the DMPM as discussed here, there are additional colour triplets that can also generate the same type of operators as in eq. (8.40), but possibly with less suppression (thus dominating over the operators discussed here) or with different ratios. It has to be checked that the symmetries

beyond $SU(5)$, assumed to obtain the right flavour structure, successfully protect the model against these contributions (as was done in [10]).

Concerning the first missing ingredient – the SUSY spectrum needed to dress the dimension five operator – we will not go into much detail for this study. It is, however, interesting to note the following: as was pointed by [142], the proton decay amplitude contribution of the second operator of $W_{p\to?}$ – the so called $RRRR$ operator – is enhanced by a factor $\tan^2\beta$ (for large $\tan\beta$), which poses a challenge for models with large $\tan\beta$. This affects the example structures at hand the following way.

Looking at the SUSY threshold correction dependence of y_τ/y_b shown in fig. 5.7, we see that the ratio $y_\tau/y_b = 3/2$ needs $\bar{\eta}_b \approx 0.11$, while $y_\tau/y_b = 1$ needs $\bar{\eta}_b \approx -0.20$. We remind ourselves that $\bar{\eta}_b \approx \bar{\varepsilon}_b \tan\beta$ where $\bar{\varepsilon}_b$ is some function of the SUSY spectrum and to a first approximation independent of $\tan\beta$. Assuming a similar SUSY spectrum and explaining the sign via a simple sign flip of μ, $\bar{\eta}_b \approx -0.20$ would thus naively need an about twice as high $\tan\beta$ as $\bar{\eta}_b \approx 0.11$ would need. In conclusion, $y_\tau/y_b = 3/2$ corresponds to a factor of four suppression compared to $y_\tau/y_b = 1$, leading to less tension with proton decay.

PART III

Summary and Conclusions

Summary and Conclusions

After establishing basics and fundamental notation in the first part of this thesis, we presented values and uncertainties for the running quark and lepton Yukawa couplings as well as quark mixing parameters calculated at various renormalisation or energy scales, intended as useful input for high-scale model building. The results calculated for the renormalisation scales $\mu = M_Z$, 1 TeV, 3 TeV and 10 TeV, as calculated within the SM in the $\overline{\text{MS}}$ scheme, can be found in tab. 5.1. The corresponding values in the $\overline{\text{DR}}$ scheme are given in tab. 5.2. Both tables can be used as convenient input for parameter fits performed after having done the RG evolution of the high-scale quantities of the respective model to the appropriate scale.

Furthermore, numerical values for the corresponding flavour quantities at the GUT scale M_{GUT} are given in figs. 5.1, 5.2, 5.3, 5.5 and 5.6. Here, the $\tan\beta$ enhanced one-loop SUSY threshold corrections are handled using a parametrisation convenient for building models of the structure of high-scale Yukawa couplings – namely, only via two significant parameters $\bar{\eta}_b$ and $\tan\bar{\beta}$, as defined in eqs. (5.6) and (5.7), which influence all parameters, and only a few other parameters that easily factor out of the RG evolution. In addition to the central values for each quantity, we also calculated their relative uncertainties at the GUT scale, as given in fig. 5.4 and tab. 5.3. While all plots shown in this thesis are obtained for $M_{\text{SUSY}} = 1$ TeV, we also provide the corresponding data for $M_{\text{SUSY}} = 3$ TeV and 10 TeV online under

`http://particlesandcosmology.unibas.ch/files/maurerv/RunningParameters-thesis.tar.gz` ,

as data tables, which also include the 1 TeV data. These allow to reproduce the GUT-scale quantities as numerical functions via simple interpolation for use in model analyses. With these results, we expect parameter fits of GUT-scale models to the experimental data to be greatly simplified and accelerated.

Next, we addressed the question of naturalness of the MSSM in the light of the Higgs discovery and mass measurement at the LHC. For this, we focused on models exhibiting non-universal high-scale boundary conditions of the soft SUSY breaking parameters and contrasted them with the cMSSM. Our basic assumption was that the non-universalities are a consequence of an underlying mechanism giving rise to fixed relations between SUSY breaking parameters which can itself be a consequence of

SUSY breaking or GUT dynamics. To identify candidates for such relations that can reduce the fine-tuning of the electroweak scale, we implemented a general high-energy parametrisation inspired by the pMSSM and obtained a semi-analytical formula for understanding fine-tuning to guide our further analysis. Based on this semi-analytical treatment, we discussed prospects of non-universal scalar and gaugino masses, coming to the conclusion – as already noticed, e.g., in [71, 72, 73] – that the latter case seems more promising. Therefore, we performed a numerical study looking into the fine-tuning Δ in the case of non-universal gaugino masses in more detail.

We found that models with non-universal gaugino masses can account for a Higgs mass in the range $125.3 \pm 0.6 \pm 3$ GeV (including the uncertainty related to the numerical calculation) with a fine-tuning of only $\Delta_{\text{min}} \sim \mathcal{O}(10)$, compared to the cMSSM, which requires $\Delta_{\text{min}} \gtrsim \mathcal{O}(100)$. Hence, the MSSM with non-universal gaugino masses is still a comparatively natural scenario. In more detail, the values of $\eta_1 = M_1/M_3$ and $\eta_2 = M_2/M_3$ giving a low fine-tuning before and after applying a constraint on the Higgs mass are shown in fig. 6.2 and 6.4. Interestingly, some of the ratios discussed in the literature as candidates for such fixed ratios lie in the low fine-tuning region or are close to it, while others that were promising before are disfavoured by including the Higgs mass constraint. Including it, we found that particularly favoured ratios are now given by, e.g., $(\eta_1,\ \eta_2) = (10, 2)$, which may originate from $SU(5)$ GUTs, and $(\eta_1, \eta_2) = (\frac{21}{5}, \frac{7}{3})$, which may be consequence of orbifold scenarios of type O-II with $\delta_{\text{GS}} = -6$.

Assuming non-universal gaugino masses at the GUT scale, we proceeded to analyse the fine-tuning price of different values of the GUT-scale Yukawa coupling ratio y_τ/y_b, representing an important cornerstone for the discrimination of GUT models. There, we found that, for $m_h \approx 125$ GeV, b-τ Yukawa unification corresponds to $\Delta \gtrsim 60$, while the alternative ratio $y_\tau/y_b = 3/2$ can be realised at the price of only $\Delta \gtrsim 30$.

Analysing the SUSY spectrum favoured by naturalness and the Higgs mass constraint, we found that for the least tuned data points with fine-tuning Δ less than 20 the lightest neutralino is expected to be lighter than about 400 GeV and the lighter stop can be as heavy as 3.5 TeV. On the other hand, the gluino mass is actually required to be above 1.5 TeV. Comparing the predicted spectra with the LHC exclusions derived in a set of simplified models, we concluded that the regions of lowest fine-tuning are at present only poorly constrained by direct SUSY searches.

In summary, while a universal high-scale boundary condition such as the cMSSM is certainly challenged from the point of view of fine-tuning by the Higgs discovery at $m_h \approx 125$ GeV, more general variants of the MSSM like the examples studied here can still provide relatively natural solutions to the hierarchy problem and will probably require several more years of data taking before they are fully tested at the LHC.

In chap. 7, motivated by current global fits [16] yielding a large leptonic mixing

angle of

$$\theta_{13}^{\text{PMNS}} = 8.5^\circ \pm 0.2^\circ \,, \tag{8.46}$$

we discussed how this value can easily emerge in theories that unify the forces of the Standard Model. In particular, we investigated how the Georgi-Jarlskog scenario with a Clebsch-Gordan factor of -3 in the connection of the 2-2 matrix elements of Y_d, Y_e can be generalised with a predictive relation for the value of $\theta_{13}^{\text{PMNS}}$.

The key towards realising this is to find a tight connection between the charged lepton Yukawa matrix and the down-type quark Yukawa matrix in the subsector of the first two generations. This can then lead to the link

$$\theta_{12}^e \approx \theta_C \,, \tag{8.47}$$

between quark and lepton mixing. This, in turn, corrects the neutrino mixing matrix in such a way that the reactor mixing angle is generated following the relation

$$\theta_{13}^{\text{PMNS}} \approx \frac{1}{\sqrt{2}}\,\theta_{12}^e \,. \tag{8.48}$$

The general conditions that characterise this scenario are the following:

- Vanishing 1-3 mixing in the neutrino and charged lepton sector
- A predictive setup in the quark sector leading to $\theta_{12}^d \approx \theta_C$ to a good approximation
- A GUT sector (or similar) linking the down type quark Yukawa matrix Y_d and the charged lepton Yukawa matrix Y_e in a definite way using discrete Clebsch-Gordan factors
- Simple equality conditions for two of the Clebsch-Gordan factors. For $SU(5)$ GUTs an additional constraint – such as symmetry of Y_d and Y_e or a vanishing 1-1 entry – is necessary.

An important reason for the last condition is given by the relation between θ_{12}^e and other flavour quantities of the form

$$\theta_{12}^e \approx \begin{cases} \left|\dfrac{c_b}{c_c}\right| \theta_{12}^d & \text{in PS} \\ \dfrac{m_e}{m_\mu}\left|\dfrac{c_c}{c_b}\right| \dfrac{1}{\theta_{12}^d} & \text{in } SU(5) \end{cases} , \tag{8.49}$$

together with the requirement to reproduce the quark-lepton mass ratios consistently and the condition on θ_{12}^d. Specifically, it turns out that, for certain cases, only one combination of Clebsch-Gordan factors is consistent with all requirements. Additionally

we found that, in $SU(5)$ GUTs under our general assumptions, the current magnitude measured for $\theta_{13}^{\text{PMNS}}$ is actually the upper limit of what you can get if a texture 0 in the 1-1 element of Y_d and Y_e is assumed.

Subsequently, we have discussed several types of corrections scenarios satisfying these four conditions receive, ranging from inaccuracy due to the approximations made, actual dependence on $\theta_{23}^{\text{PMNS}}$, renormalisation group effects to canonical normalisation. In conclusion, the corrections amount to about $\mathcal{O}(10\%)$, i.e. about a factor of three larger than current experimental uncertainty. However, most of these effects can be kept under control in an explicit model, as was shown in simple examples.

In a more model-independent way, we have also discussed how different underlying neutrino mixing schemes can be discriminated using the large value of $\theta_{13}^{\text{PMNS}}$ and the lepton mixing sum rule,

$$\theta_{12}^{\text{PMNS}} - \theta_{13}^{\text{PMNS}} \cos(\delta^{\text{PMNS}}) \approx \theta_{12}^{\nu} \, . \tag{8.50}$$

This allows to "reconstruct" the value of θ_{12}^{ν} from a future measurement of δ^{PMNS}, assuming $\theta_{13}^{\nu}, \theta_{13}^{e} \ll \theta_C$, i.e. condition 1.

Finally in chap. 8, we discussed how the double missing partner mechanism solution to the doublet-triplet splitting problem in four-dimensional supersymmetric $SU(5)$ grand unified theories can be combined with predictive models using Clebsch-Gordan (CG) factors for the quark-lepton Yukawa coupling ratios at the GUT scale.

Towards this goal, we argued that a second $SU(5)$ breaking Higgs field in the adjoint representation **24** is very advantageous. Consequently, we studied all possible renormalisable superpotentials with two adjoint Higgs fields systematically, and calculated the corresponding constraints on the GUT scale and effective triplet mass in a two-loop gauge coupling unification analysis. We found that the effective colour triplet masses, which enter dimension five and six proton decay, can easily be raised enough to avoid problems with proton decay (more than feasible with standard non-renormalisable Higgs potentials with only one adjoint GUT Higgs field). We concluded the chapter by stressing the advantage of having ratios fixed by group theoretical structure between not only Higgs doublet but also colour triplet Yukawa couplings and other advantages of the used approach.

In summary, we demonstrated via multiple avenues how the structure of a grand unified theory (of flavour and in general) can be inferred from low energy observables: most directly via flavour observables themselves, but also via other means such as fine-tuning of the electroweak scale, new input from neutrino physics and the non-observation of proton decay. As such, we expect this thesis together with its appendices to be valuable to the scientific community for future research on GUT model building.

Acknowledgements

Foremost, I thank my supervisor Prof. Stefan Antusch for his advice, help and guidance during my time as his doctoral student. Besides my advisor, I would like to thank Dr. Sabine Kraml for being co-referee for this thesis.

I also want to express my gratitude towards my other collaborators Dr. Lorenzo Calibbi, Dr. Martin Spinrath, Dr. Ivo de Medeiros Varzielas, Dr. Christian Gross, Dr. Maurizio Monaco and Constantin Sluka for many useful discussions and pleasant work together.

I am also highly grateful for my great office mates and colleagues – Eros Cazzato, Francesco Cefala, Ivo de Medeiros Varzielas, Oliver Fischer, Christian Gross, Giti Khavari, David Nolde, Mansoor Ur Rehman, Constantin Sluka – for many hours of fruitful discussions whether it was physics, politics, proof-reading parts of my thesis, or hilariously stupid videos on the internet and for enduring the mensa food together.

My thanks also go to my parents, grand-parents, uncle and aunt, and other relatives for supporting me throughout my studies as much as they were able to.

PART IV

Appendix

APPENDIX A

Quark Masses at the Z Mass Scale

In the following, we show in more detail how the quark masses at the renormalisation scale $\mu = M_Z$ are calculated using the Mathematica package `RunDec` [62]. For more information on the parameters of each function, see therein. As mentioned in chap. 5, we use the notation, where pole masses are denoted as upper case M_q and running masses in QCD with n_f active flavours are denoted as $m_q^{(n_f)}(\mu)$. As such, we take as input parameters: $m_{u,d,s}^{(3)}(2\text{ GeV})$, $m_c^{(4)}(m_c)$, $m_b^{(5)}(m_b)$, M_t, $\alpha_s^{(5)}(M_Z)$. The following algorithm takes care of the QCD calculation in an iterative way. In practice, however, after the second iteration the accuracy is good enough and this part of the calculation concludes.

As the first step, we run α_s from M_Z to the running bottom mass with $n_f = 5$ and 4 loop accuracy – the latter applies to every step in the calculation.

$$\alpha_s^{(5)}(m_b^{(5)}(m_b)) = \texttt{AlphasExact}[\alpha_s^{(5)}(M_Z),\ M_Z,\ m_b^{(5)}(m_b),\ 5,\ 4];$$

Using this value for α_s, we can determine the bottom quark pole mass. It depends weakly on the lighter quark masses of which the only (mildly) significant one is the charm quark mass. Due to the structure of `RunDec`, we need the running charm quark mass at $m_b^{(5)}(m_b)$, which we do not have during the first iteration, hence the iterative structure.

$$\begin{aligned} M_b = \texttt{mMS2mOS}[&\\ &m_b^{(5)}(m_b),\\ &\texttt{If}[m_c =!= \texttt{None},\ \{m_c\},\ \{\}],\\ &\alpha_s^{(5)}(m_b^{(5)}(m_b)),\\ &m_b^{(5)}(m_b),\ 5,\ 4\\ ];& \end{aligned}$$

With the bottom pole mass at hand, we can run α_s from M_Z to 2 GeV and $m_c^{(4)}(m_c)$, while taking into account the bottom threshold at its pole mass.

$$\alpha_s^{(4)}(2\text{ GeV}) = \texttt{AlH2AlL}[\alpha_s^{(5)}(M_Z),\ M_Z,\ \{\{5,\ M_b,\ M_b\}\},\ 2\text{ GeV},\ 4];$$
$$\alpha_s^{(4)}(m_c^{(4)}(m_c)) = \texttt{AlH2AlL}[\alpha_s^{(5)}(M_Z),\ M_Z,\ \{\{5,\ M_b,\ M_b\}\},\ m_c^{(4)}(m_c),\ 4];$$

Next, we run up again in $n_f = 4$ to the bottom quark mass scale.

$$\alpha_s^{(4)}(m_b^{(5)}(m_b)) = \texttt{AlphasExact}[\alpha_s^{(4)}(2\text{ GeV}),\ 2\text{ GeV},\ m_b^{(5)}(m_b),\ 4,\ 4];$$

Based on this value for α_s, we obtain the charm quark mass at the bottom quark mass scale for $n_f = 4$ and subsequently de-decouple the bottom quark to obtain the value for $n_f = 5$. Note that the latter is what is passed as m_c to the next iteration.

$$m_c^{(4)}(m_b^{(5)}(m_b)) = \texttt{mMS2mMS}[m_c^{(4)}(m_c),\ \alpha_s^{(4)}(m_c^{(4)}(m_c)),\ \alpha_S^{(4)}(m_b^{(5)}(m_b)),\ 4,\ 4];$$
$$m_c^{(5)}(m_b^{(5)}(m_b)) = \texttt{DecMqUpOS}[m_c^{(4)}(m_b^{(5)}(m_b)),\ \alpha_S^{(4)}(m_b^{(5)}(m_b)),\ M_b,\ M_b,\ 4,\ 4];$$

Going back to the values at the scale $m_c^{(4)}(m_c)$, we run the charm quark mass to 2 GeV for $n_f = 4$.

$$m_c^{(4)}(2\text{ GeV}) = \texttt{mMS2mMS}[m_c^{(4)}(m_c),\ \alpha_s^{(4)}(m_c^{(4)}(m_c)),\ \alpha_s^{(4)}(2\text{ GeV}),\ 4,\ 4];$$

Using this value, we determine the charm quark pole mass. Since $m_c^{(4)}(m_c)$ is below 2 GeV, we expect this way of calculating it to be more accurate as α_s runs to smaller values with increasing scale.

$$M_c = \texttt{mMS2mOS}[m_c^{(4)}(2\text{ GeV}),\ \{\},\ \alpha_s^{(4)}(2\text{ GeV}),\ 2\text{ GeV},\ 4,\ 4];$$

Next, we determine the value of α_s relevant for the three light quarks by decoupling the charm quark at 2 GeV from the $n_f = 4$ theory.

$$\alpha_s^{(3)}(2\text{ GeV}) = \texttt{DecAsDownMS}[\alpha_s^{(4)}(2\text{ GeV}),\ m_c^{(4)}(2\text{ GeV}),\ 2\text{ GeV},\ 3,\ 4];$$

Using this, we calculate the three light quark masses for $n_f = 4$ at the scale 2 GeV by de-decoupling the charm quark.

$$m_u^{(4)}(2\text{ GeV}) = \texttt{DecMqUpMS}[m_u^{(3)}(2\text{ GeV}),\ \alpha_s^{(3)}(2\text{ GeV}),\ m_c^{(4)}(2\text{ GeV}),\ 2\text{ GeV},\ 3,\ 4];$$
$$m_d^{(4)}(2\text{ GeV}) = \texttt{DecMqUpMS}[m_d^{(3)}(2\text{ GeV}),\ \alpha_s^{(3)}(2\text{ GeV}),\ m_c^{(4)}(2\text{ GeV}),\ 2\text{ GeV},\ 3,\ 4];$$
$$m_s^{(4)}(2\text{ GeV}) = \texttt{DecMqUpMS}[m_s^{(3)}(2\text{ GeV}),\ \alpha_s^{(3)}(2\text{ GeV}),\ m_c^{(4)}(2\text{ GeV}),\ 2\text{ GeV},\ 3,\ 4];$$

Turning our attention back to higher scales, we determine the running top mass in the $n_f = 5$ theory based on the lighter quark masses of charm and bottom (neglecting even lighter ones).

$$m_t^{(5)}(M_Z) = \texttt{mOS2mMS}[M_t,\ \{M_c,\ M_b\},\ \alpha_s^{(5)}(M_Z),\ M_Z,\ 5,\ 4];$$

Using this running top mass, we determine the $n_f = 6$ value for α_s by de-decoupling the top quark at the scale M_Z.

$$\alpha_s^{(6)}(M_Z) = \texttt{DecAsUpMS}[\alpha_s^{(5)}(M_Z),\ m_t^{(5)}(M_Z),\ M_Z,\ 5,\ 4];$$

Finally, we determine the running top quark mass at the scale M_Z from its on-shell mass.

$$m_t^{(6)}(M_Z) = \texttt{mOS2mMS}[M_t,\ \{M_c,\ M_b\},\ \alpha_s^{(6)}(M_Z),\ M_Z,\ 6,\ 4];$$

Of the other quark masses, the up, down, strange and charm quark running masses (denoted collectively as m_q) are then determined from their $n_f = 4$ values at 2 GeV by running them to M_Z, taking into account the $n_f = 5$ threshold at M_b and the top threshold to $n_f = 6$ just before M_Z (the result does not significantly change when moving this threshold closer to M_Z).

$$\begin{aligned} m_q^{(6)}(M_Z) = \texttt{mL2mH}[&\\ &m_q^{(4)}(2\text{ GeV}),\ \alpha_s^{(4)}(2\text{ GeV}),\ 2\text{ GeV},\\ &\{\{5,\ M_b,\ M_b\},\ \{6,\ M_t,\ 0.99M_Z\}\},\ M_Z,\ 4\\ ];& \end{aligned}$$

Lastly, the bottom quark mass is determined the same way, but, of course, without the bottom threshold.

$$\begin{aligned} m_b^{(6)}(M_Z) = \texttt{mL2mH}[&\\ &m_b^{(5)}(m_b),\ \alpha_s^{(5)}(m_b^{(5)}(m_b)),\ m_b^{(5)}(m_b),\\ &\{\{6,\ M_t,\ 0.99M_Z\}\},\ M_Z,\ 4\\ ];& \end{aligned}$$

APPENDIX B

Electroweak Corrections to Running Fermion Masses

When the SM is matched to the low-energy theory of $SU(3)_C \times U(1)_{em}$, in principle, one has to take into account contributions to the running Dirac fermion masses from the electroweak gauge bosons $W^\pm$ and Z^0 as well as the Higgs boson h^0 and associated Goldstone bosons (depending on the gauge). The relevant one-particle irreducible one-loop diagrams, shown in fig. B.1, lead to corrections to the Lagrangian density of the form

$$\Delta\mathcal{L} = \Delta K_f^L \,\overline{\psi}_f \,\mathrm{i}\not{p}\, P_L \,\psi_f + \Delta K_f^R \,\overline{\psi}_f \,\mathrm{i}\not{p}\, P_R \,\psi_f - \Delta m_f \,\overline{\psi}_f \psi_f \;, \tag{B.1}$$

where $\overline{\text{MS}}$ divergences are already assumed to be subtracted. After canonical normalisation, this results in the relation between low-energy running masses m_f^{low} and SM running masses m_f^{SM},

$$m_f^{\text{SM}} = m_f^{\text{low}} \left(1 - \frac{\Delta m_f}{m_f} + \tfrac{1}{2}\left(\Delta K_f^L + \Delta K_f^R\right)\right) \equiv m_f^{\text{low}} \left(1 + \frac{\delta m_f}{m_f}\right) \;, \tag{B.2}$$

where the specific choice which m_f to use in the brackets only amounts to a higher order effect. Determination of the corrections for up-type quarks u_i, down-type quarks d_i and charged leptons e_i using `FeynArts` [143] and `FormCalc` [144] yields the formulae

$$\begin{aligned}
\frac{\delta m_{u_i}}{m_{u_i}} = \frac{\alpha}{288\,\pi\, c_W^2\, s_W^2\, M_W^2} \Big[& M_W^2(-9 + 8\, s_W^2\,(-3 + 4\, s_W^2)) \\
& - \left[18\, c_W^2\, m_{u_i}^2 + 32\, M_W^2\, s_W^2\,(-3 + 4\, s_W^2)\right] B_0(m_{u_i}^2, m_{u_i}^2, M_Z^2) \\
& - \left[18\, c_W^2\, m_{u_i}^2 + 2\, M_W^2\,(9 + 8\, s_W^2\,(-3 + 4\, s_W^2))\right] B_1(m_{u_i}^2, m_{u_i}^2, M_Z^2) \\
& - 18\, c_W^2 \sum_{k=1}^{3} \left|V_{ik}^{\text{CKM}}\right|^2 \Big(M_W^2 + 2\, m_{d_k}^2\, B_0(m_{u_i}^2, m_{d_k}^2, M_W^2) \\
& \quad + (m_{d_k}^2 + m_{u_i}^2 + 2\, M_W^2)\, B_1(m_{u_i}^2, m_{d_k}^2, M_W^2) \Big)
\end{aligned}$$

$$
\begin{aligned}
&+ 18\, c_W^2\, m_{u_i}^2 \left(B_0(m_{u_i}^2, m_{u_i}^2, m_{h^0}^2) - B_1(m_{u_i}^2, m_{u_i}^2, m_{h^0}^2)\right) \Big] \,, \\
\frac{\delta m_{d_i}}{m_{d_i}} &= \frac{\alpha}{288\,\pi\, c_W^2\, s_W^2\, M_W^2} \Big[M_W^2(-9 + 4\, s_W^2\,(-3 + 2\, s_W^2)) \\
&- [18\, c_W^2\, m_{d_i}^2 + 16\, M_W^2\, s_W^2\,(-3 + 2\, s_W^2)]\, B_0(m_{d_i}^2, m_{d_i}^2, M_Z^2) \\
&- [18\, c_W^2\, m_{d_i}^2 + 2\, M_W^2\,(9 + 4\, s_W^2(-3 + 2\, s_W^2))]\, B_1(m_{d_i}^2, m_{d_i}^2, M_Z^2) \\
&- 18\, c_W^2 \sum_{k=1}^{3} \left|V_{ki}^{\mathrm{CKM}}\right|^2 \Big(M_W^2 + 2\, m_{u_k}^2\, B_0(m_{d_i}^2, m_{u_k}^2, M_W^2) \\
&\quad + (m_{d_i}^2 + m_{u_k}^2 + 2\, M_W^2)\, B_1(m_{d_i}^2, m_{u_k}^2, M_W^2) \Big) \\
&+ 18\, c_W^2\, m_{d_i}^2 \left(B_0(m_{d_i}^2, m_{d_i}^2, m_{h^0}^2) - B_1(m_{d_i}^2, m_{d_i}^2, m_{h^0}^2)\right) \Big] \,, \\
\frac{\delta m_{e_i}}{m_{e_i}} &= \frac{\alpha}{32\,\pi\, c_W^2\, s_W^2\, M_W^2} \Big[M_W^2(-3 - 2\, s_W^2\,(1 - 4\, s_W^2)) \\
&- [2\, c_W^2\, m_{e_i}^2 + 16\, M_W^2\, s_W^2\,(-1 + 2 s_W^2)]\, B_0(m_{e_i}^2, m_{e_i}^2, M_Z^2) \\
&- [2\, c_W^2\, m_{e_i}^2 + 2\, M_W^2\,(1 - 4\, s_W^2(1 - 2\, s_W^2))]\, B_1(m_{e_i}^2, m_{e_i}^2, M_Z^2] \\
&- 2\, c_W^2\,(m_{e_i}^2 + 2\, M_W^2)\, B_1(m_{e_i}^2, 0, M_W^2) \\
&+ 2\, c_W^2\, m_{e_i}^2 \left(B_0(m_{e_i}^2, m_{e_i}^2, m_{h^0}^2) - B_1(m_{e_i}^2, m_{e_i}^2, m_{h^0}^2)\right) \Big] \,,
\end{aligned}
$$

with $s_W = \sin\theta_W$, $c_W = \cos\theta_W$ and the one loop Passarino-Veltman functions B_0 and B_1 [145]. With the $\overline{\mathrm{MS}}$ divergence term already subtracted, they are given by

$$
\begin{aligned}
B_0(p^2, m_0^2, m_1^2) &= -\int_0^1 \log\left[\frac{-x(1-x)p^2 + x m_1^2 + (1-x) m_0^2}{\mu^2}\right] \mathrm{d}x \,, \\
B_1(p^2, m_0^2, m_1^2) &= \int_0^1 x \log\left[\frac{-x(1-x)p^2 + x m_1^2 + (1-x) m_0^2}{\mu^2}\right] \mathrm{d}x \,.
\end{aligned}
$$

The calculation was done in Feynman gauge $\xi = 1$ and in the main text the threshold renormalisation scale $\mu = M_Z$ was used. In the case of top quarks, this correction develops an imaginary part which is interpreted as contribution to the decay width due to the process $t \to Wb$ and is thus dropped for the calculation of the mass correction.

Note that these relative corrections are $\mathcal{O}(10^{-3})$ for bottom and top quark and $\mathcal{O}(10^{-4})$ for all other fermions. Thus, they are only statistically relevant for charged lepton masses.

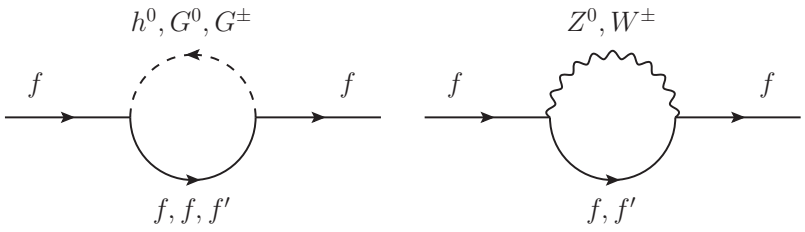

Figure B.1: Feynman diagrams involving scalar and vector boson particles contributing to the self-energy of the SM fermions. Electroweak doublet Goldstone bosons are denoted as G^0 and $G^\pm$. For uncharged bosons, the relevant internal fermion f is the same as the external one. For charged bosons, the internal fermion f' is the one with opposite weak isospin, i.e. $f' = \nu_i$ for $f = e_i$ or $f' = d_k$ for $f = u_i$.

APPENDIX C

Useful Statistical Relations

In the following, we give a brief definition of the concepts and algorithms used in the statistical analysis of chap. 5.

Let us start with the definition of highest posterior density (HPD) intervals. As stated in [15], the HPD interval $[a; b]$ of a random variable x to a given confidence level P is defined by

$$\int_a^b p(x)\,\mathrm{d}x = P \quad \text{and} \quad p(x) < p(y) \;\; \forall\, x \in [a; b], y \notin [a; b]\;, \tag{C.1}$$

where $p(x)$ is the probability distribution function (p.d.f.) of x. For random samples (of uni-modal distributions), it is more convenient to use the equivalent definition where $[a; b]$ is the smallest interval in which a fraction P of all sample elements are contained.

Since some experimental data has non-symmetrical uncertainties, it is also important to treat this case properly. Thus, we use a slightly more involved random sample drawing algorithm as follows. Recall that given a random variable x with p.d.f $p(x)$ and a cumulative distribution function

$$F(x) = \int_{-\infty}^{x} p(y)\,\mathrm{d}y\;, \tag{C.2}$$

and a random variable t that is uniformly distributed on the interval $[0; 1]$, we can replicate samples of x by drawing a number t_0 from t and obtaining the corresponding x value of

$$x_0 = F^{-1}(t_0)\;, \tag{C.3}$$

which is well defined assuming positivity of $p(x)$ and subsequent strict monotony and invertibility of $F(x)$. This is referred to as inversion sampling. Thus, using the error

function $\mathrm{erf}(x)$ defined by

$$\mathrm{erf}(x) = \frac{2}{\sqrt{\pi}} \int_0^x \mathrm{e}^{-t^2}\,\mathrm{d}t\ , \tag{C.4}$$

we model a measurement of the form μ^{+b}_{-a} with a function F^{-1} as in eq. (C.3) of the form

$$F^{-1}(t) = \begin{cases} \mu + \sqrt{2}\,a \cdot \mathrm{erf}^{-1}\left[\left(t - \dfrac{a}{a+b}\right)\dfrac{a+b}{a}\right] & \text{for } t < \dfrac{a}{a+b} \\ \mu + \sqrt{2}\,b \cdot \mathrm{erf}^{-1}\left[\left(t - \dfrac{a}{a+b}\right)\dfrac{a+b}{b}\right] & \text{for } t \geq \dfrac{a}{a+b} \end{cases} . \tag{C.5}$$

The obtained random variable x has three desirable properties: it has a continuous p.d.f. $p(x)$ especially at the measured value μ, where it has its maximum, and fulfils the property

$$\int_{\mu - n\,a}^{\mu + n\,b} p(x)\,\mathrm{d}x = \int_{-n}^{+n} \mathcal{N}(x)\,\mathrm{d}x\ , \tag{C.6}$$

where $\mathcal{N}$ is the p.d.f. for a standard normal distribution with mean value $\mu = 0$ and standard deviation $\sigma = 1$. In particular, $p(x)$ is positive for all x, meaning that all real values are realised. As can be checked quite easily, in the limit $a \to b \equiv \sigma$ the function F^{-1} of eq. (C.5) converges continuously to the one of a normal distribution with mean value μ and standard deviation σ. Note that only in this limit the relation $\int_{x<\mu} p(x)\,\mathrm{d}x = \int_{x>\mu} p(x)\,\mathrm{d}x$ is true.

APPENDIX D

Yukawa Coupling Ratios in $SU(5)$

D.1 Explicit Tensor Decomposition in $SU(N)$

In the following, we specify the algorithm for $SU(N)$ tensor decomposition with which the results in sec. D.2 were derived. Note that it is a very explicit and possibly time consuming algorithm which has not been optimised and can contain extraneous steps. In practice, it makes little difference as long as the dimension of the relevant tensors is small enough, since the results only have to be calculated once and can then be reused, similar to branching rules of $SU(N)$ representations to subalgebra representations.

Let the $SU(N)$ algebra be given by the generators T_a as hermitian $N \times N$ matrices. We take the first $N(N-1)$ generators to be the non-diagonal ones (analogous to $SU(2)$) paired up as

$$(T_{a(m,n)})^i{}_j = \frac{1}{2}\left(\delta_{in}\delta_{jm} + \delta_{im}\delta_{jn}\right) \ , \tag{D.1a}$$

$$(T_{a(m,n)+1})^i{}_j = \frac{\mathrm{i}}{2}\left(\delta_{in}\delta_{jm} - \delta_{im}\delta_{jn}\right) \ , \tag{D.1b}$$

where $m = 1, \ldots, N$ and $n = m+1, \ldots, N$ (and $a(m,n) = (2N-m)(m-1) + 2(n-m) - 1$, such that $a(1,2) = 1, a(1,3) = 3, \ldots, a(2,3) = 2(N-1)+1, a(2,4) = 2(N-1)+3, \ldots$)[1]. The $N-1$ traceless diagonal generators are not directly important for this algorithm. The $N(N-1)$ ladder operators T_a^+ and T_a^- are then given by

$$T_a^{\pm} = T_a \pm \mathrm{i}\, T_{a+1} \ , \tag{D.2}$$

for which it is easy to show that they have the generalised form and properties of ladder operators of $SU(2)$.

Now, let $R^{i_1 i_2 \ldots i_n}$ be a general tensor of $SU(N)$. Since each index corresponds to a fundamental representation $\mathbf{N}$ of $SU(N)$, the action of a generator T_a on the tensor R

[1] However, iterating over m (outer) and n (inner) will ensure this ordering automatically.

is given by

$$(T_a R)^{j_1 j_2 \ldots j_n} = \left((T_a)^{j_1}{}_{i_1} \prod_{k \neq 1} \delta^{j_k}{}_{i_k} + (T_a)^{j_2}{}_{i_2} \prod_{k \neq 2} \delta^{j_k}{}_{i_k} + \cdots + (T_a)^{j_n}{}_{i_n} \prod_{k \neq n} \delta^{j_n}{}_{i_n} \right) R^{i_1 i_2 \ldots i_n} \ , \tag{D.3}$$

meaning that all indices transform separately[2]. If R is completely general, this is the transformation rule of the reducible representation $\mathbf{R} = \mathbf{N}^n$, where $\mathbf{N}$ is the fundamental representation of $SU(N)$. What we are interested in at first is the unitary transformation $\hat{O}$ that relates this tensor R with its reduction into irreducible representations $\mathbf{R}_i$, with $\mathbf{R} = \mathbf{R}_1 + \mathbf{R}_2 + \ldots$ such that the irreducible components $R_{\mathbf{R}_i,k}$ are given by

$$R_{\mathbf{R}_i,k} = \hat{O}_{\mathbf{R}_i,k;j_1 j_2 \ldots j_n} \ R^{j_1 j_2 \ldots j_n} \ , \tag{D.4}$$

where k runs from 1 to $\dim \mathbf{R}_i$ for each i and summation over j_n is implied. Assuming that $SU(N)$ is subsequently broken into a semi-simple subgroup $\mathcal{G}$, the irreducible representations $\mathbf{R}_i$ each branch off into several irreducible representations of the factors of $\mathcal{G}$ labelled as $(\mathbf{r}_1, \mathbf{r}_2, \ldots, \mathbf{r}_m)$, where m is the number of simple Lie group factors of $\mathcal{G}$. Decomposing the $SU(N)$ tensor R also into these representations of $\mathcal{G}$ leads to an analogous definition of an orthogonal matrix O with the property

$$R_{(\mathbf{r}_1,\mathbf{r}_2,\ldots,\mathbf{r}_m),k} = O_{(\mathbf{r}_1,\mathbf{r}_2,\ldots,\mathbf{r}_m),k;j_1 j_2 \ldots j_n} \ R^{j_1 j_2 \ldots j_n} \ , \tag{D.5}$$

where k runs from 1 to $\dim (\mathbf{r}_1, \mathbf{r}_2, \ldots, \mathbf{r}_m)$ as before. Going further, we make a change of basis by collapsing multi-indices into single indices, such that eq. (D.5) reads

$$\tilde{R}_\mu = \tilde{O}_{\mu j} \, \tilde{R}^j \ , \tag{D.6}$$

where both μ and j run from 1 to $\dim \mathbf{R} = N^n$. Since this is just a numbering of the multi-index values of before, it is trivially an isomorphism on both sides of $\tilde{O}$ or O. For the following, it is not important how exactly this numbering proceeds as long as one keeps track of it and uses it consistently. Also note that it is in these simplified bases where $\tilde{O}$ can be directly understood as a unitary matrix with $\tilde{O}^\dagger \tilde{O} = \tilde{O} \tilde{O}^\dagger = \mathbb{1}$. In the same sense, eq. (D.3) now defines a hermitian $N^n \times N^n$ matrix $\tilde{T}_a$ for each a.

The determination of the matrix $\tilde{O}$ (or rather its rows) for a given tensor $R^{i_1 i_2 \ldots i_n}$ now proceeds via the following algorithm:

(1) We start with the full group $SU(N)$ and determine all ladder operators $T_a^\pm$ in the fundamental representation. The set of rows of $\tilde{O}$ is initialised as empty[3]

[2]Note that this equation and the following discussion can also be extended to encompass 'conjugated' indices corresponding to the $\overline{\mathbf{N}}$ representation by replacing $(T_a)^j{}_i$ with $-(T_a^T)^j{}_i$ for such indices. Otherwise, it is not relevant for the presented algorithm.

[3]Actually, since we use the full group in the first iteration, it will rather determine $\tilde{\hat{O}}$. The decomposition into subgroup representations will proceed with step (8).

(2) The ladder operators are converted to their analogues $\tilde{T}_a^{\pm}$ in the reducible tensor representation $\mathbf{R}$.

(3) We take a unit vector v from the kernel of the first $\tilde{T}_a^{+}$.

(4) We apply each ladder up operator $\tilde{T}_a^{+}$ to v repeatedly yielding a new v until $\tilde{T}_a^{+}v = 0$, one a after the other going over all a twice. At this point, the direction of v corresponds to a superposition of directions that are highest-weight-like of the considered group and ones that are total singlets.

(5) We split total singlet components off by going through all ladder operators $\tilde{T}_a^{\pm}$, for each a we do the following: if $\tilde{T}_a^{+}\tilde{T}_a^{-}v \neq 0$, replace v with $\tilde{T}_a^{+}\tilde{T}_a^{-}v$ and go to the next a, otherwise replace v with $\tilde{T}_a^{-}\tilde{T}_a^{+}v$ if it is not zero and proceed to the next a. This makes sure that at least one of the two combinations is applied if v is a combination of $|j, \pm j\rangle$ and $|0, 0\rangle$ of this $SU(2)$ subalgebra. Having done this, v points into a direction associated with only a single irreducible representation of the group.

(6) We decompose the full representation space associated with the vector v by applying all ladder operators $\tilde{T}_a^{\pm}$ to v and again to all vectors resulting from this and so on until further applications of $\tilde{T}_a^{\pm}$ yield only vectors that are linearly dependent on the set of vectors $\hat{V} = \{v_i\}$ we already have. The vector set $\hat{V}$ is then orthonormalised using the Gram-Schmidt process and added as rows to $\tilde{O}$. Alternatively, one can project out components of already encountered directions after each application of a ladder operator and thus also obtain a set of orthonormal vectors $\hat{V}$.

(7) Repeat steps (4) to (6) with v now being a vector perpendicular to all rows of $\tilde{O}$ found up to now. When the number of found rows is equal to the dimension of $\mathbf{R}$, we have found the full orthogonal square matrix $\tilde{O}$ that decomposes the component space of $\mathbf{R}$ into sub-blocks that are not mixed by the generators of the current group – namely the subspaces corresponding to the irreducible representations $\mathbf{R}_i$ in the tensor product $\mathbf{N}^n$.

(8) To actually arrive at the decomposition matrix $\tilde{O}$ into subgroup representations, we further decompose the subspaces of $\mathbf{R}_i$ via a change of basis using $\tilde{O}$ and applying steps (3) to (7) with the ladder operators that are contained in the unbroken subgroup, e.g. the ones commuting with predetermined direction in the adjoint representation such as hypercharge for breaking $SU(5)$ to the SM. The full $\tilde{O}$ is then given by the product of both sub-transformation matrices.

Note that via this procedure one usually only learns the dimension of the representations under the subgroup directly, e.g. it is then not immediately obvious whether a 6

dimensional representation of the SM is a $(\mathbf{6},\mathbf{1})_y$ or a $(\mathbf{3},\mathbf{2})_{y'}$ of $(SU(3)_C, SU(2)_L)_{U(1)_Y}$. It is thus necessary to break the symmetry group down to QCD alone to extract the QCD representation, while the hypercharge can be extracted by applying the corresponding diagonal generator obtained via eq. (D.3). Information on the difference between for example $\mathbf{3}$ and $\overline{\mathbf{3}}$ can only be obtained via other means entirely.

We also stress that, while we do not prove the correctness of this algorithm, we have checked that it produces correct results for all tensor structures encountered in the next section. For this, we checked that the resulting transformation matrix have square form, are unitary (actually orthogonal in all cases) and that they correctly reduce all $SU(N)$ generators into the representation blocks as quoted in the literature, see e.g. [47].

D.2 Yukawa Coupling Ratios for Higgs Doublets and Triplets

The full explicit form of the MSSM superpotential shall be given by[4]

$$W = \epsilon_{\alpha\beta}\left((Y_e)^{ij} H_d^\alpha L_i^\beta \bar{E}_j + (Y_d)^{ij} H_d^\alpha Q_i^{\beta a} \bar{D}_j^a + (Y_u)^{ij} H_u^\beta Q_i^{\alpha a} \bar{U}_j^a + \mu H_u^\alpha H_d^\beta\right) , \quad \text{(D.7)}$$

where i,j are generation indices, $\epsilon_{\alpha\beta}$ the Levi-Civita tensor ($\epsilon_{12}=1$), α, β are $SU(2)$ indices and a, b and c are $SU(3)$ indices. For clarity, we switched to the notation $\bar{U}$, $\bar{D}$, $\bar{E}$ for the right-handed up quark, down quark and charged lepton superfields instead of u^c, d^c, e^c respectively, in order to minimise the amount of indices in the next few formulae. Adding a pair of colour triplets T and $\bar{T}$ to the MSSM, we get the additional terms

$$\begin{aligned} W_T = \epsilon_{\alpha\beta}\Bigg(&-\frac{1}{2}(Y_{qq})_{ij}\epsilon_{abc} T^a Q_i^{\alpha b} Q_j^{\beta c} + (Y_{ql})_{ij} \bar{T}^a Q_i^{\alpha a} L_j^\beta\Bigg) \\ &+ (Y_{ue})_{ij} T^a \bar{U}_i^a \bar{E}_j - (Y_{ud})_{ij}\epsilon_{abc}\bar{T}^a \bar{U}_i^b \bar{D}_j^c + M_T T^a \bar{T}^a , \end{aligned} \quad \text{(D.8)}$$

where ϵ_{abc} is the three indices Levi-Civita tensor (with $\epsilon_{123}=1$).

When extending the SM gauge group to $SU(5)$, we embed the MSSM superfields in a 5-plet H_5, $\bar{5}$-plets $\bar{H}_5$ and $\mathcal{F}_i$, and 10-plets $\mathcal{T}_i$ as in

$$H_5 = \begin{pmatrix} T^r & T^g & T^b & H_u^+ & H_u^0 \end{pmatrix}^T , \quad \text{(D.9a)}$$

$$\bar{H}_5 = \begin{pmatrix} \bar{T}^r & \bar{T}^g & \bar{T}^b & H_d^- & -H_d^0 \end{pmatrix} , \quad \text{(D.9b)}$$

$$\mathcal{F}_i = \begin{pmatrix} \bar{D}_i^r & \bar{D}_i^g & \bar{D}_i^b & E_i & -\nu_i \end{pmatrix} , \quad \text{(D.9c)}$$

[4] This definition coincides with the definition of [146].

and

$$\mathcal{T}_i = \frac{1}{\sqrt{2}} \begin{pmatrix} 0 & -\bar{U}_i^b & \bar{U}_i^g & -U_i^r & -D_i^r \\ \bar{U}_i^b & 0 & -\bar{U}_i^r & -U_i^g & -D_i^g \\ -\bar{U}_i^g & \bar{U}_i^r & 0 & -U_i^b & -D_i^b \\ U_i^r & U_i^g & U_i^b & 0 & -\bar{E}_i \\ D_i^r & D_i^g & D_i^b & \bar{E}_i & 0 \end{pmatrix} , \tag{D.9d}$$

where r, g, b are the $SU(3)$ colours and U, D and ν, E denote the components of $SU(2)$-doublets Q and L.[5] In this embedding, the hypercharge operator is given by $Y \propto \mathrm{diag}(3, 3, 3, -2, -2)$. We can write down the renormalisable superpotential terms

$$W = (Y_{TF})_{ij} \mathcal{T}_i^{ab} (\mathcal{F}_j)_a (\bar{H}_5)_b + \frac{1}{2} (Y_{TT})_{ij} \epsilon_{abcde} \mathcal{T}_i^{ab} \mathcal{T}_j^{cd} H_5^e + \mu_5 H_5^a (\bar{H}_5)_a , \tag{D.10}$$

where now a, b, c, d, e are $SU(5)$-indices and ϵ_{abcde} is the respective Levi-Civita tensor. From the embedding of the MSSM fields, one obtains the minimal $SU(5)$ GUT-scale relations

$$\mu = M_T = \mu_5 , \tag{D.11a}$$

$$Y_d = Y_e^T = Y_{ql} = Y_{ud} = \frac{1}{\sqrt{2}} Y_{TF} , \tag{D.11b}$$

$$Y_u = Y_u^T = Y_{qq} = Y_{ue} = 2\, Y_{TT} . \tag{D.11c}$$

In order to fix undesirable relation $Y_d = Y_e^T$, one approach is to add a 45-dimensional Higgs representation which generates a relative factor of -3 between the Yukawa couplings of the charged leptons and down-type quarks [48]. Here, we implement the extended approach where the ratios between Yukawa couplings are fixed by the CG coefficients of higher-dimensional operators where in addition an adjoint Higgs representation **24** of $SU(5)$ is added [49, 51]. In addition, we also present the relative CG coefficents to the triplets. Namely, while in [49, 51] only Y_d, Y_e and Y_u were discussed, here we will also discuss in detail the implications of this approach for Y_{ql}, Y_{ud}, Y_{qq}, Y_{ue}. The list of the resulting ratios for dimension 4 and 5 operators with Higgs fields in a 5- and 45-dimensional representation can be found in tabs. D.1 and D.2, where the labels for the representations is defined by fig. D.1. The corresponding results for dimension six operators are given in tabs. D.3–D.6.

There are a few comments in order. First, note that several topologies involving a 45-dimensional messenger field exhibit a free parameter, due to the fact that the tensor product $\mathbf{45} \times \mathbf{24}$ contains two 45-dimensional representations. Hence, there are two operators possibly giving two different ratios so that a continuous line of ratios is

[5] Likewise $H_d = \begin{pmatrix} H_d^0 & H_d^- \end{pmatrix}^T$ and $H_u = \begin{pmatrix} H_u^+ & H_u^0 \end{pmatrix}^T$.

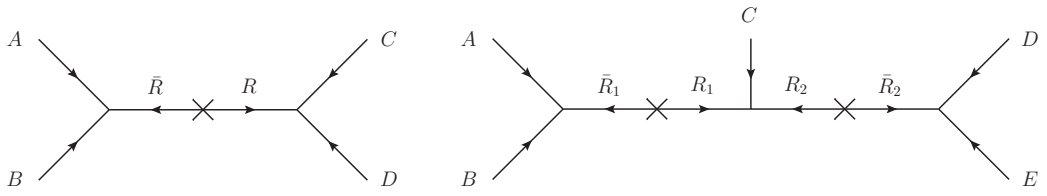

Figure D.1: Supergraphs generating Yukawa couplings upon integrating out messengers fields in representation R,$\bar{R}$, etc.

possible depending on the coefficients of the two operators. For these cases, we write x in the tables.

We also want to mention that, unlike at the renormalisable level, the up-type quark Yukawa and related matrices do not have to be symmetric or antisymmetric. Consider, for example, the operator $(H_{24}\mathcal{T}_1)_{\mathbf{10}}(H_5\mathcal{T}_2)_{\overline{\mathbf{10}}}$. Due to flavour symmetries and messenger content the operator $(H_{24}\mathcal{T}_2)_{\mathbf{10}}(H_5\mathcal{T}_1)_{\overline{\mathbf{10}}}$ could be forbidden. In that case, we find $(Y_u)_{12}/(Y_u)_{21} = -4$. Hence we have adopted the following notation for the ratios in the tables for the Yukawa couplings related to Y_u

$$(Y_u)_{ij} : (Y_u)_{ji} : (Y_{qq})_{ij} : (Y_{ue})_{ij} : (Y_{ue})_{ji} = a : b : c : d : e \ , \tag{D.12}$$

which reduces for the diagonal entries of the Yukawa matrices to

$$(Y_u)_{ii} : (Y_{qq})_{ii} : (Y_{ue})_{ii} = (a+b) : c : (d+e) \ . \tag{D.13}$$

The ratios related to Y_d do not have this extra complication since none of them could be expected to be symmetric or anti-symmetric in the first place.

If the considered model contains Higgs fields both in 5- and 45-dimensional representations[6], there are two Higgs doublet pairs in the spectrum and care should be taken that unification is still possible. One solution is mixing both and making one linear combination heavy while one stays at the electroweak scale. The simplest term generating such a mixing is

$$W \supset H_{24}H_5\bar{H}_{45} \propto H_u H_d^{\overline{45}} - \frac{2}{\sqrt{3}} T\bar{T}^{\overline{45}} + \dots \ , \tag{D.14}$$

where the dots stand for terms involving additional MSSM multiplets in $\bar{H}_{45}$. Since a $\overline{\mathbf{45}}$ contains more potentially dangerous MSSM multiplets, it is natural to have the heavy linear combination be predominantly in the $\overline{\mathbf{45}}$. Then it is possible to

[6]One could also imagine using 45-dimensional Higgs fields exclusively. However, this severely exacerbates the doublet-triplet splitting problem as now one has to split the doublets from even more component fields that can generate proton decay operators.

$A\,B$	$C\,D$	R	$(Y_d)_{ij}$	:	$(Y_e)_{ji}$	:	$(Y_{ql})_{ij}$	:	$(Y_{ud})_{ij}$
$\mathcal{F}_j\,\mathcal{T}_i\,\bar{H}_5$		—	1	:	1	:	1	:	1
$H_{24}\,\mathcal{T}_i$	$\mathcal{F}_j\,\bar{H}_5$	10	1	:	6	:	1	:	-4
$H_{24}\,\mathcal{T}_i$	$\mathcal{F}_j\,\bar{H}_5$	15	1	:	0	:	-1	:	0
$H_{24}\,\bar{H}_5$	$\mathcal{F}_j\,\mathcal{T}_i$	$\bar{5}$	1	:	1	:	$-\frac{2}{3}$	:	$-\frac{2}{3}$
$H_{24}\,\bar{H}_5$	$\mathcal{F}_j\,\mathcal{T}_i$	$\overline{45}$	1	:	-3	:	-2	:	2
$H_{24}\,\mathcal{F}_j$	$\mathcal{T}_i\,\bar{H}_5$	$\bar{5}$	1	:	$-\frac{3}{2}$	:	$-\frac{3}{2}$	:	1
$H_{24}\,\mathcal{F}_j$	$\mathcal{T}_i\,\bar{H}_5$	$\overline{45}$	1	:	$\frac{3}{2}$	:	$-\frac{1}{2}$	:	-1
$\mathcal{F}_j\,\mathcal{T}_i\,\bar{H}_{45}$		—	1	:	-3	:	$\sqrt{3}$	:	$-\sqrt{3}$
$H_{24}\,\mathcal{T}_i$	$\mathcal{F}_j\,\bar{H}_{45}$	10	1	:	-18	:	$\sqrt{3}$	:	$4\sqrt{3}$
$H_{24}\,\mathcal{T}_i$	$\mathcal{F}_j\,\bar{H}_{45}$	40	1	:	0	:	$-\frac{\sqrt{3}}{2}$	:	$-\frac{\sqrt{3}}{2}$
$H_{24}\,\mathcal{T}_i$	$\mathcal{F}_j\,\bar{H}_{45}$	175	1	:	$\frac{36}{23}$	:	$-\frac{19\sqrt{3}}{23}$	:	$-\frac{16\sqrt{3}}{23}$
$H_{24}\,\bar{H}_{45}$	$\mathcal{F}_j\,\mathcal{T}_i$	$\bar{5}$	1	:	1	:	$-\frac{2}{\sqrt{3}}$	:	$-\frac{2}{\sqrt{3}}$
$H_{24}\,\bar{H}_{45}$	$\mathcal{F}_j\,\mathcal{T}_i$	$\overline{45}$	1	:	-3	:	x	:	$-x$
$H_{24}\,\mathcal{F}_j$	$\mathcal{T}_i\,\bar{H}_{45}$	$\bar{5}$	1	:	$\frac{9}{2}$	:	$-\frac{3\sqrt{3}}{2}$	:	$-\sqrt{3}$
$H_{24}\,\mathcal{F}_j$	$\mathcal{T}_i\,\bar{H}_{45}$	$\overline{45}$	1	:	$-\frac{1}{2}$	:	$-\frac{\sqrt{3}}{2}$	:	$-\frac{1}{\sqrt{3}}$
$H_{24}\,\mathcal{F}_j$	$\mathcal{T}_i\,\bar{H}_{45}$	$\overline{70}$	1	:	$\frac{9}{4}$	:	$-\frac{3\sqrt{3}}{4}$	:	$-\sqrt{3}$

Table D.1: Y_{TF}-like CG ratios for the dimension 4 operator and effective dimension five operators $W \supset (AB)_R(CD)_{\bar{R}}$ (involving 5- and 45-dimensional Higgs fields) corresponding to the left diagram in fig. D.1. Note that one combination has a free parameter x due to the ambiguity of the index contraction. See main text for more details.

treat $\bar{H}_{45}$ like a messenger field[7] and the renormalisable operator $\mathcal{F}\mathcal{T}\bar{H}_{45}$ turns into the non-renormalisable operator $(\mathcal{F}\mathcal{T})_{45}(H_{24}\bar{H}_5)_{\overline{45}}$, cf. tab. D.1. If the approximation $M_{45} \gg \langle H_{24}\rangle$ does not hold, one has to take into account the full mass matrix for the Higgs doublets including the term in eq. (D.14).

[7]For reasons of anomaly cancellation, a $\overline{\mathbf{45}}$ must be paired with a $\mathbf{45}$.

$A\,B$	$C\,D$	R	$(Y_u)_{ij}$	:	$(Y_u)_{ji}$	:	$(Y_{qq})_{ij}$	:	$(Y_{ue})_{ij}$	:	$(Y_{ue})_{ji}$
$\mathcal{T}_i\mathcal{T}_j H_5$		—	1	:	1	:	1	:	1	:	1
$H_{24}H_5$	$\mathcal{T}_i\mathcal{T}_j$	5	1	:	1	:	$-\frac{2}{3}$	:	$-\frac{2}{3}$	:	$-\frac{2}{3}$
$H_{24}H_5$	$\mathcal{T}_i\mathcal{T}_j$	45	1	:	-1	:	0	:	-2	:	2
$H_{24}\mathcal{T}_i$	$\mathcal{T}_j H_5$	10	1	:	-4	:	1	:	-4	:	6
$H_{24}\mathcal{T}_i$	$\mathcal{T}_j H_5$	40	1	:	$\frac{1}{2}$	:	$-\frac{1}{2}$	:	-1	:	0
$\mathcal{T}_i\mathcal{T}_j H_{45}$		—	1	:	-1	:	0	:	$\sqrt{3}$	:	$-\sqrt{3}$
$H_{24}\mathcal{T}_i$	$\mathcal{T}_j H_{45}$	10	1	:	4	:	0	:	$-4\sqrt{3}$	:	$-6\sqrt{3}$
$H_{24}\mathcal{T}_i$	$\mathcal{T}_j H_{45}$	15	1	:	0	:	$-\frac{\sqrt{3}}{2}$	:	0	:	0
$H_{24}\mathcal{T}_i$	$\mathcal{T}_j H_{45}$	40	1	:	$-\frac{7}{2}$	:	$\frac{3\sqrt{3}}{2}$	:	$-\sqrt{3}$	:	0
$H_{24}\mathcal{T}_i$	$\mathcal{T}_j H_{45}$	175	1	:	$\frac{16}{19}$	:	$-\frac{21\sqrt{3}}{38}$	:	$-\frac{16\sqrt{3}}{19}$	:	$-\frac{12\sqrt{3}}{19}$
$H_{24}H_{45}$	$\mathcal{T}_i\mathcal{T}_j$	5	1	:	1	:	$-\frac{2}{\sqrt{3}}$	:	$-\frac{2}{\sqrt{3}}$	:	$-\frac{2}{\sqrt{3}}$
$H_{24}H_{45}$	$\mathcal{T}_i\mathcal{T}_j$	45	1	:	-1	:	0	:	x	:	$-x$
$H_{24}H_{45}$	$\mathcal{T}_i\mathcal{T}_j$	50	0	:	0	:	1	:	-2	:	-2

Table D.2: Y_{TT}-like CG ratios for the dimension 4 operator and effective dimension five operators $W \supset (AB)_R(CD)_{\bar{R}}$ (involving 5- and 45-dimensional Higgs fields) corresponding to the left diagram in fig. D.1. Note that one combination has a free parameter x due to the ambiguity of the index contraction. See main text for more details.

$A\,B$	C	$D\,E$	R_1, R_2	$(Y_d)_{ij}$	:	$(Y_e)_{ji}$	:	$(Y_{ql})_{ij}$	:	$(Y_{ud})_{ij}$
$\mathcal{T}_i\,\bar{H}_5$	$\mathcal{F}_j$	$H_{24}\,H_{24}$	5, 1	1	:	1	:	1	:	1
$\mathcal{T}_i\,\bar{H}_5$	$\mathcal{F}_j$	$H_{24}\,H_{24}$	5, 24	1	:	$-\frac{3}{2}$	:	$-\frac{3}{2}$	:	1
$\mathcal{T}_i\,\bar{H}_5$	$\mathcal{F}_j$	$H_{24}\,H_{24}$	45, 24	1	:	$\frac{3}{2}$	:	$-\frac{1}{2}$	:	-1
$\mathcal{T}_i\,\bar{H}_5$	$\mathcal{F}_j$	$H_{24}\,H_{24}$	45, 75	1	:	-3	:	1	:	-1
$H_{24}\,\bar{H}_5$	H_{24}	$\mathcal{F}_j\,\mathcal{T}_i$	$\bar{5}$, 5	1	:	1	:	$\frac{4}{9}$	:	$\frac{4}{9}$
$H_{24}\,\bar{H}_5$	H_{24}	$\mathcal{F}_j\,\mathcal{T}_i$	$\bar{5}$, 45	1	:	-3	:	$\frac{4}{3}$	:	$-\frac{4}{3}$
$H_{24}\,\bar{H}_5$	H_{24}	$\mathcal{F}_j\,\mathcal{T}_i$	$\overline{45}$, 5	1	:	1	:	$\frac{4}{3}$	:	$\frac{4}{3}$
$H_{24}\,\bar{H}_5$	H_{24}	$\mathcal{F}_j\,\mathcal{T}_i$	$\overline{45}$, 45	1	:	-3	:	x	:	$-x$
$H_{24}\,\bar{H}_5$	H_{24}	$\mathcal{F}_j\,\mathcal{T}_i$	$\overline{70}$, 5	1	:	1	:	$\frac{8}{9}$	:	$\frac{8}{9}$
$H_{24}\,\bar{H}_5$	H_{24}	$\mathcal{F}_j\,\mathcal{T}_i$	$\overline{70}$, 45	1	:	-3	:	$\frac{8}{3}$	:	$-\frac{8}{3}$
$\mathcal{F}_j\,\mathcal{T}_i$	$\bar{H}_5$	$H_{24}\,H_{24}$	5, 1	1	:	1	:	1	:	1
$\mathcal{F}_j\,\mathcal{T}_i$	$\bar{H}_5$	$H_{24}\,H_{24}$	5, 24	1	:	1	:	$-\frac{2}{3}$	:	$-\frac{2}{3}$
$\mathcal{F}_j\,\mathcal{T}_i$	$\bar{H}_5$	$H_{24}\,H_{24}$	45, 24	1	:	-3	:	-2	:	2
$\mathcal{F}_j\,\mathcal{T}_i$	$\bar{H}_5$	$H_{24}\,H_{24}$	45, 75	1	:	-3	:	1	:	-1
$H_{24}\,\bar{H}_5$	$\mathcal{T}_i$	$H_{24}\,\mathcal{F}_j$	$\bar{5}$, $\bar{5}$	1	:	$-\frac{3}{2}$	:	1	:	$-\frac{2}{3}$
$H_{24}\,\bar{H}_5$	$\mathcal{T}_i$	$H_{24}\,\mathcal{F}_j$	$\bar{5}$, $\overline{45}$	1	:	$\frac{3}{2}$	:	$\frac{1}{3}$	:	$\frac{2}{3}$
$H_{24}\,\bar{H}_5$	$\mathcal{T}_i$	$H_{24}\,\mathcal{F}_j$	$\overline{45}$, $\bar{5}$	1	:	$\frac{9}{2}$	:	3	:	2
$H_{24}\,\bar{H}_5$	$\mathcal{T}_i$	$H_{24}\,\mathcal{F}_j$	$\overline{45}$, $\overline{45}$	1	:	$-\frac{1}{2}$	:	1	:	$\frac{2}{3}$
$H_{24}\,\bar{H}_5$	$\mathcal{T}_i$	$H_{24}\,\mathcal{F}_j$	$\overline{45}$, $\overline{70}$	1	:	$\frac{9}{4}$	:	$\frac{3}{2}$	:	2
$H_{24}\,\bar{H}_5$	$\mathcal{T}_i$	$H_{24}\,\mathcal{F}_j$	$\overline{70}$, $\overline{45}$	1	:	$\frac{3}{2}$	:	$\frac{2}{3}$	:	$\frac{4}{3}$
$H_{24}\,\bar{H}_5$	$\mathcal{T}_i$	$H_{24}\,\mathcal{F}_j$	$\overline{70}$, $\overline{70}$	1	:	$\frac{3}{4}$	:	1	:	$\frac{2}{3}$
$\mathcal{F}_j\,\bar{H}_5$	H_{24}	$H_{24}\,\mathcal{T}_i$	$\overline{10}$, 10	1	:	36	:	1	:	16
$\mathcal{F}_j\,\bar{H}_5$	H_{24}	$H_{24}\,\mathcal{T}_i$	$\overline{10}$, 15	1	:	0	:	1	:	0
$\mathcal{F}_j\,\bar{H}_5$	H_{24}	$H_{24}\,\mathcal{T}_i$	$\overline{10}$, 40	1	:	0	:	1	:	1
$\mathcal{F}_j\,\bar{H}_5$	H_{24}	$H_{24}\,\mathcal{T}_i$	$\overline{10}$, 175	1	:	$\frac{72}{61}$	:	1	:	$\frac{64}{61}$
$\mathcal{F}_j\,\bar{H}_5$	H_{24}	$H_{24}\,\mathcal{T}_i$	$\overline{15}$, 10	1	:	0	:	-1	:	0
$\mathcal{F}_j\,\bar{H}_5$	H_{24}	$H_{24}\,\mathcal{T}_i$	$\overline{15}$, 15	1	:	0	:	-1	:	0
$\mathcal{F}_j\,\bar{H}_5$	H_{24}	$H_{24}\,\mathcal{T}_i$	$\overline{15}$, 175	1	:	0	:	-1	:	0

Table D.3: Y_{TF}-like CG ratios for the effective dimension six operators $W \supset (AB)_{R_1} C (DE)_{R_2}$ corresponding to the right diagram in fig. D.1. Note one combination has a free parameter x. See main text for more details.

$A\,B$	C	$D\,E$	R_1, R_2	$(Y_d)_{ij}$	:	$(Y_e)_{ji}$	:	$(Y_{ql})_{ij}$	:	$(Y_{ud})_{ij}$
$H_{24}\,\mathcal{F}_j$	H_{24}	$\mathcal{T}_i\,\bar{H}_5$	$\bar{5}$, 5	1	:	$\frac{9}{4}$	:	$\frac{9}{4}$	:	1
$H_{24}\,\mathcal{F}_j$	H_{24}	$\mathcal{T}_i\,\bar{H}_5$	$\bar{5}$, 45	1	:	$-\frac{9}{4}$	:	$\frac{3}{4}$	:	-1
$H_{24}\,\mathcal{F}_j$	H_{24}	$\mathcal{T}_i\,\bar{H}_5$	$\overline{45}$, 5	1	:	$\frac{3}{4}$	:	$\frac{3}{4}$	:	1
$H_{24}\,\mathcal{F}_j$	H_{24}	$\mathcal{T}_i\,\bar{H}_5$	$\overline{45}$, 45	1	:	x	:	$-\frac{x}{3}$	:	-1
$H_{24}\,\mathcal{F}_j$	H_{24}	$\mathcal{T}_i\,\bar{H}_5$	$\overline{70}$, 5	1	:	$\frac{9}{8}$	:	$\frac{9}{8}$	:	1
$H_{24}\,\mathcal{F}_j$	H_{24}	$\mathcal{T}_i\,\bar{H}_5$	$\overline{70}$, 45	1	:	$-\frac{9}{8}$	:	$\frac{3}{8}$	:	-1
$H_{24}\,\mathcal{F}_j$	$\bar{H}_5$	$H_{24}\,\mathcal{T}_i$	$\bar{5}$, 10	1	:	-9	:	$-\frac{3}{2}$	:	-4
$H_{24}\,\mathcal{F}_j$	$\bar{H}_5$	$H_{24}\,\mathcal{T}_i$	$\bar{5}$, 15	1	:	0	:	$\frac{3}{2}$	:	0
$H_{24}\,\mathcal{F}_j$	$\bar{H}_5$	$H_{24}\,\mathcal{T}_i$	$\overline{45}$, 10	1	:	9	:	$-\frac{1}{2}$	:	4
$H_{24}\,\mathcal{F}_j$	$\bar{H}_5$	$H_{24}\,\mathcal{T}_i$	$\overline{45}$, 40	1	:	0	:	1	:	1
$H_{24}\,\mathcal{F}_j$	$\bar{H}_5$	$H_{24}\,\mathcal{T}_i$	$\overline{45}$, 175	1	:	$\frac{18}{19}$	:	$\frac{23}{38}$	:	$\frac{16}{19}$
$H_{24}\,\mathcal{F}_j$	$\bar{H}_5$	$H_{24}\,\mathcal{T}_i$	$\overline{70}$, 15	1	:	0	:	$\frac{3}{4}$	:	0
$H_{24}\,\mathcal{F}_j$	$\bar{H}_5$	$H_{24}\,\mathcal{T}_i$	$\overline{70}$, 175	1	:	$\frac{9}{7}$	:	$\frac{33}{28}$	:	$\frac{8}{7}$
$H_{24}\,\bar{H}_5$	$\mathcal{F}_j$	$H_{24}\,\mathcal{T}_i$	$\bar{5}$, 10	1	:	6	:	$-\frac{2}{3}$	:	$\frac{8}{3}$
$H_{24}\,\bar{H}_5$	$\mathcal{F}_j$	$H_{24}\,\mathcal{T}_i$	$\bar{5}$, 15	1	:	0	:	$\frac{2}{3}$	:	0
$H_{24}\,\bar{H}_5$	$\mathcal{F}_j$	$H_{24}\,\mathcal{T}_i$	$\overline{45}$, 10	1	:	-18	:	-2	:	-8
$H_{24}\,\bar{H}_5$	$\mathcal{F}_j$	$H_{24}\,\mathcal{T}_i$	$\overline{45}$, 40	1	:	0	:	1	:	1
$H_{24}\,\bar{H}_5$	$\mathcal{F}_j$	$H_{24}\,\mathcal{T}_i$	$\overline{45}$, 175	1	:	$\frac{36}{23}$	:	$\frac{38}{23}$	:	$\frac{32}{23}$
$H_{24}\,\bar{H}_5$	$\mathcal{F}_j$	$H_{24}\,\mathcal{T}_i$	$\overline{70}$, 15	1	:	0	:	$\frac{4}{3}$	:	0
$H_{24}\,\bar{H}_5$	$\mathcal{F}_j$	$H_{24}\,\mathcal{T}_i$	$\overline{70}$, 175	1	:	$\frac{12}{11}$	:	$\frac{28}{33}$	:	$\frac{32}{33}$
$\mathcal{F}_j\,\bar{H}_5$	$\mathcal{T}_i$	$H_{24}\,H_{24}$	$\overline{10}$, 1	1	:	1	:	1	:	1
$\mathcal{F}_j\,\bar{H}_5$	$\mathcal{T}_i$	$H_{24}\,H_{24}$	$\overline{10}$, 24	1	:	6	:	1	:	-4
$\mathcal{F}_j\,\bar{H}_5$	$\mathcal{T}_i$	$H_{24}\,H_{24}$	$\overline{10}$, 75	1	:	-3	:	1	:	-1
$\mathcal{F}_j\,\bar{H}_5$	$\mathcal{T}_i$	$H_{24}\,H_{24}$	$\overline{15}$, 24	1	:	0	:	-1	:	0

Table D.4: Continuation of table D.3: Y_{TF}-like CG ratios for the effective dimension six operators $W \supset (AB)_{R_1} C (DE)_{R_2}$ corresponding to the right diagram in fig. D.1. Note another combination with a free parameter x. See main text for more details.

$A\,B$	C	$D\,E$	R_1, R_2	$(Y_u)_{ij}$	:	$(Y_u)_{ji}$	:	$(Y_{qq})_{ij}$	:	$(Y_{ue})_{ij}$	:	$(Y_{ue})_{ji}$
$H_{24}\mathcal{T}_i$	H_5	$H_{24}\mathcal{T}_j$	$10, 10$	1	:	1	:	$-\frac{1}{4}$	:	6	:	6
$H_{24}\mathcal{T}_i$	H_5	$H_{24}\mathcal{T}_j$	$10, 40$	1	:	-8	:	-1	:	0	:	-12
$H_{24}\mathcal{T}_i$	H_5	$H_{24}\mathcal{T}_j$	$15, 40$	1	:	0	:	1	:	0	:	0
$H_{24}\mathcal{T}_i$	H_5	$H_{24}\mathcal{T}_j$	$40, 10$	1	:	$-\frac{1}{8}$	:	$\frac{1}{8}$	:	$\frac{3}{2}$	:	0
$H_{24}\mathcal{T}_i$	H_5	$H_{24}\mathcal{T}_j$	$40, 15$	0	:	1	:	1	:	0	:	0
$H_{24}\mathcal{T}_i$	H_5	$H_{24}\mathcal{T}_j$	$40, 175$	1	:	$\frac{23}{32}$	:	$\frac{19}{32}$	:	$\frac{3}{4}$	:	0
$H_{24}\mathcal{T}_i$	H_5	$H_{24}\mathcal{T}_j$	$175, 40$	1	:	$\frac{32}{23}$	:	$\frac{19}{23}$	:	0	:	$\frac{24}{23}$
$H_{24}\mathcal{T}_i$	H_5	$H_{24}\mathcal{T}_j$	$175, 175$	1	:	1	:	$\frac{41}{40}$	:	$\frac{6}{5}$	:	$\frac{6}{5}$
$\mathcal{T}_i\mathcal{T}_j$	H_5	$H_{24}H_{24}$	$\bar{5}, 1$	1	:	1	:	1	:	1	:	1
$\mathcal{T}_i\mathcal{T}_j$	H_5	$H_{24}H_{24}$	$\bar{5}, 24$	1	:	1	:	$-\frac{2}{3}$	:	$-\frac{2}{3}$	:	$-\frac{2}{3}$
$\mathcal{T}_i\mathcal{T}_j$	H_5	$H_{24}H_{24}$	$\overline{45}, 24$	1	:	-1	:	0	:	-2	:	2
$\mathcal{T}_i\mathcal{T}_j$	H_5	$H_{24}H_{24}$	$\overline{45}, 75$	1	:	-1	:	0	:	1	:	-1
$\mathcal{T}_i\mathcal{T}_j$	H_5	$H_{24}H_{24}$	$\overline{50}, 75$	0	:	0	:	1	:	-2	:	-2
$\mathcal{T}_iH_5$	$\mathcal{T}_j$	$H_{24}H_{24}$	$\overline{10}, 1$	1	:	1	:	1	:	1	:	1
$\mathcal{T}_iH_5$	$\mathcal{T}_j$	$H_{24}H_{24}$	$\overline{10}, 24$	1	:	$-\frac{1}{4}$	:	$-\frac{1}{4}$	:	$-\frac{3}{2}$	:	1
$\mathcal{T}_iH_5$	$\mathcal{T}_j$	$H_{24}H_{24}$	$\overline{10}, 75$	1	:	-1	:	-1	:	3	:	1
$\mathcal{T}_iH_5$	$\mathcal{T}_j$	$H_{24}H_{24}$	$\overline{40}, 24$	1	:	2	:	-1	:	0	:	-2
$\mathcal{T}_iH_5$	$\mathcal{T}_j$	$H_{24}H_{24}$	$\overline{40}, 75$	1	:	-1	:	$\frac{1}{2}$	:	0	:	-2

Table D.5: Y_{TT}-like CG ratios for the effective dimension six operators $W \supset (AB)_{R_1}C(DE)_{R_2}$ corresponding to the right diagram in fig. D.1.

AB	C	DE	R_1, R_2	$(Y_u)_{ij}$	:	$(Y_u)_{ji}$	:	$(Y_{qq})_{ij}$	:	$(Y_{ue})_{ij}$	:	$(Y_{ue})_{ji}$
$H_{24}\mathcal{T}_i$	$\mathcal{T}_j$	$H_{24}H_5$	$10, 5$	1	:	-4	:	$-\frac{2}{3}$	:	$\frac{8}{3}$	:	-4
$H_{24}\mathcal{T}_i$	$\mathcal{T}_j$	$H_{24}H_5$	$10, 45$	1	:	4	:	0	:	8	:	12
$H_{24}\mathcal{T}_i$	$\mathcal{T}_j$	$H_{24}H_5$	$15, 45$	1	:	0	:	1	:	0	:	0
$H_{24}\mathcal{T}_i$	$\mathcal{T}_j$	$H_{24}H_5$	$40, 5$	1	:	$\frac{1}{2}$	:	$\frac{1}{3}$	:	$\frac{2}{3}$	:	0
$H_{24}\mathcal{T}_i$	$\mathcal{T}_j$	$H_{24}H_5$	$40, 45$	1	:	$-\frac{7}{2}$	:	-3	:	2	:	0
$H_{24}\mathcal{T}_i$	$\mathcal{T}_j$	$H_{24}H_5$	$40, 70$	1	:	$\frac{1}{2}$	:	$\frac{2}{3}$	:	$\frac{4}{3}$	:	0
$H_{24}\mathcal{T}_i$	$\mathcal{T}_j$	$H_{24}H_5$	$175, 45$	1	:	$\frac{16}{19}$	:	$\frac{21}{19}$	:	$\frac{32}{19}$	:	$\frac{24}{19}$
$H_{24}\mathcal{T}_i$	$\mathcal{T}_j$	$H_{24}H_5$	$175, 70$	1	:	$\frac{8}{7}$	:	$\frac{20}{21}$	:	$\frac{16}{21}$	:	$\frac{8}{7}$
$\mathcal{T}_i\mathcal{T}_j$	H_{24}	$H_{24}H_5$	$\bar{5}, 5$	1	:	1	:	$\frac{4}{9}$	:	$\frac{4}{9}$	:	$\frac{4}{9}$
$\mathcal{T}_i\mathcal{T}_j$	H_{24}	$H_{24}H_5$	$\bar{5}, 45$	1	:	1	:	$\frac{4}{3}$	:	$\frac{4}{3}$	:	$\frac{4}{3}$
$\mathcal{T}_i\mathcal{T}_j$	H_{24}	$H_{24}H_5$	$\bar{5}, 70$	1	:	1	:	$\frac{8}{9}$	:	$\frac{8}{9}$	:	$\frac{8}{9}$
$\mathcal{T}_i\mathcal{T}_j$	H_{24}	$H_{24}H_5$	$\overline{45}, 5$	1	:	-1	:	0	:	$\frac{4}{3}$	:	$-\frac{4}{3}$
$\mathcal{T}_i\mathcal{T}_j$	H_{24}	$H_{24}H_5$	$\overline{45}, 45$	1	:	-1	:	0	:	x	:	$-x$
$\mathcal{T}_i\mathcal{T}_j$	H_{24}	$H_{24}H_5$	$\overline{45}, 70$	1	:	-1	:	0	:	$\frac{8}{3}$	:	$-\frac{8}{3}$
$\mathcal{T}_i\mathcal{T}_j$	H_{24}	$H_{24}H_5$	$\overline{50}, 45$	0	:	0	:	1	:	-2	:	-2
$H_{24}\mathcal{T}_i$	H_{24}	$\mathcal{T}_jH_5$	$10, \overline{10}$	1	:	16	:	1	:	16	:	36
$H_{24}\mathcal{T}_i$	H_{24}	$\mathcal{T}_jH_5$	$10, \overline{40}$	1	:	-2	:	$-\frac{1}{2}$	:	4	:	0
$H_{24}\mathcal{T}_i$	H_{24}	$\mathcal{T}_jH_5$	$15, \overline{10}$	1	:	0	:	1	:	0	:	0
$H_{24}\mathcal{T}_i$	H_{24}	$\mathcal{T}_jH_5$	$40, \overline{10}$	1	:	1	:	1	:	1	:	0
$H_{24}\mathcal{T}_i$	H_{24}	$\mathcal{T}_jH_5$	$40, \overline{40}$	1	:	x	:	$-\frac{1}{2}$	:	$-2x$	:	0
$H_{24}\mathcal{T}_i$	H_{24}	$\mathcal{T}_jH_5$	$175, \overline{10}$	1	:	$\frac{64}{61}$	:	1	:	$\frac{64}{61}$	:	$\frac{72}{61}$
$H_{24}\mathcal{T}_i$	H_{24}	$\mathcal{T}_jH_5$	$175, \overline{40}$	1	:	4	:	$-\frac{1}{2}$	:	-8	:	0

Table D.6: Continuation of table D.5: Y_{TT}-like CG ratios for the effective dimension six operators $W \supset (AB)_{R_1}C(DE)_{R_2}$ corresponding to the right diagram in fig. D.1. Note two combinations have a free parameter x.See main text for more details.

APPENDIX E

Two-loop Beta Functions of Extensions to the MSSM

In a general renormalisable supersymmetric theory, the renormalisation group equations for gauge couplings g_a at two-loop are given by [147]

$$\mu \frac{d}{d\mu} g_a = \frac{g_a^3}{16\pi^2} b_a + \frac{g_a^3}{(16\pi^2)^2} \left(\sum_b B_{ab} g_b^2 - \sum_f C_a^f \mathrm{tr}(Y_f^\dagger Y_f) \right) , \tag{E.1}$$

in the $\overline{\mathrm{DR}}$ renormalisation scheme, where μ is the renormalisation scale and f runs over all Yukawa coupling matrices. In the MSSM, the beta function coefficients are given by (in GUT normalisation for g_1)

$$b_a = \begin{pmatrix} \frac{33}{5} \\ 1 \\ -3 \end{pmatrix} , \; B_{ab} = \begin{pmatrix} \frac{199}{25} & \frac{27}{5} & \frac{88}{5} \\ \frac{9}{5} & 25 & 24 \\ \frac{11}{5} & 9 & 14 \end{pmatrix} , \tag{E.2}$$

and

$$C_a^{u,d,e} = \begin{pmatrix} \frac{26}{5} & \frac{14}{5} & \frac{18}{5} \\ 6 & 6 & 2 \\ 4 & 4 & 0 \end{pmatrix} . \tag{E.3}$$

where the first column of C corresponds for u, the second to d and the third to e. Additional colour triplet and electroweak doublet pairs, i.e. particle plus distinct antiparticle, such as those contained in $\mathbf{5}$, $\bar{\mathbf{5}}$ representations, contribute (per pair) at one-loop with

$$b_a^{(5,T)} = \begin{pmatrix} \frac{2}{5} \\ 0 \\ 1 \end{pmatrix} , \; b_a^{(5,D)} = \begin{pmatrix} \frac{3}{5} \\ 1 \\ 0 \end{pmatrix} , \tag{E.4}$$

and at two-loop with

$$B_{ab}^{(5,T)} = \begin{pmatrix} \frac{8}{75} & 0 & \frac{32}{15} \\ 0 & 0 & 0 \\ \frac{4}{15} & 0 & \frac{34}{3} \end{pmatrix}, \; B_{ab}^{(5,D)} = \begin{pmatrix} \frac{9}{25} & \frac{9}{5} & 0 \\ \frac{3}{5} & 7 & 0 \\ 0 & 0 & 0 \end{pmatrix} . \tag{E.5}$$

The $SU(2)$ triplets, $SU(3)$ octets and leptoquark superfields[1] from an adjoint **24** of $SU(5)$ contribute (per chiral superfield) at one-loop with

$$b_a^{(24,T)} = \begin{pmatrix} 0 \\ 2 \\ 0 \end{pmatrix}, \; b_a^{(24,O)} = \begin{pmatrix} 0 \\ 0 \\ 3 \end{pmatrix}, \; b_a^{(24,L)} = \begin{pmatrix} \frac{5}{2} \\ \frac{3}{2} \\ 1 \end{pmatrix}, \tag{E.6}$$

and at two-loop with

$$B_{ab}^{(24,T)} = \begin{pmatrix} 0 & 0 & 0 \\ 0 & 24 & 0 \\ 0 & 0 & 0 \end{pmatrix}, \; B_{ab}^{(24,O)} = \begin{pmatrix} 0 & 0 & 0 \\ 0 & 0 & 0 \\ 0 & 0 & 54 \end{pmatrix}, \; B_{ab}^{(24,L)} = \begin{pmatrix} \frac{25}{6} & \frac{15}{2} & \frac{40}{3} \\ \frac{5}{2} & \frac{21}{2} & 8 \\ \frac{5}{3} & 3 & \frac{34}{3} \end{pmatrix} . \tag{E.7}$$

Additional Yukawa couplings between SM fermion superfields and the Higgs colour (anti-)triplet contribute with

$$C_a^{qq,ue,ql,ud} = \begin{pmatrix} \frac{6}{5} & \frac{28}{5} & \frac{14}{5} & \frac{24}{5} \\ 6 & 0 & 6 & 0 \\ 6 & 2 & 4 & 6 \end{pmatrix} . \tag{E.8}$$

In our numerical analysis we have assumed that $Y_{qq} = Y_{ue} = Y_u$ and $Y_{ql} = Y_{ud} = Y_d$ (as motivated by minimal $SU(5)$). We have checked that this approximation changes our results only negligibly.

[1] Note that leptoquark superfields can only appear in Dirac pairs due to their charges.

Bibliography

[1] S. L. Glashow, *Partial Symmetries of Weak Interactions*, Nucl. Phys. **22** (1961) 579–588.

S. Weinberg, *A Model of Leptons*, Phys. Rev. Lett. **19** (1967) 1264–1266.

A. Salam, *Weak and Electromagnetic Interactions*, Originally printed in *Svartholm: Elementary Particle Theory, Proceedings Of The Nobel Symposium Held 1968 At Lerum, Sweden*, Stockholm 1968, 367-377 (1968).

S. L. Glashow, J. Iliopoulos and L. Maiani, *Weak Interactions with Lepton-Hadron Symmetry*, Phys. Rev. **D2** (1970) 1285–1292.

D. J. Gross and F. Wilczek, *Asymptotically Free Gauge Theories. 1*, Phys. Rev. **D8** (1973) 3633–3652.

D. J. Gross and F. Wilczek, *Asymptotically Free Gauge Theories. 2*, Phys. Rev. **D9** (1974) 980–993.

H. D. Politzer, *Reliable Perturbative Results for Strong Interactions?*, Phys. Rev. Lett. **30** (1973) 1346–1349.

[2] H. Fritzsch, M. Gell-Mann and H. Leutwyler, *Advantages of the Color Octet Gluon Picture*, Phys. Lett. **B47** (1973) 365–368.

[3] E. Witten, *Dynamical Breaking of Supersymmetry*, Nucl. Phys. **B188** (1981) 513.

R. K. Kaul and P. Majumdar, *Cancellation of Quadratically Divergent Mass Corrections in Globally Supersymmetric Spontaneously Broken Gauge Theories*, Nucl. Phys. **B199** (1982) 36.

[4] L. E. Ibanez and G. G. Ross, *Low-Energy Predictions in Supersymmetric Grand Unified Theories*, Phys. Lett. **B105** (1981) 439.

S. Dimopoulos, S. Raby and F. Wilczek, *Supersymmetry and the Scale of Unification*, Phys. Rev. **D24** (1981) 1681–1683.

[5] S. Antusch and V. Maurer, *Running quark and lepton parameters at various scales*, JHEP **1311** (2013) 115 [arXiv:1306.6879].

[6] S. Antusch, L. Calibbi, V. Maurer, M. Monaco and M. Spinrath, *Naturalness and GUT Scale Yukawa Coupling Ratios in the CMSSM*, Phys.Rev. **D85** (2012) 035025 [arXiv:1111.6547].

[7] S. Antusch, L. Calibbi, V. Maurer, M. Monaco and M. Spinrath, *Naturalness of the Non-Universal MSSM in the Light of the Recent Higgs Results*, JHEP **1301** (2013) 187 [arXiv:1207.7236].

[8] S. Antusch and V. Maurer, *Large neutrino mixing angle θ_{13}^{MNS} and quark-lepton mass ratios in unified flavour models*, Phys.Rev. **D84** (2011) 117301 [arXiv:1107.3728].

[9] S. Antusch, C. Gross, V. Maurer and C. Sluka, $\theta_{13}^{PMNS} = \theta_C/\sqrt{2}$ *from GUTs*, Nucl.Phys. **B866** (2013) 255–269 [arXiv:1205.1051].

[10] S. Antusch, I. de Medeiros Varzielas, V. Maurer, C. Sluka and M. Spinrath, *Towards predictive flavour models in SUSY SU(5) GUTs with doublet-triplet splitting*, JHEP **1409** (2014) 141 [arXiv:1405.6962].

[11] G. 't Hooft, *Renormalizable Lagrangians for Massive Yang-Mills Fields*, Nucl. Phys. **B35** (1971) 167–188.

[12] H. K. Dreiner, H. E. Haber and S. P. Martin, *Two-component spinor techniques and Feynman rules for quantum field theory and supersymmetry*, Phys.Rept. **494** (2010) 1–196 [arXiv:0812.1594].

[13] F. Englert and R. Brout, *Broken Symmetry and the Mass of Gauge Vector Mesons*, Phys. Rev. Lett. **13** (1964) 321–322.

P. W. Higgs, *Broken symmetries, massless particles and gauge fields*, Phys. Lett. **12** (1964) 132–133.

P. W. Higgs, *Broken Symmetries and the Masses of Gauge Bosons*, Phys. Rev. Lett. **13** (1964) 508–509.

G. S. Guralnik, C. R. Hagen and T. W. B. Kibble, *Global Conservation Laws and Massless Particles*, Phys. Rev. Lett. **13** (1964) 585–587.

[14] N. Cabibbo, *Unitary Symmetry and Leptonic Decays*, Phys. Rev. Lett. **10** (1963) 531–533.

M. Kobayashi and T. Maskawa, *CP Violation in the Renormalizable Theory of Weak Interaction*, Prog. Theor. Phys. **49** (1973) 652–657.

[15] **Particle Data Group**, K. Olive *et. al.*, *Review of Particle Physics*, Chin.Phys. **C38** (2014) 090001.

[16] **NuFIT Collaboration**, M. Gonzalez-Garcia, M. Maltoni and T. Schwetz, *Updated fit to three neutrino mixing: status of leptonic CP violation*, JHEP **1411** (2014) 052 [arXiv:1409.5439].

[17] B. Pontecorvo, *Mesonium and anti-mesonium*, Sov.Phys.JETP **6** (1957) 429.

B. Pontecorvo, *Neutrino Experiments and the Problem of Conservation of Leptonic Charge*, Sov.Phys.JETP **26** (1968) 984–988.

[18] Z. Maki, M. Nakagawa and S. Sakata, *Remarks on the unified model of elementary particles*, Prog.Theor.Phys. **28** (1962) 870–880.

[19] J. Davis, Raymond, D. S. Harmer and K. C. Hoffman, *Search for neutrinos from the sun*, Phys.Rev.Lett. **20** (1968) 1205–1209.

[20] B. Cleveland, T. Daily, J. Davis, Raymond, J. R. Distel, K. Lande *et. al.*, *Measurement of the solar electron neutrino flux with the Homestake chlorine detector*, Astrophys.J. **496** (1998) 505–526.

Kamiokande Collaboration, Y. Fukuda *et. al.*, *Solar neutrino data covering solar cycle 22*, Phys.Rev.Lett. **77** (1996) 1683–1686.

GALLEX Collaboration, W. Hampel *et. al.*, *GALLEX solar neutrino observations: Results for GALLEX III.*, Phys.Lett. **B388** (1996) 384–396.

D. Abdurashitov, V. Gavrin, S. Girin, V. Gorbachev, T. V. Ibragimova *et. al.*, *The Russian-American gallium experiment (SAGE) Cr neutrino source measurement*, Phys.Rev.Lett. **77** (1996) 4708–4711.

Super-Kamiokande Collaboration, Y. Fukuda *et. al.*, *Measurements of the solar neutrino flux from Super-Kamiokande's first 300 days*, Phys.Rev.Lett. **81** (1998) 1158–1162 [hep-ex/9805021].

[21] **Super-Kamiokande Collaboration**, Y. Fukuda *et. al.*, *Evidence for oscillation of atmospheric neutrinos*, Phys.Rev.Lett. **81** (1998) 1562–1567 [hep-ex/9807003].

Kamiokande Collaboration, Y. Fukuda *et. al.*, *Atmospheric muon-neutrino / electron-neutrino ratio in the multiGeV energy range*, Phys.Lett. **B335** (1994) 237–245.

R. Becker-Szendy, C. Bratton, D. Casper, S. Dye, W. Gajewski *et. al.*, *Neutrino measurements with the IMB detector*, Nucl.Phys.Proc.Suppl. **38** (1995) 331–336.

W. Allison, G. Alner, D. Ayres, W. Barrett, C. Bode *et. al.*, *Measurement of the atmospheric neutrino flavor composition in Soudan-2*, Phys.Lett. **B391** (1997) 491–500 [hep-ex/9611007].

MACRO Collaboration, M. Ambrosio *et. al.*, *Measurement of the atmospheric neutrino induced upgoing muon flux using MACRO*, Phys.Lett. **B434** (1998) 451–457 [hep-ex/9807005].

[22] **T2K Collaboration**, K. Abe *et. al.*, *Indication of Electron Neutrino Appearance from an Accelerator-produced Off-axis Muon Neutrino Beam*, Phys.Rev.Lett. **107** (2011) 041801 [arXiv:1106.2822].

DOUBLE-CHOOZ Collaboration, Y. Abe *et. al.*, *Indication for the disappearance of reactor electron antineutrinos in the Double Chooz experiment*, Phys.Rev.Lett. **108** (2012) 131801 [arXiv:1112.6353].

DAYA-BAY Collaboration, F. An *et. al.*, *Observation of electron-antineutrino disappearance at Daya Bay*, Phys.Rev.Lett. **108** (2012) 171803 [arXiv:1203.1669].

RENO collaboration, J. Ahn *et. al.*, *Observation of Reactor Electron Antineutrino Disappearance in the RENO Experiment*, Phys.Rev.Lett. **108** (2012) 191802 [arXiv:1204.0626].

[23] **Particle Data Group**, J. Beringer *et. al.*, *Review of Particle Physics (RPP)*, Phys.Rev. **D86** (2012) 010001.

[24] S. Weinberg, *Baryon and Lepton Nonconserving Processes*, Phys.Rev.Lett. **43** (1979) 1566–1570.

[25] M. Gell-Mann, P. Ramond and R. Slansky, *Complex Spinors and Unified Theories*, Print-80-0576 (CERN) (1980).

T. Yanagida, *Horizontal gauge symmetry and masses of neutrinos*, In Proceedings of the Workshop on the Baryon Number of the Universe and Unified Theories, Tsukuba, Japan, 13-14 Feb 1979 (1979).

R. N. Mohapatra and G. Senjanovic, *Neutrino Masses and Mixings in Gauge Models with Spontaneous Parity Violation*, Phys. Rev. **D23** (1981) 165.

[26] M. Magg and C. Wetterich, *Neutrino Mass Problem and Gauge Hierarchy*, Phys.Lett. **B94** (1980) 61.

G. Lazarides, Q. Shafi and C. Wetterich, *Proton Lifetime and Fermion Masses in an SO(10) Model*, Nucl.Phys. **B181** (1981) 287–300.

E. Ma and U. Sarkar, *Neutrino masses and leptogenesis with heavy Higgs triplets*, Phys.Rev.Lett. **80** (1998) 5716–5719 [hep-ph/9802445].

[27] R. Foot, H. Lew, X. He and G. C. Joshi, *Seesaw Neutrino Masses Induced by a Triplet of Leptons*, Z.Phys. **C44** (1989) 441.

[28] S. P. Martin, *A Supersymmetry Primer*, [hep-ph/9709356].

[29] J. Wess and B. Zumino, *Supergauge Transformations in Four-Dimensions*, Nucl. Phys. **B70** (1974) 39–50.

[30] H. P. Nilles, *Supersymmetry, Supergravity and Particle Physics*, Phys. Rept. **110** (1984) 1–162.

H. E. Haber and G. L. Kane, *The Search for Supersymmetry: Probing Physics Beyond the Standard Model*, Phys. Rept. **117** (1985) 75–263.

R. Barbieri, *Looking Beyond the Standard Model: The Supersymmetric Option*, Riv. Nuovo Cim. **11N4** (1988) 1–45.

[31] L. J. Hall, R. Rattazzi and U. Sarid, *The Top quark mass in supersymmetric SO(10) unification*, Phys.Rev. **D50** (1994) 7048–7065 [hep-ph/9306309].

M. S. Carena, M. Olechowski, S. Pokorski and C. Wagner, *Electroweak symmetry breaking and bottom - top Yukawa unification*, Nucl.Phys. **B426** (1994) 269–300 [hep-ph/9402253].

R. Hempfling, *Yukawa coupling unification with supersymmetric threshold corrections*, Phys.Rev. **D49** (1994) 6168–6172.

[32] T. Blazek, S. Raby and S. Pokorski, *Finite supersymmetric threshold corrections to CKM matrix elements in the large tan Beta regime*, Phys.Rev. **D52** (1995) 4151–4158 [hep-ph/9504364].

[33] S. Antusch and M. Spinrath, *Quark and lepton masses at the GUT scale including SUSY threshold corrections*, Phys.Rev. **D78** (2008) 075020 [arXiv:0804.0717].

[34] A. Crivellin and C. Greub, *Two-loop SQCD corrections to Higgs-quark-quark couplings in the generic MSSM*, Phys.Rev. **D87** (2013) 015013 [arXiv:1210.7453].

[35] A. Y. Smirnov and F. Vissani, *Upper bound on all products of R-parity violating couplings λ' and λ'' from proton decay*, Phys. Lett. **B380** (1996) 317–323 [hep-ph/9601387].

G. Bhattacharyya and P. B. Pal, *Upper bounds on all R-parity-violating lambda lambda" combinations from proton stability*, Phys. Rev. **D59** (1999) 097701 [hep-ph/9809493].

R. Barbier *et. al.*, *R-parity violating supersymmetry*, Phys. Rept. **420** (2005) 1–202 [hep-ph/0406039].

[36] G. R. Farrar and P. Fayet, *Phenomenology of the Production, Decay, and Detection of New Hadronic States Associated with Supersymmetry*, Phys. Lett. **B76** (1978) 575–579.

[37] S. Dimopoulos and H. Georgi, *Softly Broken Supersymmetry and SU(5)*, Nucl. Phys. **B193** (1981) 150.

S. Weinberg, *Supersymmetry at Ordinary Energies. 1. Masses and Conservation Laws*, Phys. Rev. **D26** (1982) 287.

N. Sakai and T. Yanagida, *Proton Decay in a Class of Supersymmetric Grand Unified Models*, Nucl. Phys. **B197** (1982) 533.

S. Dimopoulos, S. Raby and F. Wilczek, *Proton Decay in Supersymmetric Models*, Phys. Lett. **B112** (1982) 133.

[38] L. Girardello and M. T. Grisaru, *Soft Breaking of Supersymmetry*, Nucl. Phys. **B194** (1982) 65.

[39] D. Chung, L. Everett, G. Kane, S. King, J. D. Lykken *et. al.*, *The Soft supersymmetry breaking Lagrangian: Theory and applications*, Phys.Rept. **407** (2005) 1–203 [hep-ph/0312378].

[40] S. Dimopoulos and D. W. Sutter, *The Supersymmetric flavor problem*, Nucl. Phys. **B452** (1995) 496–512 [hep-ph/9504415].

[41] D. Z. Freedman, P. van Nieuwenhuizen and S. Ferrara, *Progress Toward a Theory of Supergravity*, Phys. Rev. **D13** (1976) 3214–3218.

S. Deser and B. Zumino, *Consistent Supergravity*, Phys. Lett. **B62** (1976) 335.

J. Wess and J. Bagger, *Supersymmetry and supergravity*, . Princeton, USA: Univ. Pr. (1992) 259 p.

[42] A. H. Chamseddine, R. L. Arnowitt and P. Nath, *Locally Supersymmetric Grand Unification*, Phys.Rev.Lett. **49** (1982) 970.

R. Barbieri, S. Ferrara and C. A. Savoy, *Gauge Models with Spontaneously Broken Local Supersymmetry*, Phys.Lett. **B119** (1982) 343.

L. E. Ibanez, *Locally Supersymmetric SU(5) Grand Unification*, Phys.Lett. **B118** (1982) 73.

L. J. Hall, J. D. Lykken and S. Weinberg, *Supergravity as the Messenger of Supersymmetry Breaking*, Phys.Rev. **D27** (1983) 2359–2378.

N. Ohta, *Grand Unified Theories Based on Local Supersymmetry*, Prog.Theor.Phys. **70** (1983) 542.

[43] M. Dine and W. Fischler, *A Phenomenological Model of Particle Physics Based on Supersymmetry*, Phys.Lett. **B110** (1982) 227.

C. R. Nappi and B. A. Ovrut, *Supersymmetric Extension of the SU(3) x SU(2) x U(1) Model*, Phys.Lett. **B113** (1982) 175.

L. Alvarez-Gaume, M. Claudson and M. B. Wise, *Low-Energy Supersymmetry*, Nucl.Phys. **B207** (1982) 96.

M. Dine and A. E. Nelson, *Dynamical supersymmetry breaking at low-energies*, Phys.Rev. **D48** (1993) 1277–1287 [hep-ph/9303230].

M. Dine, A. E. Nelson and Y. Shirman, *Low-energy dynamical supersymmetry breaking simplified*, Phys.Rev. **D51** (1995) 1362–1370 [hep-ph/9408384].

M. Dine, A. E. Nelson, Y. Nir and Y. Shirman, *New tools for low-energy dynamical supersymmetry breaking*, Phys.Rev. **D53** (1996) 2658–2669 [hep-ph/9507378].

[44] L. Randall and R. Sundrum, *Out of this world supersymmetry breaking*, Nucl.Phys. **B557** (1999) 79–118 [hep-th/9810155].

G. F. Giudice, M. A. Luty, H. Murayama and R. Rattazzi, *Gaugino mass without singlets*, JHEP **9812** (1998) 027 [hep-ph/9810442].

T. Gherghetta, G. F. Giudice and J. D. Wells, *Phenomenological consequences of supersymmetry with anomaly induced masses*, Nucl.Phys. **B559** (1999) 27–47 [hep-ph/9904378].

[45] A. Djouadi, J.-L. Kneur and G. Moultaka, *SuSpect: A Fortran code for the supersymmetric and Higgs particle spectrum in the MSSM*, Comput.Phys.Commun. **176** (2007) 426–455 [hep-ph/0211331].

[46] H. Georgi and S. Glashow, *Unity of All Elementary Particle Forces*, Phys.Rev.Lett. **32** (1974) 438–441.

[47] R. Slansky, *Group Theory for Unified Model Building*, Phys. Rept. **79** (1981) 1–128.

R. Feger and T. W. Kephart, *LieART - A Mathematica Application for Lie Algebras and Representation Theory*, [arXiv:1206.6379].

[48] H. Georgi and C. Jarlskog, *A New Lepton - Quark Mass Relation in a Unified Theory*, Phys.Lett. **B86** (1979) 297–300.

[49] S. Antusch and M. Spinrath, *New GUT predictions for quark and lepton mass ratios confronted with phenomenology*, Phys.Rev. **D79** (2009) 095004 [arXiv:0902.4644].

[50] L. Brizi, M. Gomez-Reino and C. A. Scrucca, *Globally and locally supersymmetric effective theories for light fields*, Nucl. Phys. **B820** (2009) 193–212 [arXiv:0904.0370].

[51] S. Antusch, S. F. King and M. Spinrath, *GUT predictions for quark-lepton Yukawa coupling ratios with messenger masses from non-singlets*, Phys.Rev. **D89** (2014) 055027 [arXiv:1311.0877].

[52] H. Georgi, *The State of the Art - Gauge Theories. (Talk)*, AIP Conf.Proc. **23** (1975) 575–582.

H. Fritzsch and P. Minkowski, *Unified Interactions of Leptons and Hadrons*, Annals Phys. **93** (1975) 193–266.

[53] J. C. Pati and A. Salam, *Lepton Number as the Fourth Color*, Phys.Rev. **D10** (1974) 275–289.

[54] B. Allanach, S. King, G. Leontaris and S. Lola, *Yukawa textures in string unified models with SU(4) x O(4) symmetry*, Phys.Rev. **D56** (1997) 2632–2655 [hep-ph/9610517].

[55] C. F. Kolda and S. P. Martin, *Low-energy supersymmetry with D term contributions to scalar masses*, Phys.Rev. **D53** (1996) 3871–3883 [hep-ph/9503445].

[56] J. Chakrabortty and A. Raychaudhuri, *A Note on dimension-5 operators in GUTs and their impact*, Phys.Lett. **B673** (2009) 57–62 [arXiv:0812.2783].

S. P. Martin, *Non-universal gaugino masses from non-singlet F-terms in non-minimal unified models*, Phys.Rev. **D79** (2009) 095019 [arXiv:0903.3568].

[57] A. Brignole, L. E. Ibanez and C. Munoz, *Towards a theory of soft terms for the supersymmetric Standard Model*, Nucl.Phys. **B422** (1994) 125–171 [hep-ph/9308271].

[58] P. Nath and P. Fileviez Perez, *Proton stability in grand unified theories, in strings and in branes*, Phys.Rept. **441** (2007) 191–317 [hep-ph/0601023].

[59] T. Goto and T. Nihei, *Effect of RRRR dimension five operator on the proton decay in the minimal SU(5) SUGRA GUT model*, Phys.Rev. **D59** (1999) 115009 [hep-ph/9808255].

[60] See e.g.:

H. Fusaoka and Y. Koide, *Updated estimate of running quark masses*, Phys.Rev. **D57** (1998) 3986–4001 [hep-ph/9712201].

C. Das and M. Parida, *New formulas and predictions for running fermion masses at higher scales in SM, 2 HDM, and MSSM*, Eur.Phys.J. **C20** (2001) 121–137 [hep-ph/0010004].

Z.-z. Xing, H. Zhang and S. Zhou, *Updated Values of Running Quark and Lepton Masses*, Phys.Rev. **D77** (2008) 113016 [arXiv:0712.1419].

[61] G. Colangelo, S. Durr, A. Juttner, L. Lellouch, H. Leutwyler *et. al.*, *Review of lattice results concerning low energy particle physics*, Eur.Phys.J. **C71** (2011) 1695 [arXiv:1011.4408].

[62] K. Chetyrkin, J. H. Kuhn and M. Steinhauser, *RunDec: A Mathematica package for running and decoupling of the strong coupling and quark masses*, Comput.Phys.Commun. **133** (2000) 43–65 [hep-ph/0004189].

[63] **UTfit Collaboration**, M. Bona *et. al.*, *The 2004 UTfit collaboration report on the status of the unitarity triangle in the standard model*, JHEP **0507** (2005) 028 [hep-ph/0501199]. Summer 2014 (pre-ICHEP) updated fit results available at www.utfit.org/UTfit/ResultsSummer2014PostMoriond.

[64] H. Arason, D. Castano, B. Keszthelyi, S. Mikaelian, E. Piard *et. al.*, *Renormalization group study of the standard model and its extensions. 1. The Standard model*, Phys.Rev. **D46** (1992) 3945–3965.

[65] S. Antusch, J. Kersten, M. Lindner, M. Ratz and M. A. Schmidt, *Running neutrino mass parameters in see-saw scenarios*, JHEP **0503** (2005) 024 [hep-ph/0501272].

[66] M.-x. Luo and Y. Xiao, *Two loop renormalization group equations in the standard model*, Phys.Rev.Lett. **90** (2003) 011601 [hep-ph/0207271].

[67] S. P. Martin and M. T. Vaughn, *Two loop renormalization group equations for soft supersymmetry breaking couplings*, Phys.Rev. **D50** (1994) 2282 [hep-ph/9311340].

[68] S. P. Martin and M. T. Vaughn, *Regularization dependence of running couplings in softly broken supersymmetry*, Phys.Lett. **B318** (1993) 331–337 [hep-ph/9308222].

[69] **CMS Collaboration**, S. Chatrchyan *et. al.*, *Search for physics beyond the standard model in events with a Z boson, jets, and missing transverse energy in pp collisions at* $\sqrt{s} = 7$ *TeV*, Phys.Lett. **B716** (2012) 260–284 [arXiv:1204.3774].

ATLAS Collaboration, G. Aad *et. al.*, *Search for squarks and gluinos using final states with jets and missing transverse momentum with the ATLAS detector in* $\sqrt{s} = 7$ *TeV proton-proton collisions*, Phys.Lett. **B710** (2012) 67–85 [arXiv:1109.6572].

ATLAS Collaboration, G. Aad *et. al.*, *Search for gluinos in events with two same-sign leptons, jets and missing transverse momentum with the ATLAS detector in pp collisions at* $\sqrt{s} = 7$ *TeV*, Phys.Rev.Lett. **108** (2012) 241802 [arXiv:1203.5763].

ATLAS Collaboration, G. Aad *et. al.*, *Search for supersymmetry in pp collisions at* $\sqrt{s} = 7$ *TeV in final states with missing transverse momentum and* b^- *jets with the ATLAS detector*, Phys.Rev. **D85** (2012) 112006 [arXiv:1203.6193].

ATLAS Collaboration, G. Aad *et. al.*, *Search for scalar bottom pair production with the ATLAS detector in pp Collisions at* $\sqrt{s} = 7$ *TeV*, Phys.Rev.Lett. **108** (2012) 181802 [arXiv:1112.3832].

[70] A. Arbey, M. Battaglia, A. Djouadi, F. Mahmoudi and J. Quevillon, *Implications of a 125 GeV Higgs for supersymmetric models*, Phys.Lett. **B708** (2012) 162–169 [arXiv:1112.3028].

[71] H. Abe, T. Kobayashi and Y. Omura, *Relaxed fine-tuning in models with non-universal gaugino masses*, Phys.Rev. **D76** (2007) 015002 [hep-ph/0703044].

[72] I. Gogoladze, M. U. Rehman and Q. Shafi, *Amelioration of Little Hierarchy Problem in SU(4)(c) x SU(2)(L) x SU(2)(R)*, Phys.Rev. **D80** (2009) 105002 [arXiv:0907.0728].

[73] D. Horton and G. Ross, *Naturalness and Focus Points with Non-Universal Gaugino Masses*, Nucl.Phys. **B830** (2010) 221–247 [arXiv:0908.0857].

[74] D. M. Ghilencea, H. M. Lee and M. Park, *Tuning supersymmetric models at the LHC: A comparative analysis at two-loop level*, JHEP **1207** (2012) 046 [arXiv:1203.0569].

[75] F. Brummer and W. Buchmuller, *The Fermi scale as a focus point of high-scale gauge mediation*, JHEP **1205** (2012) 006 [arXiv:1201.4338].

[76] L. J. Hall, D. Pinner and J. T. Ruderman, *A Natural SUSY Higgs Near 126 GeV*, JHEP **1204** (2012) 131 [arXiv:1112.2703].

A. Arvanitaki and G. Villadoro, *A Non Standard Model Higgs at the LHC as a Sign of Naturalness*, JHEP **1202** (2012) 144 [arXiv:1112.4835].

Z. Kang, J. Li and T. Li, *On Naturalness of the MSSM and NMSSM*, JHEP **1211** (2012) 024 [arXiv:1201.5305].

M. Asano and T. Higaki, *Natural supersymmetric spectrum in mirage mediation*, Phys.Rev. **D86** (2012) 035020 [arXiv:1204.0508].

H. M. Lee, V. Sanz and M. Trott, *Hitting sbottom in natural SUSY*, JHEP **1205** (2012) 139 [arXiv:1204.0802].

J. L. Feng and D. Sanford, *A Natural 125 GeV Higgs Boson in the MSSM from Focus Point Supersymmetry with A-Terms*, Phys.Rev. **D86** (2012) 055015 [arXiv:1205.2372].

K. Blum, R. T. D'Agnolo and J. Fan, *Natural SUSY Predicts: Higgs Couplings*, JHEP **1301** (2013) 057 [arXiv:1206.5303].

M. W. Cahill-Rowley, J. L. Hewett, A. Ismail and T. G. Rizzo, *The Higgs Sector and Fine-Tuning in the pMSSM*, Phys.Rev. **D86** (2012) 075015 [arXiv:1206.5800].

L. Randall and M. Reece, *Single-Scale Natural SUSY*, JHEP **1308** (2013) 088 [arXiv:1206.6540].

B. Kyae and J.-C. Park, *A Singlet-Extension of the MSSM for 125 GeV Higgs with the Least Tuning*, Phys.Rev. **D87** (2013) 075021 [arXiv:1207.3126].

H. Baer, V. Barger, P. Huang, A. Mustafayev and X. Tata, *Radiative natural SUSY with a 125 GeV Higgs boson*, Phys.Rev.Lett. **109** (2012) 161802 [arXiv:1207.3343].

P. Grothaus, M. Lindner and Y. Takanishi, *Naturalness of Neutralino Dark Matter*, JHEP **1307** (2013) 094 [arXiv:1207.4434].

[77] R. Barbieri and G. Giudice, *Upper Bounds on Supersymmetric Particle Masses*, Nucl.Phys. **B306** (1988) 63.

[78] M. Papucci, J. T. Ruderman and A. Weiler, *Natural SUSY Endures*, JHEP **1209** (2012) 035 [arXiv:1110.6926].

[79] S. Cassel, D. Ghilencea and G. Ross, *Fine tuning as an indication of physics beyond the MSSM*, Nucl.Phys. **B825** (2010) 203–221 [arXiv:0903.1115].

S. Cassel, D. Ghilencea and G. Ross, *Testing SUSY*, Phys.Lett. **B687** (2010) 214–218 [arXiv:0911.1134].

S. Cassel, D. Ghilencea and G. Ross, *Testing SUSY at the LHC: Electroweak and Dark matter fine tuning at two-loop order*, Nucl.Phys. **B835** (2010) 110–134 [arXiv:1001.3884].

S. Cassel, D. Ghilencea, S. Kraml, A. Lessa and G. Ross, *Fine-tuning implications for complementary dark matter and LHC SUSY searches*, JHEP **1105** (2011) 120 [arXiv:1101.4664].

[80] B. de Carlos and J. Casas, *One loop analysis of the electroweak breaking in supersymmetric models and the fine tuning problem*, Phys.Lett. **B309** (1993) 320–328 [hep-ph/9303291].

A. Romanino and A. Strumia, *Are heavy scalars natural in minimal supergravity?*, Phys.Lett. **B487** (2000) 165–170 [hep-ph/9912301].

J. L. Feng and K. T. Matchev, *Focus point supersymmetry: Proton decay, flavor and CP violation, and the Higgs boson mass*, Phys.Rev. **D63** (2001) 095003 [hep-ph/0011356].

[81] L. Giusti, A. Romanino and A. Strumia, *Natural ranges of supersymmetric signals*, Nucl.Phys. **B550** (1999) 3–31 [hep-ph/9811386].

[82] **Particle Data Group**, K. Nakamura *et. al.*, *Review of particle physics*, J.Phys. **G37** (2010) 075021.

[83] P. Bechtle, K. Desch, H. K. Dreiner, M. Hamer, M. Krmer *et. al.*, *Constrained Supersymmetry after the Higgs Boson Discovery: A global analysis with Fittino*, PoS **EPS-HEP2013** (2013) 313 [arXiv:1310.3045].

[84] B. Allanach, *SOFTSUSY: a program for calculating supersymmetric spectra*, Comput.Phys.Commun. **143** (2002) 305–331 [hep-ph/0104145].

[85] K. L. Chan, U. Chattopadhyay and P. Nath, *Naturalness, weak scale supersymmetry and the prospect for the observation of supersymmetry at the Tevatron and at the CERN LHC*, Phys.Rev. **D58** (1998) 096004 [hep-ph/9710473].

J. L. Feng, K. T. Matchev and T. Moroi, *Multi - TeV scalars are natural in minimal supergravity*, Phys.Rev.Lett. **84** (2000) 2322–2325 [hep-ph/9908309].

J. L. Feng, K. T. Matchev and T. Moroi, *Focus points and naturalness in supersymmetry*, Phys.Rev. **D61** (2000) 075005 [hep-ph/9909334].

S. Akula, B. Altunkaynak, D. Feldman, P. Nath and G. Peim, *Higgs Boson Mass Predictions in SUGRA Unification, Recent LHC-7 Results, and Dark Matter*, Phys.Rev. **D85** (2012) 075001 [arXiv:1112.3645].

[86] S. Akula, M. Liu, P. Nath and G. Peim, *Naturalness, Supersymmetry and Implications for LHC and Dark Matter*, Phys.Lett. **B709** (2012) 192–199 [arXiv:1111.4589].

[87] A. Arbey, M. Battaglia and F. Mahmoudi, *Implications of LHC Searches on SUSY Particle Spectra: The pMSSM Parameter Space with Neutralino Dark Matter*, Eur.Phys.J. **C72** (2012) 1847 [arXiv:1110.3726].

H. K. Dreiner, M. Kramer and J. Tattersall, *How low can SUSY go? Matching, monojets and compressed spectra*, Europhys.Lett. **99** (2012) 61001 [arXiv:1207.1613].

[88] S. Antusch, L. Calibbi, V. Maurer and M. Spinrath, *From Flavour to SUSY Flavour Models*, Nucl.Phys. **B852** (2011) 108–148 [arXiv:1104.3040].

[89] A. Freitas, E. Gasser and U. Haisch, *Supersymmetric large tan(beta) corrections to DeltaM(d, s) and B(d, s)* $\to \mu^+\mu^-$ *revisited*, Phys.Rev. **D76** (2007) 014016 [hep-ph/0702267].

[90] M. Spinrath, New Aspects of Flavour Model Building in Supersymmetric Grand Unification. PhD thesis, Max Planck Institute for Physics, Munich, 2010. [arXiv:1009.2511].

[91] F. Mahmoudi, *SuperIso v2.3: A Program for calculating flavor physics observables in Supersymmetry*, Comput.Phys.Commun. **180** (2009) 1579–1613 [arXiv:0808.3144].

F. Mahmoudi, *SuperIso: A Program for calculating the isospin asymmetry of B* $\to$ *K* gamma in the MSSM*, Comput.Phys.Commun. **178** (2008) 745–754 [arXiv:0710.2067].

[92] **Heavy Flavor Averaging Group**, D. Asner *et. al.*, *Averages of b-hadron, c-hadron, and* τ*-lepton properties*, [arXiv:1010.1589].

[93] **LHCb Collaboration**, R. Aaij *et. al.*, *Strong constraints on the rare decays* $B_s \to \mu^+\mu^-$ *and* $B^0 \to \mu^+\mu^-$, Phys.Rev.Lett. **108** (2012) 231801 [arXiv:1203.4493].

[94] **Heavy Flavor Averaging Group**, E. Barberio *et. al.*, *Averages of b−hadron and c−hadron Properties at the End of 2007*, [arXiv:0808.1297].

[95] J. M. Frere, D. R. T. Jones and S. Raby, *Fermion Masses and Induction of the Weak Scale by Supergravity*, Nucl. Phys. **B222** (1983) 11.

[96] M. Passera, W. Marciano and A. Sirlin, *The Muon g-2 and the bounds on the Higgs boson mass*, Phys.Rev. **D78** (2008) 013009 [arXiv:0804.1142].

K. Hagiwara, R. Liao, A. D. Martin, D. Nomura and T. Teubner, $(g-2)_m u$ *and* $\alpha(M_Z^2)$ *re-evaluated using new precise data*, J.Phys. **G38** (2011) 085003 [arXiv:1105.3149].

[97] **J-PARC g-2 Collaboration**, T. Mibe, *New g-2 experiment at J-PARC*, Chin.Phys. **C34** (2010) 745–748.

[98] R. Carey, K. Lynch, J. Miller, B. Roberts, W. Morse *et. al.*, *The New (g-2) Experiment: A proposal to measure the muon anomalous magnetic moment to +-0.14 ppm precision*, .

[99] **ATLAS Collaboration**, G. Aad *et. al.*, *Search for squarks and gluinos with the ATLAS detector in final states with jets and missing transverse momentum using* $\sqrt{s} = 8$ *TeV proton–proton collision data*, JHEP **1409** (2014) 176 [arXiv:1405.7875].

[100] **ATLAS Collaboration**, G. Aad *et. al.*, *Search for strong production of supersymmetric particles in final states with missing transverse momentum and at least three b-jets at* $\sqrt{s}$*= 8 TeV proton-proton collisions with the ATLAS detector*, JHEP **1410** (2014) 24 [arXiv:1407.0600].

[101] **ATLAS Collaboration**, G. Aad *et. al.*, *Search for squarks and gluinos in events with isolated leptons, jets and missing transverse momentum at* $\sqrt{s} = 8$ *TeV with the ATLAS detector*, [arXiv:1501.0355].

[102] **ATLAS Collaboration**, G. Aad *et. al.*, *Observation of a new particle in the search for the Standard Model Higgs boson with the ATLAS detector at the LHC*, Phys.Lett. **B716** (2012) 1–29 [arXiv:1207.7214].

CMS Collaboration, S. Chatrchyan *et. al.*, *Observation of a new boson at a mass of 125 GeV with the CMS experiment at the LHC*, Phys.Lett. **B716** (2012) 30–61 [arXiv:1207.7235].

[103] A. Arbey, M. Battaglia, A. Djouadi and F. Mahmoudi, *The Higgs sector of the phenomenological MSSM in the light of the Higgs boson discovery*, JHEP **1209** (2012) 107 [arXiv:1207.1348].

[104] J. Alwall, P. Schuster and N. Toro, *Simplified Models for a First Characterization of New Physics at the LHC*, Phys.Rev. **D79** (2009) 075020 [arXiv:0810.3921].

D. S. Alves, E. Izaguirre and J. G. Wacker, *Where the Sidewalk Ends: Jets and Missing Energy Search Strategies for the 7 TeV LHC*, JHEP **1110** (2011) 012 [arXiv:1102.5338].

LHC New Physics Working Group, D. Alves *et. al.*, *Simplified Models for LHC New Physics Searches*, J.Phys. **G39** (2012) 105005 [arXiv:1105.2838].

[105] C. D. Froggatt and H. B. Nielsen, *Hierarchy of Quark Masses, Cabibbo Angles and CP Violation*, Nucl. Phys. **B147** (1979) 277.

[106] P. Harrison, D. Perkins and W. Scott, *Tri-bimaximal mixing and the neutrino oscillation data*, Phys.Lett. **B530** (2002) 167 [hep-ph/0202074].

[107] C. H. Albright and M.-C. Chen, *Model Predictions for Neutrino Oscillation Parameters*, Phys.Rev. **D74** (2006) 113006 [hep-ph/0608137].

[108] S. Antusch, S. F. King, M. Malinsky and M. Spinrath, *Quark mixing sum rules and the right unitarity triangle*, Phys.Rev. **D81** (2010) 033008 [arXiv:0910.5127].

[109] S. King, *Constructing the large mixing angle MNS matrix in seesaw models with right-handed neutrino dominance*, JHEP **0209** (2002) 011 [hep-ph/0204360].

[110] S. Antusch and S. F. King, *Charged lepton corrections to neutrino mixing angles and CP phases revisited*, Phys.Lett. **B631** (2005) 42–47 [hep-ph/0508044].

[111] D. Marzocca, S. T. Petcov, A. Romanino and M. Spinrath, *Sizeable θ_{13} from the Charged Lepton Sector in SU(5), (Tri-)Bimaximal Neutrino Mixing and Dirac CP Violation*, JHEP **1111** (2011) 009 [arXiv:1108.0614].

[112] S. King, *Tri-bimaximal-Cabibbo Mixing*, Phys.Lett. **B718** (2012) 136–142 [arXiv:1205.0506].

[113] H. Leutwyler, *The Ratios of the light quark masses*, Phys.Lett. **B378** (1996) 313–318 [hep-ph/9602366].

[114] S. Antusch, J. Kersten, M. Lindner and M. Ratz, *Running neutrino masses, mixings and CP phases: Analytical results and phenomenological consequences*, Nucl.Phys. **B674** (2003) 401–433 [hep-ph/0305273].

[115] S. Antusch, S. F. King and M. Malinsky, *Third Family Corrections to Quark and Lepton Mixing in SUSY Models with non-Abelian Family Symmetry*, JHEP **0805** (2008) 066 [arXiv:0712.3759].

[116] S. Antusch, S. F. King and M. Malinsky, *Third Family Corrections to Tri-bimaximal Lepton Mixing and a New Sum Rule*, Phys.Lett. **B671** (2009) 263–266 [arXiv:0711.4727].

S. Antusch, S. F. King and M. Malinsky, *Perturbative Estimates of Lepton Mixing Angles in Unified Models*, Nucl.Phys. **B820** (2009) 32–46 [arXiv:0810.3863].

[117] S. Antusch, C. Gross, V. Maurer and C. Sluka, *A flavour GUT model with* $\theta_{13}^{PMNS} \simeq \theta_C/\sqrt{2}$, Nucl.Phys. **B877** (2013) 772–791 [arXiv:1305.6612].

[118] S. Antusch, C. Gross, V. Maurer and C. Sluka, *Inverse neutrino mass hierarchy in a flavour GUT model*, Nucl.Phys. **B879** (2014) 19–36 [arXiv:1306.3984].

[119] S. King, *Predicting neutrino parameters from SO(3) family symmetry and quark-lepton unification*, JHEP **0508** (2005) 105 [hep-ph/0506297].

[120] I. Masina, *A Maximal atmospheric mixing from a maximal CP violating phase*, Phys.Lett. **B633** (2006) 134–140 [hep-ph/0508031].

S. Antusch, P. Huber, S. King and T. Schwetz, *Neutrino mixing sum rules and oscillation experiments*, JHEP **0704** (2007) 060 [hep-ph/0702286].

[121] S. Boudjemaa and S. King, *Deviations from Tri-bimaximal Mixing: Charged Lepton Corrections and Renormalization Group Running*, Phys.Rev. **D79** (2009) 033001 [arXiv:0808.2782].

[122] S. Antusch, S. F. King, C. Luhn and M. Spinrath, *Right Unitarity Triangles and Tri-Bimaximal Mixing from Discrete Symmetries and Unification*, Nucl.Phys. **B850** (2011) 477–504 [arXiv:1103.5930].

[123] V. D. Barger, S. Pakvasa, T. J. Weiler and K. Whisnant, *Bimaximal mixing of three neutrinos*, Phys.Lett. **B437** (1998) 107–116 [hep-ph/9806387].

[124] A. Y. Smirnov, *Neutrinos: '...Annus mirabilis'*, [hep-ph/0402264].

M. Raidal, *Relation between the neutrino and quark mixing angles and grand unification*, Phys.Rev.Lett. **93** (2004) 161801 [hep-ph/0404046].

P. Frampton and R. Mohapatra, *Possible gauge theoretic origin for quark-lepton complementarity*, JHEP **0501** (2005) 025 [hep-ph/0407139].

S. Antusch, S. F. King and R. N. Mohapatra, *Quark-lepton complementarity in unified theories*, Phys.Lett. **B618** (2005) 150–161 [hep-ph/0504007].

N. Li and B.-Q. Ma, *Relations between quark and lepton mixing angles and matrices*, Eur.Phys.J. **C42** (2005) 17–24 [hep-ph/0504161].

H. Minakata, *Quark-lepton complementarity: A Review*, [hep-ph/0505262].

K. Hochmuth, S. Petcov and W. Rodejohann, *U(PMNS) = U**dagger (l) U(nu)*, Phys.Lett. **B654** (2007) 177–188 [arXiv:0706.2975].

S. Goswami, S. T. Petcov, S. Ray and W. Rodejohann, *Large —U(e3)— and Tri-bimaximal Mixing*, Phys.Rev. **D80** (2009) 053013 [arXiv:0907.2869].

N. Qin and B.-Q. Ma, *A New simple form of quark mixing matrix*, Phys.Lett. **B695** (2011) 194–198 [arXiv:1011.6412].

N. Qin and B.-Q. Ma, *Parametrization of fermion mixing matrices in Kobayashi-Maskawa form*, Phys.Rev. **D83** (2011) 033006 [arXiv:1101.4729].

Y. Ahn, H.-Y. Cheng and S. Oh, *Quark-lepton complementarity and tribimaximal neutrino mixing from discrete symmetry*, Phys.Rev. **D83** (2011) 076012 [arXiv:1102.0879].

Y. Ahn, H.-Y. Cheng and S. Oh, *Recent Neutrino Data and a Realistic Tribimaximal-like Neutrino Mixing Matrix*, Phys.Lett. **B715** (2012) 203–207 [arXiv:1105.4460].

Y.-j. Zheng and B.-Q. Ma, *Re-Evaluation of Neutrino Mixing Pattern According to Latest T2K result*, Eur.Phys.J.Plus **127** (2012) 7 [arXiv:1106.4040].

Y. Ahn, H.-Y. Cheng and S. Oh, *An extension of tribimaximal lepton mixing*, Phys.Rev. **D84** (2011) 113007 [arXiv:1107.4549].

[125] H. Minakata and A. Y. Smirnov, *Neutrino mixing and quark-lepton complementarity*, Phys.Rev. **D70** (2004) 073009 [hep-ph/0405088].

[126] K. M. Patel, *An SO(10)XS4 Model of Quark-Lepton Complementarity*, Phys.Lett. **B695** (2011) 225–230 [arXiv:1008.5061].

[127] Z. Berezhiani and Z. Tavartkiladze, *Anomalous U(1) symmetry and missing doublet SU(5) model*, Phys.Lett. **B396** (1997) 150–160 [hep-ph/9611277].

[128] G. Altarelli, F. Feruglio and I. Masina, *From minimal to realistic supersymmetric SU(5) grand unification*, JHEP **0011** (2000) 040 [hep-ph/0007254].

[129] H. Murayama, Y. Okada and T. Yanagida, *The Georgi-Jarlskog mass relation in a supersymmetric grand unified model*, Prog.Theor.Phys. **88** (1992) 791–796.

[130] D.-X. Zhang and J.-h. Zheng, *A Missing Partner Model With 24-plet Breaking SU(5)*, JHEP **1212** (2012) 087 [arXiv:1212.5852].

[131] A. Masiero, D. V. Nanopoulos, K. Tamvakis and T. Yanagida, *Naturally Massless Higgs Doublets in Supersymmetric SU(5)*, Phys.Lett. **B115** (1982) 380.

[132] B. Grinstein, *A Supersymmetric SU(5) Gauge Theory with No Gauge Hierarchy Problem*, Nucl.Phys. **B206** (1982) 387.

[133] J. Hisano, T. Moroi, K. Tobe and T. Yanagida, *Suppression of proton decay in the missing partner model for supersymmetric SU(5) GUT*, Phys.Lett. **B342** (1995) 138–144 [hep-ph/9406417].

[134] A. Meroni, S. Petcov and M. Spinrath, *A SUSY SU(5)xT' Unified Model of Flavour with large θ_{13}*, Phys.Rev. **D86** (2012) 113003 [arXiv:1205.5241].

[135] H. Murayama and A. Pierce, *Not even decoupling can save minimal supersymmetric SU(5)*, Phys.Rev. **D65** (2002) 055009 [hep-ph/0108104].

[136] B. Bajc, P. Fileviez Perez and G. Senjanovic, *Minimal supersymmetric SU(5) theory and proton decay: Where do we stand?*, [hep-ph/0210374].

[137] L. J. Hall, *Grand Unification of Effective Gauge Theories*, Nucl.Phys. **B178** (1981) 75.

[138] M. Fallbacher, M. Ratz and P. K. Vaudrevange, *No-go theorems for R symmetries in four-dimensional GUTs*, Phys.Lett. **B705** (2011) 503–506 [arXiv:1109.4797].

[139] D. Emmanuel-Costa and S. Wiesenfeldt, *Proton decay in a consistent supersymmetric SU(5) GUT model*, Nucl.Phys. **B661** (2003) 62–82 [hep-ph/0302272].

[140] S. Wiesenfeldt, *Proton decay in supersymmetric GUT models*, Mod.Phys.Lett. **A19** (2004) 2155 [hep-ph/0407173].

[141] P. Nath, *Hierarchies and textures in supergravity unification*, Phys.Rev.Lett. **76** (1996) 2218–2221 [hep-ph/9512415].

[142] V. Lucas and S. Raby, *Nucleon decay in a realistic SO(10) SUSY GUT*, Phys.Rev. **D55** (1997) 6986–7009 [hep-ph/9610293].

[143] T. Hahn, *Generating Feynman diagrams and amplitudes with FeynArts 3*, Comput.Phys.Commun. **140** (2001) 418–431 [hep-ph/0012260].

[144] T. Hahn and M. Perez-Victoria, *Automatized one loop calculations in four-dimensions and D-dimensions*, Comput.Phys.Commun. **118** (1999) 153–165 [hep-ph/9807565].

T. Hahn and M. Rauch, *News from FormCalc and LoopTools*, Nucl.Phys.Proc.Suppl. **157** (2006) 236–240 [hep-ph/0601248].

[145] G. Passarino and M. Veltman, *One Loop Corrections for e+ e- Annihilation Into mu+ mu- in the Weinberg Model*, Nucl.Phys. **B160** (1979) 151.

[146] P. Z. Skands, B. Allanach, H. Baer, C. Balazs, G. Belanger *et. al.*, *SUSY Les Houches accord: Interfacing SUSY spectrum calculators, decay packages, and event generators*, JHEP **0407** (2004) 036 [hep-ph/0311123].

[147] D. Jones, *Asymptotic Behavior of Supersymmetric Yang-Mills Theories in the Two Loop Approximation*, Nucl.Phys. **B87** (1975) 127.

D. Jones and L. Mezincescu, *The Beta Function in Supersymmetric Yang-Mills Theory*, Phys.Lett. **B136** (1984) 242.